Clinical Significance of SphK1 in Chemotherapy Resistance of Gastric Cancer Patients

by

Xiangyu Gao
Cardiff China Medical Research Collaborative
School of Medicine, Cardiff University
Cardiff

June 2019

Thesis submitted to Cardiff University for the degree of Doctor of Medicine

DECLARATION

This work has not been submitted in substance for any other degree or award at this or any other university or place of learning, nor is being submitted concurrently in candidature for any degree or other award.

Signed …… (candidate) Date ……

STATEMENT 1

This thesis is being submitted in partial fulfilment of the requirements for the degree of MD.

Signed …… (candidate) Date ……

STATEMENT 2

This thesis is the result of my own independent work/investigation, except where otherwise stated. Other sources are acknowledged by explicit references. The views expressed are my own.

Signed …… (candidate) Date ……

STATEMENT 3

I hereby give consent for my thesis, if accepted, to be available for photocopying and for inter-library loan, and for the title and summary to be made available to outside organisations.

Signed …… (candidate) Date ……

STATEMENT 4: PREVIOUSLY APPROVED BAR ON ACCESS

I hereby give consent for my thesis, if accepted, to be available for photocopying and for inter-library loans after expiry of a bar on access previously approved by the Academic Standards & Quality Committee.

Signed …… (candidate) Date ……

Word count…….
(excluding summary, acknowledgments, declarations, contents pages, appendices, tables, diagrams and figures, references, bibliography, footnotes and endnotes

Acknowledgements

After two years' study in Clinical Significance of SphK1in Chemotherapy Resistance of Gastric Cancer Patients, and another more than half year's writing, this thesis was finally accomplished. Without the help of many people, it could never have been completed; thus here I would like to extend my deep gratitude to all that have offered me practical, cordial and selfless support in accomplishing this thesis.

First and foremost, I owe my heartfelt thanks to my two distinguished supervisors, DR. Jun Cai, who influenced me with his insightful ideas and meaningful inspirations, and guided me with practical academic advice and feasible instructions at the stage of research, and Ms. Rachel Hargest, who instructed me in clinical work and set me a vivid example by her rigorous attitude and exceeding enthusiasm in clinical work. Without both of their dedicated assistance and insightful supervision, this thesis would have gone nowhere.

Then, my faithful appreciation also goes to Dr. Andrew Sanders for enlightening me while I was confused during the experiment and writing procedure. His thought-provoking comments and patient encouragements are indispensable for my accomplishment of this thesis.

I would also like to express my sincere gratitude to Prof. Wenguo Jiang for his help and encouragement in my studies and life during my stay in the Cardiff China Medical Research Collaborative (CCMRC). The numerous academic discussions between us have helped broaden my research ideas.

I am also grateful to Ms. Fiona Ruge, Dr Lin Ye, Dr Tracey Martin, Dr. Liam Morgan, Dr. Jane Lane and Dr. Nicola Jordan for their help during the project.

Moreover, I have been given a lot of help from China. Thanks to Prof Jiafu Ji, helping me to research on patients of Peking University Cancer Hospital with his high perspective sight and Prof. Ziyu Li for providing detailed help in collecting samples

in our department and his suggestions and individual time on my clinical research. Apart from these, I would like to thank all my friends, especially Nikki and Levon, as no matter what I am doing, their support and encouragement are always there. Ultimately, my thanks go to my wife Leilei and my daughter Seren and my parents. It is their consistent support that gives me the courage to confront any obstacles along the way and enables me to finally complete my MD program.

Finally, I would like to thank the paper review experts and the respondents for their review and guidance.

Summary

Sphingosine kinase 1 (SphK1) is a biologically active lipid which plays a significant role in the growth, survival, migration of the cell, as well as a role in anti-apoptosis and enhances cell immortalization. SphK1 is involved in the crucial S1P signalling pathway which can catalyse sphingosine phosphorylates to S1P in an ATP-dependent manner. Our study examined the effect of SphK1 on gastric cancer cell line, its clinical significance in gastric cancer progression and the role in chemoresistance with the prediction that SphK1 is a potential pharmacologic target.Our results demonstrated that the inhibition of SphK1 expression and/or its kinase activity could down-regulate AKT/mTOR survival signalling pathway, leading to reduced chemoresistance of gastric cancer cells, suggesting that SphK1might be a potential novel target for the treatment of gastric cancer.

Publications and Presentations

1. Xiangyu Gao, Ke Ji, Jun Cai, Wenguo Jiang, Jiafu Ji, et al. Inhibition of sphingosine-1-phosphate phosphatase 1 (SGPP1) promotes cancer cell migration in gastric cancer, clinical implications [J]，Oncology Reports 34: 1977-1987, 2015
2. Jun Li, Xiangyu Gao, Wenguo Jiang, Jiafu Ji, Lin Ye, et al. Differential expression of CNN family members CYR61, CTGF and NOV in gastric cancer and association with disease progression [J], Oncology Reports 36: 2517-2525, 2016
3. Xiangyu Gao, Ke Ji, Jun Cai, Wenguo Jiang, Jiafu Ji, et al. Inhibitor effects of sphingosine-1-phosphate phosphatase 1 (SGPP1) in migration of gastric cancer cell [C]. 11th International Gastric Cancer Congress (IGCC) :2015
4. Xiangyu Gao, Ke Ji, Jun Cai, Wenguo Jiang, Jiafu Ji, et al. Activation of PI3K/Akt signaling pathway in gastric cancer through active sphingosine kinase-1 [C]. China United Kingdom Cancer Conference (CUKC) :2015
5. Xiangyu Gao, Ke Ji, Jun Cai, Wenguo Jiang, Jiafu Ji, et al. Activation of MMPs to enhance the invasion of gastric cancer cell through inhibiting sphingosine-1-phosphatereceptor 1: clinical implications [C]. European cancer congress (ECC) :2015
6. Xiangyu Gao, Ke Ji, Lin Ye, Wenguo Jiang, Jiafu Ji, et al. Differential expression of CNN family members CYR61, CTGF and NOV in gastric cancer and association with disease progression [C]. European cancer congress (ECC) :2015
7. Xiangyu Gao., Ji Ke, Jiafu Ji, Wenguo Jiang and Lin Ye (2015). "2215 Differential expression of CNN family members CYR61, CTGF and NOV in gastric cancer and association with disease progression." European Journal of Cancer 51: S404.
8. Xiangyu Gao, Ke Ji, Jun Cai, Chunyi Hao, Wenguo Jiang et al. Promotion of Cell Growth and Migration in Pancreatic Cancer

through Active Sphingosine Kinase-1: Clinical Implications [C]. China United Kingdom Cancer Conference (CUKC) :2016

9. Xiangyu Gao, Ke Ji, Jun Cai, Wenguo Jiang, Jiafu Ji, et al. Clinical significance of SphK1 related to chemotherapy resistance in gastric cancer patients [C]. 12th International Gastric Cancer Congress (IGCC) :2017

Abbreviations

ABC	ATP-binding Cassette
ABCA1	ATP-binding Cassette A1
ABCC1	ATP-binding Cassette C1
ABCG1	ATP-binding Cassette G1
ACTS-GC	Adjuvent Chemotherapy Trial of TS-1 for Gastric Cancer
ADP	Adenosine diphophate
AJCC	American Joint Committee on Cancer
Akt/PKB	Protein Kinase B
AOM	Azoxymethane
APS	Ammonium Persulphate
ARHGAP	Rho GTPase activating protein
ATCC	American Type Culture Collection
ATG5	Autophagy related 5
ATM	Ataxia Telangiectasia Mutated protein
AVAGAST	Avastin in Gastric Cancer
BCL-2	B-cell lymphoma-2
BECN1	Beclin-1
bFGF	Basic fibroblast growth factor
BRCA	BReast CAncer
BSA	Bovine Serum Albumin
CCMRC	Cardiff China Medical Research Collaborative
CCND1	Cyclin D1
CCNE1	Cyclin E1
CD274	Cluster of differentiation 274
CDH1	Genome-stable phenotypes include Cadherin-1

CDK6	Cyclin dependent kinase 6
CDKN2A	Cyclin-dependent kinase Inhibitor 2A
CDX1	Caudal type homeobox 1
CI	Confidence interval
CIN	Chromosomally unstable tumour
CK-19	Cytokeratin-19
CLASS	The Chinese Laparoscopic Gastrointestinal Surgery Study
CLASSIC	The capecitabine and oxaliplatin adjuvant study in stomach cancer
CLDN18	Claudin 18
COX	Cytochrome c Oxidase
COX-2	Cyclooxygenase-2
CpG	5'-C-phosphate-G-3'
CRC	Colon Rectal Cancer
CTD	C-terminal domain
Cyp-D	Cyclophilin-D
DEPC	Diethyl Pyrocarbonate
DFS	Disease-free survival
DMEM	Dulbecco's Modified Eagle Medium
DMSO	Dimethylsulphoxide
DNA	Deoxyribonucleic acid
EBV	Epstein barr virus
ECACC	European Collection of Authenticated Cell Cultures
ECF	Epirubicin, cisplatin, fluorouracil
ECM	Extracellular matrix
EDG1	Endothelial differentiation gene 1
EDTA	Ethylene Diaminetetraacetic Acid
EGFR	Epidermal growth factor receptor

EGC	Early Gastric cancer
EGJ	Gastroesophageal junction
EMR	Endoscopic Mucosa Resection
ERK	Extracellular signal-regulated kinase
ESD	Endoscopic Submucosa Disection
ESMO	European Society for Medical Oncology-
EMT	Epithelial Mesenchymal Transition
ERBB2/3	Epidermal Growth Factor Receptor 2/3
EVOS	Environmental Virtual Observatories
EXPAND	Erbitux (cetuximab) in combination with Xeloda (capecitabine) and cisplatin in advanced esophago-gastric cancer
FAK	Focal adhesion kinase
FCS	Fetal calf serum
FDA	Food and Drugs Administration
FFCD	The Fe´de´ration Francophone de Cance´rologie Digestive
FLOT4	Fluorouracil, Leucovorin, Oxaliplatin and Docetaxel
FNCLCC	The Fe´de´ration Nationale des Centres de Lutte contre le Cancer
FSCN1	Fascin1
FTC	Follicular Thyroid Carcinoma
FTY720	Fingolimod
GAPDH	Dehydrogenase
GC	Gastric cancer
GEO	Gene Expression Omnibus
GPCR	G Protein Coupled Receptor
GS	Genomically stable tumour
GTPase	Guanosine triohosphte
GZMB	Granzyme B

HDACs	Histone Deacetylases
HDGC	Hereditary diffuse gastric cancer
HER2	Human Epidermal Growth Factor Receptor2
HGF	Hepatocyte growth factor
HNSCC	Head and neck squamous cell carcinomas
HP	Helicobacter pylori
HPMC	Human peritoneal mesothelial cells
HR	Hazard ratio
HRAS	Harvey rat sarcoma viral oncogene homolog
HRP	Horseradish peroxidase
ICL	Intracellular loops
IHC	Immunohistochemical
IL6	Interleukin-6
I2PP2A/SET	Inhibitor 2 of Protein phosphatase 2A
IκBα	Nuclear factor of kappa light polypeptide gene enhancer in B-cells inhibitor alpha
JACCRO GC	Japan Clinical Cancer Research Organization Gastric Cancer
JAK	Janus kinase
JCOG	Japan Clinical Oncology Group
KDa	Kilo Dalton
LB	Lysogeny Broth
LBA	Late-Breaking Abstract
LC	Lung Cancer
LDH	Lactate dehydrogenase
LG	Laparoscopic Gastrectomy
mAb	Monoclonal antibody
MAGIC	Council Adjuvant Gastric Infusional Chemotherapy
MLH1	MutL Homolog 1

MM	Multiple myemola
MMP	Matrix metalloproteinases
mRNA	Message Ribonucleic Acid
miRNA	Micro Ribonucleic Acid
MS	Multiple sclerosis
MSI	Microsatellite instability
MSI-H	Microsatellite instability High
mTOR	Mammalian target of rapamycin
MTT	3-(4,5-dimetheylthiazol-2-yl)-2,5-diphenyltetrazolium bromide
NCCN	National Comprehensive Cancer Network
NCCRC	National Central Cancer Registry of China
NSCLC	Non-small Cell Lung Cancer
NF-κB	Nuclear factor of kappa light polypeptide gene enhancer in B-cells
NTD	N-terminal domain
OG	Opem Gastrectomy
OR	Odds Ratio
ORR	Objective response rate
OS	Overall survival
PalCoA	Palmitoyl-CoA
PARP	Poly-ADP ribose polymerase
PBS	Phosphate buffered saline
PCR	Polymerase Chain Reaction
PD-1/2	Programmed deat 1 and 2
PD-L1/2	Programmed death ligand 1 and 2
PDCD1LG2	Programmed cell death 1 ligand 2
PDGF	Platelet derived growth factor
PDO	Patient Derived Organoids

PDTX	Patient Derived Tumour Xenograft
PE	Phosphoethanol-amine
PGE2	Prostaglandin E2
PFK	Phosphofructokinase
PFS	Progression free survival
PHB2	Prohibitin 2
PI3K	Phosphatidylinositol-3-kinase
PIK3CA	Phospatidylinositol-4,5-Bisphosphate 3-Kinase Catalytic Subunit Alpha
PKUCH	Peking University Cancer Hospital
PP2A	Protein phosphatase 2A
PTC	Papillary Thyroid Carcinoma
PVDF	Polyvinylidene fluoride or polyvinylidene difluoride
qPCR	Quantitative Real-time Polymerase Chain Reaction
RCC	Renal Cell Carcinoma
RCF	Relative Centrifugal Force
RFS	Relapse Free Survival
RHO	Ras Homolog Family
RHOA	Ras Homolog Family Member A
RIPK	Receptor interacting protein kinase
RT-PCR	Reverse Transcription Polymerase Chain Reaction
RTK	Receptor tyrosine kinases
S-1	Tegafur/gimeracil/oteracil
S1P	Sphingosine-1-phosphate
S1PRs	Sphingosine-1-phosphate receptors
SDS	Sodium Dodecyl Sulphate
SDS-PAGE	Sodium Dodecyl Sulfate-Polyacrylamide Gel Electrophoresis
SFM	Serum free medium

SFRP4	Secreted frizzled-related protein 4
SGPP1	Sphingosine 1phosphate phosphatase 1
SGPL1	Sphingosine 1phosphate Lyase 1
shRNA	Short Hairpin Ribonucleic Acid
SphK1	Sphingosine kinase 1
STAT3	Signal transducer and activator of transcription
SYBR	(Z)-4-((3-Methylbenzo[d]thiazol-2(3H)-ylidene)methyl)-1-propylquinolin-1-ium 4-methylbenzenesulfonate
TBE	Tris-Boric-Acid-EDTA
TBS	Tris Buffered Saline
TCGA	The Cancer Genome Atlas
TEMED	Tetramethylethylenediamine
TNBC	Triple Negative Breast Cancer
TNF	Tumour necrosis factor
TNFR1	Tumour necrosis factor receptor 1
TNM	Tumour Node Metastases
ToGA	Trastuzumab for Gastric Cancer
TP53	Tumour protein 53
TRAF2	Tumour-necrosis factor receptor-associated factor 2
TRAILR1/2	TNF related apoptosis inducing ligand receptors1/2
UICC	Union for International Cancer Control
UTR	Untranslated Region
WARS	Tryptophanyl-tRNA Synthetase
VEGF	Vascular endothelial growth factor
WB	Western Blot
XELOX/CapOX	Capecitabine Oxaliplatin,

Contents

List of Figures

List of Tables

Chapter I

General Introduction

1.1 Gastric cancer

1.1.1 General introduction

Gastric cancer (GC) causes a significant health issue worldwide, being the fifth most common cancer and second leading cause of cancer related death. An estimated 1,033,701 new cases and 782,685 deaths occured in 2018, ranking the fifth leading cause of morbidity and the third leading cause of mortality around the world (Bray et al., 2018).

China has the largest number of GC patients worldwide, and according to the National Central Cancer Registry of China (NCCRC), 410,400 new GC cases were diagnosed, and about 293,800 GC-related deaths occurred in 2014 in China (Yang et al., 2018). The incidence in men is 2-fold higher than that in women. The incidence rate of GC is approximately 30/100,000. GC is more common in rural areas rather than urban areas. The incidence in men is 2.4 times as high as that in women. Among patients older than 44 years, the morbidity rate is higher in men than in women. It is estimated that there was an increase of 365,000 GC cases in comparison with those in 1990, leading to more than 96,000 deaths.

Although the absolute number is increased, the incidence of new GC cases has declined since 1990 (Collaborators, 2020).The slowing decline is most likely explained by the long-term low and stable prevalence of *Helicobacter pylori* (HP) infection (Ferro et al., 2014). By contrast, incidence rates of gastro-oesophageal-junction adenocarcinomas are on the rise (Pohl et al., 2010).

Despite declining incidence and mortality rates, advancements in the understanding of the epidemiology, pathology, molecular mechanisms and therapeutic options and strategies for gastric cancer, the burden and strain on healthcare systems remains high. Due to the large number of GC patients in China and Asia, tailor-made treatment strategies are still needed.

1.1.2 Aetiology

1.1.2.1 *Helicobacter pylori* (HP)

HP infection is the most important cause of sporadic gastric cancer (Bornschein et al., 2010). Persistent HP infection can promote normal epithelium atrophy, and then intestinal epithelium, dysplasia and adenocarcinoma (Leung et al., 2004, Mera et al., 2005, Fukase et al., 2008). Studies have confirmed that HP infection can cause interactions among bacteria, hosts and the environment, promote tissue damage, and cause chronic inflammatory lesions and tumours (Wang et al., 2014b). In addition, HP is involved in tumour cell proliferation, apoptosis, and epigenetic modification of oncogenes, leading to tumorigenesis associated with inflammatory lesions (Wang et al., 2014b). However, the question remains as to whether the eradication of HP can prevent the process of gastric cancer? After 15 years of follow-up, it has been demonstrated in a large sample population that HP eradication significantly reduces the incidence of gastric cancer (Odds Ratio, OR = 0.61, 95% CI 0.38-0.96) (Ma et al., 2012). In addition, in severe mucosal lesions and the elderly group, eradication of HP can also prevent the occurrence of gastric cancer (Li et al., 2014b). For patients with early gastric cancer after surgery, whether the eradication of HP is effective is inconclusive, a study has shown that after surgery, HP eradication significantly reduces the incidence of metachronous gastric cancer compared to placebo (HR = 0.50, $p = 0.03$) (Choi et al., 2018). Furthermore, recent research result showed that patients who had a family history could also benefit from eradication of HP (Choi et al., 2020).

1.1.2.2 Epstein Barr Virus (EBV)

EBV preferentially exists in gastric cancer cells and lymphoid stroma, and normal epithelial cells are mostly free of EBV (Wu et al., 2000). In recent years, with the

establishment of molecular classification of gastric cancer and the rise of immunotherapy, EBV-related gastric cancer has gradually received attention. It is suggested that EBV-related gastric cancer may have independent biological and clinical characteristics. A study showed that patients with EBV-positive metastatic gastric cancer treated with pembrolizumab had an amazing objective response rate (ORR) which initially confirmed that EBV-positivity could be used as a potential molecular marker to predict the response of immunotherapy (Kim et al., 2018). However, it is limited by the characteristics of retrospective studies and needs further verification. It is believed that the in-depth study of the molecular mechanism of EBV-related gastric cancer could provide a theoretical basis for the refinement of the molecular classification of gastric cancer and development of new drugs.

1.1.2.3 Hereditary diffuse gastric cancer (HDGC)

Hereditary diffuse gastric cancer (HDGC) is an autosomal dominant genetic disease with CDH1 (Cadherin 1) mutation. For CDH1 mutation carriers, prophylactic total gastrectomy is recommended between the ages of 18 and 40 years. Baseline endoscopy is required before preventive total gastrectomy. A frozen section should be performed during the operation to confirm that the proximal edge contains oesophageal squamous mucosa and the distal edge contains duodenal mucosa to ensure complete removal of gastric tissue. Prophylactic total gastrectomy does not require D2 lymphadenectomy. Prophylactic gastrectomy is not recommended before the age of 18, unless there are members of the family who have been diagnosed with gastric cancer before the age of 25. Carriers of CDH1 mutations who choose not to undergo prophylactic gastrectomy should receive an endoscopy every 6-12 months and undergo multiple random biopsies for screening. Women with CDH1 mutations have an increased risk of breast cancer (cited from NCCN Guidelines Version 4.2019 Gastric Cancer).

1.1.3 Classification

1.1.3.1 Anatomical

1.1.3.1.1 Siewert classification

Due to the fact that the incidence, geographical distribution, causes, clinical disease course and treatment are different in non-cardia gastric cancers and gastro-oesophageal-junction cancers (cardia), it is of great importance to classify the anatomical location in tumour. The Siewert classification is widely used to categorise gastro-oesophageal-junction cancers (Siewert and Stein, 1998):

- Siewert I: The epicentre of tumour is located 1-5cm above the gastro-oesophageal junction
- Siewert II: The epicentre of tumour is located 1-2cm above and below the gastro-oesophageal junction
- Siewert III: The epicentre of tumour is located 2-5cm below the gastro-oesophageal junction.

However, it is not clear whether there are biological differences between Siewert type II and type III (Demicco et al., 2011). Furthermore, due to the lack of precise criteria for identifying gastro-oesophageal-junction adenocarcinomas, the Siewert classification has been under criticism.

In the 8th edition of the TNM staging of gastric cancer published by the Union for International Cancer Control (UICC) and the American Joint Committee on Cancer (AJCC) in 2018, tumours where the epicentre is located within 2cm distal to gastro-oesophageal-junction and tumour does not invade gastro-oesophageal-junction are classified as gastric cancer. Therefore, some cases of Siewert type II gastroesophageal junction cancer were reclassified as gastric cancer, which will inevitably affect the future treatment strategy of gastroesophageal junction cancer.

1.1.3.1.2 Borrmann's classification

Borrmann's classification was established in 1926. This classification has 4 subtypes, depending on the macroscopic appearance of the lesion (Sendler et al., 1995).

- Type I: polypoid fungating,
- Type II: ulcerative with elevated distinct borders,
- Type III: ulcerative with indistinct borders,
- Type IV: diffuse, indistinct borders.

Type I and II: localized types, Types III and IV: infiltrative Types (Figure 1.1)

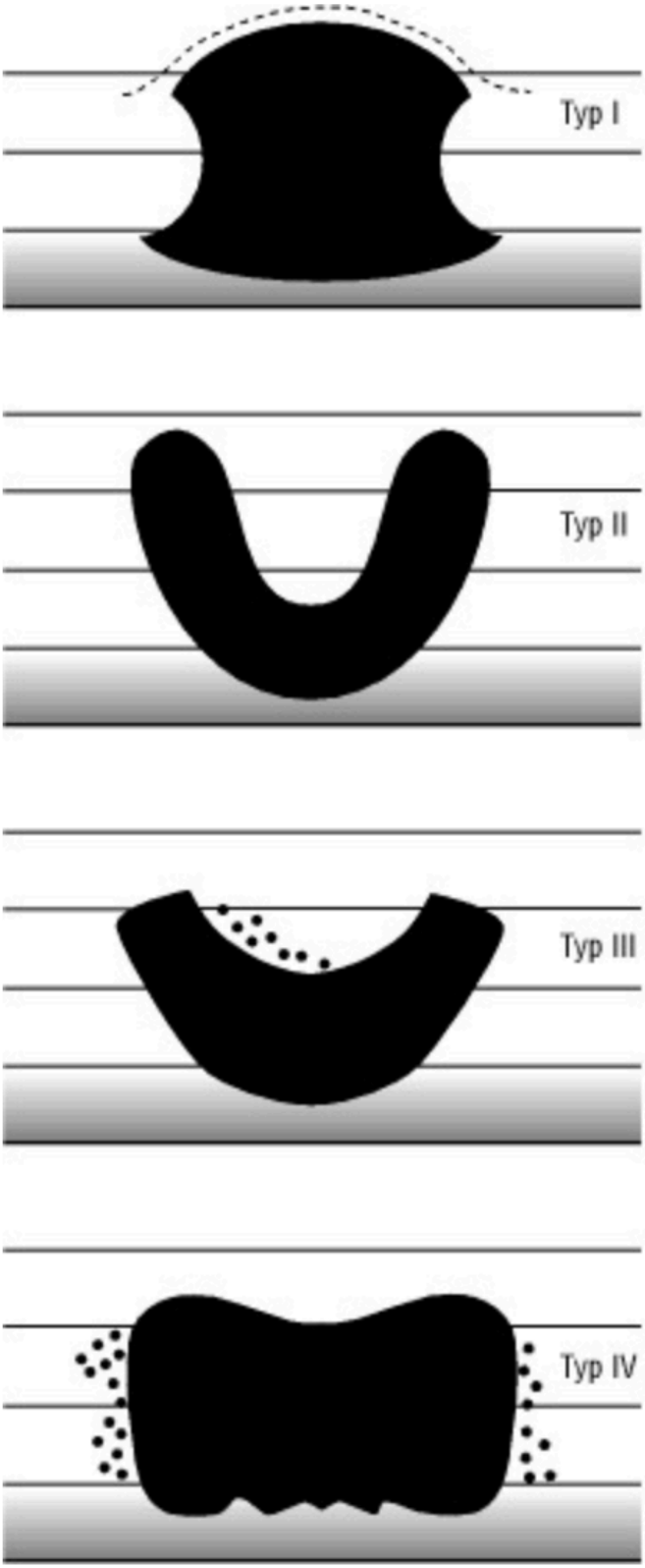

Figure 1.1Borrmann's classification. Figure reproduced from Surgical Treatment: Evidence-Based and Problem-Oriented, Chapter-Preoperative staging for gastric cancer, writing by J R Siewert et al.

1.1.3.2 Histological

Although the majority of GC are gastric adenocarcinomas, their architecture, growth, cell differentiation, histogenesis, and molecular pathogenesis vary, which accounts for the diversity of histopathological classifications. The Lauren (Lauren, 1965) and WHO classifications are currently the most commonly used classifications.

1.1.3.2.1 Lauren classification

There are two main types of GC according to Lauren classification, termed intestinal type and diffuse type. These two types of GC have different biological, aetiological and epidemiological characteristics.

Intestinal type: tumour cells are arranged in a tubular or glandular structure and are often associated with intestinal metaplasia (Lauren, 1965). This type of GC has a tendency to lymphoid or vascular invasion and is most commonly seen in older male patients. It occurs in the antrum of the stomach, and shows a better prognosis (Qiu et al., 2013, Zheng et al., 2007).

Diffuse type: Tumour cells lack glandular structure (Lauren, 1965). The mucus inside the cell pushes the nucleus to one side to form signet-ring cell carcinoma. Diffuse type presents in the body of stomach in women and young people and is prone to peritoneal metastasis and worse prognosis (Qiu et al., 2013, Chen et al., 2016).

1.1.3.2.2 WHO classification

The WHO classification is composed of five main histopathological types. Compared with the simple and powerful Lauren classification, the advantage of the WHO classification is that the system allows comparison with the histological classifications of cancers in other parts of the gut. The WHO classification is based

on the predominant histological patterns of the carcinoma, namely tubular, papillary, mucinous, poorly cohesive and rare variants. In contrast to the Lauren classification, the WHO tubular and papillary carcinomas are histologically similar to the intestinal type. Likewise poorly cohesive carcinomas (including those composed partly or totally of signet ring cells) is equivalent to the diffuse type histologically (Waldum and Brenna, 1993).

1.1.3.3 Molecular classification

As a part of The Cancer Genome Atlas (TCGA) project, the TCGA research team integrated the analysis of total cell-based array analysis based on somatic cell number analysis of 295 gastric cancer patients' tissues and blood samples without chemotherapy. Subsequence analysis, DNA methylation array analysis, mRNA sequence analysis, microRNA sequence analysis, and data measured based on protein array analysis were undertaken. In 2014, the molecular classification of GC was published (Cancer Genome Atlas Research, 2014) (Figure 1. 2).

GC was divided into 4 subtypes, namely:

- Chromosomally unstable tumour (CIN) (50%)
- Microsatellite instability tumour (MSI) (21%)
- Genomically stable tumour (GS) (20%)
- EBV-infected tumour (EBV) (9%)

1.1.3.3.1 CIN type

This type accounts for about 50% of GC. It usually occurs at the gastro-oesophageal-junction, and most of them belong to the intestinal type of Lauren (Lauren, 1965). Chromosomal instability often exhibits significant aneuploidy and in-situ

amplification of receptor tyrosine kinases (RTK). Almost all RTKs have in situ amplification of genes, and many of them have been blocked by existing or developing drugs (Cancer Genome Atlas Research, 2014). In addition, due to amplification of cell cycle regulatory genes, inhibiting cyclin dependent kinases，such as cyclin E1 (CCNE1), cyclin D1 (CCND1) and cyclin dependent kinase 6 (CDK6)) could represent potential therapeutic targets. In addition, there are many Tumour Protein (TP53) mutations (71%) in chromosomal instability. Frequent TP53 mutations are related to chromosomal aneuploidy (Cancer Genome Atlas Research, 2014).

1.1.3.3.2 MSI type

MSI type accounts for about 21% of gastric cancers. It usually occurs in the gastric antrum or pylorus and is more common in women and the elderly. The age at first diagnosis is high (median age 72 years). This type of DNA hypermethylation includes MSI-associated gastric 5'-C-phosphate-G-3' (CpG) island methylation and hypermethylation of the characteristic MutL Homolog 1 (MLH1) promoter (Cancer Genome Atlas Research, 2014). Hypermethylation of the MLH1 promoter can cause defects in the mismatch repair system, leading to the occurrence of gastric cancer (Wen et al., 2017). Due to abnormal DNA repair mechanisms, high DNA mutation rates include mutations in several genes that activate oncogenic signalling proteins, such as mutations in Phospatidylinositol-4,5-Bisphosphate 3-Kinase Catalytic Subunit Alpha (PIK3CA), Epidermal Growth Factor Receptor 3 (ERBB3), Epidermal Growth Factor Receptor 2 (ERBB2), and epidermal growth factor receptor (EGFR) (Cancer Genome Atlas Research, 2014).

1.1.3.3.3 GS type

This type accounts for about 20% of gastric cancers, and the age at first diagnosis is low (median age 59 years). Most of them are Lauren diffuse type (73%) (Cancer Genome Atlas Research, 2014). Genome-stable phenotypes include Cadherin-1 (CDH1) mutations (37%), Ras Homolog Family Member A (RHOA) mutations, or RHO family GTPase-activated protein gene fusion (Claudin l8-Rho GTPase activating protein, CLDN18-ARHGAP fusion) (Cancer Genome Atlas Research, 2014). CDH1 germline mutations are closely related to hereditary diffuse gastric cancer. However, germline analysis only shows that two CDH1 genes are polymorphic, but neither is a causative factor for hereditary diffuse gastric cancer. RHOA mutations are characteristic mutations that are stable in the genome (Thumkeo et al., 2013). CLDN18-ARHGAP fusion and RHOA mutations are mutually exclusive, and their incidence in GS gastric cancer accounts for 62% (Cancer Genome Atlas Research, 2014). Recognition of the fusion of these mutant genes indicates that genes can provide new ideas for future research and development of drugs.

1.1.3.3.4 EBV type

This type accounts for about 9% of all patients. It mostly occurs in the fundus and body of stomach and is more common in men. EBV-positive types have high levels of CpG island methylation, and EBV-positive DNA hypermethylation levels are higher than any other cancer (colorectal cancer, endometrial cancer, etc.) reported by TCGA (Cancer Genome Atlas, 2012, Cancer Genome Atlas Research et al., 2013, Brennan et al., 2013). Cyclin-dependent kinase Inhibitor 2A （CDKN2A) (p16INK4A) promoter hypermethylation is common in EBV-positive types. CDKN2A is an important tumour suppressor gene, which belongs to the cell cycle-dependent kinase inhibitor gene family. It can regulate cell proliferation and

apoptosis, and methylation of its promoter can promote tumorigenesis (Lee et al., 2012c). PIK3CA mutations are common in EBV-positive types, 80% of EBV-positive types have non-silent PIK3CA mutations and their mutation sites are scattered; while other subtypes have only 3% to 42% PIK3CA mutations. A new frequent amplification site on chromosome 9p24, including Janus kinase 2 (JAK2), cluster of differentiation 274 (CD274), and programmed cell death 1 ligand 2 (PDCD1LG2) gene amplification has been found (Cancer Genome Atlas Research, 2014). The JAK2 gene encodes a receptor tyrosine kinase and is a potential therapeutic target. The CD274 and PDCD1LG2 genes encode Programmed death ligand 1 and 2 (PD-L1 and PD-L2) proteins, respectively. PD-L1 and PD-L2 are immunosuppressive proteins and may become therapeutic targets for anti-tumour immune responses. The results of the TCGA study indicate that JAK2 inhibitors and PD-1/2 antagonists may be effective in the treatment of EBV-positive gastric cancer (Cancer Genome Atlas Research, 2014).

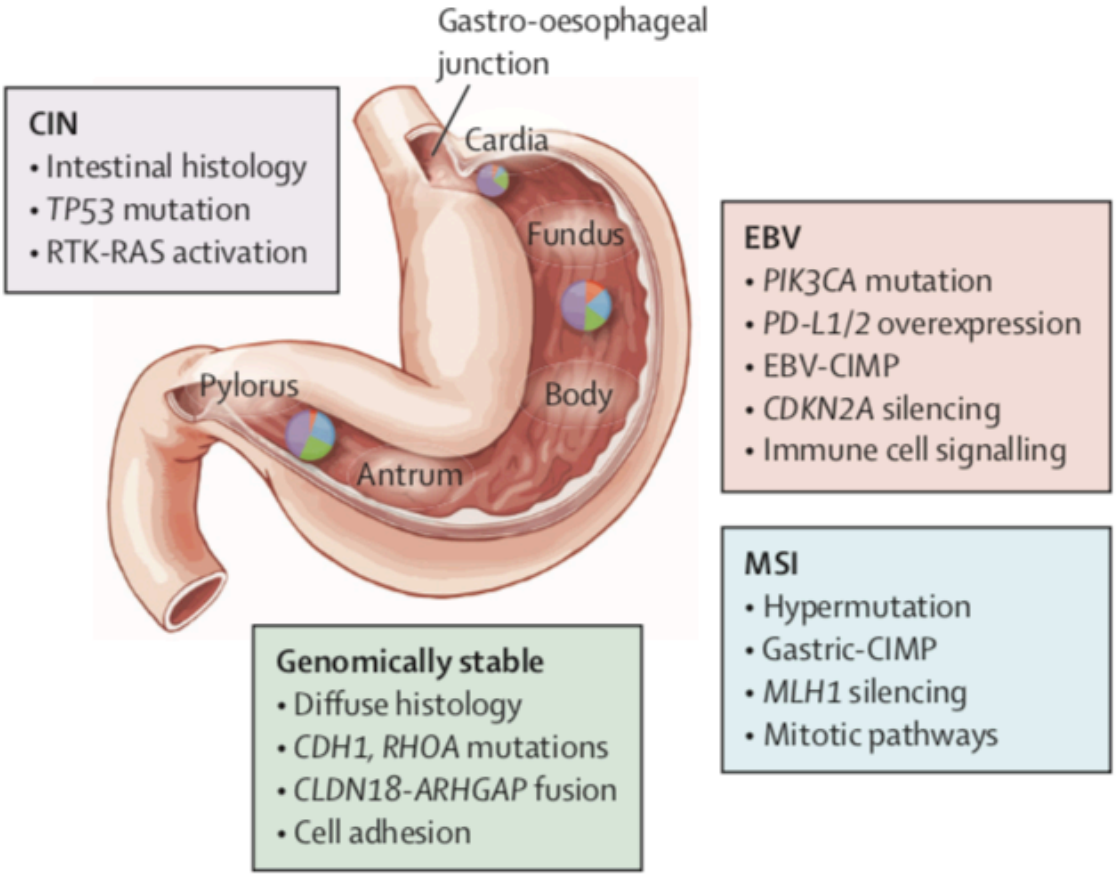

Figure 1.2 Molecular characterisation of gastric carcinomas subtypes
CIN=chromosomally unstable tumours. EBV=Epstein-Barr virus-infected tumours. CIMP=CpG island methylation phenotype. MSI=microsatellite unstable tumours. Figure reproduced from (The Cancer Genome Atlas Research et al., 2014).

1.1.4 Therapy

1.1.4.1 Staging

The most widely used method for staging is the American Joint Committee on Cancer (AJCC) TNM staging. The latest 8th staging system was released in 2018. This staging system is based on tumour invasion depth (T), lymph node metastasis (N), and with or without distant metastasis (M). This staging system requires at least 15 lymph nodes for accurate staging (Table 1.1).

The 8th edition of the TNM staging system for gastric cancer changed the single staging system to three staging systems, including clinical staging (cTNM), pathological staging (pTNM), and pathological staging (ypTNM) after neoadjuvant therapy. This new classification system solves the shortcomings of patients who cannot be well stratified in a single stage and guided for treatment. Based on previous data, Li et al. has verified the rationality of ypTNM staging. It is the largest study on the prognostic value of ypTNM staging at present (Li et al., 2018b), and proposes that the new classification of ypTNM staging may be helpful for predicting patient prognosis (Table 1.2).

Table 1.1 TNM classification of carcinoma of the stomach

T	Primary Tumor
Tx	Primary tumor cannot be assessed
T0	No evidence of primary tumor
Tis	Carcinoma *in situ*: intraepithelial tumor without invasion of the lamina propria, high-grade dysplasia
T1	Tumor invades the lamina propria, muscularis mucosae, or submucosa
T1a	Tumor invades the lamina propria or muscularis mucosae
T1b	Tumor invades the submucosa
T2	Tumor invades the muscularis propria*
T3	Tumor penetrates the subserosal connective tissue without invasion of the visceral peritoneum or adjacent structures**, ***
T4	Tumor invades the serosa (visceral peritoneum) or adjacent structures**, ***
T4a	Tumor invades the serosa (visceral peritoneum)
T4b	Tumor invades adjacent structures/organs

*A tumor may penetrate the muscularis propria with extension into the gastrocolic or gastrohepatic ligaments, or into the greater or lesser omentum, without perforation of the visceral peritoneum covering these structures. In this case, the tumor is classified as T3. If there is perforation of the visceral peritoneum covering the gastric ligaments or the omentum, the tumor should be classified as T4.

**The adjacent structures of the stomach include the spleen, transverse colon, liver, diaphragm, pancreas, abdominal wall, adrenal gland, kidney, small intestine, and retroperitoneum.

***Intramural extension to the duodenum or esophagus is not considered invasion of an adjacent structure, but is classified using the depth of the greatest invasion in any of these sites.

N	Regional Lymph Nodes
Nx	Regional lymph node(s) cannot be assessed
N0	No regional lymph node metastasis
N1	Metastasis in one or two regional lymph nodes
N2	Metastasis in three to six regional lymph nodes
N3	Metastasis in seven or more regional lymph nodes
N3a	Metastasis in seven to 15 regional lymph nodes
N3b	Metastasis in 16 or more regional lymph nodes

M	Distant Metastasis
M0	No distant metastasis
M1	Distant metastasis

Reproduced from NCCN Guidelines Version 4.2019 Gastric Cancer

Table 1.2 AJCC cTNM 8th

	N0	N1	N2	N3
T1	I	IIA	IIA	IIA
T2	I	IIA	IIA	IIA
T3	IIB	III	III	III
T4a	IIB	III	III	III
T4b	IVA	IVA	IVA	IVA
M1	IVB	IVB	IVB	IVB

AJCC pTNM 8th

	N0	N1	N2	N3a	N3b
T1	IA	IB	IIA	IIB	IIIB
T2	IB	IIA	IIB	IIIA	IIIB
T3	IIA	IIB	IIIA	IIIB	IIIC
T4a	IIB	IIIA	IIIA	IIIB	IIIC
T4b	IIIA	IIIB	IIIB	IIIC	IIIC

AJCC ypTNM 8th

	N0	N1	N2	N3
T1	I	I	II	II
T2	I	II	II	III
T3	II	II	III	III
T4a	II	III	III	III
T4b	III	III	III	III
M1	IV	IV	IV	IV

Reproduced from NCCN Guidelines Version 4.2019 Gastric Cancer

1.1.4.2 Surgical Treatment

1.1.4.2.1 Early gastric cancer treatment (EGC)

Early gastric cancer (EGC) is a tumour of T1 and N+/-. Treatment for early gastric cancer can be roughly divided into 3 categories (Japanese Gastric Cancer, 2020).

- T1a patients without lymph node metastasis-suitable for ESD / EMR.
- T1b patients without lymph node metastasis -suitable for D1+/D1.
- T1 patients with lymph node metastasis -suitable for D2.

1.1.4.2.1.1 Definition of EGC

Early gastric cancer is defined as infiltration of the mucosa or submucosa, with or without lymph node metastasis (T1a, N+/-). For some early gastric cancers, endoscopy (EMR / ESD) can be used as an alternative to gastrectomy (Isomoto et al., 2009), but it should be performed in a medical centre with extensive experience.

1.1.4.2.1.2 Definition of endoscopic resection

- Endoscopic mucosal resection (EMR)

The submucosal injection of normal saline lifts the lesion and surrounding mucosa and removes it with a high-frequency steel trap snare.

- Endoscopic Submucosal Dissection (ESD)

The submucosal injection of normal saline lifts the lesion and surrounding mucosa and use a high-frequency electrosurgical knife to remove the mucosa around the lesion and the submucosa from the appropriate muscle layer (Japanese Gastric Cancer, 2017).

1.1.4.2.1.3 Indications for ESD

Tumours with less likelihood of lymph node metastasis, accompanied by no lymphovascular invasion, which is suitable for endoscopic resection (Hirasawa et al., 2009).

Tumours clinically diagnosed as T1a and differentiated-type, non-ulcer, ≤2cm.

1.1.4.2.1.4 New indication for ESD

JCOG0607 (Hasuike et al., 2018) conducted long-term follow-up of two types of patients who previously belonged to the ESD expanded indications (non-ulcer > 2cm and ulcer ≤ 3cm). The results showed that the 5-yrs OS was 97.0% (95% CI, 95.0-98.2%), therefore, the original expanded indication was changed to absolute indication.

1.1.4.2.2 Localised gastric cancer treatment

1.1.4.2.2.1 Definition of gastrectomy, D1 and D2

Radical gastrectomy is the main treatment for localised gastric cancer. Gastrectomy has undergone more than 100 years development since Billroth completed the first human gastrectomy in 1881. During the whole of the last century, efforts to improve the quality of surgery, improve patient survival and reduce postoperative complications have never stopped. Gastrectomy is a procedure that removes a part of the stomach or the whole stomach which can be divided into total gastrectomy, distal gastrectomy and proximal gastrectomy. Gastrectomy for gastric cancer should remove the stomach and lymph nodes around the stomach - the perigastric lymph nodes (D1). In addition, lymph nodes around the celiac axis vessels should be removed (D2). The total number of lymph nodes removed must not be less than 15 (cited from NCCN guideline for gastric cancer Version 4.2019-December 20, 2019).

- D1 definition

D1 resection requires removal of the stomach and the greater and lesser omenta, along with removal of the lymph nodes along left and right gastric vessels, and the left and right gastroepiploic vessels.

- D2 definition

In addition to a D1 resection, the lymph nodes along the common hepatic artery and splenic artery should be removed.

There is still controversy about the range of D2 surgery between East and West surgeons. In the East, the left gastric artery (No. 7) lymph node belongs to D1, but in the West this group of lymph nodes belongs to D2. In addition, based on the JCOG0110 study (Sano et al., 2017), splenectomy is only indicated for tumours involving the greater curve of the stomach. Removal of the No. 10 group nodes is no longer a routine requirement for D2 dissection. JCOG0110 compared the effect of splenectomy on the survival of patients and found that splenectomy resulted in increased postoperative complications (30.3% vs. 16.7%, $p = 0.0004$) with no benefit to survival. Only 6 of the 254 patients in the splenectomy group had No.10 lymph node metastasis, and the metastasis rate was only 2.36% (Sano et al., 2017). Therefore, No.10 lymph node dissection is no longer included in the range of D2 lymphadenectomy. However, in the NCCN guidelines, Western surgeons still recommend clearing No. 10 lymph node.

1.1.4.2.2.2 D2 or D1

There are still many controversies concerning gastrectomy procedure between Eastern and Western surgeons. Leading Japanese, Chinese and South Korean

surgeons contend that D2 surgery is necessary for GC patients, while in contrast, Western surgeons have traditionally argued that D1 surgery is satisfactory for GC patients. In addition, Western surgeons also argued that D2 surgery can increase the complication rate of surgery and does not improve the survival of patients. Therefore, Western surgeons actively apply neoadjuvant radiotherapy and chemotherapy to their patients, in order to supplement the disadvantage of the lesser extent of the D1 procedure. However, with the results of the 15-year follow-up Dutch study (Songun et al., 2010), Western and Eastern surgeons have begun to reach a consensus. This Dutch study has shown that the D2 procedure has a lower local recurrence rate and a lower gastric cancer-related mortality rate than the D1 procedure. However, the D2 procedure has a higher complication rate than the D1 procedure. The data from high volume cancer centres in East Asia have shown that the mortality rate of operation related complications is very low, basically less than 13-17% (Wang et al., 2019c).

1.1.4.2.2.3 Laparoscopic or Open gastrectomy (LG or OG)

In 1994 Kitano from Japan completed the first laparoscopic gastrectomy. Laparoscopy has rapidly developed in the last 20 years due to its advantages such as minimally invasive approach and magnified field of view allowing clearer identification of the fine anatomy. Laparoscopic gastrectomy has become one of the standard treatment options for early gastric cancer, and its feasibility for advanced gastric cancer is also being verified.

Yu et al. (Yu et al., 2019) recently released the 3-year follow-up results of CLASS-01, which enrolled 1056 patients from 14 centres in China. Among patients with locally advanced distal gastric cancer, the 3-year Disease Free Survival (DFS) rate was 76.5% in the laparoscopic group compared with 77.8% in the open group; the 3-year Overall Survival (OS) rate was 83.1% and 85.2% (HR 1.19; 95% CI, 0.87 to 1.64; $p = 0.28$), respectively. Recurrence rates were comparable in both groups (HR

1.15; 95% CI, 0.86 to 1.54; p = 0.35). This study provided the preliminary confirmation that the long-term efficacy of laparoscopic gastrectomy for locally advanced distal gastric cancer is not inferior to open gastrectomy, and the previous safety results have also been published (Hu et al., 2016). According to the completion rate of D2 lymphadenectomy (99.4% versus 99.6%; p = 0.845), postoperative complication rate (95% CI, -1.9 to 6.6; p = 0.285), and postoperative mortality (95% CI, -0.4 to 1.4; p = 0.289), the results were similar in both groups.

During the same period, the Korean small sample study COACT 1001 (Park et al., 2018) also released their results. 5-year OS in the study was 85.1% compared with 84.1%, respectively (laparoscopic assisted surgery group and open surgery group of patients with locally advanced distal gastric cancer). The 5-year DFS was 74.5% and 78.7%, respectively. Again, laparoscopic surgery showed the same long-term effects as open surgery. The results of the JCOG1401 (Katai et al., 2019) study in Japan confirmed the safety of laparoscopic assisted total or proximal gastrectomy in patients with clinical stage I.

The results of the trials above herald the prospect of expanding indications for laparoscopic treatment of gastric cancer. It became essential to standardise the technology and processes of laparoscopic surgery in order to roll out the service from specialist trial centres to more general hospitals. Therefore, in 2018, China also released the Expert Consensus on Gastrointestinal Reconstruction and Surgical Operation Guideline for Complete Laparoscopic Stomach Cancer Surgery (2018 Edition) in order to guide clinical surgeons to standardise the development of full laparoscopic gastrectomy.

1.1.4.2.2.4 Laparoscopic gastrectomy after neoadjuvant chemotherapy

Laparoscopic gastrectomy has become the mainstream surgical method for gastric cancer surgery in many countries. Neoadjuvant chemotherapy may cause changes in

the tissue which can alter the ease with which surgery can be performed. Whether laparoscopic surgery can achieve the same effect and safety rates after neoadjuvant chemotherapy is still controversial. Li et.al (Li et al., 2019b) initiated a randomised trial to address this question. The study enrolled 96 gastric cancer patients with cT2-4aN+M0 GC. The results showed that compared with the open group, the laparoscopic group had a reduced rate of postoperative complications (20% versus 46%; $p = 0.007$). This is the first study in the world to confirm that laparoscopic gastrectomy is as safe as open gastrectomy after neoadjuvant chemotherapy. Surprisingly, laparoscopic surgery reduces the rate of postoperative complications. However, the implications surrounding long-term oncological effects are yet to be reported.

1.1.4.3 Neoadjuvant treatment

Neoadjuvant (or perioperative) chemotherapy is administered as an approach for "downstaging and downsizing" a locally advanced tumour before curative resection and dealing with potential metastatic cells thereafter. Furthermore, for GC patients at a high risk of developing distant metastases, neoadjuvant chemotherapy helps reduce the risk by eliminating potential cancer cells and informing sensitive therapeutic regimens for postoperative adjuvant chemotherapy.

However, there has been no consensus worldwide so far. 3Neoadjuvant chemotherapy is also frequently applied in patients in Europe according to studies such as the MAGIC trail (Cunningham et al., 2006) and FLOT (Al-Batran et al., 2016). Due to the tendency of Europeans and Americans to have more intraperitoneal fat than Asians, there are fewer patients who can undergo D2 radical gastrectomy, so neoadjuvant chemotherapy and chemoradiotherapy will bring extra survival benefits to these patients. However, this is more controversial in Asia. The fact that Asian patients are thinner in body shapes makes it easier for them to achieve D2

radical gastrectomy. Chinese gastric cancer guideline recommends neoadjuvant chemotherapy should be used for T3/T4 and lymph node positive patients, but in South Korea, their guidelines do not recommend the usage of neoadjuvant chemotherapy on patients. Japan has recently started recommending neoadjuvant chemotherapy for patients with large bulky lymph nodes (Japanese Gastric Cancer, 2017).

However, in comparison with surgery alone, the benefits of this approach have been demonstrated by multiple clinical trials. In the MAGIC study (Cunningham et al., 2006), 503 stage II and III gastric cancers patients were enrolled and randomly divided into surgery group (n=253) and perioperative chemotherapy group (n=250) with 3 cycles of the epirubicin, cisplatin, and fluorouracil (ECF) regimen. The 5-year OS rate was 23% (95% CI, 16.6 to 29.4) compared with 36% (95% CI, 29.5 to 43). The OS (hazard ratio (HR) 0.75; 95% CI, 0.60 to 0.93; $p = 0.009$) and progression free survival (PFS) (HR 0.66; 95% CI, 0.53 to 0.81; $p < 0.001$) were better in the perioperative chemotherapy group than in the surgery group. The conclusions of the study show that perioperative ECF can effectively reduce tumour size, reduce tumour staging, and prolong progression-free survival and overall survival of patients, and thereby the position of neoadjuvant chemotherapy in the treatment of gastric cancer has been established and written into the NCCN guidelines.

In the FNCLCC and FFCD study (Ychou et al., 2011), 224 gastric cancer patients were assigned to neoadjuvant and adjuvant chemotherapy (n = 113) with cisplatin plus fluorouracil or surgery alone (n = 111). It also proved that perioperative chemotherapy has better OS (OS rate 38% vs 24%; HR 0.69; 95% CI, 0.50 to 0.95; $p < 0.02$) and DFS (DFS rate 34% vs 19%; HR 0.65; 95% CI, 0.48 to 0.89; $p < 0.003$). At the same time, subgroup analyses implied that gastroesophageal junction (GEJ) tumour patients benefited from this therapy. However, as some patients in the above studies did not achieve D2 radical gastrectomy, the current standard treatment for

gastric cancer is postoperative chemotherapy. Thus, these studies can only preliminarily highlight the important role of neoadjuvant chemotherapy in gastric cancer, but they cannot change clinical practice worldwide.

In the FLOT4 (Al-Batran et al., 2016) study, there were 716 patients with T2 + and N + GC at 28 centres in Germany, randomly assigned 1:1 to the ECF (n = 360) and FLOT (Fluorouracil, Leucovorin, Oxaliplatin and Docetaxel) (n = 356) groups. The OS in the ECF group (35 months) was found to be worse than that in the FLOT group (50 months, HR 0.77; 95% CI, 0.63 to 0.94; $p = 0.012$). 3-year OS rate was 48% in the ECF group in comparison with 56% in the FLOT group. PFS was also elevated in the FLOT group (30 months) compared with the ECF (18 months) group (HR 0.75; 95% CI, 0.62 to 0.91; $p = 0.004$). Perioperative study to compare ECF and FLOT regimens in the treatment of such patients and subsequently, the FLOT regimen demonstrated sufficient superiority, replacing the ECF regimen in the NCCN guidelines. FLOT regimen showed sufficient superiority and replaced the ECF regimen in the NCCN guidelines. However, because the FLOT regimen is a three-drug combination, the tolerance in the Asian population still needs to be verified, the conclusions from this trial should be carefully referenced.

Furthermore, since 2012, Ji et al. have launched and completed the first phase III international randomised controlled trial of pre-operative chemotherapy (RESOLVE), which enrolled a total of 1094 patients. It was the first to confirm that neoadjuvant chemotherapy reduced the risk of tumour recurrence by 21%, which was presented at the 2019 ESMO LBA (Late-Breaking Abstract) section and named the Latest Breaking Research. The study proved, for the first time, that preoperative chemotherapy was the preferred option for locally advanced GC and this is an important study to prove preoperative chemotherapy significantly improves survival and will become the new standard of treatment. Many Chinese patients are at

advanced stage of gastric cancer when diagnosed, and it is expected that nearly 50% of patients could benefit from the neoadjuvant model.

Therefore, the above research has illustrated that perioperative chemotherapy can improve the survival of GC patients, though not every patient can benefit from perioperative chemotherapy and the relative toxicity and side effects can significantly prolong the treatment time. Issues such as the optimal operation time, the optimal number of cycles, the optimal pre- and postoperative interval, and the effect on the operation are unresolved and still require more study.

1.1.4.4 Adjuvant treatment

The ACTS-GC study makes S-1 (Tegafur/gimeracil/oteracil) the standard adjuvant chemotherapy regimen for patients with stage II/III gastric cancer (Sakuramoto et al., 2007). These studies have shown that the patients have benefited significantly from single-agent S-1 chemotherapy. Since then, how to stratify and target treatment of patients has become a hotspot for clinical attention. Furthermore, the CLASSIC trial (Bang et al., 2012) also indicated improved OS and DFS (postoperative combined capecitabine and oxaliplatin, XELOX/CapOX). The JACCRO GC-07 (Yoshida et al., 2019) study included patients who underwent D2 radical gastrectomy for pathological stage III GC and compared the effectiveness of S-1 combined with docetaxel versus S-1 alone. The results show that S-1 combined with docetaxel can significantly improve the 3-year DFS rate (65.9% versus 49.6%, HR 0.632, p = 0.0007). Therefore, S-1 combined with docetaxel protocol is now recommended as the new standard for adjuvant chemotherapy after D2 radical surgery in patients with stage III gastric cancer (Yoshida et al., 2019). In addition, the results of the JCOG1104 study (Yoshikawa et al., 2019), which included patients with pathological stage II GC, were updated. These results have shown that the 3-year relapse-free survival (RFS) of the S-1 treatment in the 8-cycle and 4-cycle groups

was 93.1% and 89.8% (HR 1.84), with OS rates of 96.1% and 92.6% (HR 3.34), respectively. The non-inferiority of using 4-cycle S-1 has not been demonstrated. Considering the efficacy, S-1 adjuvant chemotherapy is recommended to continue for one year for patients with pathological stage II gastric cancer.

1.1.4.5 Targeted treatment

Screening for effective chemotherapy and drug-resistant populations can save patients from unnecessary pain caused by chemotherapy and reduce the burden on national health economics. Cheong et al. (Cheong et al., 2018) did a post hoc analysis for the CLASSIC trial (Bang et al., 2012) to develop gene panels of granzyme B (GZMB), Tryptophanyl-tRNA synthetase (WARS), secreted frizzled-related protein 4 (SFRP4), and caudal type homeobox 1 (CDX1) in order to predict who would benefit from adjuvant chemotherapy. The study showed that, based on this panel, patients could be divided into high-risk group (40%, 250/625), intermediate-risk group (47%, 296/625), and low-risk group (13%, 79/625). The 5-year OS rate of the three groups of patients were 66.0%, 74.8%, and 83.2% (p = 0.012). In addition, researchers used this panel to divide patients into adjuvant chemotherapy benefit group and adjuvant chemotherapy no benefit group. In the adjuvant chemotherapy benefit group, the 5-year OS rate was 80% and 64.5% in the subgroup receiving adjuvant therapy compared with the subgroup treated with surgery alone (HR 0.47, p = 0.0015). However, in the adjuvant chemotherapy non-benefit group, the 5-year OS rates of the two subgroups were 72.9% and 72.5%, respectively (p = 0.71) (Cheong et al., 2018). However, this panel was based on retrospective research data and needs to be verified in a prospective study.

In 2010, the ToGA study (Bang et al., 2010) became a milestone for targeted treatment of gastric cancer, and trastuzumab became the first-line treatment for patients with HER-2 positive metastatic gastric cancer. Later, REGARD (Fuchs et

al., 2014) and RAINBOW (Wilke et al., 2014) studies supported the use of ramucirumab combined with paclitaxel as a standard drug for second-line treatment in patients with metastatic gastric cancer. Additionally, a study by Li et al. supported the use of apatinib as a standard drug for third-line treatment of metastatic gastric cancer (Li et al., 2016a). Despite this research in the field of targeted therapy has also faced some difficulties. The failure of EXPAND (Eatock et al., 2013), REAL3 (Waddell et al., 2013) and AVAGAST (Van Cutsem et al., 2012) trials has made scholars once again recognise the importance of relevant molecular markers and the selection of indication populations.

1.1.4.5.1 HER-2 inhibitor

In 2018 the findings of the JACOB study (Tabernero et al., 2018) were published. The study included patients with metastatic gastric cancer with strong positive HER-2 expression. The results showed that the OS in pertuzumab combined with trastuzumab and chemotherapy group was 17.5 months whereas the OS of pertuzumab plus chemotherapy group was 14.2 months, and there was no statistically significant difference between the two groups ($p = 0.057$). Although pertuzumab has been successful in breast cancer, HER-2 expression in gastric cancer is heterogeneous, with weak expression and incomplete membrane staining. The pertuzumab group did not show significant survival benefit.

1.1.4.5.2 Poly-ADP ribose polymerase (PARP) inhibitor

The GOLD study included patients with metastatic gastric cancer who had progressed after or during first-line chemotherapy, compared with treatment with olaparib (PARP inhibitor) combined with paclitaxel versus paclitaxel monotherapy. In the entire population, the OS of the olaparib group was 8.8 months, and the paclitaxel only group was 6.9 months (HR 0.79, $p = 0.026$). In the ataxia

telangiectasia mutated protein (ATM)-negative population, the OS of the olaparib group and the paclitaxel group were 12.0 months and 10.0 months (HR 0.73, p = 0.25). The olaparib group did not show survival benefits (Bang et al., 2017). Olaparib has shown efficacy in a phase II study (Study 39) (Bang et al., 2015), especially in ATM-negative patients. The different doses of olaparib in both GOLD and Study 39 (namely 100mg and 300mg) could possibly be the reason. Other studies of PARP inhibitors in other tumour types showed that BRCA (BReast CAncer) mutation or gene mutations involved in homologous recombination repair can improve the efficacy after using the PRAP inhibitor, but these relationships are not clear in the GOLD study and need to be further analysed.

1.1.4.6 Immunotherapy treatment

Unlike other treatments, immunotherapy aims to fight tumours by activating the body's own immune system. It has become the fifth important tumour treatment method. The American immunologist James P Alison and the Japanese immunologist Tasuku Honjo were awarded the 2018 Nobel Prize for Physiology or Medicine in recognition of their pioneering contribution in discovering the braking mechanisms of human immune regulation. Gastric cancer research is relatively lagging due to strong heterogeneity, insufficient mutation load in tumours, and unclear pathogenic mutations. In 2018, due to improvements in the results in gastric cancer immunotherapy, the food and drug administration (FDA) approved pembrolizumab and nivolumab for the treatment of gastric cancer.

1.1.4.6.1 Pembrolizumab

In the KEYNOTE-059 study, Cohort 1 included gastric cancer patients with second-line or multi-line treatment. The safety and efficacy of 200mg of pembrolizumab was evaluated (Fuchs et al., 2018). The results showed an overall response rate (ORR)

of 11.6%. Patients were stratified according to the expression level of PD-L1. The ORR of the PD-L1 high expression group was 15.5% and the low expression group was 6.4%. Compared with third-line apatinib treatment (Ruan et al., 2017), pembrolizumab increased ORR (Li et al., 2016a), but whether the OS and PFS are prolonged remains to be verified. At the same time, phase III studies related to this study have also been initiated (NCT02872116, NCT02743494). The results of KEYNOTE-061 showed that the comparison of pembrolizumab with the standard second-line paclitaxel treatment has not indicated that pembrolizumab can achieve a significant survival benefit. The OS of the two groups was 9.1 months and 8.3 months (HR 0.82, $p = 0.4211$). The PFS was 1.5 months and 4.1 months (HR 1.27), respectively, and the safety of the pembrolizumab group was significantly better than that of the paclitaxel group (Shitara et al., 2018). In addition, subgroup analysis showed that patients with high PD-L1 expression or microsatellite instability high (MSI-H) may benefit from pembrolizumab treatment.

1.1.4.6.2 Nivolumab

The CheckMate-032 study included patients after second-line treatment of metastatic gastroesophageal junction cancer. Patients were assigned into three groups comparing nivolumab 3mg/kg, nivolumab 1mg/kg combined with ipilimumab 3mg/kg and nivolumab 3mg/kg combined with ipilimumab 1mg/kg. The results showed that the ORR of the three groups were 12%, 24%, and 8%. The 1-year PFS rates were 8%, 17%, and 10%, and the 1-year OS rates were 39%, 35%, and 24%, respectively. Grade 3-4 adverse events were 17%, 47% and 27%. In addition, ORR was not related to PD-L1 expression (Janjigian et al., 2018). Although nivolumab 1mg/kg combined with ipilimumab 3mg/kg showed good ORR and survival benefit, the adverse events of grade 3-4 toxicity were as high as 47%, which limited the clinical practical application of this regimen.

At present, other checkpoint inhibitors, tumour vaccines, and adoptive immune cell therapies have all shown good prospects for clinical application. Combining targeted therapy and chemotherapy to improve efficacy may be the future direction.

1.1.4.7 Future perspectives

GC is a serious fatal disease. In the past, due to the fact that gastric cancer is not a major tumour burden in Western countries, there has been relatively little research focusing on GC. However, in recent years, with the continuous and in-depth studies from Chinese and other oriental scholars research has advanced and is ongoing. Similarly, as discussed in previous sections, advances have been made in standard treatments and management of gastric cancer patients. Despite this gastric cancer still remains a substantial burden worldwide. As such research into novel biomarkers of new potential therapeutic targets, as well as gaining a fuller understanding of the biological mechanisms underlying the disease and the development of therapy resistance are essential.

1.1.5 Limitations and future therapy design

Whilst progress has been made in the optimisation and combination of therapies available for gastric cancer patients there remains an urgent need to further advance this field due to the high mortality and incidence rates associated with this cancer. Further work based on understanding the molecular biology and interactions involved in this cancer type as well as the identification of novel therapeutic targets are needed to improve diagnostic, detection and therapeutic options for patients as well as combating therapy resistance.

1.2 Sphingosine 1 Phosphate

The Ceramide-Sphingosine-Sphingiosine-1-phosphate (S1P) rheostat was first proposed in 1996 (Cuvillier et al., 1996). In this rheostat (Figure 1.3), Ceramide and sphingosine promote cellular apoptosis and S1P leads to cell growth.

S1P is the key molecule in the Ceramide-Sphingosine-S1P rheostat whose functions were recognised approximately 30 years ago (Zhang et al., 1991). S1P is involved in wide range of biological function (Sukocheva, 2018), including regulation of cellular proliferation (Zhang et al., 2015), survival (Datta et al., 2014), migration (Zhao et al., 2015), invasion (Li et al., 2016b) cell differentiation (Romani et al., 2018), angiogenesis (Dai et al., 2017), immune cell tracking (Liao et al., 2018) and chemoresistance (Matula et al., 2015).

The Ceramide-Sphingosine-S1P rheostat involves several important enzymes. Sphingosine is generated from the deacylation of ceramide, which is also acylated to ceramide by ceramide synthase (Ohta et al., 1994). Sphingosine kinases (SphKs), present in two isoforms, namely Sphingosine Kinase 1 and Sphingosine Kinase 2 (SphK1 and SphK2), can catalyse the phosphorylation of sphingosine to synthesise S1P (Foss et al., 2009) which is dephosphorylated by S1P phosphatases (SGPPs) to sphingosine. S1P also can be secreted from the cell by ATP-binding cassette A1 (ABCA1) (Sato et al., 2007), ATP-binding cassette C1 (ABCC1) (Mitra et al., 2006), ATP-binding cassette G2 (ABCG2) (Takabe et al., 2010) and, subsequently, can directly bind to the Sphingosine-1-phosphate receptor 1-5 (S1PR1-5) G protein-coupled receptors on the cell surface in paracrine or autocrine manners, a process termed ‘inside-out’ signalling (Takabe et al., 2008). Furthermore, S1P also can be degraded into ethanolamine-1-phosphate and C16 fatty aldehyde through S1P lyase (SGPL1) which is the only exit in the entire metabolic pathway (Pyne and Pyne, 2010, Peest et al., 2008).

Hence, the S1P rheostat and S1P signalling have key functions and disruption of this can lead to various pathological states including cancer (Gao et al., 2017) Similarly, alterations in key enzymes involved in regulating this rheostat can tip the balance between apoptosis and proliferation, promoting cell death or survival and having key implications in cancer development and progression. A key interest of the current study was the implications of SphK1 in gastric cancer. The following sections outline the related progress in mechanistic and clinical research surrounding SphK1, especially, focusing on the role of SphK1 in tumour growth and drug resistance.

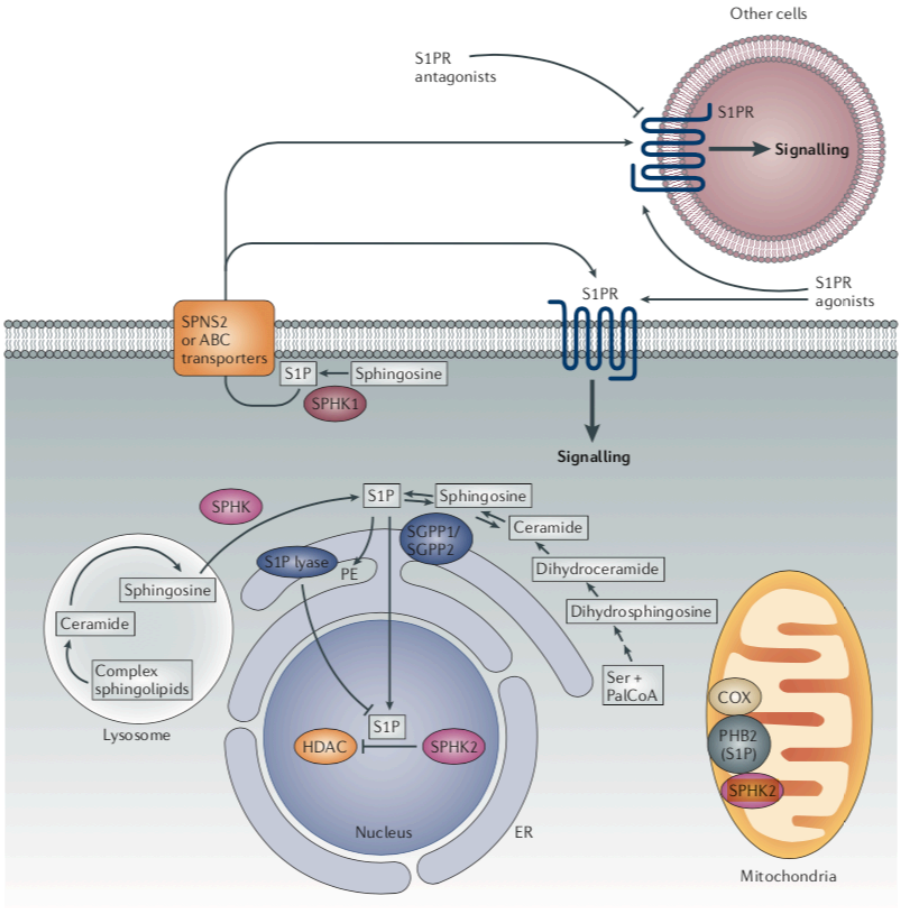

Figure 1.3 Ceramide-Sphingosine-S1P rheostat
PHB2, Prohibitin 2; COX, Cytochrome c oxidase ; HDACs, Histone deacetylases ; ABC, ATP-binding cassette; PalCoA, palmitoyl-CoA; PE, phosphoethanol-amine; SGPP1, S1P phosphatase 1. Figure reproduced from (Kunkel et al., 2013)

1.3 Sphingosine Kinases (SphKs)

There are two Sphingosine kinases, SphK1 (Kohama et al., 1998) and SphK2 (Liu et al., 2000), which have been identified and characterised in mammalian cells. Each isoform has a differing cellular location with SphK1 predominantly being located in the cytoplasm and SphK2 predominantly located in the nucleus, potentially implicating differential functions of each isoforms, though there exists the potential for both isoforms to move to other subcellular compartments (Taha et al., 2006, Alemany et al., 2007, Pyne et al., 2009). In recent years, there have already been many orally biological drugs targeting SphK1 and they have also been proved to have both anti-tumour (Kreitzburg et al., 2018) and anti-inflammatory (Nagahashi et al., 2018b) activity *in vivo* and *in vitro*. Thus, as for the treatment of cancer patients, SphK1 was regarded as a potential therapeutic target. In the following section, I will briefly introduce the role of SphK1 in cancer and cancer treatment.

1.3.1 Structural Characteristics of SphKs

As discussed above, isoforms of SphKs exist. Furthermore, through molecular identification of SphKs, a 49 kDa protein was purified from rat kidney (Olivera et al., 1998). Subsequently, two variants, namely SphK1a (382 amino acids) and SphK1b (388 amino acids) were cloned and characterised (Kohama et al., 1998).

In humans, SphK1 is located on chromosome 17q25.2 and SphK2 lies on 19q13.2 which are produced from distinct genes. Human SphK1 is 384 amino acids is size and SphK2 is 618 amino acids in size, with the two isoforms sharing 80% similarity and 45% of their sequence identities (Liu et al., 2000). There are five highly conserved regions, termed C1 to C5, existing in all known eukaryotic SphKs, and these regions are believed to be essential for ATP binding and catalysis (Leclercq and Pitson, 2006). A key report by Wang et al (Wang et al., 2013) described the

crystal structure of SphK1and provided a new direction to design SphK1 inhibitors, which has aided in the development of more effective and specific inhibitors. The crystal structure of SphK1 contained 9-364 residues and was composed of a 2 domain architecture with 9 α helices, 17 β strands and α 310-helix. N-terminal domain (NTD) residing 91-50, 357-364 and including C1-C3 domains was α/β folded and contains 6α helices and 6β chains. The C-terminal domain (CTD) residing 151-356 and containing the C4 and C5 domains contained 11 β-chains and 4 helices. Analysis of protein sequence motifs and structural classification showed that SphKs were classified to the phosphofructokinase (PFK)-like superfamily and shares the same protein folds with ceramide kinase (Wang et al., 2013) (Figure 1.4).

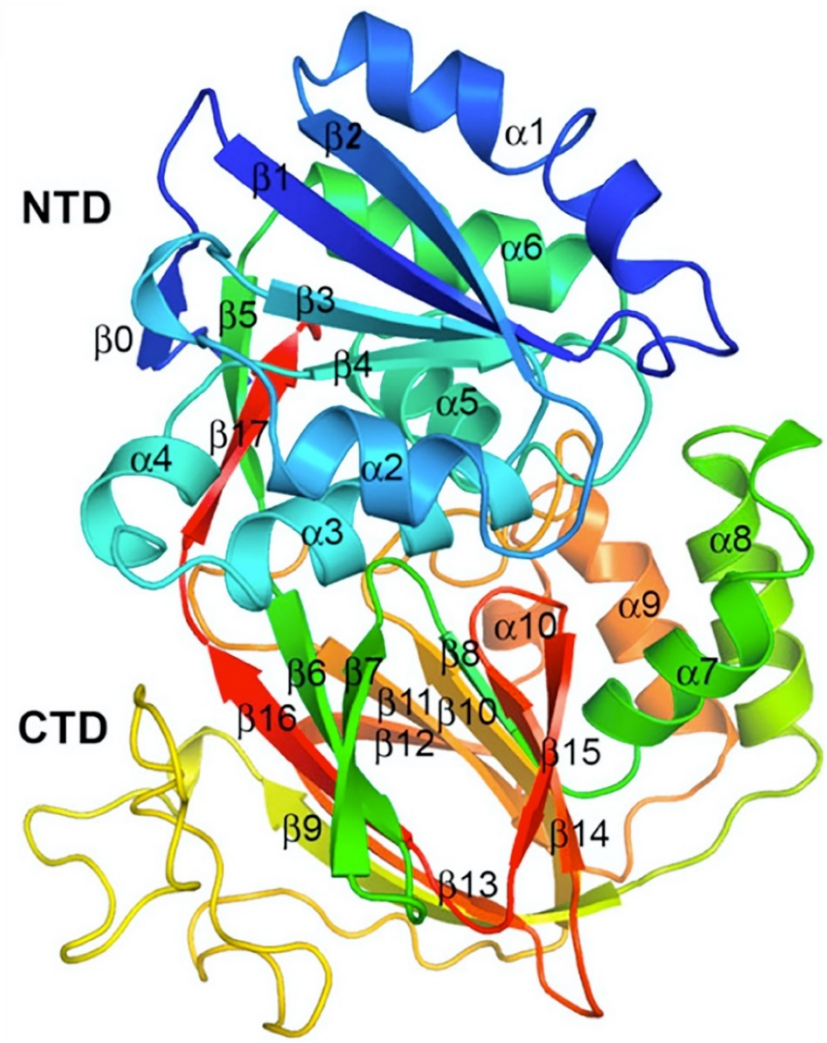

Figure 1.4 Structure of SphK1. Figure reproduced from (Wang et al., 2013), N-terminal domain (NTD), C-terminal domain (CTD).

1.3.2 Implication of SphK1 in Cancer Progression and PrognosisIn light of the role of SphK1 in generation of S1P and its potential to contribute to cancer many studies have focused on exploring the expression of SphK1 in human cancer. These studies have collectively demonstrated that the expression levels of SphK1 are frequently altered in many different types of human cancers further supporting its links to cancer and potential as either a therapeutic target or biomarker (Li et al., 2008, Kawamori et al., 2006). At the same time, more evidences indicate that high expression SphK1 is correlated with poor outcome for cancer patients (Pyne et al., 2012b, Zhang et al., 2014b).

1.3.2.1 Clinical relevance

1.3.2.1.1 Gastric Cancer (GC)

Li et al. (Li et al., 2009) reported that the mRNA and protein levels of SphK1 were higher in gastric cancer cell lines than in normal gastric epithelial cells. Compared with paired adjacent normal tissues, SphK1 protein levels were upregulated in GC tissue. In this study, in total 115 of 175 GC patients (65.7%) showed high expression of SphK1 protein, while the expression of SphK1 in adjacent normal gastric tissues was undetectable. Furthermore, significant differences in SphK1 expression levels were found in patients at different clinical stages ($p = 0.003$), T stage ($p = 0.035$), M stage ($p = 0.020$) and venous invasion ($p = 0.037$). In addition, patient with higher SphK1 expression had shorter OS compared with those with lower SphK1 expression ($p = 0.0019$), and observed a cumulative 5 year survival rates of patients with high SphK1 expression of 23.85% (95% CI 0.1585-0.3185) in upregulation group compared with 49.66% (95% CI, 0.2707-0.5225) in the downregulation group, (Li et al., 2009). Subsequently, in a more recent study, Wang et al. analysed the gene expression data from the Gene Expression Omnibus (GEO) dataset. In this study 24

common differentially expressed genes were screened, in which SphK1 was found to have a higher fold change in GC tissues and peripheral blood. The expression of SphK1 in tumour tissue was higher than that in normal tissue in one dataset. In addition, S1P produced by SphK1 was more prominent in tumour patients' serum than in normal patients' serum in another dataset (Wang et al., 2018b).

1.3.2.1.2 Colon Rectal Cancer (CRC)

In CRC, Kawamori et al., (Kawamori et al., 2009) reports that SphK1 was strongly stained in 89% (42/47) of colon cancer tissues compared with normal tissues and adenoma. At the same time, the expression of SphK1 in colon cancer with metastasis was higher than that in colon cancer without metastasis. Furthermore, it was noted that mouse model had a higher levels of S1P in the blood with colon cancer compared to controls, without colon cancer. Additionally, the SphK1-/- mouse model receiving azoxymethane (AOM) had significantly reduced incidence of colon cancer, indicating the SphK1/S1P pathway could be a key contributor to colon cancer progression and a potential target for cancer therapy (Kawamori et al., 2009). Another recent study showed that 92.4% (280/303) of patients showed SphK1 positive expression in CRC tissues. About 206 died (67.99%, 206/303) and of these patients 193 (93.7%) were SphK1 positive patients. Meanwhile, the expression of SphK1 was related to TNM stage ($p = 0.042$), with SphK1 expression shown to be positively related to mortality (Tan et al., 2014). Furuya et al., (Furuya et al., 2017) reported that 96% (27 / 28) of mice formed tumours in wild type group, while in the SphK1 knockout group, only 59% (17 / 28) of mice formed tumours ($p < 0.001$) in the study of AOM induced colon cancer formation in mice. This result indicated that SphK1 played an important role in tumour growth. Furthermore, the staining intensity of SphK1 was higher in CRC tissue compared with adjacent normal tissue ($p = 0.02$).

1.3.2.1.3 Lung Cancer (LC)

In LC, one study (Yang et al., 2019) indicated that the mRNA and protein levels of SphK1 in Non-small Cell Lung Cancer (NSCLC) tissues were significantly increased compared with normal paired tissue and it was noted that the expression of SphK1 in late stage was significantly higher than that in early stage. Wang et al. (Wang et al., 2019b) study included 1926 NSCLC patients, 720 lung adenocarcinoma (Ade) patient and 524 lung squamous cell carcinoma (SCC) patients who were followed up 20 years ago from KM plotter database. It showed that high expression of SphK1 had a better OS compared with low expression of SphK1 in NSCLC ($p < 0.0001$) and Ade patients ($p = 0.014$), but not in SCC patients ($p < 0.094$). At the same time, evaluating the prognostic value of SphK1with different clinical parameters, it was found that SphK1 was a risk factor in stage I and III patients, but a protective factor in stage II patients. Furthermore, it was also a risk factor in patients receiving chemotherapy or radiotherapy. Another recent study (Gachechiladze et al., 2019) showed that SphK1 was stronger stained in cancerous tissue than surrounding stroma ($p < 0.0001$). Interestingly, overexpression of SphK1 was related to short OS in the postoperative chemotherapy plus in the surgery group, while not in surgery alone group ($p = 0.035$). The same trend has been found in DFS analysis, but with no statistical significance ($p = 0.09$). From this study, it was found that high expression of SphK1 was related to the poor prognosis in the chemotherapy plus surgery group, but not in surgery alone group. It suggested a role of SphK1 in chemotherapy resistance and it could be a good biomarker. However, due to the retrospective study and limitation of sample size, more evidence was needed to prove the hypothesis.

1.3.2.1.4 Breast Cancer (BC)

In BC, Zhu et al. (Zhu et al., 2017) reported that Sphk1 was upregulated in BC patients ($p < 0.0001$) in which 59.4% of patients showed enhanced mRNA expression levels of SphK1 in BC tissue compared to paired normal tissue and the expression of SphK1 in 40.6% patients was downregulated. Immunochemical analysis found that the patients with SphK1 strong expression, moderate expression and weak expression were 32%, 46.7% and 21.3% respectively in 122 BC patients, but no SphK1 expression was noted in 15 normal tissues. Overexpression SphK1 was significantly related to the lymph nodes metastases, positive lymph nodes number and distant metastases. Multivariate analysis showed that SphK1 was an independent prognosis factor of OS (HR 0.196; 95% CI 0.058-0.655; $p = 0.0081$). Another study (Acharya et al., 2019) reported that the expression of SphK1 was related to poor relapse-free survival (RFS) in triple negative breast cancer (TNBC) patients. The transcript levels of SphK1 were highly expressed in TNBC-derived cell lines. These results indicate that SphK1 may play an important role in BC and might serve as a predictor. Acharya et al. (Acharya et al., 2019) reported that the mRNA expression of SphK1 in TNBC was higher than that in paired normal tissue through analysing the GEO data (GSE27447). At the same time, using TCGA data to verify the hypothesis, the expression of SphK1 in TNBC was significantly higher than that in normal tissue. Furthermore, the high expression of SphK1 was related to the poor RFS. At the same time, high expression of SphK1 was found at both mRNA and protein levels in TNBC derived cell lines.

1.3.2.1.5 Other types of Cancer

Li et al. (Li et al., 2008) reported that compared with adjacent non-cancerous brain tissue, both mRNA and protein levels of SphK1 were increased in primary astrocytomas. The high SphK1 expression was found in astrocytoma tissues (41.2%,

100 /243). The OS of patients who had high SphK1 protein levels was reduced (18 months) compared to patients who had low SphK1 protein levels (40 months). Hence this work highlights that the upregulation of SphK1 may be an independent prognostic indicator of survival for astrocytoma patients (Li et al., 2008). A study from Li et al. (Li et al., 2016c) showed that the protein expression level of SphK1 was significantly elevated in pancreatic cancer tissue compared with normal tissue. SphK1 high expression was related to OS ($p < 0.001$) of pancreatic cancer patients and different clinical parameters. Interestingly, SphK1 was associated with clinical stage not only in early stage, but also in late stage. Furthermore, SphK1 was an independent prognostic factor of pancreatic cancer patients (HR 1.395, 95% CI 1.107-1.758, $p = 0.005$). All of these indicated that SphK1 may serve as a prognosis biomarker of pancreatic cancer patients.

1.3.2 Intracellular function

SphK1 has been demonstrated to play a significant role in regulating oncogenesis, and its biological functions are associated with tipping the balance between apoptotic (Guillermet-Guibert et al., 2009) and pro-survival signalling (Akao et al., 2006, Pchejetski et al., 2005). Wang et al (Wang et al., 2018b) reported that knockdown of SphK1 inhibited cell invasion, migration, apoptosis and proliferation, leading to cell cycle arrest in vitro, as well as inhibited tumour growth in vivo. Furthermore, it was found that miR-330-3p could target the promoter region of SphK1 and inhibit the growth of tumour cells. The same effect could be observed using inhibitors (FTY720, Fingolimod). These studies indicated that SphK1 was expected to become a new molecular marker and a new therapeutic target for GC. Another study (Kohno et al., 2006) reported that mechanistically, knockdown of SphK1 reduced the expression of Cyclooxygenase-2 (COX-2) expression and prostaglandin E2 (PGE2). On the contrary, overexpression of SphK1 increased the expression of COX-2. SphK1

increase colon carcinogenesis by regulating the expression of COX 2 and PGE2. Furthermore, Knockdown of SphK1 inhibits cell growth, proliferation, migration, and invasion, and increases apoptosis. In addition, knockdown of SphK1 expression inhibited tumour growth in an animal model. Mechanistically, silencing SphK1 could inhibit the extracellular signal-regulated kinase (ERK) signalling pathway (Yang et al., 2019). It has been reported that SphK1 is the direct target of Micro-RNA-28-5p (miR-28-5p). miR-28-5p negatively regulated SphK1 and SphK1 promoted the growth, apoptosis and invasion of tumour cells *in vitro* (Chen et al., 2019). Acharya et al. (Acharya et al., 2019) also reported that high expression of SphK1 resulted in increased the lung metastasis tumour size *in vivo*. It was also found that SphK1 through regulating the downstream gene Fascin1 (FSCN1) regulated TNBC cell proliferation and apoptosis. The expression of SphK1 and FSCN1 was consistent in expression patterns in TNBC tumour. The following study showed that SphK1 regulated the NF-κB signalling pathway by regulating the transcription of FSCN1. However, the SphK1 / FSCN1 / NF-κB signalling pathway was related to the poor prognosis of TNBC patients (p = 0.003). Using small molecule targeted drugs to inhibit SphK1 and NF-κB reduced the size of primary tumour and lung metastasis (Table 1.3).

Table 1.3 Expression of SphK1 in different type of cancer

Tissue	Sample	N	Comments	OS	Refs
Gastric cancer	mRNA	4	Increased in tumour compared with paired normal tissue.	Y	(Li et al., 2009)
	Protein	175	65.7% of patients had high SphK1 in the cancer lesion compared with adjacent normal tissue. Patient survival reduced when expression of SphK1 is high		
	mRNA	3	SphK1 in tumour tissue was higher than that it is in normal tissue.	N	(Wang et al., 2018b)
	Serum	3	S1P produced by SphK1 was more expressed in tumour patients' serum than its in normal patients' serum.		
	Protein	136	44.1% of patients had high pSphK1 (Ser225) in the gastric cancer tissue compared with adjacent normal tissue. 5 year OS rate is 79.3 versus 98.3%.	Y	(Hanyu et al., 2018)
Breast cancer	mRNA	1269	SphK1 expression increased in tumour samples. Reduced DFS with high SphK1 expression in whole patient cohort.	Y	(Ruckhaberle et al., 2008)
	Protein	304	High SphK1 expression in ER+ patient tumours tissues were related to DFS.	Y	(Long et al., 2010)
	mRNA	32	59.4% patients of SphK1expression was increased and the expression of SphK1 in 40.6% patients was downregulated	Y	(Zhu et al., 2017)
	Protein	122	SphK1 was an independent prognosis factor of OS		
	mRNA	56	The mRNA expression of SphK1 in TNBC was higher than that in paired normal tissue	Y	(Acharya et al., 2019)
Lung cancer	Protein	25	5 carcinoid, 10 squamous and 10 adenocarcinoma samples. All had high SphK1 expression compared with normal matched tissue	N	(Johnson et al., 2005)
		173	Overexpression of SphK1 was related to short OS in postoperative chemotherapy plus surgery group, while not in surgery alone group (Gachechiladze et al., 2019)	Y	(Gachechiladze et al., 2019)
	mRNA	31	The levels of SphK1 in NSCLC tissues were significantly increased compared with paired normal tissue	N	(Yang et al., 2019)
	Protein				
	mRNA	3170	High expression of SphK1 had a better OS compared with low expression of SphK1 in NSCLC and Ade patients, but not in SCC patients	Y	(Wang et al., 2019b)
Colon cancer	Protein	28	(75%) of adenocarcinomas had positive SphK1 stain	N	(Kohno et al., 2006)
		47	42/47(89%) of colon cancers had higher SphK1 expression compared with normal colon tissue	N	(Kawamori et al., 2009)
		303	92.4% (280/303) patients showed SphK1 positive expression in CRC tissues.	Y	(Tan et al., 2014)

		90	The stain intensity of SphK1 was higher in CRC tissue compared with adjacent normal tissue (p = 0.02)	N	(Furuya et al., 2017)
Sacral chordoma cancer	Protein	58	69% (29/42) showed high expression of SphK1, whereas 19% (3/16) normal tissues showed a high expression of SphK1 (p = 0.001). High expression of SphK1 was related to shorter DFS.	Y	(Zhang et al., 2014a)
Uterine cervical cancer	Protein	287	High SphK1 expression was associated with different clinical parameters and OS.	Y	(Kim et al., 2015)
Pancreatic cancer	Protein	388	SphK1 was significantly elevated in pancreatic cancer tissue compared with normal tissue. SphK1 high expression was related to OS (p < 0.001)	Y	(Li et al., 2016c)
Adrenocortical carcinoma	mRNA	20	SphK1 expression was correlated with tumour size (p = 0.001) and OS (p = 0.03),	Y	(Xu et al., 2016)
	Protein	46			

Table modified from from (Pyne and Pyne, 2010)

1.3.3 Implication of SphK1 in chemotherapeutic resistance

Surgery alone is no longer considered to be the standard treatment (Cunningham and Chua, 2007). A combination of radical surgery with individualised perioperative chemotherapy (Al-Batran et al., 2016), postoperative chemotherapy (Sasako et al., 2011), radiotherapy (Lee et al., 2012b) and optimum target therapy (Bang et al., 2010) has been accepted as the optimum treatment for GC. However, there are still problems with this comprehensive treatment, that is, the cellular resistance to chemotherapy. As we can see in clinical practice, not all patients benefit from chemotherapy, therefore, identifying the patients who can benefit from chemotherapy in advance and clarifying the mechanism of chemoresistance has become the hot topic in the area of GC treatment (Cheong et al., 2018).

In recent years, research has indicated that chemotherapy resistance occurs when the expression of SphK1 is enhanced, such as, si-SphK1 significantly increased chemosensitivity of AsPC-1 and PANC-1 cells to gemcitabine. (Li et al., 2016c). Furthermore, downregulated expression of SphK1 sensitised the function of docetaxel and camptothecin in LNCaP and PC-3 cells (prostate cancer cells), respectively (Pchejetski et al., 2008). Similarly, enhanced SphK1 activity was demonstrated to result in daunorubicin resistance in leukaemia cells (Sobue et al., 2008), cisplatin resistance in lung cancer cells (Min et al., 2005) docetaxel resistance in prostate cancer cell (Alshaker et al., 2016) and oxaliplatin resistance in colon cancer cells (Nemoto et al., 2009). Furthermore, an additional study has demonstrated the ability of SphK1 to bring about the overexpression of transcript levels of the downstream transcription factor, E2F7, mediating the chemoresistance of anthracycline in head and neck squamous cell carcinomas (HNSCC) (Hazar-Rethinam et al., 2015). Another study has demonstrated the capacity of a SphK inhibitor to repair the resistance to etoposide and doxorubicin through inducing apoptosis, a finding that is identical to the observation that reduced ceramide

accumulation and sustained SphK1 activity may result in chemotherapeutic resistance (Heffernan-Stroud and Obeid, 2013). Yang et al. (Yang et al., 2014) reported that the expression of SphK1 in drug-resistant cells H69AR was significantly higher than that in H69. Downregulating the expression of SphK1 in H69AR increased the sensitivity of cells to chemotherapeutic drugs, promoted cell apoptosis and G0 / G1 phase arrest in the cell cycle. The expression of SphK1 in lung cancer chemo-resistant patients was significantly increased compared with those in sensitive patients. The expression of SphK1 was significantly related to the stage, sensitivity to chemotherapy and OS ($p < 0.05$) (Yang et al., 2014).

A relationship between bioactive sphingolipid levels and drug resistance may possibly contribute to the relationship between SphK1 and the sensitivity of cancer cells to chemotherapeutics and radiotherapeutics. Indeed, daunorubicin sensitivity, linked with low S1P and high ceramide levels, could be recovered in daunorubicin-resistant cells line if SphK1 activity was inhibited (Sobue et al., 2008). This suggested that the ceramide-sphingosine-S1P rheostat played a significant role in daunorubicin-induced cytotoxicity. Hence, taken together with the previous examples, it was clear that SphK1 played a biologically significant role in chemotherapeutic drug resistance. However, the mechanism related to SphK1 in chemotherapeutic drug resistance is still not fully understood.

Table 1.4 Chemotherapy resistance of SphK1 in different type of cancer

Drug	Cancer type	*Vivo* or *Vitro*	Comment	Ref
Docetaxel and Camptothecin	Prostate cancer (PC-3 and LNCaP)	*In vitro/ in vivo*	High expression of SphK1 inhibited sensitivity of Docetaxel/Camptothecin	(Pchejetski et al., 2005)
Camptothecin	Prostate cancer (PC-3 and LNCaP)	*In vitro*	The treatment of PC3 cells with Camptothecin induced up-regulation of the SphK1	(Akao et al., 2006)
Daunorubicin	Leukaemia	*In vitro*	Inhibited SphK increased the daunorubicin-sensitivity of daunorubicin-resistant cells.	(Sobue et al., 2008)
Docetaxel and Camptothecin	Prostate cancer (PC-3 and LNCaP)	*In vitro/ in vivo*	SphK1 inhibiter sensitized LNCaP and PC-3 cells to docetaxel and Camptothecin.	(Pchejetski et al., 2008)
Gemcitabine	Pancreatic cancer (BxPC-3 and Panc-1)	*In vitro*	A high level of SphK1was associated with a robust intrinsic pancreatic cancer cell chemoresistance toward gemcitabine.	(Guillermet-Guibert et al., 2009)
5-FU	CRC (HCT-116, RKO, SW480 and SW620)	*In vitro*	With 5-FU treatment, the siRNA-SphK1 treated HCT116 cells exhibited dose-dependent cytotoxicities.	(Tan et al., 2014)
Oxaliplatin, Cisplatin and Docetaxel	Oesophageal and gastric cancer (OE21, OE33 and AGS)	*In vitro*	Drug resistance was associated with increased SphK1 expression.	(Matula et al., 2015)
Doxorubicin	Head and neck squamous cell carcinomas (HNSCC)	*In vitro/ in vivo*	SphK1 as a potential mediator of E2F7-dependent drug resistance, due to E2F7-deficient keratinocytes were selectively sensitive to doxorubicin.	(Hazar-Rethinam et al., 2015)
Gemcitabine	Pancreatic cancer (AsPC-1 and PANC-1)	*In vitro*	si-SphK1 significantly increased chemosensitivity of AsPC-1 and PANC-1 cells to gemcitabine.	(Li et al., 2016c)
Docetaxel	Prostate cancer (PC-3)	*In vitro*	Overexpression of SphK1 cells had significant resistance to docetaxel.	(Alshaker et al., 2016)

1.3.4 Therapeutic implication of SphKs targeted therapy

As outlined in previous sections, SphK1 has been strongly linked to contributing to cancer development and progression, through its capacity to influence traits such as proliferation and chemotherapy resistance and is frequently dysregulated in numerous human cancers. Hence SphK1 has been subject to intense scientific study as a potential therapeutic target. There have already been many biological inhibitors developed targeting SphK1 and these have demonstrated both anti-tumour (French et al., 2006) and anti-inflammatory activity *in vivo* (Maines et al., 2008). Furthermore, a number have progressed to clinical trials. A number of such examples are outlined in the following section and Table 1.5.

1.3.4.1 Sonepcizumab

The anti-S1P antibody sonepcizumab targeting anti-VEGF therapy refractory renal clear cell carcinoma (RCC) patients has been evaluated in a phase II clinical trial (Pal et al., 2017). In this study, 40 RCC patients who had previously received a median of 3 therapy courses were involved in this multi-centre trial. The results showed that the OS was 21.7 months, however, it did not achieve the primary end point based on 2 months PFS (Pal et al., 2017). Although 10% of patients showed a partial response with median duration response of 5.9 months with no major toxicity, its efficacy in metastatic RCC was not impressive. However, there is need of future studies to focus on the way that systemic S1P induces tumour growth and metastasis and using lipid-specific antibodies in patients to improve the neutralisation of systematic S1P signalling.

1.3.4.2 Sphingosine Kinase 1 Inhibitor (SK1-I)

SK1-I, a sphingosine analogue and competitive inhibitor of SphK1, has been

reported to be able to decrease glioblastoma growth and proliferation in cell lines and mouse models (Kapitonov et al., 2009). Another study showed that SK1-I can induce the phosphorylation of tumour protein (TP53) at Ser15, activating the downstream pro-apoptosis B-cell lymphoma-2 (BCL-2) family. Importantly, the downregulation of Beclin-1 (BECN1) and autophagy related 5 (ATG5), the key regulators of autophagy, significantly reduced the cytotoxicity of SK1-I in cancer cells (Lima et al., 2018). A further study has indicated that SK1-I could inhibit the production of SphK1 in a mouse model, reduce the burden of primary tumours, the degree of lymph node metastasis and lung metastasis. In conjunction with this, the study also demonstrated the capacity of SK1-I to reduce peritumoral lymphatic vessel density *in vivo* (Nagahashi et al., 2012). SK1-I was a sphingosine analogue and a competitive inhibitor of SphK1, but its effect was still in preclinical research, thus more safety and effectiveness data were needed to confirm the anti-tumour function.

1.3.4.3 PF543

In addition, another specific small inhibitor, named PF-543, a powerful SphK1 selective inhibitor which has 100 times greater affinity for SphK1 over SphK2 (Schnute et al., 2012) has also been utilised as a therapeutic for targeting SphK1. However, PF543 was originally reported to be lacking in cytotoxicity in cancer cells (Wang et al., 2014c). Subsequently, PF543 has been shown to reduce S1P in cancer cells, but did not inhibit cell growth (Paugh et al., 2008). PF543 having no effect on cell growth may be due to its inability to produce ceramides that promote apoptosis (Paugh et al., 2008). However, recent studies have demonstrated PF543 efficacy where it inhibited the growth and proliferation in TNBC, CRC cells and in xenograft mouse models (Ju et al., 2016). This controversy may be due to the different tissue types. PF-543 has also be shown to induce programmed necrosis, through regulating

the expression level of lactate dehydrogenase (LDH) release, mitochondrial membrane potential collapse and mitochondrial P53-cyclophilin-D (Cyp-D) complexation. Furthermore, PF543 reduced the growth of cancer cell significantly *in vivo* (Ju et al., 2016).

1.3.4.4 Fingolimod (FTY720)

The structure of fingolimod (FTY720) was first discovered in 1995 (Cordi et al., 1995). A sphingosine analogue drug, FTY720 was approved by the American FDA for the treatment of multiple sclerosis (MS) in 2010 (Cohen et al., 2010). FTY720 can be phosphorylated by SphK2 to generate P-FTY720, functionally acting as an antagonist of S1PR1, though FTY720 and P-FTY720 possess significantly different biological functions, with FTY720 suppressing the function of SphK1 which performs related functions through the S1PR1 signalling pathway (Brinkmann et al., 2002). A subsequent study by Saddoughi et al. (Saddoughi et al., 2013) showed that FTY720 mediated protein phosphatase 2A (PP2A)/Receptor-interacting serine/threonine-protein kinase 1 (RIPK1)-dependent programmed necrosis through targeting I2PP2A/SET and inhibited lung tumour growth (Saddoughi et al., 2013). Similarly, a more recent study highlighted the efficacy of FTY720 in ovarian cancer. In their study Kreitzburg et al. (Kreitzburg et al., 2018) showed that FTY720 increased the sensitivity of tumour cells to carboplatin and tamoxifen *in vitro*. FTY720 combined with carboplatin or tamoxifen effectively inhibited tumour growth and was able to shrink tumour size *in vivo*, compared with single drug alone, effects that were mechanistically suggested to result from the capacity of FTY720 to induce the production of ceramide, enhancing apoptosis (Kreitzburg et al., 2018).

Overall, it can be concluded from the above studies that creative strategies like inducing ceramide or inhibiting S1P metabolism and/or signalling, through strategies such as targeting SphK1 have great potential as future anticancer therapies. The

development and efficacy testing of small molecule inhibitors to SphK1 and related pathways represents a key step in clinical application of such therapies. Scientific attention is required to refine improve and fully comprehend the mechanistic actions of these therapies.

Table 1.5 Small inhibitor of SphK1 in different cancer type

Drug	Cancer Type	*Vitro/ Vivo*	Comments	Refs
MP-A08	Embryonic kidney (HEK293),Lung cancer (A549) Breast cancer (MCF7)	*In vitro/ In vivo*	MP-A08 reduced the growth of human lung adenocarcinoma tumours in a mouse xenograft model.	(Pitman et al., 2015)
Safingol	Esophageal and gastric cancer (OE21, OE33 and AGS)	*In vitro*	Safingol a SphK1 inhibitor, was cytotoxic as a single agent and acted synergistically with cisplatin in gastric cancer cell lines.	(Matula et al., 2015)
SKI-II (2-(p-hydroxyanilino)-4-(p-chlorophenyl)thiazole)	Gastric cancer SGC7901e	*In vitro*	The results showed that SKI-II reversed the drug resistance in human GC cells and enhanced the antitumor effect of DDP.	(Liu et al., 2014)
	Multiple Myeloma (MM)	*In vitro/ in vivo*	Combination FTY720 with SKI-II resulted in synergistic inhibition of MM growth.	*(Beid* er et al., 2017)
SK1-I (BML-EI411)	Glioblastoma	*In vitro/ in vivo*	SK1-I decreased glioblastoma growth and proliferation *in vitro* and *in vivo*.	(Kapitonov et al., 2009
	Breast Cancer	*In vivo*	SK1-I to reduce peritumoral lymphatic vessel density *in vivo.*	(Nagahashi et al., 2012)
	Head and neck squamous cell carcinomas (HNSCC)	*In vitro/ in vivo*	SK1-I enhanced the sensitivity of SCC cells to doxorubicin *in vitro* and *in vivo*.	(Hazar-Rethinam et al., 2015)
	Colon Cancer (DLD, HT29) Brest Cancer (MCF7, BT474), Lung Cancer (H460)	*In vitro*	SK1-I induced the phosphorylation of TP53 at Ser15, activating the downstream BCL-2 family, significantly reduced the cytotoxicity of SK1-I in cancer cells.	(Lima et al., 2018)
Fingolimod (FTY720)	Lung Cancer	*In vitro*	FTY720 mediated PP2A/RIPK1-dependent programmed necrosis through targeting I2PP2A/SET and inhibited lung tumour growth.	(Sadoughi et al., 2013
	Ovarian cancer (COV362, CAOV3)	*In vitro/ in vivo*	FTY720 increased the sensitivity of tumour cells to carboplatin and tamoxifen *in vitro*.	(Kreitzburg et al., 2018)
	Multiple Myeloma (MM)	*In vitro/ in vivo*	Combination FTY720 with SKI-II resulted in synergistic inhibition of MM growth.	(Beider et al., 2017)

PF543	CRC (HCT-116)	*In vitro/ in vivo*	PF-543 intravenous injection significantly suppressed HCT-116 xenograft tumour growth.	(Ju et al., 2016)

1.3.5 SphK1 and downstream signalling pathway

As implicated previously, SphK1 has the potential to play an important role in regulating oncogenesis (Akao et al., 2006, Pchejetski et al., 2005). In keeping with this, a number of studies have demonstrated the connection between SphK1 upregulation and the development of malignant phenotypes of various cancers, such as proliferation (Yuza et al., 2018), anti-apoptosis (Tsukamoto et al., 2015), angiogenesis (Dai et al., 2017), migration (Yuza et al., 2018) and invasion (Yuza et al., 2018). Early indications of SphK1's role in cancer were reported by Xia et al. (Xia et al., 2000) who demonstrated overexpression of SphK1 could increase its enzyme activity and promote growth *in vivo* and *in vitro*. The group also found that SphK1 was involved in the regulation of Harvey Rat Sarcoma Viral Oncogene Homolog (HRAS) signalling pathway, which could be suppressed by the overexpression of the G82D dominant-negative kinase SphK1 mutant. These early findings were key in defining SphK1 as an oncogene.

Yin et al. (Yin et al., 2019) reported that GC cells promoting autophagy in human peritoneal mesothelial cells (HPMCs), was inhibited by blocking TGF-β1 secreted by GC cells, while inhibition of SphK1 expression in HPMC can inhibit TGF-β1-induced autophagy. SphK1 regulates HPMC autophagy and promotes the growth of GC cells *in vitro* and *in vivo*. Overexpression of SphK1 can induce fibrosis in HPMCs. Mechanically, elevated SphK1 levels promoted tumour bioactive sphingolipid dysregulation, of which ceramide decreased and S1P increased (Yin et al., 2019).

Furthermore, in addition to the clinical expression profiling described in the previous sections, Wang et al., also explored the functional implications of SphK1 in GC *in vitro* and *in vivo* (Wang et al., 2018b) Silenced SphK1 significantly inhibited the proliferation, migration, and invasion in cells line. Silencing the expression of SphK1 also blocked the cell cycle and induced apoptosis in cell lines, inhibiting

tumour growth and suppressing S1P levels at the same time. Furthermore, knockdown of SphK1 also inhibited tumour growth *in vivo*. The same study showed that miR-330-3p directly targets SphK1 playing an anti-tumour role. miR-330-3p could inhibit the tumour growth *in vivo*. Furthermore, using chemical inhibitors, such as FTY720 (SphK1 inhibitor) and VPC23019 (S1PR1 inhibitor), inhibited the expression of SphK1 and S1PR1 and exerted antitumor effects *in vivo* and *in vitro* (Wang et al., 2018b).

Another study demonstrated that the deletion of SphK1 inhibited the growth of thymic lymphomas in p53 null mice and extended the survival time. SphK1 enhances the expression of sphingosine and ceramide, in order to mediate P53 tumour surppressive role in cancer, and also influence the cell cycle process and chemosensitivity (Heffernan-Stroud et al., 2012). The study of Liu et al. (Liu et al., 2019) indicated that SphK1 was overexpressed in colon cancer, which affected the prognosis, metastasis and survival of patients. SphK1 affected the metastasis through affecting cancer cell epithelial-to-mesenchymal transition (EMT). At the same time, elevated expression of SphK1 promoted the expression of phosphorylated focal adhesion kinase (p-FAK), p-protein kinase B (AKT) and matrix metalloproteinase 2/9 (MMP2/9). FAK small inhibitors inhibited the expression of the above proteins and the inactivation of FAK signalling pathways (Liu et al., 2019).

In recent years, research discovered that SphK1 is a target of microRNA (miRNA), and that this will subsequently impact many downstream signalling pathways. A study by Wang et al., (Wang et al., 2019a) demonstrated that miR-506-3p directly targeted and inhibited SphK1 expression in osteosarcoma. In this study, transfection with miR-506-3p mimics reduced the ability of invasion of osteosarcoma cell lines, which could be subsequently reversed through SphK1 overexpression. Furthermore, miR-506-3p played an important role in mesenchymal to epithelial transition (MET) and autophagy. Similarly, a study by Cao et al., (Cao et al., 2019), also highlighted

a link between SphK1 and miR-128 in papillary thyroid cancer (PTC) and follicular thyroid carcinoma (FTC) (Cao et al., 2019). In this study SphK1 was identified as a target of miR-128 and the expression of SphK1 was reduced in PTC and FTC tissues where it notably showed a negative correlation with miR-128 expression. Additionally, the inhibitory effect of miR-128 on growth rate and tumour weight identified using *in vivo* models also appeared to suppress SphK1 expression suggesting that SphK1 plays an important role in the occurrence and development of cancer and affects different signalling pathways.

Nuclear Factor Kappa B (NF-κB) is well established as a key signalling pathway in apoptosis and as being involved in cancer development and progression (Zhang et al., 2017). In keeping with SphK1's role, links between SphK1 and NF-κB have been previously observed. One such study by Alvarez et al. (Alvarez et al., 2010) have demonstrated a role for SphK1/S1P in apoptosis through regulation of NF-κB signalling by ubiquitination of tumour-necrosis factor (TNF) receptor-associated factor 2 (TRAF2), the lysine 63-lpolyubiquitination of receptor-interacting serine/threonine-protein kinase 1 (RIP1), phosphorylation of inhibitor of NF-κB kinase (IκB kinase), inhibitor of NF-κB (IκBa) and the degradation of IκBa (Alvarez et al., 2010). Further links have also been demonstrated in a subsequent study by Liang et al. (Liang et al., 2013) indicating that overexpression of SphK1 and subsequent upregulation of S1P drives a persistent amplification loop from SphK1 / S1P / S1PR1 to NF-κB / IL-6 / STAT3 (Liang et al., 2013).

1.4 Sphingosine 1 phosphate receptors (S1PRs)

S1P regulate a variety of biological functions through binding to its receptors, the Sphingosine 1 phosphate receptors (S1PRs). S1PR1 was the first receptor identified in this family, discovered in 1990 and initially named endothelial differentiation

gene 1 (EDG1) (Hla and Maciag, 1990). Subsequently, the other 4 receptors in this group (S1PR2-S1PR5) were identified in the following years. These five receptors are expressed in different tissues and cells (Takabe et al., 2008) and have different biological functions (Brocklyn, 2010), but they all have a high affinity for extracellular S1P. The S1PR receptors are members of the G-protein coupled receptors (GPCRs), and widely exist in many types of cells (Jeffery et al., 2011). Due to the role in cancer progression, an increasing scientific interest has been focused on establishing the functions of the S1PRs family in a variety of cellular processes, including cell differentiation, migration, survival, angiogenesis, calcium homeostasis, inflammation and immunity which is further highlighted in section 1.4.2.

1.4.1 Structural Characteristics of S1PRs

S1PR1 is a 382 amino acids GPCR which includes a heterotrimeric G protein consisting of α, β and γ subunits to transduce intracellular signalling. Due to β and γ subunits being similar, G proteins are assorted into four different groups Gs, Gi/o, Gq/11, and G12/13 based on the difference of α subunit. S1PR1 through the binding of Gi and β-arrestin, allows binding of src proto-oncogene, non-receptor tyrosine kinase (Src) leading to receptor internalization mediated activation of downstream pathways (Pyne and Pyne, 2017).

S1PR1 consists of 3 parts (Parrill et al., 2000)

- Seven hydrophobic transmembrane a-helices (TM1-TM7)
- Three extracellular loops on N terminus (ECL1-ECL3)
- Three intracellular loops on C terminus (ICL1-ICL3)

1.4.2 Function and signalling of S1PRs

1.4.2.1 The function of S1PR1

In recent years, many studies have suggested that abnormal regulation or signalling of the Interleukin-6 (IL6)-Janus kinase (JAK)-Signal transducer and activator of transcription (STAT3) signalling pathway in tumours can be defined as a key mechanism for the initiation and progression of cancer (Bollrath et al., 2009, Grivennikov et al., 2009, Hedvat et al., 2009). S1PR1, a Gi family protein, was a key receptor found to be expressed on T and B lymphocytes (Jeffery et al., 2011). Many studies also have indicated that S1PR1 has an important role in mediating the activations of IL6-JAK-STAT3 signalling pathway (Priceman et al., 2014). S1PR1 promoted the accumulation of regulatory T cells (Tregs) in tumours, thereby affecting the recruitment and activation of $CD8^{+}$T cells. In addition, S1PR1 in $CD4^{+}$T cells activated STAT3 and JAK/STAT3-dependent Treg migration (Priceman et al., 2014). Another study showed that the expression of S1PR1 was significantly increased in STAT3-positive tumours. The same study showed that STAT3 was a transcription factor of S1PR1. STAT3 regulated the expression of S1PR1, accelerating the growth and metastasis of tumours in a STAT3-dependent manner. On the contrary, tumour STAT3 activity, tumour growth and metastasis are suppressed if S1PR1 function is lost. S1PR1 can also activate JAK2 while activating STAT3. Hence, S1PR1 signalling regulation of STAT3 activity, seemed a major positive feedback loop for persistent STAT3 activation in cancer cells and the tumour microenvironment as well as for malignant progression (Lee et al., 2010).

Scientific research has also emphasised the importance of myeloid cells in distant metastasis of tumour cell colonies. A study by Deng et al. (Deng et al., 2012) has shown that upregulation of S1PR1-STAT3 in tumour cells induced activation of S1PR1-STAT3 in various cells at the primary tumour site before metastasis, leading to the formation of a niche before metastasis. Targeting S1PR1 or STAT3 in myeloid

cells can disrupt the existing pre-metastatic niche. The S1PR1-STAT3 pathway enables myeloid cells to enter blood vessels, trigger distant organ microenvironments, and mediate the continued proliferation and survival of themselves and other stromal cells in future metastatic sites. The same study also demonstrated, through analysis of tumour-free lymph nodes from cancer patients, increased myeloid infiltration, increased STAT3 activity and survival signals (Deng et al., 2012).

More recently, a study by Pi et al., demonstrated that elevated miR-302-367 levels in endothelial cells reduced angiogenesis and promoted vascular stability *in vivo* and *in vitro*. As part of this study, it was shown that down-regulation of ERK1/2 in endothelial cells increased miR-302-367 expression and inhibited expression of S1PR1, supressing angiogenesis and improving blood vessels stability. In contrast, blocking S1PR1 in endothelial cells had anti-angiogenic and anti-vascular stabilisation effects in mouse model. Therefore, S1PR1 was shown to have a crucial role in tumour angiogenesis (Pi et al., 2017).

Taken together, S1PR1 appears to be linked to processes and signalling pathways involved in cancer development and progression and hence, S1PR1 may be a potential therapeutic target in the treatment of various tumours.

1.4.2.2 S1PR1 and Clinical significance

It has been difficult to target STAT3 therapeutically (Hong et al., 2015), as outlined above, STAT3 induced S1PR1 transcription, could result in STAT3 and IL-6 continued activation. This unique S1PR1-dependent axis may be an attractive intervention target, as some reports suggest that disruption of the S1PR1 signal eliminates this cycle of STAT3 amplification.

A study by Nagahashi et al., (Nagahashi et al., 2018b) highlighted the potential of targeting the SphK1/S1P/S1PR1 axis with FTY720 to alleviate tumour progression caused by pro-inflammatory cytokines and macrophage infiltration. During this study they demonstrated that S1P produced by tumour-induced SphK1 in the pre-metastatic niche increased recruitment of macrophages to the lung and induced IL-6 signalling pathways important for breast cancer lung metastasis. In contrast, treatment with FTY720 inhibited IL-6, macrophage infiltration, and S1P-mediated signalling pathways in the lung induced by a high-fat diet, and significantly reduced the formation of metastases. Furthermore, utilising a mouse model, the group also demonstrated that FTY720 could reduce obesity-related inflammation, S1P signalling, and lung metastasis, thereby extending survival concluding that sphingolipid signalling might be an effective target for preventing obesity-related breast cancer metastasis (Nagahashi et al., 2018b).

As outlined previously, STAT3 plays key roles in various cancers but is difficult to target clinically. Work conducted by Liu et al,, demonstrated S1PR1 persistently activated STAT3 activating B-cell-like tumour cells synergy while inhibition of S1PR1 expression, using shRNA in lymphoma cells, negatively regulated the expression of downstream genes of STAT3, which were closely related to the survival, proliferation, tumour invasion and immunosuppression of tumour cells. Furthermore, the same study showed that FTY720 inhibited S1PR1 activity, down-regulated STAT3 activity and inhibited lymphoma cell growth *in vitro* and *in vivo*. Therefore, targeting S1P / S1PR1 may be an effective new treatment modality for the treatment of cancer (Liu et al., 2012).

1.5 Conclusion

SphK1, S1P signalling and S1PRs all appear to hold great potential in therapeutic design. There is considerable information focusing on the role of S1P receptors in cancer. Similarly, SphK1 expression and importance in cancer has also been heavily documented. S1P release from the cells has the potential to function in a number of ways, influencing nearby cells to modify the environment or promote angiogenesis as well as acting in an autocrine fashion to promote growth/survival and inhibit apoptosis. Of particular importance is the association of SphK1 with therapy resistance including chemotherapy resistance, which represents a key issue arising in many cancer types and having significant impact on patient mortality and morbidity. Therapeutic targeting of this pathway or molecules involved is an exciting prospect for the generation of novel treatments to target cancer progression or therapy resistance. The current study will focus on the role of SphK1 in gastric cancer patients and its potential as a target therapy in reducing the aggressive nature or combat chemotherapy resistance in this aggressive cancer type.

1.6 Aims and objectives

The aims and objectives of the current project were as follows:

1) To assess SphK1 expression in clinical gastric cancer tissue, its relevance to patient survival and its potential as a biomarker

2) To functionally characterise the cellular role of SphK1 in gastric cancer cell models

3) To explore the potential of targeting SphK1 using inhibitor compounds in the response of gastric cancer cell and patient derived cell lines to chemotherapeutic agents

4) To gain insight into potential mechanisms that may be involved in SphK1's role in gastric cancer.

It is hypothesised that enhanced SphK1 expression will be associated with poorer clinical prognosis, a more aggressive cellular phenotype and reduced sensitivity to chemotherapeutic agents and that targeting or inhibiting SphK1 will reduce the aggressive nature of the cells and enhance sensitivity to chemotherapeutics.

Chapter II

Methods and materials

2.1 Cells

Seven gastric cancer cell lines (823, HGC27, 7901, AGS, NUGC3 and MKN28) and normal epithelium cell line (GES1) were used to explore SphK1 expression across a range of gastric cancer cell types. Subsequently, two cell lines were chosen and used for *in vitro* SphK1 knockdown model generation and functional assay investigation and are outlined in Table 2.1. The human AGS cell line was purchased from the American Type Culture Collection (ATCC, Manassas, VA, USA). The human HGC27 cell line was purchased from the European Collection of Authenticated Cell Cultures, (ECACC, UK).

Both HGC27 and AGS cell lines were routinely cultured in Dulbecco's Modified Eagle Medium (DMEM) / Ham's F12 with L-Glutamine medium (Sigma-Aldrich, Inc., Dorset, UK), supplemented with antibiotic antimycotic solution (Sigma-Aldrich, Inc. Dorset, UK), and 10% foetal calf serum (FCS) (Sigma-Aldrich, Inc., Dorset, UK), and incubated at 37.0°C, 5% CO2 and 95% humidity. The remaining five cell lines are outlined in Table 2.2.

Gastric cancer patients' primary cells were obtained from Peking University Cancer Hospital (PKUCH) (Table 2.3). Information on the isolation and culture of primary CG cells is outlined in section 2.5.4.

Table 2.1 Cell lines used for *in vitro* functional analysis

Cell line	Organism	Morphology	Ethnicity	Gender	Sources and features	Growth Conditions
AGS	*Homo sapiens*	Epithelial	Caucasian	Female	This is a hyperdiploid human cell line. The modal chromosome number was 49, occurring in 60% of cells	Grown in DMEM supplemented with 10% FCS and antibiotics at 37°C in 5% CO_2
HGC27	*Homo sapiens*	Epithelial	East Asian	NA	Tissue original from the metastatic lymph node from a gastric cancer patient diagnosed histologically as undifferentiated carcinoma.	Grown in DMEM supplemented with 10% FCS and antibiotics at 37°C in 5% CO_2

Table 2.2 Cells used for SphK1 expression screening

Cell line	Organism	Morphology	Ethnicity	Gender	Sources and features	Growth Conditions
823	*Homo sapiens*	Epithelial	African, European, East Asian, Native American	Female	This is a hyperdiploid human cell line. The modal chromosome number was 49, occurring in 60% of cells	Grown in DMEM supplemented with 10% FCS and antibiotics at 37°C in 5% CO_2
7901	*Homo sapiens*	Epithelial	Caucasian	Male	Tissue original from the metastatic lymph node from a gastric cancer patient diagnosed histologically as undifferentiated carcinoma.	Grown in DMEM supplemented with 10% FCS and antibiotics at 37°C in 5% CO_2
NUGC3	*Homo sapiens*	Epithelial	Caucasian	Male	Tissue original from gastric adenocarcinoma metastatic site: brachialis muscle.	Grown in DMEM supplemented with 10% FCS and antibiotics at 37°C in 5% CO_2
MKN28	*Homo sapiens*	Epithelial	East Asian	Male	Tissue original from gastric tubular adenocarcinoma metastatic site: liver	Grown in DMEM supplemented with 10% FCS and antibiotics at 37°C in 5% CO_2
GES1	*Homo sapiens*	Normal stomach cell	Caucasian	Male	Derived from sampling site: fetal stomach, epithelial mucosa.	Grown in DMEM supplemented with 10% FCS and antibiotics at 37°C in 5% CO_2
AGS	*Homo sapiens*	Epithelial	Caucasian	Female	This is a hyperdiploid human cell line. The modal chromosome number was 49, occurring in 60% of cells	Grown in DMEM supplemented with 10% FCS and antibiotics at 37°C in 5% CO_2
HGC27	*Homo sapiens*	Epithelial	East Asian	NA	Tissue original from the metastatic lymph node from a gastric cancer patient diagnosed histologically as undifferentiated carcinoma.	Grown in DMEM supplemented with 10% FCS and antibiotics at 37°C in 5% CO_2

Table 2.3 Gastric cancer primary cells used for drug test

Name	Origin	Tissue type	Cell morphology	Lauren Type	TNM stage	Differentiation	Location
SphK1-H	67 year-old male	Adenocarcinoma	Epithelial	Diffuse	cT3N2M0	Poorly differentiated	Gastric antrum
SphK1-L	45 year-old male	Adenocarcinoma	Epithelial	Intestinal	cT4aN1M0	Moderate- poorly differentiated	Gastric antrum

2.2 Primers

Primers used in the current study were designed using Beacon designer software (PREMIER Biosoft International, Palo Alto CA, USA), synthesised by Sigma-Aldrich (Dorest, UK) and are outlined in Table 2.4.

Table 2.4 Primers used in this study

Function	Target gene/sequence	Name of Primer	Sequence
Screening of clinical samples and cell lines using q-PCR and conventional PCR	SphK1	SphK1 F8	5'- TTGCTGATGTGGACCTAGA
		SphK1 R8	5'- CACTGCAAACACACCTTTC
		SphK1 F1	5'- ACCATTATGCTGGCTATGAG
		SphK1 ZR1	5'-*ACTGAACCTGACCGTACA*GAGACAGCAGGTTCATGG
	Cytokeratin-19 (CK-19)	CK-19 F8	5'-AGCCACTACTACACGACCAT
		CK-19 ZR8	5'-*ACTGAACCTGACCGTACA*TCGATCTGCAGGACAATC
Sequences for ribozyme synthesis	SphK1	SphK1 rib 1F	5'-CTGCAGGGCTCCAAGCGCAAGGCCTGATGATCCGTGAGGA
		SphK1 rib 1R	5'-ACTAGTGCCCCTACTTGGTATATGTGCCCGTGGTTTCGTCCTCACGGACT
		SphK1rib 2F	5'-CTGCAGTGAGCATCAGCGTGAAGGACTGATGAGTCCGTGAGGA
		SphK1 rib 2R	5'-ACTAGTGCAGCCCCTTTTGGCTGAGGCTGAAATTTCGTCCTCACGGACT
SphK1 knockdown verification by q-PCR		SphK1 F1	5'- ACCATTATGCTGGCTATGAG
		SphK1 ZR1	5'-*ACTGAACCTGACCGTACA*GAGACAGCAGGTTCATGG
Screening on cell lines by PCR	Glyceraldehyde-3-phosphate dehydrogenase (GAPDH)	GAPDH F8	5'-GGCTGCTTTTAACTCTGGTA
		GAPDH R8	5'-GACTGTGGTCATGAGTCCTT
Sphk1 knockdown verification by q-PCR		GAPDH F2	5'-CTGAGTACGTCGTGGAGTC
		GAPDH ZR2	5'-*ACTGAACCTGACCGTACA*CAGAGATGATGACCCTTTTG
Transgene insertion and orientation screening	T7F promoter	T7F	5'-TAATACGACTCACTATAGGG
	Ribozyme common sequence	RbBMR	5'-TTCGTCCTCACGGACTCATCAG
		RbToPF	5'-CTGATGAGTCCGTGAGGACGAA
	BGHR site	BGHR	5'-TAGAAGGCACAGTCGAGG

- Z Sequence '*ACTGAACCTGACCGTACA'* is italicised

2.3 Antibodies

Full details of the antibodies used throughout this this study are outlined in Table 2.5 and Table 2.6.

Table 2.5 Antibodies used for IHC analysis on gastric cancer biopsies

Antibody name	Host species	Antibody concentration	Supplier and catalogue number
SphK1 (M-209)	Rabbit	2µg/ml	Santa Cruz biotechnology, SC-48825

Table 2.6 Antibodies used for verification of SphK1 knockdown and validation of Kinexus data

Antibody name	Host species	Molecular Weight (kDa)	Antibody concentration	Supplier and catalogue number
SphK1 (M-209)	Rabbit	42	1:1,000	Santa Cruz biotechnology, SC-48825
GAPDH (6C5)	Mouse	37	1:4,000	Santa Cruz biotechnology, SC-32233
GAPDH (FL-335)	Rabbit	37	1:4,000	Santa Cruz biotechnology, SC-25778
Akt	Mouse	62	1:1,000	Santa Cruz biotechnology, SC-5298
p-Akt (Ser473)	Mouse	56	1:1,000	Santa Cruz biotechnology, SC-81433
mTOR	Rabbit	289	1:1500	Cell Signalling biotechnology, 7C10
p-mTOR (Ser 2448)	Rabbit	289	1:1500	Cell Signalling biotechnology, D9C2
Anti-Mouse IgG	Rabbit		1:100,000	Sigma-Aldrich, A9044
Anti-Rabbit IgG	Goat		1:100,000	Sigma-Aldrich, A0545

2.4 General reagents and solutions

2.4.1 Reagents and chemicals

2.4.1.1 Solutions and reagents for cell culture

Ethylene Diaminetetraacetic Acid (EDTA) trypsin

A stock solution of 10X Tryspin-EDTA (Product number T4174) was purchased from Sigma-Aldrich (Dorset, UK). For routine use, stock trypsin was diluted in phosphate buffered saline (PBS) to 1X concentration and aliquoted to 25ml aliquots before storing at -20°C for long term or 4°C for short term before use.

Phosphate buffered saline (PBS)

10X Phosphate buffered saline (P5943) was purchased from Sigma-Aldrich, (Dorset, UK). PBS was diluted to 1X concentration in distilled water before aliquoting into. T 25ml aliquots and storing at room temperature. PBS stocks prepared for tissue culture were autoclaved before aliquoting and kept under sterile conditions.

Antibiotics

A 100X Antibiotic Antimycotic solution (A5955) was purchased from Sigma-Aldrich (Dorset, UK). The solution was aliquoted into 5ml aliquots, stored at -20°C, with one aliquot being added into a 500ml bottle of medium to obtain a 1X final concentration.

Foetal Calf Serum (FCS)

Foetal Calf Serum was purchased from Sigma-Aldrich, Inc. (Dorset, UK) and aliquoted into 25ml aliquots. Aliquots were stored at -20°C until required for tissue culture.

MTT (3-(4,5-dimetheylthiazol-2-yl)-2,5-diphenyltetrazolium bromide)

Stock solutions of MTT (5.5mg/ml) were prepared by dissolving 110mg MTT powder (Sigma-Aldrich, Dorset, UK) in 20ml PBS and filtering through a 0.2μm filter. Stock solutions were then covered in foil and stored at 4°C until required.

Cytotoxic drugs

5-FU and Cisplatin were obtained from Peking University Cancer Hospital which was aliquoted into 5ml aliquots, stored at -20°C.

SphK1 inhibitor and S1P

A SphK1 inhibitor named PF543 and S1P were purchased from TOCRIS, Inc. (UK, Catalog No.: 5754; Catalog No.: 1370) and aliquoted into 25ml aliquots. Aliquots were stored at -20°C until required for tissue culture.

2.4.1.2 Solutions and reagents for molecular biology

Tris-Boric-Acid-EDTA (TBE)

A 10X concentrated TBE buffer (T4415) solution was purchased from Sigma-Aldrich (Dorset, UK). For use in electrophoresis, this was diluted with distilled water into a 1X stock and stored at room temperature.

Diethyl Pyrocarbonate (DEPC) Water

DEPC was purchased from Sigma-Aldrich (Dorset, UK). Subsequently, 250ml of DEPC solution was added to 4.75L of distilled water before autoclaving and storing at room temperature for further use.

Loading buffer (used for DNA electrophoresis)

Loading buffer was prepared by dissolving 25mg of bromophenol blue (Sigma-Aldrich, Dorset, UK) and 4g sucrose (Fisons Scientific Equipment, Loughborough, UK) in 10ml of distilled water before storing at 4°C.

2.4.1.3 Solutions and reagents for cloning

LB (Lysogeny Broth)

Eight grams of low salt granulated power LB Broth (Melford Laboratories Ltd., Suffolk, UK) was dissolved in 400ml distilled water. Subsequently the pH value was adjusted to 7.0 and the solution autoclaved before storing at room temperature for further use.

LB Agar

Ten grams of low salt granulated powder LB Broth (Melford Laboratories Ltd., Suffolk, UK), combined with 7.5g of agar (A1296) (Sigma-Aldrich, Dorset, UK) was dissolved in 500ml of distilled water and the pH adjusted to 7.0. Following this, the solution was autoclaved and stored at room temperature (forming a solid gel). Prior to use, the gel was placed in a microwave and heated until completely melted.

Ampicillin

A stock solution of 100mg/ml ampicillin (Melford Laboratories Ltd., Suffolk, UK) was prepared by dissolving 1g of ampicillin powder in 10ml of sterile PBS.

2.4.1.4 Solutions and reagents for western blotting

Lysis Buffer

Eight point seven six grams of NaCl (150mM), 6.05g of Tris (50mM), 200mg Sodium azaide (0.02%, w/v) and 5g Sodium deoxycholate (0.5%, w/v) were dissolved in distilled water before adding 15ml Triton X-100 (1.5%, v/v) to a final volume of 1L. This lysis buffer stock solution was stored at 4°C. Subsequently, one cOmplete™, EDTA-free protease inhibitor cocktail tablet (Roche Diagnostics, Mannheim, Germany) was dissolved in 50ml of the lysis buffer before being aliquoted into 1ml aliquots and stored at -20°C. For phosphorylation studies, 100mM of Na_3VO_4 was added to the lysis buffer at the working concentration of 1mM.

10% (w/v) Ammonium Persulphate (APS)

One gram of Ammonium Persulphate (Melford Laboratories Ltd., Suffolk, UK) was added and dissolved in 10ml of distilled water before being stored at 4°C for future use.

10% (w/v) Sodium Dodecyl Sulphate (SDS)

Fifty grams of Sodium Dodecyl Sulphate (Melford Laboratories Ltd., Suffolk, UK) was added and dissolved in 500ml distilled water. The resultant solution was stored at room temperature for future use.

Tris Buffered Saline (TBS)

One Litre of 10X Tris Buffered Saline solution (T5912) (Sigma-Aldrich, Dorset, UK) was diluted in 9L of distilled water, to give a 1X concentration, and stored at room temperature for future use.

Running buffer (for Sodium Dodecyl Sulfate-Polyacrylamide Gel Electrophoresis, SDS-PAGE)

One Litre of 10X Tris-Glycine-SDS Buffer solution (T7777) (Sigma-Aldrich, Dorset, UK) was diluted in 9L of distilled water, to give a 1X concentration, and stored at room temperature for future use.

Transfer buffer

One Litre of 10X Tris-Glycine Buffer solution (T4904) (Sigma-Aldrich, Dorset, UK) was diluted in 9L of distilled water containing 2L methanol, to give a 1X concentration, (Fisher Scientific UK, Loughborough, UK) and stored at room temperature for future use.

Ponceau S stain

Ponceau S (P3504) (Sigma-Aldrich, Dorset, UK) was used to prepare a stock solution containing 0.1% Ponceau S (and 5% acetic acid (w/v). This solution was subsequently stored at room temperature for future use.

2.4.1.5 Solutions and reagents for Kinexus microarray protein lysis

Six grams of Tris powder (Melford Laboratories Ltd., Suffolk, UK) was dissolved in 1.5L distilled water to obtain a 100mM Tris buffer solution. To 50ml of the Tris buffer one cOmplete^{TM}, EDTA-free protease inhibitor cocktail tablet (Roche

Diagnostics, Mannheim, Germany), 5ml of 2-mercaptoethonal (10%, v/v), nonident P-40 (1%, v/v) and 5ml of 500mM NaFl (50mM) were added before mixing the solution thoroughly, aliquoting into 1ml aliquots and storing at -20°C for future use.

2.4.1.6 Solutions and reagents for immunohistochemical (IHC) staining

Avidin-biotin complex (ABC)

The VECTASTAIN® ABC Kit (Vector Laboratories, Inc., CA, USA) was used to prepare the ABC complex for use in IHC staining. Four drops of reagent A and reagent B were added into 20ml of wash buffer, mixed well and left at 4°C for 30 minutes prior to use.

2.5 Cell culture, maintenance, storage and revival

2.5.1 Preparation of growth medium and cell maintenance

Medium for routine cell culture was prepared by adding 10% FCS ((Sigma-Aldrich, Dorset, UK) and antibiotic/antimyotic solution (1% final) (Sigma-Aldrich., Dorset, UK) into DMEM Nutrient Mixture F-12 Ham with 15mM HEPES, $NaHCO_3$, pyridoxine and L-glutamine (Sigma-Aldrich, Dorset, UK).

Following transfection of gastric cancer cells, medium was further supplemented with 5µg/ml blasticidin (Melford Laboratories Ltd., Suffolk, UK) (selection medium) and was used for initial selection of cells that had been transfected with the pEF6 plasmid vector. Following the initial selection period, medium containing 0.5µg/ml blasticidin (maintenance medium) was used to maintain transfected cells during routine culture.

Cells were cultured in 25 cm^2 (T25) and 75cm^2 (T75) culture flasks (Greiner Bio-One Ltd., Gloucestershire, UK) incubated at 37°C, 5% CO_2 and 95% humidity.

2.5.2 Trypsinisation of adherent cells and cell counting

Upon reaching 80-90% confluency, cells were typsinised and sub-cultured to maintain them and prevent over-confluence. Firstly, the medium was aspirated using a glass pipette and the remaining monolayer washed with sterile PBS to ensure complete removal of serum which may disrupt the action of trypsin. Subsequently, trypsin was added to the flask (1ml for T25 flask, 2ml for T75 flask), agitated to ensure coverage of the monolayer and incubated at 37°C, 5% CO_2 and 95% humidity for a suitable time (dependent on nature of cell line). Following incubation visual confirmation of cell detachment was undertaken using the microscope. Detached cells were then resuspended in fresh medium to neutralise the trypsin, collected into a 30ml universal container (Greiner Bio-One Ltd,. Gloucestershire, UK) and centrifuged at 1,700rpm for 5 minutes to pellet cells. Following this, the supernatant was removed, using a glass pipette, and the remaining cell pellet re-suspended in a suitable volume of fresh medium (dependent on cell size and required cell density for application). A Neubauer haemocytometer counting chamber (Mod-Fuchs Rosenthal, Hawksley, UK) was then used to count cell numbers in the suspension under an Olympus CKX31 microscope at X10 objective magnification (Olympus, Tokyo, Japan) and the resulting number converted to number of cells/ml.

2.5.3 Storage and revival of cells

Cells were detached and resuspended as described in the previous section before being divided into 900µl aliquots in pre-labelled CRYO.S^{TM} cryotube (Greiner Bio-One Ltd,. Gloucestershire, UK). Following this, an additional 100µl of Dimethylsulphoxide (DMSO) (Sigma-Aldrich, Dorset, UK) was added (10% final concentration) and the cryovials capped and then wrapped in tissue paper before

placing in the -80°C freezer for short term storage or transferred to liquid nitrogen for long term storage.

For cell revival, the cryotube was removed from either the -80°C freezer or the liquid nitrogen stocks and rapidly thawed. Subsequently, the cell suspension was transferred to 10mls of pre-warmed medium in a universal container before centrifuging at 1700rpm for 5 minutes pellet cells. Following this the supernatant, containing remnant DMSO from the preservation step, was removed using a glass pipette and the remaining pellet re-suspended in 5ml fresh growth medium before transferring to a T25 flask and culturing as described previously.

2.5.4 Primary GC cell isolation and culture

Gastric tissues were washed three times with PBS and were cleared of the connective and necrotic sections. The samples were cut into small fragments of approximately 1 mm, with 1% collagenase IV (Biosharp, China) incubation at 37℃ for 1h. Then, centrifuge the sample to remove undigested tissue and to keep the pellet. The pellet was subsequently cultured in Roswell Park Memorial Institute (RPMI) 1640 (Hyclone, USA) containing 10% FBS (Gibco, Grand Island, NY, USA), 100 U/ml penicillin and 100 ug/ml streptomycin at 37℃ in an atmosphere of 5% CO2 and 95% air.

2.6 Tissue collection and processing

2.6.1 Cohort 1

322 fresh-frozen tissues were used to undertake qPCR transcript analysis in which we got total 322 patients in which 183 were paired with tumour tissue and normal tissue. Tissue was obtained from cT2-4N0M0 or cT1-4N1-3M0 gastric cancer

patients treated between January 2006 and December 2007 in Peking University Cancer Hospital. All specimens were stored in one of the best bio-bank in China with global standards. All protocols were reviewed and approved by the local ethics committee and informed consent was obtained from the patients before therapy.

2.6.2 Cohort 2

263 paraffin-embedded tissues were used to undertake IHC protein analysis, Tissue was obtained from cT2-4N0M0 or cT1-4N1-3M0 gastric cancer patients treated between January 2003 and December 2011 in Peking University Cancer Hospital. All protocols were reviewed and approved by the local ethics committee and informed consent was obtained from the patients before therapy.

2.7 Total RNA isolation

RNA was isolated using TRI-reagent (Sigma-Aldrich, Dorset, UK) in accordance with the manufacturer's instructions. RNA was extracted from both cell lines and also from patient tissues.

Tissue extraction

Multiple sections were cut from the same clinical patient sample and were collected and combined in a 7ml Bijou container before homogenising in 1ml of ice-cold TRI-reagent with a handheld homogeniser (Cole-Parmer, London, UK). Following homogenisation, the lysate was transferred to a 1.5ml Eppendorf tube before continuing with the remaining extraction steps outlined in the manufacturer’s instructions.

Cell lysate

Following confluency, cell medium was aspirated using a glass pipette and 1ml of TRI-reagent was added to the monolayer and a cell scraper (Greiner Bio-one, Frickenhausen, Germany) used to ensure full detachment and lysis of cells before transferring the lysate to a 1.5ml Eppendorf tube. Subsequently, remaining extraction steps outlined in the manufacturer instructions were followed.

Following lysis (as outlined above), the homogenate was kept at room temperature for 5 minutes before adding 100µl of 1-bromo-3-chloropane (Sigma-Aldrich, Dorset, UK) and shaking vigorously for 15 seconds. The resulting mixture was left for 5-10 minutes at room temperature before centrifuging at 4°C, 12,000g for 15 minutes resulting in phase formation. The upper aqueous phase (containing RNA) was transferred into a new, pre-labelled 1.5ml Eppendorf tube containing 500µl of isopropanol (Fisher Scientific UK, Loughborough, UK) before shaking vigorously for 10 seconds and centrifuging at 4°C, 12,000g for 10 minutes. Following this a visible RNA pellet was obtained and the supernatant removed and discarded, before washing the pellet in 75% ethanol in DEPC water, through vortexing briefly and centrifuging at 7,500g for 5 minutes. Subsequently, the Eppendorf was placed in a Techne, Hybrdiser HB-1D drying oven at 50°C to dry out any remaining liquid before dissolving the RNA pellet in 20-80µl of DEPC (depending on pellet size) and freezing at -80°C until required.

At the same time, we did have limitations in our study. Firstly, we used fresh frozen samples from 2006 to 2007, and we extracted RNA in 2014. Therefore, there is the possibility that such long storage could increase RNA degradation and thus affect the results of our study. However, it is suggested from the literature that Kelly et al. (Kelly et al., 2019) reported that 11 years didn't affect the integrity and

histomorphology preserved under qualified preservation conditions. Biobank of PKUCH has been a qualified one with worldwide standards.

2.8 Reverse transcription polymerase chain reaction (RT-PCR)

RNA samples were first quantified using a NanoPhotometer™ (IMPLEN; Geneflow ltd., Lichfield, UK) and standardised to 500ng before being used to generate cDNA using the GoScript™ Reverse Transcription System kit (Promega, Southampton, UK).

Five hundred nanograms sample RNA was mixed with 1µl of Oligo (dT)15 and brought up to 5µl with PCR water in a thin-walled 200µl PCR tube before heating in a 2720 Thermal Cycler (Applied Biosystems, Paisley, UK) at 70°C for 5 minutes followed by immediately being transfered to ice for 5 minutes. Subsequently, the tube was removed from the ice and 15µl of a pre-prepared Mastermix, containing 4µl GoScript™ 5X Reaction Buffer, 1.2µl $MgCl_2$, 1µl Nucleotide mix, 0.5µl Recombinant RNasin Ribonuclease Inhibitor, 1µl GoScript™ Reverse Transcriptase and 7.3µl nuclease-free water, was added. The sample was then centrifuged briefly before being subjected to 25°C for 5 minutes, 42°C for 60 minutes and 75°C for 15 minutes in a thermocycler.

cDNA generated was then diluted 1 in 4 with PCR water and was stored at -20°C for future use.

2.9 Polymerase chain reaction (PCR)

GoTaq Green master mix (Promega, Southampton, UK) was used to undertake PCR in conjunction with molecule specific primers (outlined in section 2.2). Each 16µl reaction contained 8µl GoTaq Green master mix, 1µl forward primer, 1µl reverse

primer, 5µl PCR water and 1µl sample cDNA. Following reaction preparation the sample was centrifuged briefly before being placed in a 2720 Thermal Cycler (Applied Biosystems, Paisley, UK) and undergoing an initial 94°C denaturing for 5 minutes, followed by 30 -36 cycles of 94°C for 30 seconds, 55°C for 40 seconds, 72°C for 1 minute and a final 10 minute 72°C extension before holding at 4°C.

2.10 Agarose gel electrophoresis

Following amplification in the thermocycler, samples were separated using gel electrophoresis. Gels were prepared using either a 0.8% or 2% agarose gel, dependent on predicted product size. The gels were made by adding the appropriate amount of agarose (Melford Chemicals, Suffolk, UK) to 1X TBE and heating in a microwave to fully dissolve the powder. Following this, the gel solution was removed from the microwave and allowed to cool partially before adding (Z)-4-((3-Methylbenzo[d]thiazol-2(3H)-ylidene)methyl)-1-propylquinolin-1-ium 4-methylbenzenesulfonate (SYBR) safe DNA gel stain (Invitrogen, Paisley, UK) at a 1:10,000 dilution. The gel solution was then poured into an electrophoresis tank assembled with plastic combs (SCIE-PLAS, Cambridge, UK) resulting in loading well formation when combs were removed. Once the agarose gel had set it was submerged in 1X TBE buffer before loading either 4µl of PCR Ranger 100bp DNA Ladder/ High Ranger 1000bp DNA Ladder (Geneflow, Litchfield, UK) or 8µl of cDNA samples. Samples were then separated at 100V, 50mA and 50W for a sufficient amount of time (20-50 minutes). Following separation, the gel and product bands were visualised under Blue light and images captured using a Syngene gel doc system (Syngene, Cambridge, UK).

2.11 Generation of mutant AGS and HGC27 cell lines

2.11.1 Generation of ribozyme transgenes

Hammerhead ribozyme transgenes were used to target SphK1 expression in AGS and HGC27 cell lines. Hammerhead ribozymes are able to cleave RNA at specific cleavage sites (GTG, ATC and TTC). Ribozymes were designed based on the predicted secondary structure of SphK1 mRNA (Figure 2.1) according to Zukers RNA mFold software (Zuker, 2003). The secondary structure of SphK1 was examined for suitable cleavage sites, sitting in the loop regions of the mRNA structure, and regions surrounding this used to design complementary sequences to specifically target the ribozyme catalytic region to this site. Once designed, ribozyme transgene sequences were synthesised by Sigma-Aldrich (Dorset, UK; Table 2.4) and were combined using touchdown PCR over a range of annealing temperatures. The transgene products were subsequently separated on a 2% agarose gel to confirm successful generation of the ribozyme product and the remaining reaction product stored at 4°C before cloning using the pEF6/His TOPO system.

Figure 2.1 Predicted secondary structure of human SphK1 mRNA predicted by Zukers mFold software

2.11.2 TOPO TA gene cloning and generation of stable transfectants

The pEF6/V5-His TOPO® TA expression system (Invitrogen, Paisley, UK) was used to generate plasmids for SphK1 knockdown. The expression system allows insertion of *Taq* polymerase-amplified PCR products into the pEF6 plasmid enabling constitutive expression in mammalian cells. The structure of the pEF6 plasmid is outlined in Figure 2.2

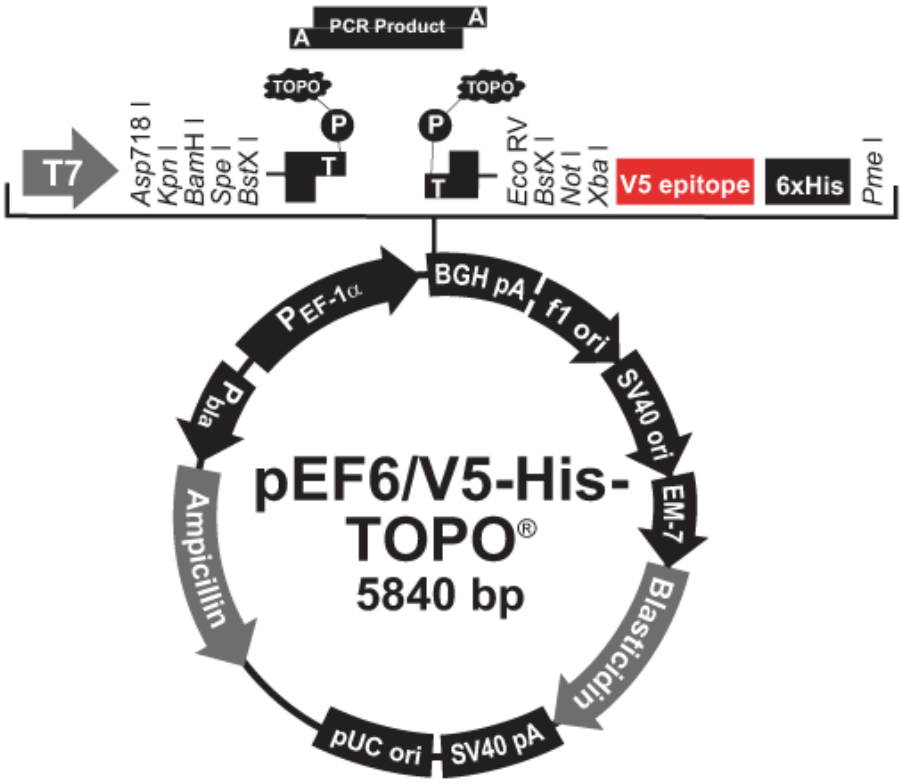

Figure 2.2 Structure of the pEF6/V5-His TOPO vector. Image reproduced from pEF6-His TOPO® TA Expression Kit manual, (Invitrogen)

The generated ribozyme transgene PCR products were cloned into pEF6/V5-His TOPO® plasmid in accordance with the manufacturer's guidance. A 6µl cloning reaction, containing 4µl PCR product, 1µl salt solution and 1µl TOPO vector, was prepared, mixed gently and stored on ice before adding 5µl of the cloning reaction mix to a vial of One Shot TOP10 *Escherichia coli* (*E. coli*) and mixing gently. The vial was then left on ice for between 5 and 30 minutes before transferring the vial to a 42°C water bath and heat shocking for 30 seconds. The vial was then immediately transferred back into the ice before adding 250µl of S.O.C medium (at room temperature) and agitating the tubes at a 45^{o} angle and 225rpm and 37°C for 1 hour on an orbital shaker (Bibby Stuart Scientific, UK). The vial contents were then spread onto a pre-prepared ampicillin selective (100µg/ml) agar petri dish and incubated overnight at 37°C allowing colony formation.

Orientation checking was then undertaken on random colonies to ensure the product had inserted in the correct orientation and would form a viable product. Ribozyme orientation was confirmed using a range of plasmid specific (T7F and BGHR) and ribozyme specific (RbToPF and RbBMR). A portion of each tested colony was added to three reactions, outlined below:

Reaction 1: Product insertion check

- GoTaq Green master mix - 8µl
- T7F plasmid specific forward primer - 1µl
- BGHR plasmid specific reverse primer - 1µl
- PCR water -6µl

Reaction 2: Correct orientation check

- GoTaq Green master mix - 8µl

- T7F plasmid specific forward primer - 1µl
- RbBMR ribozyme specific reverse primer - 1µl
- PCR water -6µl

Reaction 3: Incorrect orientation check

- GoTaq Green master mix - 8µl
- T7F plasmid specific forward primer - 1µl
- RbToPF ribozyme specific forward primer - 1µl
- PCR water -6µl

Following set up and inoculation of the colony into all reactions, the mixes were heated in a 2720 Thermal Cycler (Applied Biosystems, Paisley, UK) using the following conditions: 94°C for 5 minutes; 30 cycles of 94°C for 30 seconds, 55°C for 40 seconds and 72°C for 1 minute; final extension of 72°C for 10 minutes; 4°C hold. The products were then run on a 2% agarose gel stained with SYBR safe before analysing the orientation profiles and inoculating those with correct orientation into 5ml of ampicillin (100µg/ml) selective LB broth in a universal container and incubating overnight at 37°C under angled agitation at 225rpm.

2.11.3 Plasmid amplification and extraction

A GenElute Plasmid MiniPrep Kit (Sigma-Aldrich, Dorset, UK) was used to extract plasmid from the amplified bacteria in accordance with the manufacturer guidelines. Overnight cultures were centrifuged at 5,000 Relative Centrifugal Force (RCF) to pellet the bacteria and the supernatant removed before resuspending the pellet in 200µl Resuspension Solution containing RNase A and transferring into a 1.5ml Eppendorf. Following this, 200µl of Lysis Solution was added and the tube inverted

8 times before adding, within 5 minutes, 350µl of Neutralisation and inverting again 6 times. The solution was then centrifuged at 12,000g for 10 minutes to pellet the cell debris and the cleared lysate transferred into a Miniprep Binding Column (pre-washed with Column Preparation Solution) placed in a Microcentrifuge Tube. The tube was then centrifuged for 1 minute at 12,000g and the flow-through liquid was discarded before adding 700µl of Wash Solution (containing ethanol) into the Miniprep Binding Column and centrifugation at 12,000g for 1 minute followed by removal of the flow-through liquid. A final centrifugation at 12,000g for 1 minute was undertaken to remove any remaining Wash solution before placing the Miniprep Binding Column into a fresh Collection Tube and eluting the plasmid by adding 50µl of Elution Solution and centrifuging at 12,000g for 1 minute. The eluted plasmid, quantified using the nanophotometer (IMPLEN; Geneflow ltd., Lichfield, UK),was then stored at -20°C until required.

2.11.4 Plasmid transfection via electroporation into AGS and HGC27 cell lines

Wild type AGS and HGC27 cells were grown in T75 culture flasks. Upon reaching approximately 70-80% confluency cells were trypsinised as previously described, transferred into a universal container and centrifuged before resuspending the cell pellet in medium and counting cells as previously described. One million cells in 1ml was added into a 4mm cuvette (Geneflow ltd., Lichfield, UK) along with 3-5µg of plasmid, inverted several times and then electroporated under 310V and 1500µA. Following electroporation, the cell suspension was seeded into a T25 flask containing pre-warmed medium and incubated as described previously. Plasmids containing ribozyme transgenes and closed pEF6 control plasmids were used for electroporation into cells. In addition, a mock transfection was undertaken for wild

type cells without the addition of any plasmid. Following overnight culture, all cells were placed in selection medium containing 5µg/ml blasticidin. Selection was continued over a 5-14 days period based on how quickly the mock transfected cells were killed by the selective antibiotic. Following selection, transfected cells were placed and maintained in maintenance medium containing 0.5µg/ml balsticidin.

2.12 Real time quantitative polymerase chain reaction (qPCR)

qPCR was used to quantify the transcript expression of target genes in cell lines and tissue cohorts. AmplifluorTM UniprimerTM Universal system (Intergen company®, New York, USA) was utilised in the current study. In this system the Amplifluor probe (Uniprimer) contains a 3' region which is identical to the Z-sequence (ACTGAACCTGACCGTACA), contained on one of the qPCR primers for each molecule, and a 5' hairpin structure containing a fluorescent (FAM) tag.

In its natural state, it forms a hairpin structure and the fluorescent tag is linked to an acceptor moiety (DABSYL), quenching the fluorescent signal. Target molecule primers were designed as described in section 2.2 with one containing a Z-sequence facilitating incorporation of the Amplifluor Uniprimer probe during PCR. This incorporation then acts as a template for the Amplifluor Uniprimer probe (outlined in Figure 2.3) in later cycles as the Z-tagged primer (present at a lower concentration) exhausts, causing break down of the hairpin structure and unfolding by DNA polymerase, disrupting the fluorophore - quencher structure and resulting in fluorescence emission to be detected.

Ten microlitre reactions were prepared consisting of 5µl of Precision FAST 2X qPCR Mastermix (Primerdesign, Eastleigh, UK), 0.3µl target forward primer, 0.3µl target reverse primer [$1/10^{th}$ concentration of forward primer] containing Z-sequence, 0.3µl Ampliflour Uniprimer probe and a 4.1µl of cDNA and PCR water. The

reactions were loaded into a 96 well optical plate (Applied Biosystems, Paisley, UK) and run in a StepOne plus Real-Time PCR System (Applied Biosystems, Paisley, UK) under the following conditions: 94°C, 10 minute initial denaturing followed by 60-100 cycles of 94°C for 10 seconds, 55°C for 30 seconds, 72°C for 10 seconds.

The fluorescent signal was detected during the annealing stage and the threshold cycle for each sample determined. Reactions were run simultaneously alongside a standard plate containing known transcript concentration of PDPL (10^8-10^1), allowing formation of a standard curve (example shown in Figure 2.4) and subsequently calculation of relative transcript copy number per sample. Sample transcript copy number was also normalised against the expression of either the Glyceraldehyde 3-phosphate dehydrogenase (GAPDH) or cytokeratin 19 (CK-19) housekeeping genes.

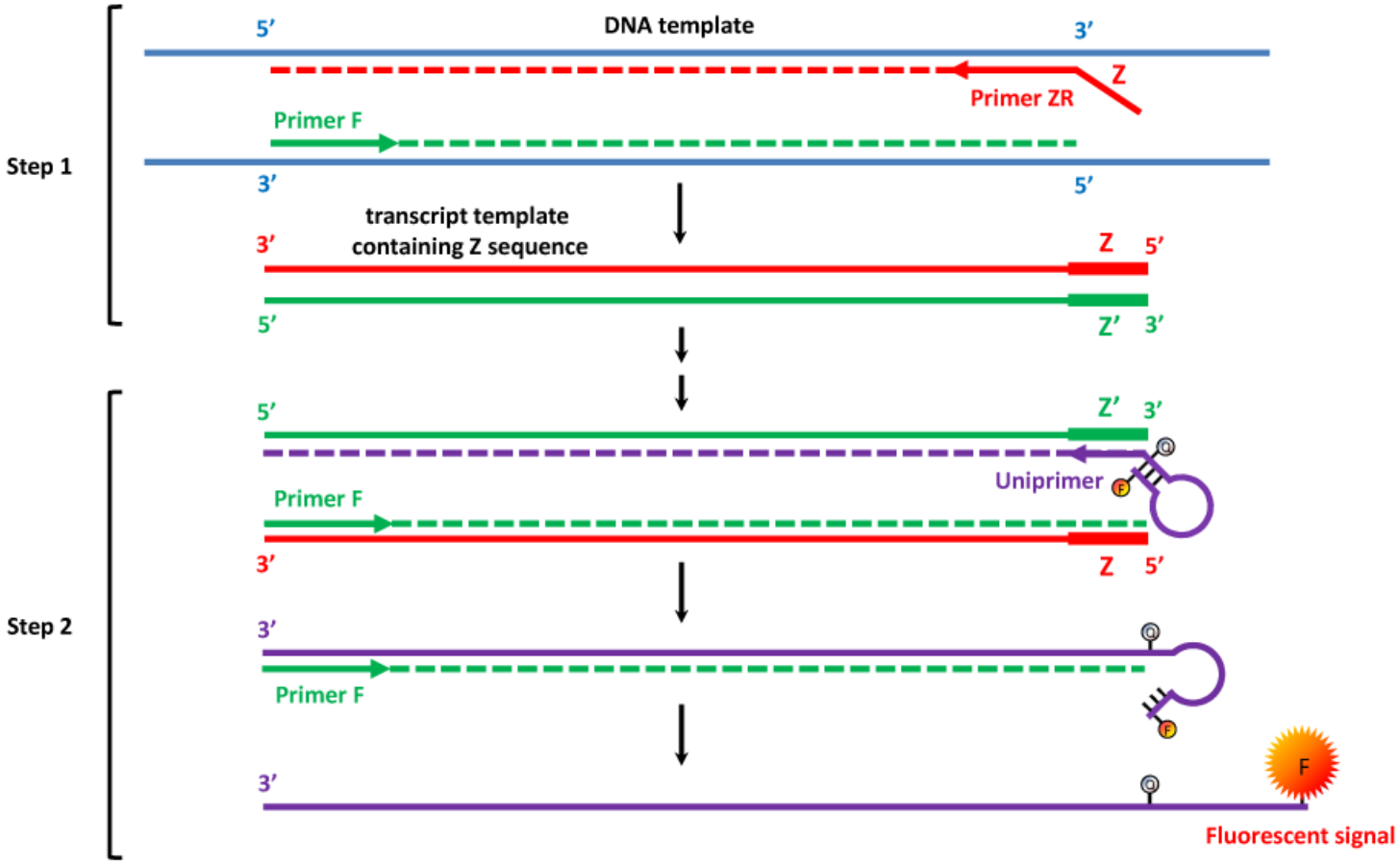

Figure 2.3 Outline of the Amplifluor Uniprimer Universal system

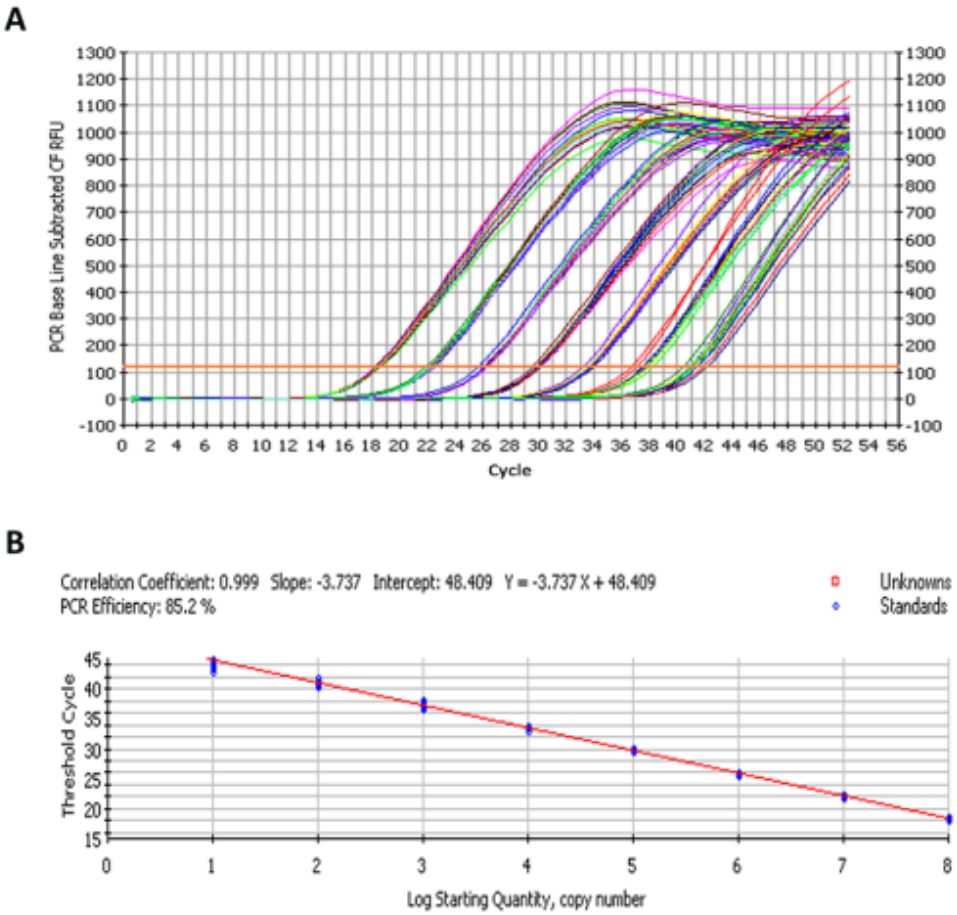

Figure 2.4 Example of standard curve used in transcript quantification
A. Reaction curves for range of PDPL standard samples (10^8 to 10 copy number) **B.** Resultant standard curve based on the threshold cycle and copy number of the of the PDPL standard samples.

2.13 Immunohistochemistry (IHC)

Sections of 4-mm thickness from formalin-fixed, paraffin-embedded tissues were mounted on poly-L-lysine-coated slides and then deparaffinised in xylene and rehydrated through alcohol to distilled water. Endogenous peroxidase activity was blocked with 3% hydrogen peroxide for 15 min at room temperature. After pressure cooking the slides in 10 mmoll-1 EDTA (pH 8.0) for 3 min, the sections were incubated with 5% goat serum, then incubated overnight at 4°C with SphK1 antibody (1:200, Santa Cruz Biotechnologies, Santa Cruz, CA, USA) and also without primary antibody as a negative control. Primary antibodies were detected using a two-step EnVision System (Dako, Glostrup, Denmark). Horseradish peroxidase and diaminobenzedene hydrochloride were the enzyme and chromogen used, respectively. Staining score was independently assessed by two pathologists. The percentage of positive cells and the intensity of cytoplasmic staining were analyzed. Thus all final scoring estimations were stratified into four categories: -, 0% of stained cells; +, <20% weakly to moderately stained cells; ++, 10–20% intensively stained cells and 20–50% weakly stained cells; and +++, 20–50% positive cells with moderate-to-marked staining or >50% positive cells. There was a low level of discrepancy (<5% cases) among the pathologists in terms of scoring, but a consensus was reached after joint review.

The judgment standard referred to the standard of HER2 in NCCN guide. If heterogeneity was also found in the tissues, it will be resected, stained, and revaluated by the pathologist.

2.14 Cellular lysis and protein extraction

At approximately 80-90% confluence cells were harvested for protein extraction. Medium was first aspirated and the monolayer washed in PBS. Subsequently PBS

was replaced with 5ml of fresh PBS and cells were scraped from the flask using a cell scraper, collected and transferred into a universal container. The universal container was centrifuged at 2000rpm for 10 minutes to pellet the cells, before removing the supernatant and resuspending the cell pellet in 150-300µl of protein lysis buffer. The lysate was then transferred to a 1.5ml Eppendorf and placed on a Labinoco rotating wheel (Wolf laboratories, York, UK) (25rpm) for a minimum of 40 minutes at 4°C. Following this, samples were centrifuged at 13,000rpm and 4°C for 15 minutes with the resulting supernatant, containing the protein lysate, transferred to a new 1.5ml Eppendorf and the pellet, containing insoluble discarded. Protein samples were then stored at -20°C until required.

2.15 Protein sample quantification and standardisation

A Bio-Rad *DC*^{TM} protein assay kit (Bio-Rad, Laboratories, Hemel-Hempstead, UK) was used for protein quantification, using the microplate technique. A serially diluted standard was first prepared from 10mg/ml bovine serum albumin (BSA). Subsequently, 5µl of either the standard or sample was transferred to fresh wells of a 96-well plate. Reagent A' was then prepared by combining 20µl of reagent S with 1000µl of reagent A, and 25µl of this reagent A' solution was added to each standard or unknown protein sample. Following this 200µl of reagent B was added to each reaction and the plate incubated for 30 minutes for the colorimetric reaction to occur Absorbance was then read at 620nm on a ELx800 plate reader (Bio-Tek, Wolf laboratories, York, UK) and a standard curve prepared and used to calculate the protein concentration of the unknown samples. All samples were diluted to a standardised concentration before adding an equal volume of 2x Laemmli sample buffer (Sigma-Aldrich, Dorset, UK), boiling at 100°C for 5 minutes and storing at -20°C until required.

2.16 Protein extraction and quantification for Kinexus™ antibody microarrays

AGS cells were cultured in two T75 flasks until reaching 80% confluence before placing in serum hunger followed by addition of treatments or left in control conditions. Cells were then lysed as described in section 2.14, using 500-600µl of the Kinexus lysis buffer outlined in section 2.4.1.5.

A fluorescamine based assay was used to quantify protein samples for the Kinexus microarray due to incompatibility of the lysis buffer with the Bio-Rad DC kit. Fluorescamine acetone was made by dissolving 15mg of fluorescamine (Sigma-Aldrich, Dorset, UK) in 5ml absolute acetone (Fisher Scientific UK, Loughborough, UK) in a glass vial and stored at 4°C until required in the assay. A standard was prepared as described earlier from a BSA stock in PBS and the protein samples were diluted 1:10 in PBS. Subsequently, 150µl of each BSA standard or diluted protein samples were aliquoted into triplicate wells of a 96-well plate. Following this, 50µl of fluorescamine acetone, previously prepared, was added and the plate agitated for 1 minute. Fluorescence was then detected using a GloMax®-Multi Microplate Multimode Reader (Promega, Southampton, UK) with a 365nm excitation and 410-460nm emission filter and a standard curve generated from the BSA standards. Subsequently, sample concentration was determined using the standard curve and protein samples standardised to 4mg/ml. Following standardisation, half of the sample was sent to Kinexus Bioinformatics (Vancouver, Canada) for analysis on the protein antibody microarray and the remaining sample frozen at -20°C.

2.17 Tris-glycine sodium dodecyl sulphate polyacrylamide gel electrophoresis (SDS-PAGE) and western blotting

2.17.1 Gel preparation and PAGE

Tris-glycine SDS-PAGE was conducted to explore protein expression using an OmniPAGE VS10DSYS vertical electrophoresis system (OmniPAGE, Cleaver Scientific Ltd., Rugby, UK). The apparatus was assembled in line with the manufacturer guidance. Based on protein predicted size, 15ml (enough for two resolving gels) of either 8% or 10% resolving gels were prepared according to Table 2.7 and 5ml (enough for two stacking gels) of stacking gels were prepared according to Table 2.8.

Table 2.7: Composition of 8% and 10% resolving gel

Component	8% Resolving gel	10% Resolving gel
Distilled water	6.9ml	5.9ml
30% acrylamide mix (Sigma-Aldrich, Inc., Dorset, UK)	4.0ml	5.0ml
1.5M Tris-HCl buffer pH8.8 (Bio-Rad Laboratories, Hemel Hempsead, UK)	3.8ml	3.8ml
10% SDS	0.15ml	0.15ml
10% Ammonium persulphate	0.15ml	0.15ml
Tetramethylethylenediamine TEMED (Sigma-Aldrich, Inc., Dorset, UK)	0.009ml	0.006ml

*8% gel was used to separate proteins with larger molecular weights (>100kDa) with 10% gels being used for lower molecular weight proteins (<100kDa)

Table 2.8: Composition of stacking gel

Component	Stacking gel
Distilled water	3.4ml
30% acrylamide mix (Sigma-Aldrich, Inc., Dorset, UK)	0.83ml
0.5M Tris-HCl buffer pH6.8 (Bio-Rad Laboratories, Hemel Hempsead, UK)	0.63ml
10% SDS	0.05ml
10% Ammonium persulphate	0.05ml
TEMED (Sigma-Aldrich, Inc., Dorset, UK)	0.005ml

The resolving gel was firstly prepared, mixed and loaded between the two glass plates, leaving sufficient space for the comb and stacking gel. Once added, ethanol was added over the top of the resolving gel to prevent an uneven formation. Following polymerisation (approximately 30 minutes) the ethanol was tipped off the top of the resolving gel and the stacking gel prepared, mixed and added over the top of the resolving gel before inserting a Teflon comb into the stacking gel solution. After polymerisation of the stacking gel, the loading cassette, containing the glass plates was inserted into the electrophoresis tank and 1X running buffer added upto the maximum limits. Following this the comb was removed and an appropriate volume of protein sample (dependent on comb size) or 8µl of a BLUeye Prestained Protein Ladder (Geneflow ltd., Lichfield, UK) was loaded into the wells before running the gel at 120V, 50mA and 50W using a EV243 power consort (Topac Inc., Cohasset, MA, USA) until sufficient separation had occurred.

2.17.2 Protein transfer to PVDF membrane

Immobilon-Polyvinylidene fluoride or polyvinylidene difluoride (PVDF) transfer membrane (EMD Millipore Corporation, Billerica, MA, USA) was cut to 7.5 x 7.5cm dimensions before soaking in methanol (Fisher Scientific UK, Loughborough, UK) for 30 seconds, rinsing and placing in 1x transfer buffer. In addition, six squares of filter paper (Sigma-Aldrich, Dorset, UK) were cut to 8 x 8cm dimensions and soaked in 1X transfer buffer.

Mini Trans-Blot cell (Bio-Rad Laboratories, Hemel-Hempstead, UK) was used to transfer proteins from an acrylamide gel to a PVDF membrane. Following electrophoresis completion, the electrophoresis tank and cassette was dismantled and the stacking gel cut away from the resolving gel. The resolving gel was then carefully transferred onto a PVDF membrane in a sandwich like structure consisting of

Cathode: fibre pad:3X filter paper: Gel: PVDF membrane:3X filter paper: fibre pad: Anode This was then placed into the electrode assembly in the buffer tank before filling with 1X transfer buffer, covering with the lid, placing the tank at 4°C and running at 100V, 200mA, 50W for 1-2 hours (depending on protein size).

2.17.3 Protein staining and immunoprobing

2.17.3.1 Ponceau S membrane staining

Ponceau S stain was used to stain membranes in order to confirm transfer or to aid in cutting of membranes. Following transfer the membrane was placed in a weighing boat and immersed in Ponceau S whilst shaking. Following this, the membrane was washed with distilled water to allow visual confirmation of protein bands.

2.17.3.2 Immunoprobing

Following blotting the membrane was placed into a 50ml falcon tube, with the protein side facing inwards, containing 10ml of blocking buffer (5% low fat milk and 0.1% Tween 20 in PBS) before transferring the tube to a roller (Stuart, Wolf Laboratories, York), and incubating for one hour at room temperature. Following the blocking stage, blocking buffer was discarded and the primary antibody was diluted in fresh 5ml blocking solution as outlined in Table 2.6, added into the falcon tube and incubated overnight at 4°C. Following incubation with the primary antibody, the primary antibody solution was removed and three 10 minutes washes with 10ml of wash buffer (0.1% Tween 20 in PBS) conducted to remove unbound primary antibody. Following the removal of the last wash buffer, a horseradish peroxidase (HRP) conjugated secondary antibody, specific to the species used in the primary antibody, was added in 5ml blocking buffer to the falcon tube at concentrations outlined in Table 2.6, which was then placed on the roller for 1 hour at room

temperature. Following incubation with the secondary antibody, the buffer was removed and the membrane washed again 3 times with wash buffer. Following this, the EZ-ECL Chemiluminescent Detection Kit (Geneflow ltd., Lichfield, UK) was used to detect proteins. Solution A and B were mixed in equal volumes in a Bijou and incubated at room temperature for 5 minutes in the dark to equilibrate. Once equilibrated, the membrane was removed from the falcon tube and excess wash buffer removed before adding the combined EZ-ECL solution over the membrane and incubating for 1 minute in the dark. Excess combined EZ-ECL solution was then removed and the membrane placed in a G:BOX Chemi XRQ imaging system (Syngene, Cambridge, UK) to detect and capture images. In addition to detecting proteins of interest, GAPDH expression was also detected as a housekeeping control.

Image J v1.50c (downloaded from https://imagej.nih.gov/ij/) was used to quantify band densities. Densities of the bands obtained for the proteins of interests were normalised based on GAPDH expression within the samples.

2.18 Cell functional assays

2.18.1 *In vitro* thiazolyl blue tetrazolium bromide (MTT) and crystal violet for cell proliferation assay

MTT (3-(4,5-dimetheylthiazol-2-yl)-2,5-diphenyltetrazolium bromide) tetrazolium was used for cell viability assays and response of cells to cytotoxic agents. Viable, metabolically active cells convert MTT into a purple coloured formazan product, which can subsequently be dissolved in DMSO and the resulting absorbance read on a plate spectrophotometer, corresponding to viable cell numbers (Riss et al., 2004).

Sub confluent flasks were trypsinised and counted as described in section 2.5.2. Subsequently, 2,000 cells were seeded into replicate wells of a 96 well plate in 100µl. Appropriate concentrations of inhibitors or cytotoxic drugs were then added to obtain

a final volume and desired concentration in 200µl and incubated at 37.0°C, 5% CO_2 and 95% humidity for 48 hours. Following incubation, 20µl of sterile MTT stock solution was added (providing working concentration of 0.5mg/m) and the plates incubated for a further 4 hours. Following this, the medium was gently aspirated to avoid disturbing crystals and 200µl of DMSO added and mixed resulting in a coloured solution. The absorbance of each well of the 96 well plate was then read on an ELx800 plate spectrophotometer at 540nm wavelength. Experiments were repeated a minimum of three times. Cell viability was determined based on the percentage difference between untreated control cells (chemotherapy and SphK1 small inhibitor).

Crystal violet based assays were undertaken by seeding 3,000 cells per well, in replicate wells and replicate plates (one plate per incubation point). At each incubation point, the medium was aspirated, cells fixed in 4% Formalin (Sigma-Aldrich, Dorset, UK) for 10 minutes before aspiration of the Formalin and cell staining with 0.5% (v/v in distilled water) crystal violet (Sigma-Aldrich, Dorset, UK) for 5 minutes. Subsequently, crystal violet stain was dissolved in 10% acetic acid (Sigma-Aldrich, Dorset, UK) (v/v in distilled water) and read on ELx800 plate spectrophotometer at 540nm wavelength.

2.18.2 *In vitro* Matrigel cell adhesion assay

Matrigel cell adhesion assays were used to examine cell-matrix adhesion based on the cell' capacity to attach to a Matrigel® Basement Membrane Matrix (Corning Incorporated, Flintshire, UK). 100µl of serum free medium (SFM) containing 5µg of matrigel was added to the wells of a 96 well plate and dehydrated at 55°C for 2 hours in a Hybrdiser HB-1D drying oven. Subsequently, 100µl of SFM was used to rehydrate the matrigel for 30 minutes before gently removing the SFM and seeding

40,000 cells in 200µl of medium in replicate wells. The plate was then incubated for 45 minutes before removing medium and washing thoroughly with PBS to remove non-adherent cells. Following washing, adherent cells were fixed in 4% formalin (Sigma-Aldrich, Dorset, UK) for 10 minutes before aspirating the formalin and staining with 0.5% (v/v) crystal violet (Sigma-Aldrich, Dorset, UK) for 5 minutes. Subsequently, stain was dissolved in 10% (v/v) acetic acid (Sigma-Aldrich, Dorset, UK) and read on an ELx800 plate spectrophotometer at 540nm wavelength. Experiments were repeated a minimum of three times.

2.18.3 *In vitro* cell migration assay (wound healing assay)

An Environmental Virtual Observatories (EVOS®) FL Auto Imaging System (Life technologies, CA, USA) equipped with EVOS® Onstage Incubator (Life technologies, CA, USA) was used to quantify the migration rate of control and SphK1 knockdown AGS and HGC27 cells in an *in vitro* scratch/wound healing migration assay. Cells were seeded in a 24 well (Greiner Bio-One Ltd., Gloucestershire, UK) plate and grown to confluence. The monolayer was then scraped using a sterile 200µl pipette tip to create a wound in each well before aspirating the medium, washing with PBS and replacing with fresh medium. The plate was then returned to the incubator and allowed to recover for 10 minutes before placing in the onstage incubator of the EVOS system, programmed to maintain an environment of 37°C, 5% CO_2 and 80% humidity. The EVOS system was then programmed to capture multiple images of the wound at specific co-ordinates following 6, 12, 18 and 22 hours in each well.

The distance between the two wound fronts was quantified using Image J at each time point, allowing cell migration to be monitored as the distance between the wound fronts reduced. Experiments were repeated a minimum of three times.

2.18.4 *In vitro* Matrigel invasion assay

Impact of SphK1 knockdown on AGS and HGC27 cell invasion was quantified using a Matrigel cell invasion assay. Inserts with 8.0µm pores (Becton Dickinson, Oxford, UK), placed into wells of a 24 well plate, were coated with 100µl of SFM containing 50µg of Matrigel before dehydration at 55°C for 2 hours in a Hybrdiser HB-1D drying oven. Subsequently, 100µl of SFM was used to rehydrate the matrigel for 30 minutes before gently removing the SFM and seeding 30,000 cells in 200µl of medium. 1ml of growth medium was added to the wells of the 24 well housing the inserts to sustain invasive cells and the plate was incubated for 3 days. Following incubation, cells / Matrigel remaining in the inside of the insert were removed with tissue paper and cells present on the underside of the insert were fixed in 4% formalin for 10 minutes, stained in 0.5% crystal violet for 5 minutes, washed, air dried and visualised under a Leica DMi1 microscope equipped with a MC120 HD camera. Images of several random fields were captured and quantified. The experiment was repeated a minimum of three times.

2.19 Statistical analysis

Statistical analysis was undertaken using the SPSS 24 and graphs prepared using Graph Pad Prism 8. Data was analysed using t-test or Mann Whitney test depending on data parameters. Clinical data was analysed using chi-squared tests, uni- and multi-variant analysis. Values of $p < 0.05$ were regarded as statistically significant.

Chapter III

Expression of sphingosine kinase 1 (SphK1) in human gastric cancer tissues: potential clinical implications for SphK1 in gastric cancer

3.1 Introduction

The area of gastric cancer research has drawn much attention from many healthcare professionals due to the high cost of healthcare resources and high mortality/morbidity for patients seeking appropriate treatment based on the complexity of its underlying mechanisms. Despite advances in understanding of this disease research is still required to identify molecules that may be of therapeutic benefit, either as biomarkers of disease or to aid in the development of new therapeutic strategies.

One such molecule is SphK1, a protein kinase involved in generation of S1P (Moruno Manchon et al., 2016). A pathway which, when subject to improper regulation has been linked to cancer development/progression (Nagahashi et al., 2018a). Similarly, SphK1 has been implicated to play a role in cancer, with an early key study, highlighting SphK1 as an oncogene, demonstrating enhanced *in vitro and in vivo* growth following SphK1 overexpression, which could be supressed following overexpression of a G82D dominant-negative kinase SphK1 mutant or through treatment with an SphK1 inhibitor In keeping with this role of SphK1 transcript and/or protein expression is frequently up-regulated in various types of cancer. Enhanced expression of SphK1 in cancerous, in comparison to normal adjacent tissues has been reported both in mRNA level and protein level, including gastric cancer (Li et al., 2009, Wang et al., 2018b), brain cancer (Li et al., 2008, Van Brocklyn et al., 2005), colon cancer (Kohno et al., 2006, Kawamori et al., 2009, Kawamori et al., 2006) and lung cancer (French et al., 2003, Johnson et al., 2005, Song et al., 2011, Yang et al., 2019), as well as in blood cancer (Bayerl et al., 2008, Le Scolan et al., 2005) and breast cancer (Ruckhaberle et al., 2008, Erez-Roman et al., 2010, Zhu et al., 2017). This research demonstrated that SphK1 played an important role in carcinogenesis. Furthermore, there are a growing number of studies that have associated that enhanced SphK1 expression with poorer patient outlooks, where it has been linked to enhanced tumour malignancy, disease progression, decreased patient survival rates and poor prognosis (Zhang et al., 2014b, Ruckhaberle et al., 2008, Van Brocklyn et al., 2005), Taken together, the above studies and wider literature strongly suggests an association

between SphK1 and cancer, with enhanced expression being linked to cancer development and/or disease progression (Zhang et al., 2014b).

The aim of the current chapter was to explore the expression of SphK1 within a number of cohorts at both transcript and protein level and to further clarify its potential to act as a biomarker for progression and patient prognosis in gastric cancer.

3.2 Methods and materials

3.2.1.1 Cohort 1

This method is fully described in section 2.6 of the main methodology. Briefly, 322 fresh-frozen tissues were used to undertake qPCR transcript analysis in which we got 183 paired normal tissue. Tissue was obtained from cT2-4N0M0 or cT1-4N1-3M0 gastric cancer patients treated between January 2006 and December 2007 in Peking University Cancer Hospital. All protocols were reviewed and approved by the local ethics committee and informed consent was obtained from the patients before therapy.

3.2.1.2 Cohort 2

263 paraffin-embedded tissues were used to undertake IHC protein analysis. Tissue was obtained from cT2-4N0M0 or cT1-4N1-3M0 gastric cancer patients treated between January 2003 and December 2011 in Peking University Cancer Hospital. All protocols were reviewed and approved by the local ethics committee and informed consent was obtained from the patients before therapy.

3.2.2 Immunohistochemisty

This method is fully described in section 2.13 of the main methodology and as previously described (Gao et al., 2015). Staining score was independently assessed by two pathologists. Percentage of positive cells and intensity of cytoplasmic staining were analysed.

3.2.3 Total RNA isolation and quantification

This method is fully described in section 2.7 of the main methodology. In brief, total RNA isolation was performed with TRI Reagent kit (Sigma-Aldrich, Dorset, UK) as previously

described (Ye et al., 2014). RNA concentration and purity were measured on a Nanophotometer (IMPLEN; Geneflow ltd., Lichfield, UK) and samples standardised.

3.2.4 Reverse Transcription (RT)

This method is fully described in section 2.8 of the main methodology. Briefly a 20µl RT reaction was performed using 500ng total RNA template and the GoScript™ Reverse Transcription System (Promega, Southampton, UK). The complementary DNA (cDNA) was then diluted with PCR water by a factor of 1:4 and stored at -20 °C.

3.2.5 Quantitative real-time polymerase chain reaction (qPCR)

The method is fully described in section 2.12 of the main methodology section. In brief, the current study quantified transcript copy number of interest using the Amplifluor™ Uniprimer system (Intergen company®, New York, USA). Primers sequences are shown in Table 3.1.

3.2.6 Conventional polymerase chain (PCR) reaction and agarose gel electrophoresis

This method is fully described in section 2.9 and 2.10 of the general methodology. In brief, PCR was performed with the Promega Green master mix (Promega, Southampton, UK) and 1µl cDNA samples. SphK1 primer sequences used are indicated in table 3.2

Table 3.1. Primers used in qPCR analysis

Primer	Forward primer	Reverse primer
SphK1	5'-ACCATTATGCTGGCTATGAG-3'	5'-*ACTGAACCTGACCGTACA*GAGACAGCAGGTTCATGG-3'
CK19	5'-CAGGTCCGAGGTTACTGAC-3'	5'-*ACTGAACCTGACCGTACA*CCGTTTCTGCCAGT GTGTCTTC-3'

ACTGAACCTGACCGTACA represents the Z sequence

Table 3.2. Primers used in the PCR analysis.

Primer	Forward primer	Reverse primer
SphK1	5'- TGAACCATTATGCTGGCTA-3'	5'- GTGCAGCAAACATCTCACT-3'
GAPDH	5'-GGGCAACGAACTCTTCTAC-3'	5'-TCCAGGTGTCAAGAGTGAA-3'

3.2.7 Protein extraction, quantification and western blotting

This method is fully described in sections 2.14, 2.15 and 2.17 of the main methodology. In brief, following confluence, cells were extracted using a cell scraper, centrifuged to pellet and lysed in a lysis buffer for 1 hour on a rotating wheel. Subsequently, insolubles were removed through centrifugation, the samples quantified using a DC protein assay kit (Bio-Rad, Hemel Hempstead, UK), standardised, mixed 1:1 with 2X laemmli sample buffer (Sigma-Aldrich, Dorset, UK) and boiled for 5 minutes. Sodium Dodecyl Sulphate Poly Acrylamide Gel Electrophoresis (SDS-PAGE) was used to separate protein samples before blotting onto PVDF membranes. Subsequently, the membranes were blocked in 10% skimmed milk for 60 min at room temperature before being probed with anti-SphK1 and anti-GAPDH antibodies (Santa-Cruz Biotechnologies, CA, USA). Membranes were then incubated with a peroxidase-conjugated secondary antibody (Sigma-Aldrich, Dorset, UK) and the protein bands visualised using the EZ-ECL Chemiluminescent Detection Kit (Geneflow ltd., Lichfield, UK).

3.2.8 Statistical analysis

Statistical analysis was performed using the SPSS statistical software package (SPSS Mac Standard version 24.0, SPSS Inc.). The relationship between SphK1 expression and tumour grade, TNM staging and nodal status was assessed using the Mann-Whitney U (mRNA), Chi-square (protein) and Log-rank (protein) tests. Survival was analysed using Kaplan-Meier survival analysis (*p*-values by Cox Proportion Hazardous Analysis). $p < 0.05$ was considered statistically significant.

3.3 Results

3.3.1 Gastric cancer patient cohort

The gastric cancer clinical cohort (Cohort 1) (n = 322) was used to probe SphK1 expression using quantitative PCR. The cohort consisted of 229 men (71.1%) and 93 women (28.9%). All the patients underwent surgery without any prior treatment. The result was that 134 patients were alive, 185 patients died of gastric cancer, 15 patients had metastasis and 119 remained disease-free survival.

Cardiff China Medical Research Collaborative (CCMRC) have a long-term relationship with PKUCH. Therefore, the team used GC patients tissue sample storing in PKUCH biobank. In 2013, RNA of GC samples were extracted and cDNA were reverse-transcribed and multiple genes were detected by qPCR. The above work is the basis on the previous work of whole team before I started to work in the laboratory. I used the qPCR data that had been generated and made statistical analysis.

3.3.2 Gene expression of SphK1 in gastric cancer patients and association with clinicopathological parameters

We evaluated the transcript copies of SphK1 in all patient tissues using real-time quantitative PCR is expressed as median SphK1 transcript copies/µl of cDNA from 50ng total RNA and was standardised using CK19) and compared expression levels to patient clinicopathological data (Table 3.3). The results showed that SphK1 expression was upregulated in tumour tissue compared to adjacent normal tissue ($p < 0.001$). Transcript levels of SphK1 were significantly upregulated in tumours at more advanced depth of invasion (T1+T2 versus T3+T4, $p = 0.009$), further lymph node metastasis (N0 versus N3, $p = 0.0244$) and more advanced grade of TNM stage

(TNM1 versus TNM4, TNM1+TNM2 versus TNM3 + TNM4, $p = 0.0334$, $p = 0.0225$, respectively). Furthermore, statistical analysis revealed significant links between the different clinical outcomes and transcript levels (Alive versus Death, $p = 0.0379$). However, there was no significant correlation between the transcript level of SphK1 and distant metastasis, vascular invasion, tumour location or differentiation (all $p > 0.05$).

Table 3.3. The association of SphK1 transcript expression and clinical parameters.

Category		No.	Median	Q1	Q3	p^a
T/N[b]						<0.001
	Normal	183	0.10	0	21	
	Tumour	322	2.50	0	56	
Gender						0.7876
	Male	229	0.10	0	16	
	Female	93	0.10	0	29	
Location						
	Cardia	66	0.30	0	53	
	Fundus	21	2.90	0	52	0.3310
	Corpus	61	0.10	0	27	0.4796
	Pylorus	130	0.00	0	16	0.1696
Differentiation						
	Diff-H	1	0.00	N/A	N/A	
	Diff-HM	6	0.03	0	1.69	
	Diff-M	62	0.03	0	6	0.3812
	Diff-ML	81	0.08	0	28	0.2121
	Diff-L	137	0.10	0	29	0.2510
T stage						
	T1	16	0.01	0	0.64	
	T2	25	0.00	0	0	0.3706
	T3	31	6.20	0	83	0.0586
	T4	232	0.08	0	26	0.2526
	T1+T2	41	0.00	0	0	
	T3+T4	273	0.10	0	28	0.009
N stage				0		
	N0	71	0.00	0	5	
	N1	48	0.00	0	8	0.8221
	N2	64	0.00	0	24	0.1375
	N3	133	0.00	0	45	0.0244
			0.00			
	N0	71	0.00	0	5	
	N1+N2+N3	245	0.00	0	29	0.0519
M stage				0		0.7139
	M0	280	0.10	0	13	
	M1	41	0.00	0	93	
TNM stage				0		
	I	25	0.00	0	0.60	
	II	59	0.02	0	10	0.5474
	III	220	0.20		30	0.0516
	IV	9	1.00	0	258	0.0334
	I+II	84	0.00	0	4	
	III+IV	229	0.00	0	32	0.0255
Vascular invasion						0.6462
	No invasion	152	0.00	0	23	
	Invasion	155	0.10	0	19	

Clinical outcome			0		0.0379
Alive	134	0.00	0	4	
Death	185	0.40	0	45	

p^a: Mann-Whitney U test

3.3.3 Association between SphK1 transcript expression and gastric cancer patient survival

Using median value as the cut off to define high and low transcript level of SphK1, Kaplan-Meier survival curves revealed that patients with a low expression of SphK1 generally had a better overall survival (OS) and disease-free survival (DFS) than those with SphK1 high expression in gastric cancer patients. However, this difference did not reach statistical significance ($p = 0.196$ and $p = 0.570$, respectively) (Figure 3.1. A).

Although there was no statistical difference in the survival time in our own cohort, we examined the expression of SphK1 in GEO database to check whether the expression of SphK1 contributed to survival. In the GEO database (GSE26253) cohort, we found that the low expression of SphK1 had a better RFS compared to the high expression of SphK1 in GC patients ($p = 0.034$) (Lee et al., 2014) (Figure 3.1. B).

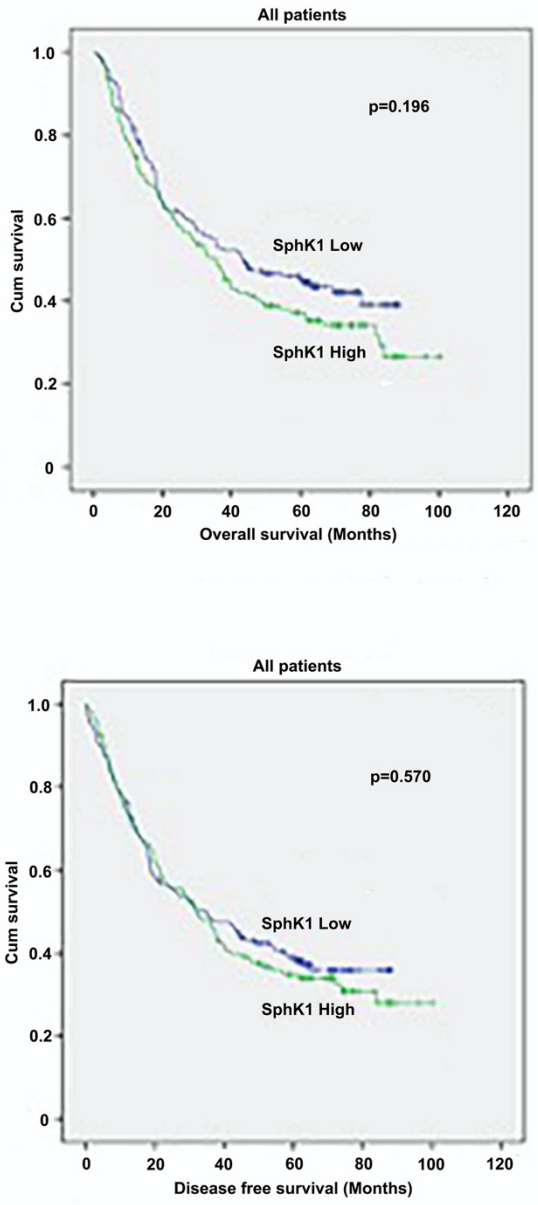

Figure 3.1.A. Kaplan-Meier survival curves demonstrating the relationship between SphK1 mRNA expression and overall survival (Top panel) and disease-free survival (bottom panel)

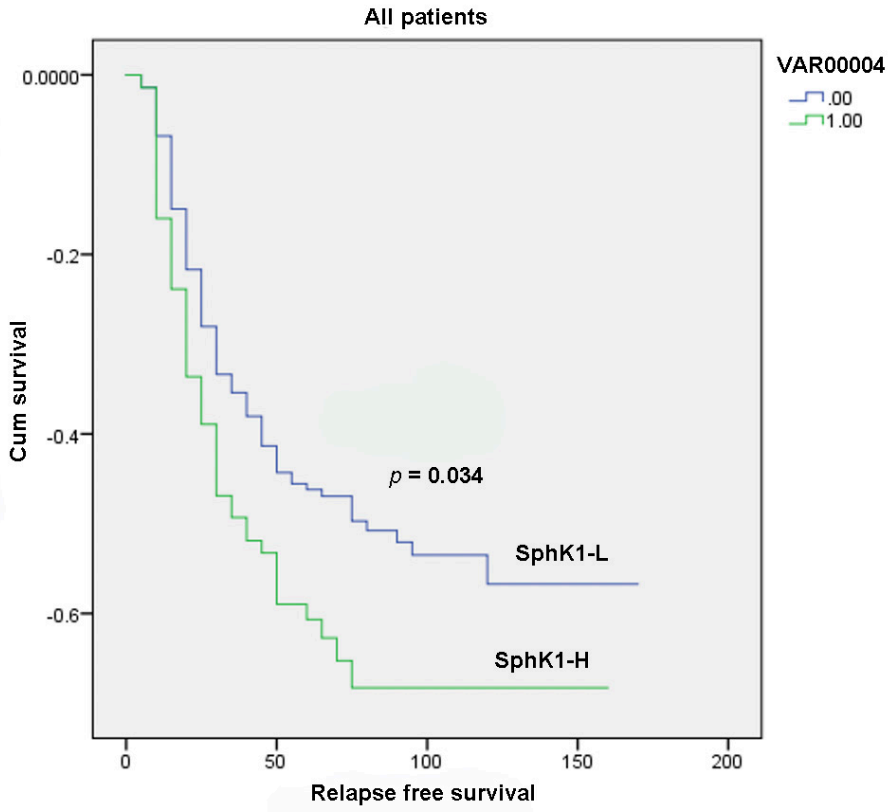

Figure 3.1. B. Kaplan-Meier survival curves demonstrating the relationship between SphK1 mRNA expression and relapse free survival from GEO database (GSE26253).

3.3.4 Conventional PCR analysis of SphK1 expression in paired tissues in gastric cancer patients

A subset of 10 gastric cancer samples and paired adjacent normal samples (5cm away from tumour margin), taken from the Biobank of Peking University Cancer Hospital, were used to explore the mRNA expression of SphK1 within gastric cancer and paired normal tissue samples (Figure 3.2). The results indicate that SphK1 is routinely higher in the tumour tissue in comparison to the paired normal equivalent, with the vast amounts of pairs demonstrating a substantially higher level in the tumour component that the normal paired equivalent.

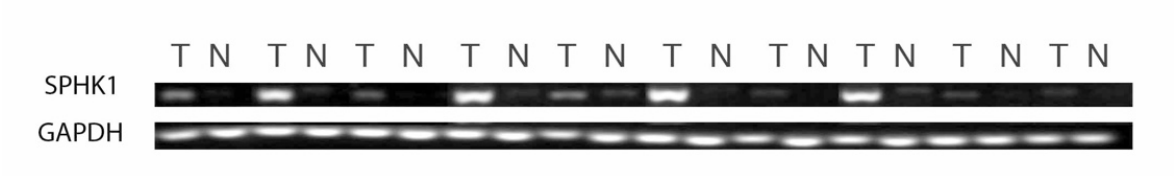

Figure 3.2. Representative images of SphK1 mRNA expression in gastric tissue of 10 different patients showing tumour (T) and paired adjacent normal (N) tissues.

3.3.5 Protein expression levels of SphK1 in gastric cancer tissues

Another gastric cancer clinical cohort (Cohort 2) (n = 263) was used to explore SphK1 protein expression using immunohistochemistry (IHC) analysis. Staining intensity was assigned as negative expression '-' and '+', '++', '+++' as positive expression. Immunostaining data were available for 100% (263/263) of cases, with 6 cases lacking interpretable staining data. SphK1 expression was moderately positive (++) in 7.75% of cases (23/263), faintly positive (+) in 25.86% of cases (68/263) and the remaining 65.40% (172/263) of cases showed negative staining (-). In addition, SphK1 was found to be highly expressed in gastric cancer tissue in comparison to paired adjacent normal tissue ($p < 0.001$), and its distribution was mainly confined in the cytoplasm (Figure 3D). Representative staining patterns from 3 patients are shown in Figure 3.3A.B.C.

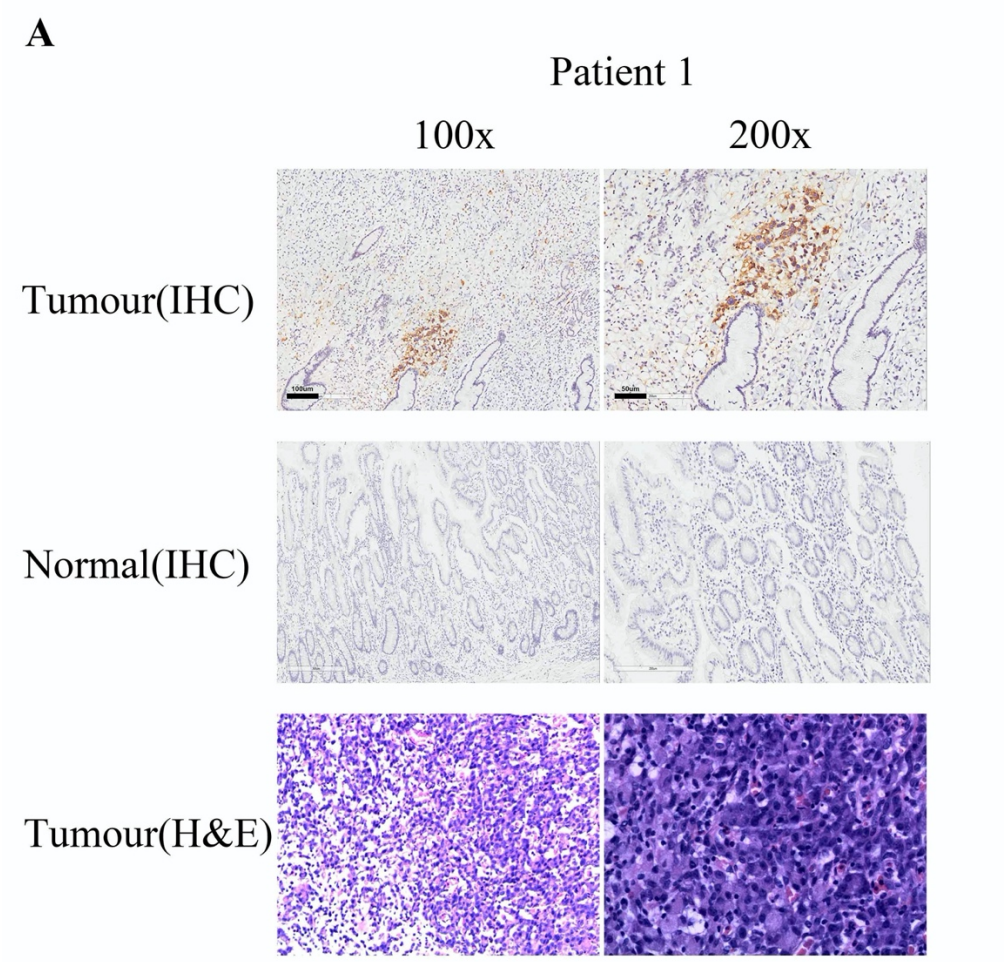

Figure 3.3. A. Representative images of SphK1 immunohistochemical staining in gastric tissue of Patient 1(No. 62629) showing tumour (Top panel; Tumour), adjacent normal tissue (Middle panel; Normal) and H&E staining in the same patient tumour tissue (Bottom panel) (100x & 200x, respectively).

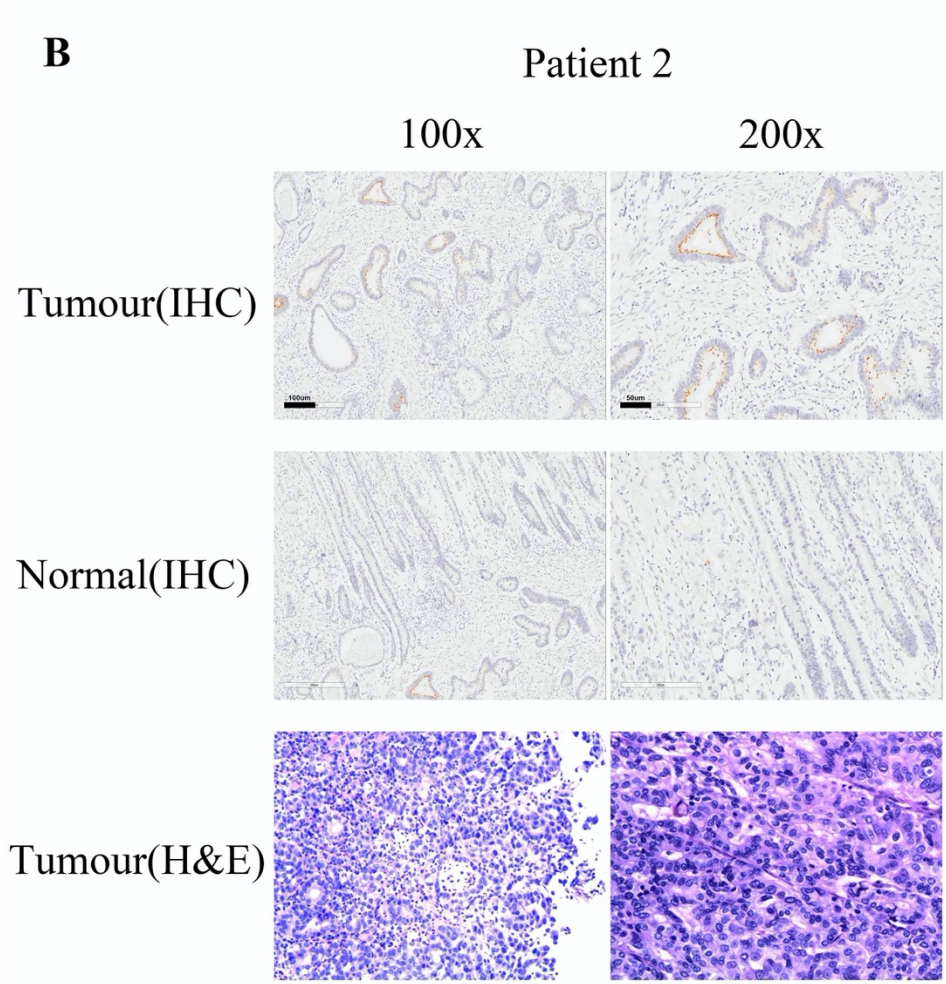

Figure 3.3. B. Representative images of SphK1 immunohistochemical staining in gastric tissue of Patient 2 (No. 62969) showing tumour (Top panel; Tumour), adjacent normal tissue (Middle panel; Normal) and H&E staining in the same patient tumour tissue (Bottom panel) (100x & 200x, respectively).

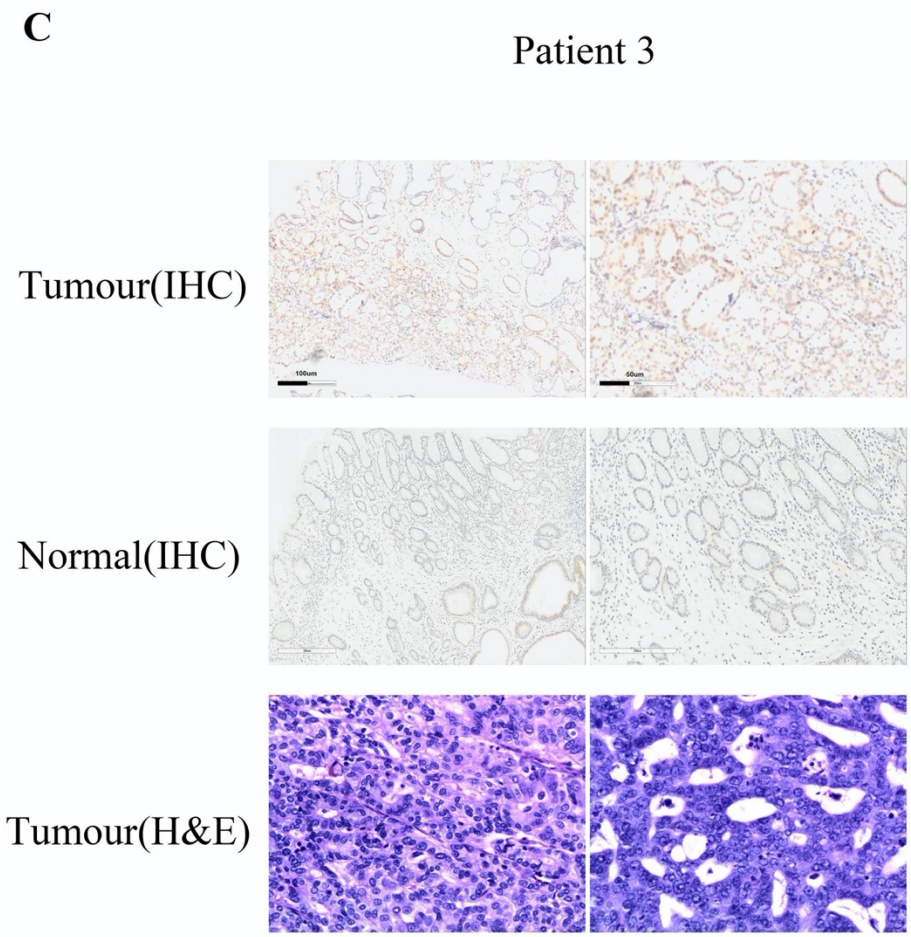

Figure 3.3. C. Representative images of SphK1 immunohistochemical staining in gastric tissue of Patient 3 (No. 65078) showing tumour (Top panel; Tumour), adjacent normal tissue (Middle panel; Normal) and H&E staining in the same patient tumour tissue (Bottom panel) (100x & 200x, respectively).

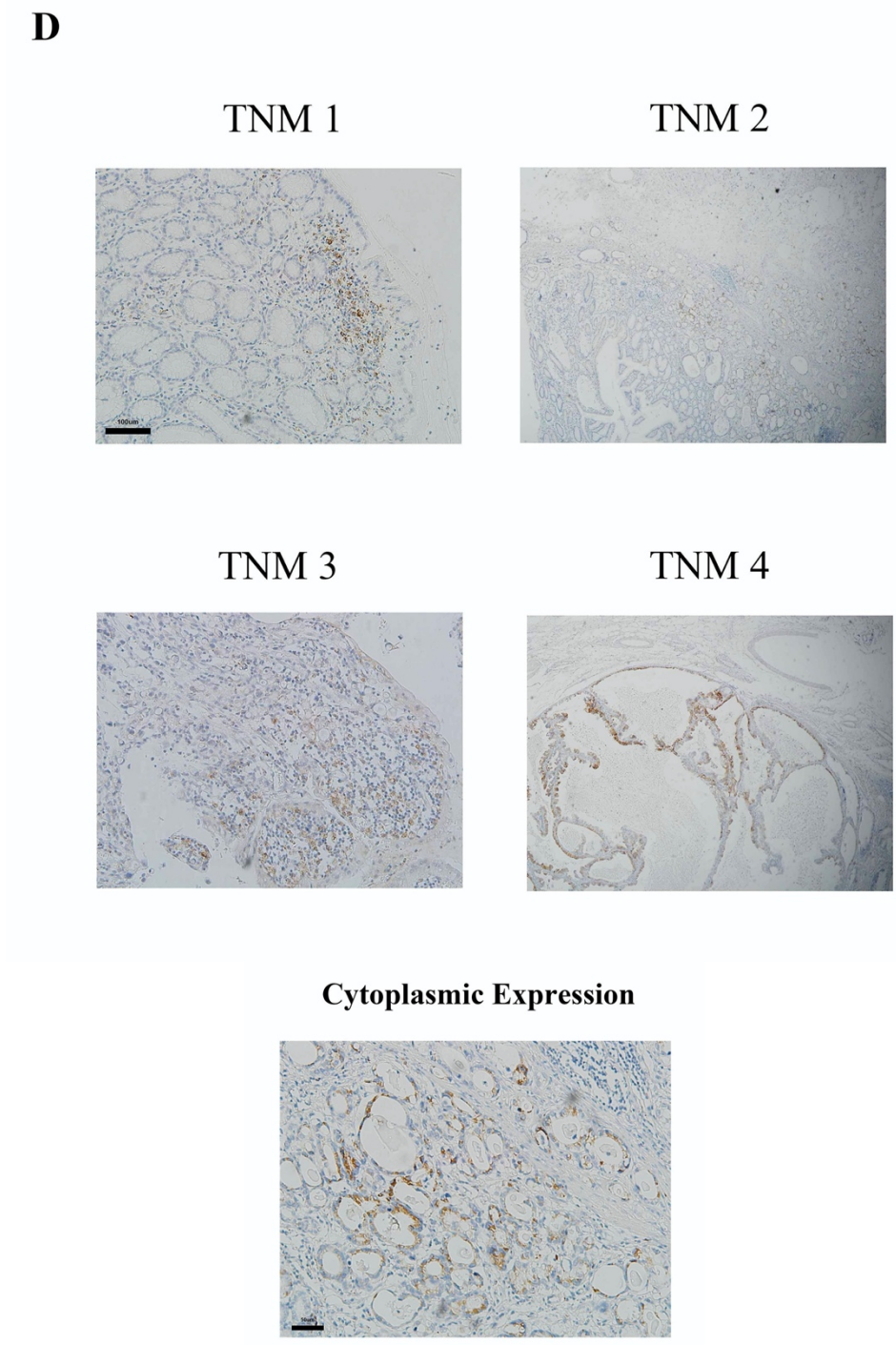

Figure 3.3. D. Representative images of SphK1 immunohistochemical staining in gastric tissue demonstrating higher SphK1 expression in higher TNM stage tissues and the cytoplasmic distribution of SphK1.

3.3.6 Expression of SphK1 in gastric cancer tissues and association with clinicopathological parameters

The staining profile of SphK1 in gastric cancer tissues was further compared to patient clinical pathological information (Table 3.4; Figure 3.3D). Upon analysis it was seen that positive expression of SphK1 was positively associated with lymph node metastasis (N0 versus N1 versus N2 versus N3; $p = 0.003$, N0 versus N1 + N2 + N3; $p = 0.003$), distant metastasis ($p = 0.004$) and TNM stage (TNM1 versus TNM2 versus TNM3 versus TNM4; $p < 0.004$, TNM1 + TNM2 versus TNM3 + TNM4; $p = 0.005$). There was no significant correlation between SphK1 expression and gender, age, tumour location, tumour size, Lauren type, differentiation, histology, lymphovascular invasion and depth of invasion (all $p > 0.05$). However, an increasing trend in the expression of SphK1 was observed from T1+T2 to T3+T4, and from T1 to T2+T3+T4. Also, comparison between the absence and presence of lymphovascular invasion showed an increasing trend and near statistical significance ($p = 0.084$) (Table 3.4).

Table 3.4. Association of SphK1 expression with clinicopathological features in gastric cancer patients

Clinicopathological Features	SphK1 expression		p^b
	Negative (%)	Positive (%)	
Gender			0.640
Male	120 (64.5)	66 (35.5)	
Female	52 (67.5)	25 (32.5)	
Age (year)			0.932
>60	86 (71.4)	46 (28.6)	
≤60	86 (74.1)	45 (25.9)	
Tumour location			0.950
Upper 1/3	36 (61.7)	17 (38.3)	
Middle 1/3	40 (67.2)	20 (32.8)	
Low 1/3	90 (78.3)	51(21.7)	
Total	6 (100.0)	3 (0.0)	
Cardia & Non-			0.671
Cardia cancer	30 (68.2)	14 (31.8)	
Non-cardia cancer	144 (64.8)	71 (35.2)	
Tumour size (cm)			0.512
>4.0	81 (67.5)	39 (32.5)	
≤4.0	91 (63.6)	52 (36.4)	
Lauren type			0.752
Intestinal type	32 (61.5)	20 (38.5)	
Diffuse	95 (65.5)	50 (34.5)	
Mixed type	45 (68.2)	21 (31.8)	
Differentiation			0.685
Well-Moderate	82 (69.2)	41 (30.8)	
Poor	90 (75.8)	50 (24.2)	
			0.573
Well	6 (66.7)	3 (33.3)	
Moderate	76 (66.7)	38 (33.3)	
Poor	78 (62.4)	47 (37.6)	
Singnet	12 (80.0)	3 (20.0)	
Histology			0.604
Adenocarcinoma	146 (66.1)	75 (33.9)	
Other types*	26 (61.9)	16 (38.1)	
Lymphovascular			0.084
Absent	93 (70.5)	39 (29.5)	
Present	79 (60.3)	52 (39.7)	
Depth of invasion			0.286

T_1	13 (68.4)	6 (31.6)	
T_2	24 (72.7)	9 (27.3)	
T_3	1 (25.0)	3 (75.0)	
T_4	134 (64.7)	73 (35.3)	
			0.330
T_1+T_2	37 (71.2)	15 (28.8)	
T_3+T_4	135 (64.0)	76 (36.0)	
			0.774
T_1	13 (68.4)	6 (31.6)	
T_2+ T_3+T_4	159 (65.2)	85 (34.8)	
Lymph node			0.003
N_0	49 (81.7)	11 (18.3)	
N_1	36 (73.5)	13 (26.5)	
N_2	26 (60.5)	17 (39.5)	
N_3	61 (55.0)	50 (45.0)	
			0.003
No	49 (81.7)	11 (18.3)	
Yes	123 (60.6)	80 (39.4)	
Distant metastasis			0.004
No	160 (68.4)	74 (31.6)	
Yes	12 (41.4)	17 (58.6)	
TNM stage			0.004
I	25 (75.8)	8 (24.2)	
II	31 (81.6)	7 (18.4)	
III	104 (63.8)	59 (36.2)	
IV	12 (41.4)	17 (58.6)	
			0.181
I	25 (75.8)	8 (24.2)	
II-IV	147 (63.9)	83 (36.1)	
			0.005
I+II	56 (78.9)	15 (21.1)	
III+IV	116 (60.4)	76 (39.6)	

Other types*: Signet-ring cell carcinoma, mucinous adenocarcinoma and et al.
p^b: Chi-square test

3.3.7 Association of SphK1 staining in gastric cancer tissue with patient survival time

Kaplan-Meier survival curves using data from all gastric cancer patients (n = 257) (Cohort 2) revealed that patients with positive SphK1 expression had worse overall survival (OS; $p < 0.001$) and disease-free survival (DFS; $p < 0.001$) than those that were negative for SphK1. Patients were divided into subgroups according to T stage, N stage, M stage and TNM stage. We found that positive SphK1 expression was associated with worse OS in patients with T2+T3+T4 ($p < 0.001$) (n = 85); and also in those patients in the TNM2+TNM3 ($p = 0.002$) (n = 66), N1+N2+N3 ($p = 0.006$) (n = 80), M0 ($p = 0.003$) (n = 74) and M1 ($p = 0.028$) (n = 17) subgroups. Although there was no statistical significance in N0 subgroup, SphK1 negative expression still showed a better OS and DFS in N0 subgroup (Figure 3.4).

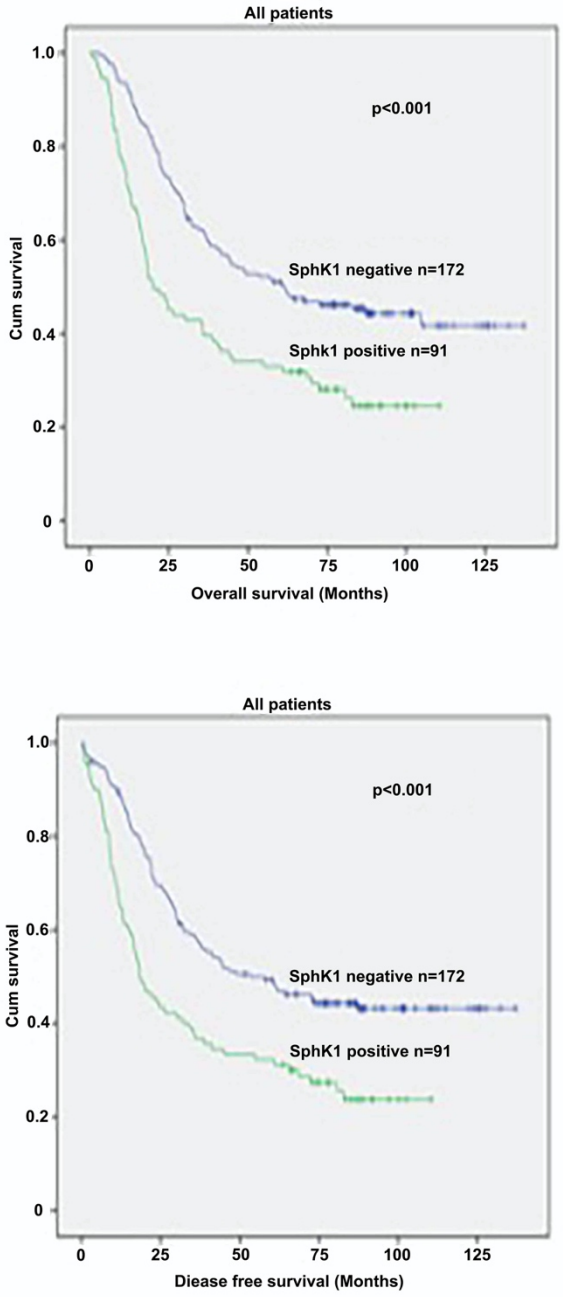

Figure 3.4. Kaplan-Meier survival curves demonstrating the relationship between SphK1 protein level and overall survival (Top panel) and disease-free survival (Bottom panel)

3.3.8 Univariate and multivariate analysis of SphK1 staining in gastric cancer tissues

It was revealed using Univariate analysis (Table 3.5) that the protein expression of SphK1 correlated with tumour location (p = 0.021), tumour size (p = 0.002), lymphovascular invasion ($p < 0.001$), depth of invasion (T1+T2 versus T3+T4, $p < 0.001$), lymph node metastasis (N0 versus N+, $p < 0.001$), distant metastasis (M0 versus M1, $p < 0.001$) and SphK1 (Negative versus Positive, $p < 0.001$). However, there was no significant correlation between the expression level of SphK1 and gender, age, differentiation, Lauren type and histology (all $p > 0.05$). Multivariate analysis revealed that the expression of SphK1 was an independent prognostic factor in gastric cancer patients ($p = 0.001$). Analysis using all parameters as variants also showed that invading cardia ($p < 0.001$), differentiation ($p = 0.011$), lymphovascular invasion ($p = 0.003$), T status ($p < 0.001$), N status ($p < 0.001$) and M status ($p < 0.001$) are independent factors for the overall survival (Table 3.5).

Table 3.5.Univariate and multivariate survival analysis of clinicopathological features of gastric carcinoma patients

Clinicopathological Features	Univariate analysis			Multivariate analysis		
	HR	95% CI	p^c	HR	95% CI	p^d
Gender						
Male vs. Female	1.12	0.790-1.579	0.53			
Age (year)						
≤60 vs. >60	0.830	0.610-1.132	0.240			
Cardia & Non-cardia						
Cardia vs Non-cardia	1.69	1.160-2.476	0.006	2.396	1.607-3.573	<0.001
Tumour location						
Upper 1/3	0.424	0.204-0.878	0.021			
Middle 1/3	0.237	0.112-0.499	<0.001			
Low 1/3	0.259	0.130-0.520	<0.001			
Total			<0.001			
Tumour size (cm)						
>4.0 vs. ≤4.0	0.620	0.455-0.845	0.002			
Lauren type						
Intestinal vs.	0.975	0.668-1.424	0.898			
Differentiation						
Well-Moderate vs.	1.30	0.954-1.776	0.096	1.503	1.098-2.057	0.011
Histology						
Adenocarcinoma vs. Other	1.350	0.907-2.007	0.138			
Lymphovascular invasion						
Absent vs. Present	2.056	1.502-2.815	<0.001	1.637	1.184-2.265	0.003
Depth of invasion						
T_1	0.000		0.937			
T_2	0.256	0.130-0.502	<0.001			
T_3	0.548	0.145-2.359	0.451			
T_4			0.001			
T_1+T_2 vs. T_3+T_4	6.462	3.293-12.677	<0.001	3.611	1.787-7.295	<0.001
Lymph node						
N_0	0.114	0.062-0.209	<0.001			
N_1	0.247	0.152-0.402	<0.001			
N_2	0.636	0.428-0.946	0.025			
N_3			<0.001			
No vs. Yes	5.597	3.104-10.095	<0.001	3.370	1.797-6.319	<0.001
Distant metastasis	0.177	0.116-0.271	<0.001	0.277	0.179-0.428	<0.001
SphK1						
Negative vs. Positive	1.895	1.385-2.594	<0.001	1.726	1.253-2.378	0.001

Other types*: Signet-ring cell carcinoma, mucinous adenocarcinoma and et al;
CI: Confidence Interval; HR, Hazard ratio.
p^c: Log-rank test; p^d: Cox regression test

3.3.9 Protein expression of SphK1 in gastric cancer patients

A subset of 12 gastric cancer samples and paired normal samples, taken from Biobank of Peking University Cancer Hospital, were used to explore the protein expression of SphK1 within gastric cancer samples using western blot (Figure 3.5). Similar to the earlier conventional PCR analysis, SphK1 protein levels were seen to be elevated in the majority of tumour tissues compared to their paired normal equivalents.

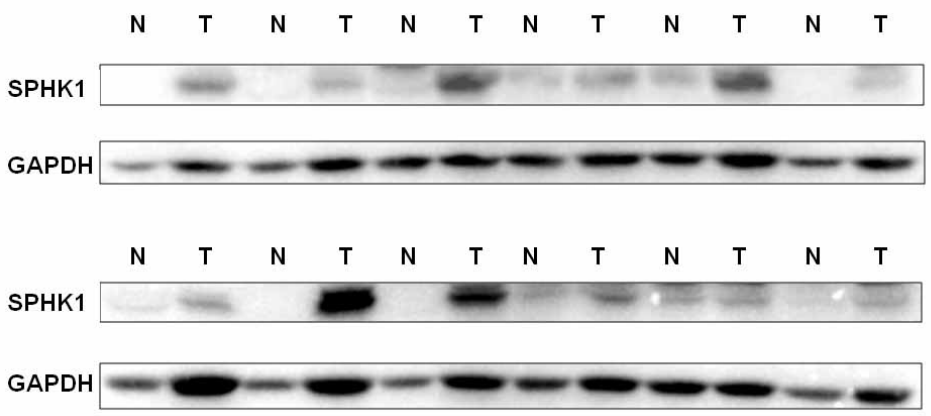

Figure 3.5: Representative images of SphK1 protein expression in gastric tissue of 12 different patients showing tumour (T) and paired adjacent normal (N) tissue

3.4 Discussion

GC represents the third greatest cause of cancer-related mortality and has the fifth highest incidence around the world (Torre et al., 2015). It is a key concern in China which almost half of GC patients worldwide (Ferlay et al., 2015). As early GC has no obvious symptoms, therefore, GC was mostly found in the advance and late stage. As a result, the 5-year survival rate in most countries is usually maintained at 20-40% (Allemani et al., 2018, Arnold et al., 2019). However, South Korea and Japan, with early gastroscopy screening, have a five-year survival rate of 60% . GC is a highly heterogeneous tumour, and there is an urgent need to understand the molecular mechanisms involved in the development and progression of gastric cancer in order to find better molecular markers and therapeutic targets. The identification of novel targets for use in the development of more effective anti-gastric cancer chemotherapy resistant strategies is urgent. Hence, developing new biomarkers for early detection of the tumour and more accurate prediction of disease outcomes as well as the patients' response to chemotherapy regimens could significantly improve efficacy of the treatments and greatly decrease the mortality of gastric cancer.

The current chapter explored the potential of SphK1, a molecule known to play a significant role in regulating oncogenesis, and which has been proposed to alter the balance between apoptotic (Guillermet-Guibert et al., 2009) and pro-survival signalling (Akao et al., 2006, Pchejetski et al., 2005). Previous studies have demonstrated that the expression level of SphK1 is frequently up-regulated in various types of cancer, both at mRNA level and protein level, including gastric cancer (Li et al., 2009), brain cancer (Li et al., 2008, Van Brocklyn et al., 2005), colon cancer (Kohno et al., 2006, Kawamori et al., 2009, Kawamori et al., 2006) and lung cancer (French et al., 2003, Johnson et al., 2005, Song et al., 2011). Similar observations have also been identified in blood cancer (Bayerl et al., 2008, Le Scolan et al., 2005) and breast cancer (Ruckhaberle et al., 2008, Erez-Roman et al., 2010).

and enhanced SphK1 expression has also been linked with poorer patient outlooks, where it has been linked to enhanced tumour malignancy, disease progression, decreased patient survival rates and poor prognosis (Zhang et al., 2014b, Ruckhaberle et al., 2008, Van Brocklyn et al., 2005).

In keeping with these observations in other cancers the data presented in the current chapter has shown that SphK1 expression is enhanced in tumour tissue compared to normal counterparts and is significantly correlated with depth of invasion, lymph node metastasis, distant metastasis, clinical stage and prognosis in gastric cancer patients, whether in the mRNA or protein level. This chapter has also demonstrated that the high expression of SphK1 is associated with poor prognosis of gastric cancer patients. Compared with previous work, the current study demonstrated poor prognosis in patients with high SphK1 expression at both mRNA and protein levels and is supported by the relatively large sample sizes to illustrate the relationship between SphK1 and prognosis. In addition, following multivariate analysis, SphK1 was found to be an independent prognostic factor in patients with gastric cancer which also indicates that SphK1 may be a promising prognosis biomarker of gastric cancer patients. Protein level studies have found that OS of patients with high expression of SphK1 significantly better than patients with low SphK1 expression. However, in the study of mRNA levels, the survival curves of SphK1 high and low expression patients were not separated, which may be due to the large variability of real-time quantitative PCR and the expression of SphK1 at the gene level and protein level were not same.

Hence, the data presented in this chapter supports previous studies focused on GC (Li et al., 2009, Wang et al., 2018b). Li et al., demonstrated enhanced SphK1 expression at both mRNA and protein level in gastric cancer tissues and cell lines compared to the normal equivalents, with higher expression associated with clinical stage, T stage, M stage and survival rates, reporting it as an independent prognostic

factor (Li et al., 2009). More recently Wang et al., (Wang et al., 2018b) showed SphK1 was elevated in GC tumour tissue and also increased the S1P level. Knockdown SphK1 was related to tumour growth. In addition, the expression rate of SphK1 at the protein level was about 34%, and the expression rate of SphK1 in Li et.al., (Li et al., 2009) article is as high as 66%. The reason for this difference might be due to the antibody factor and the lower indoor temperature in the laboratory.

In conclusion, the data presented in this chapter demonstrates and supports a link between SphK1 expression and gastric cancer prognosis and progression. Subsequent chapters will aim to explore the cellular significance and function of SphK1 in gastric cancer cells and its role in chemotherapeutic resistance.

Chapter IV

Establishment of SphK1 knockdown models and its functional significance

4.1 Introduction

The expression of SphK1 is frequently dysregulated in a range of human cancers (Wang et al., 2019b). SphK1 has been established as playing a role in regulating oncogenesis and is able to alter the balance between apoptotic and survival signals (Limaye et al., 2005, Guillermet-Guibert et al., 2009, Akao et al., 2006, Pchejetski et al., 2005). The potential for shifting the balance away from S1P production and towards sphingosine and ceramide production has been investigated as a method to promote apoptosis and inhibit growth (Hannun and Obeid, 2008). Here, SphK1 plays an important role, acting as a kinase which can catalyse conversion of sphingosine into S1P and bring about biological function.

Given its dysregulation in cancer and role in these important processes, the functional role of SphK1 has been investigated in a number of published studies exploring various type of cancer. Recently, a study by Cao et al. has showed that miR-128 can directly target 3'-untranslated region (UTR) of SphK1 and plays a vital role in thyroid carcinoma progression (Cao et al., 2019). Another study also showed *in vivo* that SphK1 contributes to hepatocarcinogenesis, using SphK1 knockout ($SphK1^{-/-}$) mouse models (Chen et al., 2018a). Shimizu's study also demonstrates a link where ER- /PR- /HER2+ human breast cancer cells and mouse models display a reduced level of claudin-2 (CLDN2) expression in mice deficient in SphK1, highlighting a potential link between CLDN2 and SphK1. Hence, therapeutic targeting of SphK1 may present an interesting approach for HER2-positive breast cancer therapies (Shimizu et al., 2018). Furthermore, A recent study has demonstrated poorer prognosis of colorectal cancer patients with SphK1-positive expression compared with those displaying SphK1-negative expression and SphK1 knockdown could inhibit EMT and cellular migratory capacity through focal adhesion kinase/protein kinase B / Matrix metalloproteinase (FAK /AKT / MMPs) axis (Liu et al., 2019).

Hence, SphK1 appears to be an interesting molecule that could influence the aggressive nature of cancer cells. The current chapter aims to assess the functional role of SphK1 in gastric cancer cells and its potential to regulate aggressive cellular characteristics.

4.2 Methods and materials

4.2.1 Synthesis of SphK1 targeting ribozyme by touchdown PCR

This method is described in section 2.11.1 of chapter II. In brief, touchdown PCR was carried out with specific sequences to synthesise different transgenes, labelled as ribozyme 1 and ribozyme 2, targeting different specific GTC or ATC sites with SphK1. Following this a portion of the products were run on a 2% agarose gel to confirm presence before undertaking cloning with the remaining product.

4.2.2 TOPO TA cloning of SphK1 targeting ribozyme into the pEF6/V5-His-TOPO plasmid vector, incorporated transgene orientation check, plasmid amplification and extraction

This methodology is described in section 2.11.2 of Chapter II. In brief, ribozyme transgenes were inserted into a pEF6 / V5-His-TOPO plasmid vector in accordance with the manufacturer's instructions. Subsequently, insert orientation was confirmed using RbBMR and RbToPF (Table 4.1) primers and PCR, before amplifying colonies and harvesting plasmids using a Sigma GenElute plasmid kit in accordance with the manufacturer's instructions (see section 2.11.3 of Chapter II).

4.2.3 Transfection of gastric cancer cells using electroporation and generation of knockdown models

This methodology is described in full in section 2.11.4 of Chapter II. In brief, HGC27 and AGS cells were detached and seeded into electroporation curvettes together with either pEF control plasmid or plasmid containing SphK1 ribozyme transgene before being subjected to electroporation. Cells were subsequently transferred to fresh

flasks and underwent a selective period (5µg/ml blasticidin) before being transferred and routinely cultured in maintenance medium (0.5µg/ml blasticidin).

4.2.4 Total RNA isolation and quantification

This method is fully described in section 2.7 of Chapter II. In brief, total RNA isolation was performed with TRI Reagent kit (Sigma-Aldrich, Dorset, UK) as previously described (Ye et al., 2014). RNA concentration and purity were measured on a Nanophotometer (IMPLEN; Geneflow ltd., Lichfield, UK) and standardised.

4.2.5 Reverse transcription (RT)

This method is fully described in section 2.8 of Chapter II. Briefly a 20µl RT reaction was performed with 500ng total RNA and the GoScript^{TM} Reverse Transcription System (Promega, Southampton, UK). The complementary DNA (cDNA) was then diluted with PCR water by a factor of 1:4 and stored at -20 °C for further use.

4.2.6 Polymerase Chain reaction (PCR) and agarose gel electrophoresis

This method is fully described in section 2.9 and 2.10 of Chapter II. In brief, PCR was performed with the Promega Mix PCR Reaction mix (Promega, Southampton, UK) and 1µl cDNA samples. SphK1 primer sequences used are indicated in Table 4.1.

4.2.7 Quantitative real-time polymerase chain reaction (qPCR)

The method is fully described in section 2.12 of Chapter II. In brief, the current study quantified transcript copy number of interest using the Amplifluor^{TM} Uniprimer system (Intergen company®, New York, USA). Primers sequences are shown in Table 4.1.

4.2.8 Protein extraction, quantification and western blotting

This method is fully described in sections 2.14, 2.15 and 2.17 of Chapter II. In brief, following confluence, cells were extracted using a cell scraper, centrifuged to pellet and lysed in a lysis buffer for 1 hour on a rotating wheel. Subsequently, insolubles were removed through centrifugation, the samples quantified using a DC protein assay kit (Bio-Rad, Hemel Hempstead, UK), standardised, mixed 1:1 with 2X laemmli sample buffer (Sigma-Aldrich, Dorset, UK) and boiled for 5 minutes. SDS-PAGE was used to separate protein samples before blotting onto PVDF membranes. Subsequently, the membranes were blocked in 10% skimmed milk for 60 min at room temperature before being probed with anti-SphK1 (1:1000) and anti-GAPDH (1:4000) antibodies (Santa-Cruz Biotechnologies, CA, USA). Membranes were then incubated with a peroxidase-conjugated secondary antibody (1:10000) (Sigma-Aldrich, Dorset, UK) and the protein bands visualised using EZ-ECL Chemiluminescent Detection Kit (Geneflow ltd., Lichfield, UK).

4.2.9 Invasion assay

This method is described in section 2.18 of Chapter II. In brief, cancer cells were seeded into inserts containing 8µm pores pre-coated with 50µg of Matrigel, suspended above a 24 well plate containing growth medium. Following 3 days

incubation, invaded cells, on the underside of the insert, were fixed in formalin, stained in crystal violet and visualised and counted under the microscope.

4.2.10 Matrix-adhesion assay

This method is described in section 2.18 of Chapter II. In brief, cancer cells were seeded into wells of a 96 well plate pre-coated with 5µg of Matrigel and incubated for 40 minutes. Following incubation, the plate was washed in PBS and adherent cells fixed in formalin and stained in crystal violet before extracting stain in acetic acid and measuring absorbance.

4.2.11 Proliferation assay

This method is described in section 2.18 of Chapter II. In brief, cancer cells were seeded into 96 well plates. Following 0, 1, 3 or 5 day incubation, media was removed from one plate and cells were formalin fixed and stained in crystal violet before extracting stain in acetic acid and measuring absorbance. Growth over the incubation periods was compared to original reference plates.

4.2.12 Migration assay

This method is described in full in section 2.18 of Chapter II. In brief, cancer cells were grown in a 24 well plate until confluent monolayers were formed. Cell monolayers were then scratched with a pipette tip to create a scratch or wound. Images of the wound were taken at several time points and the rate of migration as the wound closed calculated by determining the distance between the wound edges.

4.2.13 Statistical analysis

Statistical analysis was undertaken using the SPSS 24 and Graphpad Prism 8 statistical software packages. Data was found to be normalised and was therefore analysed using t-test. Values of $p < 0.05$ were regarded as statistically significant.

Table 4.1. Primers used in the study

Name of Primer	Sequence of Primer
SphK1 F8	5'- TGAACCATTATGCTGGCTA-3'
SphK1 R8	5'- GTGCAGCAAACATCTCACT-3'
SphK1 F9	5'- TGAACCATTATGCTGGCTA-3'
SphK1 R9	5'- GTGCAGCAAACATCTCACT-3'
SphK1 F1	5'- ACCATTATGCTGGCTATGAG
SphK1 Zr1	5'-ACTGAACCTGACCGTACA GAGACAGCAGGTTCATGG-3'
GAPDH F8	5'-GGGCAACGAACTCTTCTAC-3'
GAPDH R8	5'-TCCAGGTGTCAAGAGTGAA-3'
GAPDH F1	5'- AAGGTCATCCATGACAACTT-3'
GAPDH Zr1	5'-ACTGAACCTGACCGTACA GCCATCCACAGTCTTCTG-3'
T7F	5'-TAATACGACTCACTATAGGG-3'
RbBMR	5'-TTCGTCCTCACGGACTCATCAG-3'
RbToPF	5'-CTGATGAGTCCGTGAGGACGAA-3'
BGHR	5'-TAGAAGGCACAGTCGAGG-3'

Z Sequence 'ACTGAACCTGACCGTACA'

4.3 Results

4.3.1 Expression profile of SphK1 in gastric cancer cell line candidates

The expression levels of SphK1 were examined to determine the strategy for the establishment of *in vitro* models. RNA was isolated from 823, HGC27, 7901, AGS, NUGC3, MKN28 gastric cancer cells and GES1 normal epithelial cells followed by reverse transcription to cDNA and PCR.

SphK1 was expressed in 823, HGC27, 7901, AGS, NUGC3, MKN28 and GES1 cell lines, furthermore, the gene expression levels of SphK1 exhibited moderate expression in most of cell lines. However, low expression of SphK1 was observed in 823 and NUGC3 cells (Figure 4.1).

Following the gene expression profile of SphK1 in the clinical cohort in Chapter III and the expression levels of this molecule in gastric cancer cell lines, it was decided to establish knockdown cell lines for SphK1 to further explore the significance of SphK1in gastric cancer cell model systems. AGS and HGC27 lines were chosen for knockdown models.

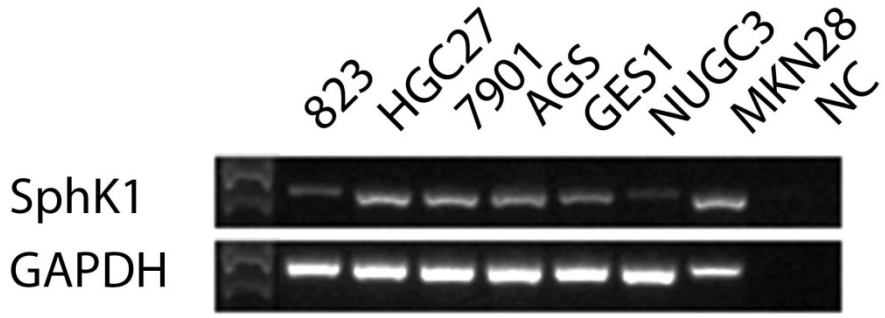

Figure 4.1 Profiling of SphK1 in different gastric cancer cell line
Different gastric cancer cell line cDNA samples were profiled for SphK1 and GAPDH. Representative RT-PCR demonstrating SphK1 expression in different gastric cancer cell lines. GAPDH is presented as a housekeeping control, negative control (NC) represents amplification of PCR water instead of cDNA.

4.3.2 Generation of SphK1 knockdown models using ribozyme transgene

Touchdown PCR was carried out to synthesise transgenes. The products were visualised below 100bp which is in agreement with the size of the two transgenes (Figure 4.2 Top panel). The synthesised transgenes were cloned into a pEF6/V5-His-TOPO plasmid vector, and the transgene orientation was checked using PCR and a combination of plasmid specific and ribozyme specific primers as previously described in the methodology sections. Examples of orientation checks are demonstrated in Figure 4.2 bottom panel.

T7F vs BGHR gave an indication of the inserted product size, with T7F versus RbBMR indicating correct orientation and T7F versus RbToPF indicating incorrect orientation. Positive expression following amplification with the incorrect orientation (T7F versus RbToPF) primer pair rather than the correct orientation pair (T7F versus RbBMR), indicating that the transgene was mostly incorporated into those colonies in the incorrect orientation.

Two randomly picked colonies with correctly orientation transgene inserts from each petri dish were chosen for further incubation. These colonies were inoculated and incubated in two universal tubes containing 5ml of selective LB broth (containing 100µg/ml ampicillin) before plasmid extraction was undertaken.

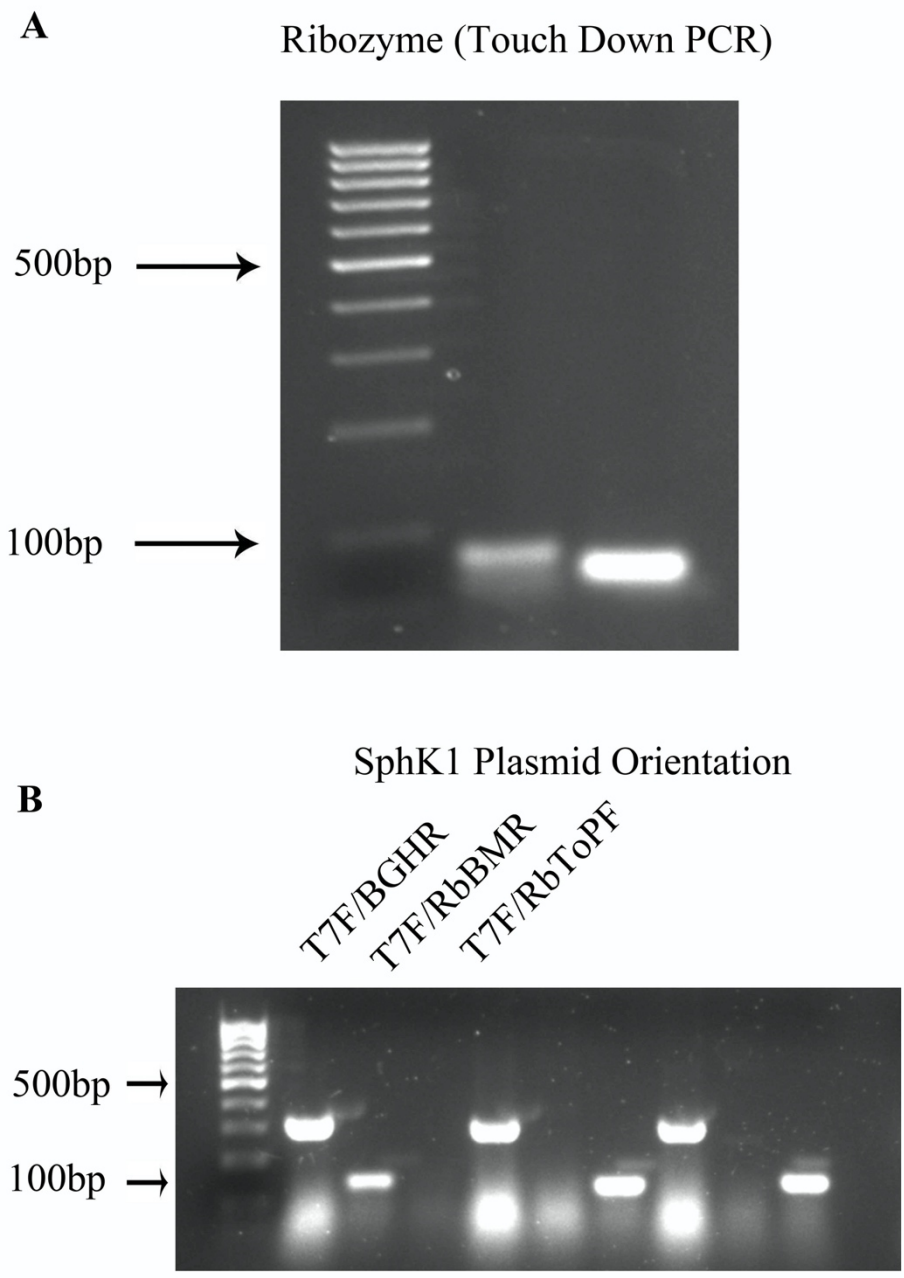

Figure 4.2 Ribozyme transgene synthesis, incorporation and plasmid extraction
Ribozyme transgenes, synthesised by touchdown PCR, were loaded on 2% agarose gel and separated by gel electrophoresis and two bands were visualised below 100bp marker. The predicted size of ribozyme 1 and ribozyme 2 transgene are 85bp and 81bp respectively (A top panel). Colonies had been transfected with ribozyme 1 and 2 incorporated plasmid were inoculated into PCR reaction mix for transgene orientation check (representative examples shown in B bottom panel).

4.3.3 Verification of SphK1 knockdown by ribozyme transgene in gastric cancer cell models

SphK1 targeting ribozyme transgene incorporated plasmids (KD) and control plasmids (pEF) were transfected via electroporation into AGS and HGC27 gastric cancer cell lines. After the blasticidin selection period, RT-PCR, qPCR and western blot were used to verify knockdown of SphK1 in HGC27 and AGS.

SphK1 knockdown was achieved using ribozyme transgene technology in both HGC27 and AGS cell models. Transcript expression levels of SphK1 in the transfected cells were examined using RT-PCR which demonstrated a reduction in SphK1 transcript in comparison to control (pEF) and wild type equivalent cells (Figure 4.3 A and B). The expression of SphK1 in two transfected cell lines (HGC27 and AGS) was found to be significantly reduced, and by more than 50%, compared to the respective control cells (transfected with empty pEF6 plasmids alone) following band quantification ($p < 0.01$ in both cases). SphK1 knockdown in gastric cancer cell lines were further verified using qPCR (Figure 4.3 C) and western blotting, with subsequent band semi-quantification (Figure 4.3 D and E) to explore transcript and protein level respectively. Both qPCR and western blot analysis, similarly, suggested a significant and greater than 50% reduction in SphK1 levels in both knockdown cells compared to controls. Transfected HGC27 and AGS cells containing the ribozyme transgene plasmids were routinely tested to confirm continued knockdown of SphK1 expression in comparison to control cells. Cells transfected with control and transgene plasmid were designated as HGC27 pEF6, HGC27 SphK1-KD, AGS pEF6, AGS SphK1-KD.

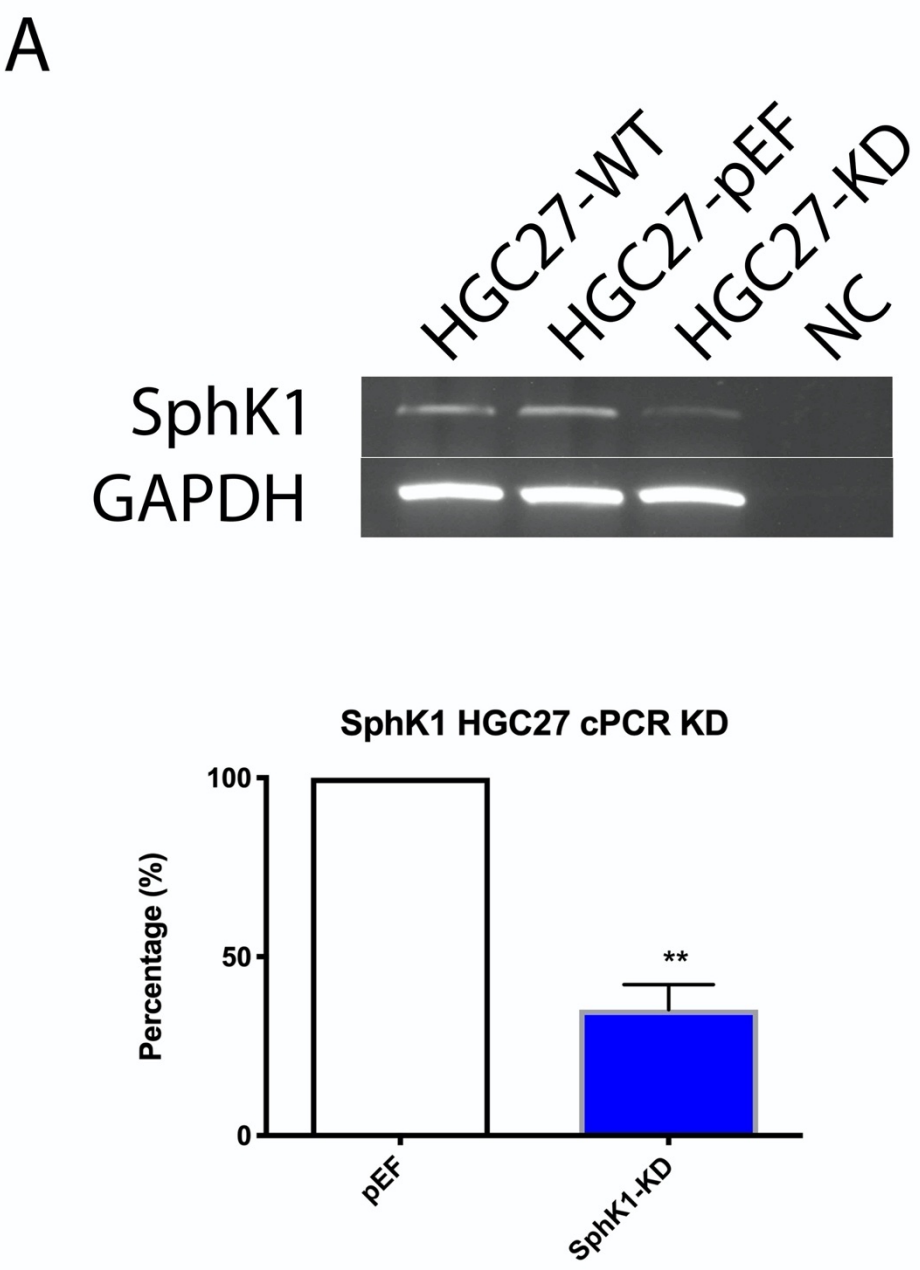

Figure 4.3 Verification of SphK1 knockdown in HGC27 by RT-PCR
A. The transcript level of SphK1 in wild type HGC27 cells transfected with control plasmid (pEF) and ribozyme sequence transgene incorporated plasmids (SphK1-KD) were detected by RT-PCR and normalised by the expression level of GAPDH, with band densitometry shown below blot.
Experiments were repeated a minimum of three times. Data shown represents Mean ± SEM. * represents $p<0.05$, ** represents $p<0.01$.

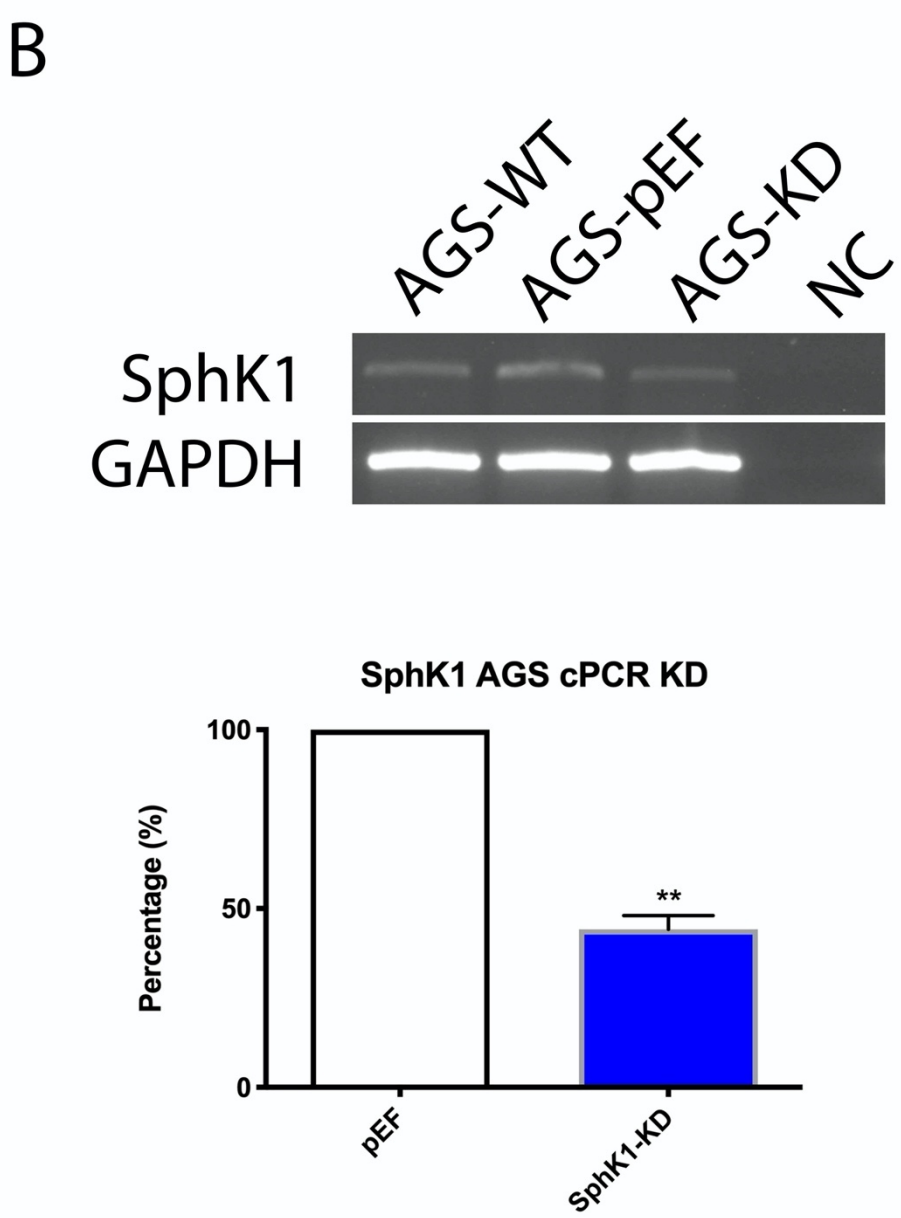

Figure 4.3 Verification of SphK1 knockdown in AGS by RT-PCR
B. The transcript level of SphK1 in AGS cells transfected with control plasmid (pEF) and ribozyme sequence transgene incorporated plasmids (SphK1-KD) were detected by RT-PCR and normalised by the expression level of GAPDH.
Experiments were repeated a minimum of three times. Data shown represents Mean ± SEM. * represents $p<0.05$, ** represents $p<0.01$.

C

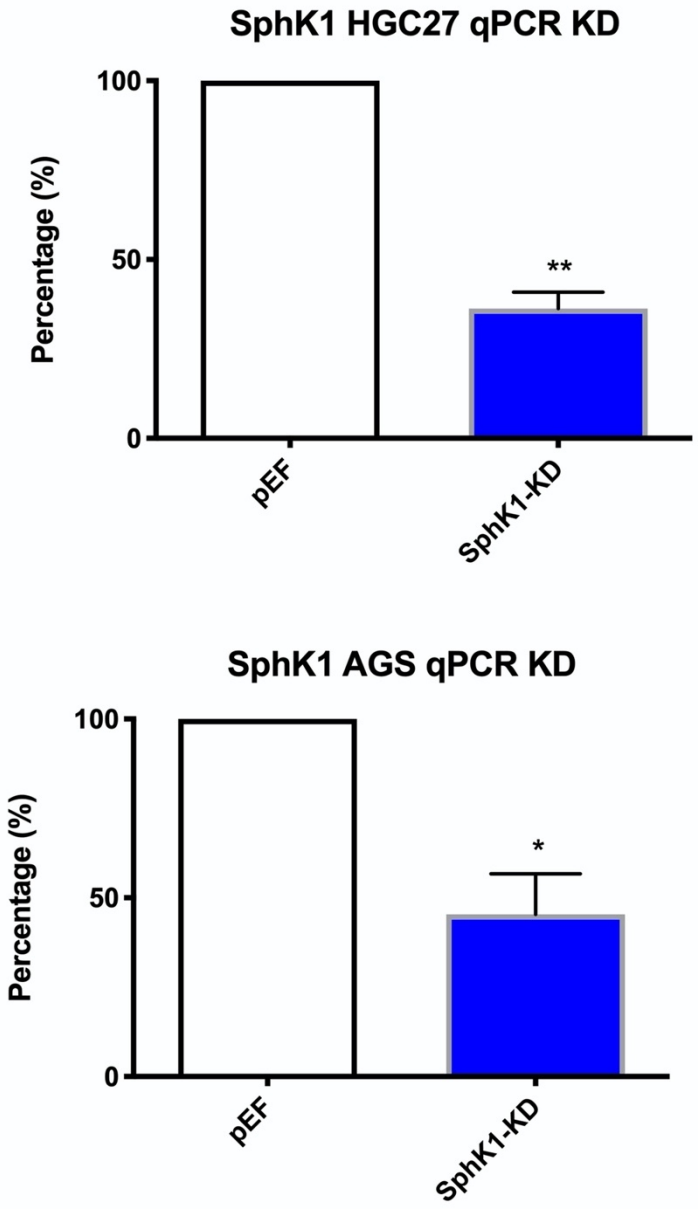

Figure 4.3 Verification of SphK1 knockdown in HGC27 and AGS by qPCR
C. The transcript level of SphK1 in HGC27 and AGS cells transfected with control plasmid (pEF) and ribozyme sequence transgene incorporated plasmids (SphK1-KD) were detected by qPCR and normalised by the expression level of GAPDH.
Experiments were repeated a minimum of three times. Data shown represents Mean ± SEM. * represents $p<0.05$, ** represents $p<0.01$.

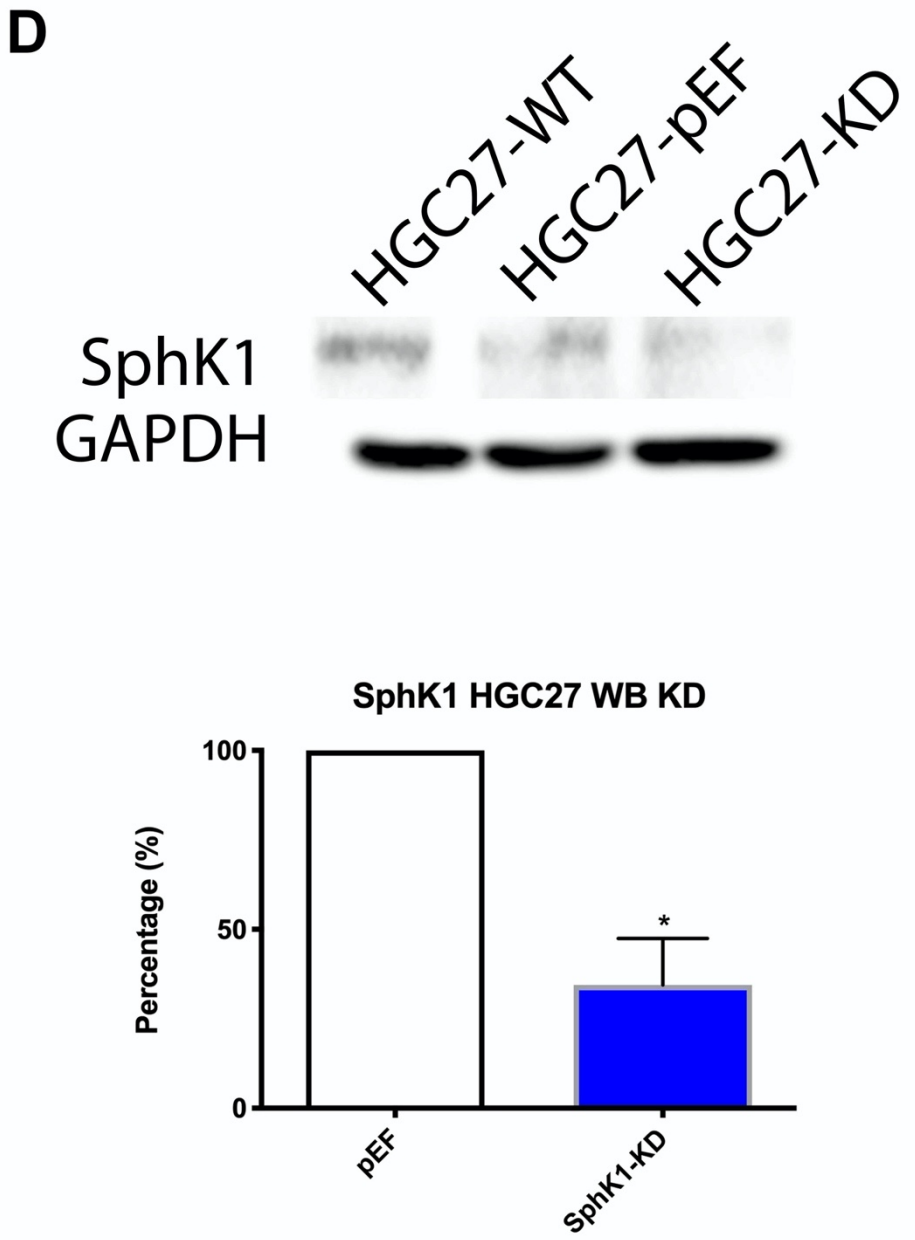

Figure 4.3 Verification of SphK1 knockdown in HGC27 by western blotting
D. The protein expression level of SphK1 and GAPDH in HGC27 cells transfected with control plasmid (pEF) and ribozyme sequence transgene incorporated plasmids (SphK1-KD) were detected by western blotting, with band densitometry shown below blot. Experiments were repeated a minimum of three times. Data shown represents Mean ± SEM. * represents $p<0.05$, ** represents $p<0.01$.

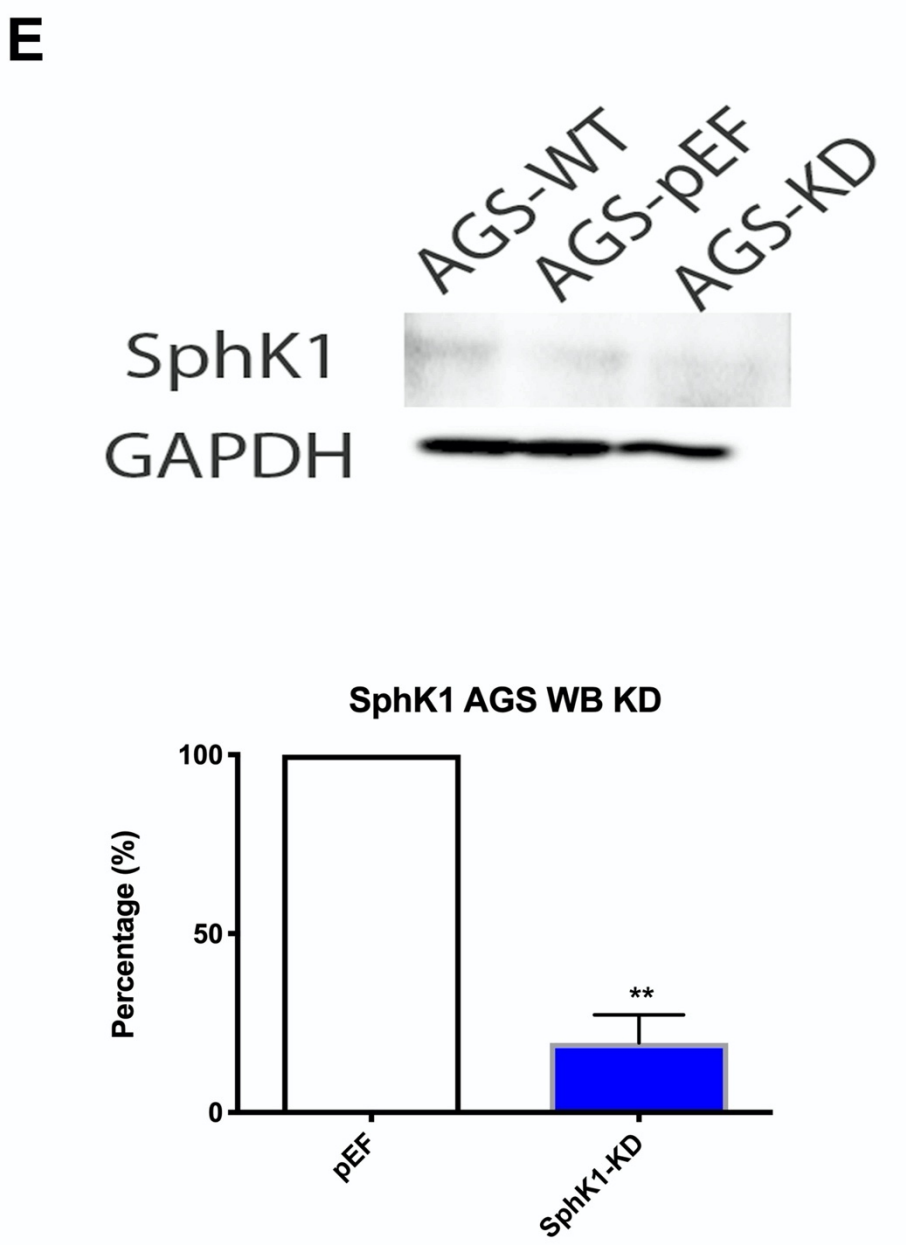

Figure 4.3 Verification of SphK1 knockdown in AGS by RT-PCR, qPCR and western blotting

E. The protein expression level of SphK1 and GAPDH in AGS cells transfected with control plasmid (pEF) and ribozyme sequence transgene incorporated plasmids (SphK1-KD) were detected by western blotting, with band densitometry shown below blot, Experiments were repeated a minimum of three times. Data shown represents Mean ± SEM. * represents $p<0.05$, ** represents $p<0.01$.

4.3.4 *In vitro* cell invasion assay

In order to examine the impact of SphK1 knockdown on the invasion ability of HGC27 and AGS cell lines, an *in vitro* cell invasion assay was conducted using both the HGC27 and AGS SphK1 knockdown cell models.

In vitro invasion assay demonstrated that decreased expression of SphK1 did not lead to significant changes in the invasive capabilities of the HGC27 cell line (Figure 4.4). Similarly, *in vitro* invasion assay demonstrated that decreased expression of SphK1 did not lead to significant changes in the invasive capabilities of the AGS cell line (Figure 4.5).

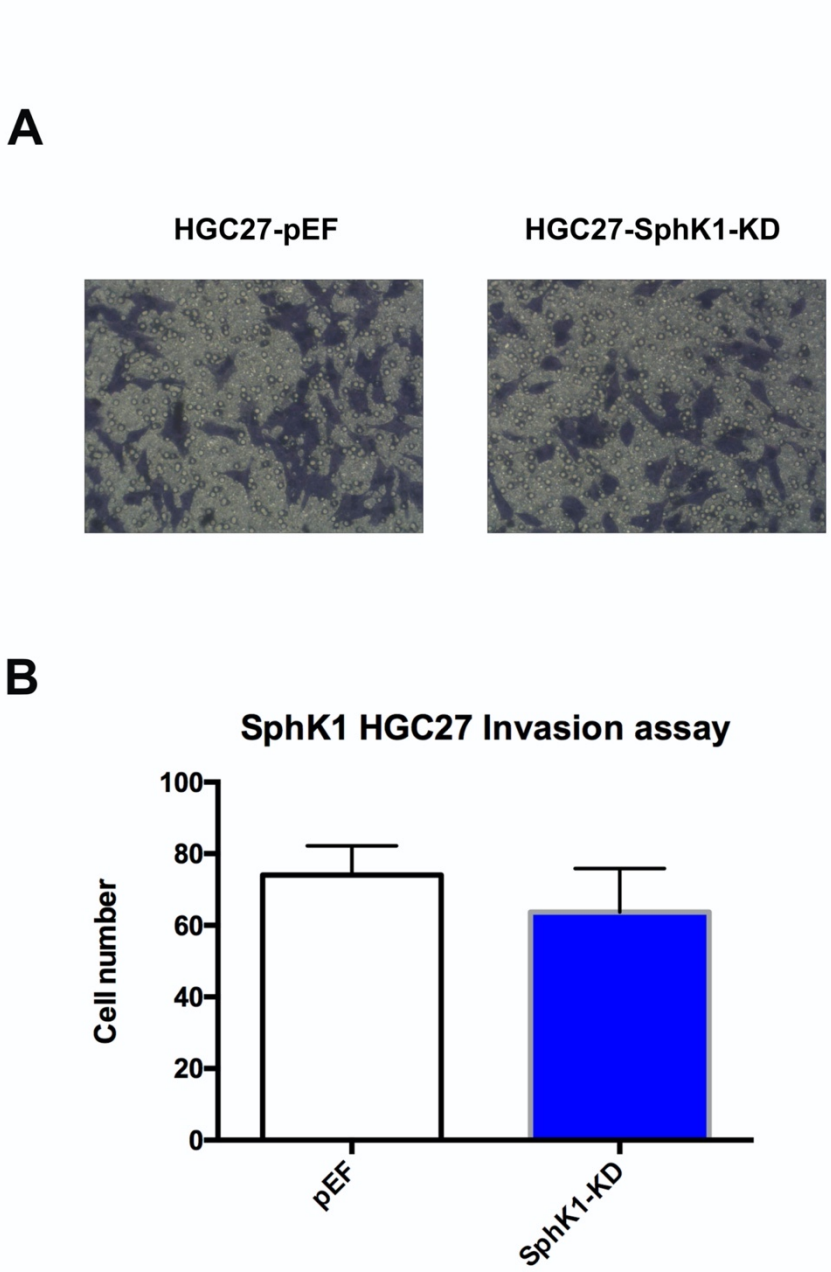

Figure 4.4 *In vitro* cell invasion assay on SphK1 knockdown HGC27 cell line
A. Representative images of invaded cells. **B.** Graphical representation of quantified invaded cells on the underside of the insert. Experiments were repeated a minimum of three times. Data shown represents Mean ± SEM.

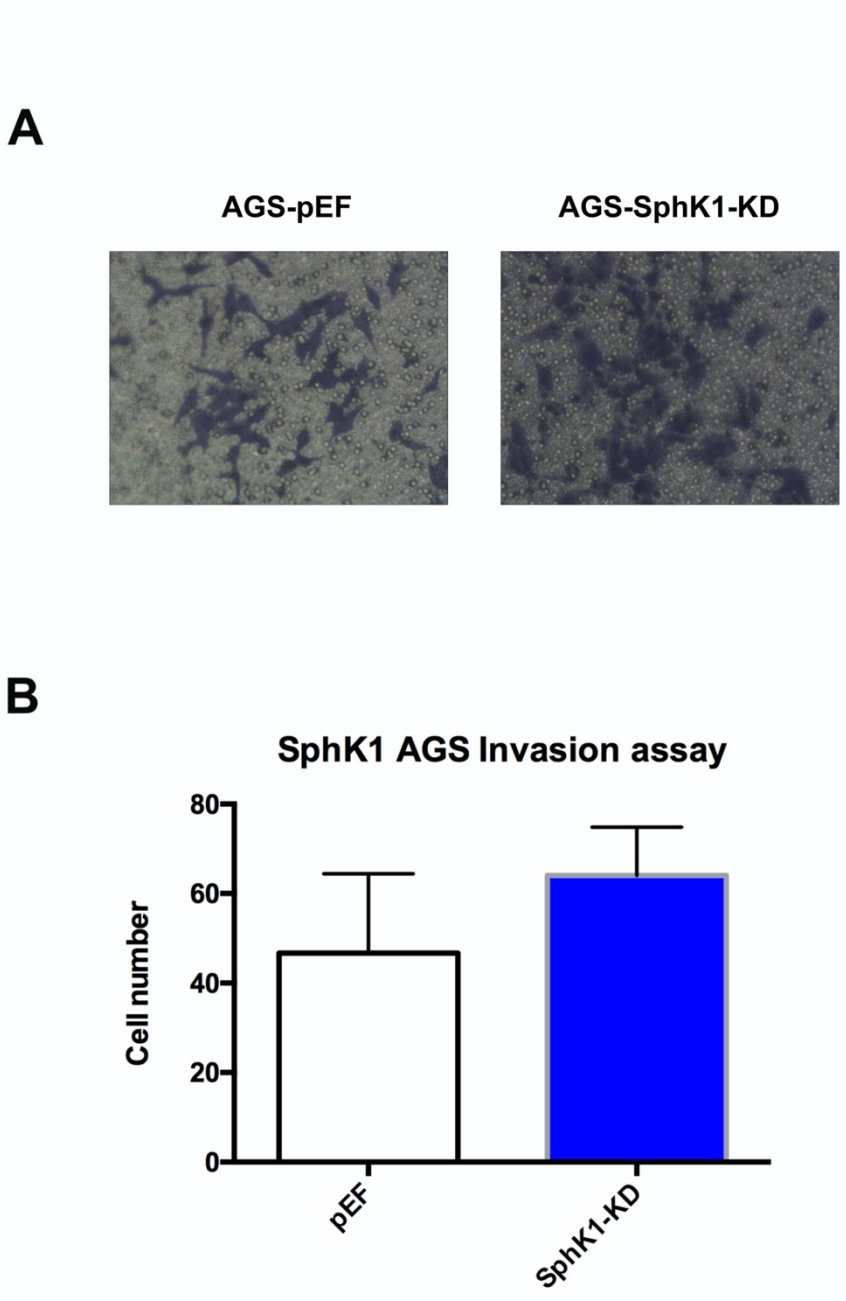

Figure 4.5 *In vitro* cell invasion assay on SphK1 knockdown AGS cell line
A. Representative images of invaded cells. **B.** Graphical representation of quantified invaded cells on the underside of the insert. Experiments were repeated a minimum of three times. Data shown represents Mean ± SEM.

4.3.5 *In vitro* cell adhesion assay

In vitro cell adhesion assays were performed to determine if SphK1 affects the adhesive ability of HGC27 and AGS on Matrigel matrix. Absorbance of cellular crystal violet stain dissolved in acetic acid was used to indicate levels of adherent cells.

Enhanced levels of cell-matrix attachment were seen in both HGC27 (Figure 4.6A) and AGS (Figure 4.6B) SphK1 knockdown cells compared to the respective pEF control. In both HGC27 and AGS cells SphK1 knockdown significantly enhanced the quantity of attached cells when compared to the respective pEF control cell line ($p < 0.01$ and $p < 0.001$ respectively).

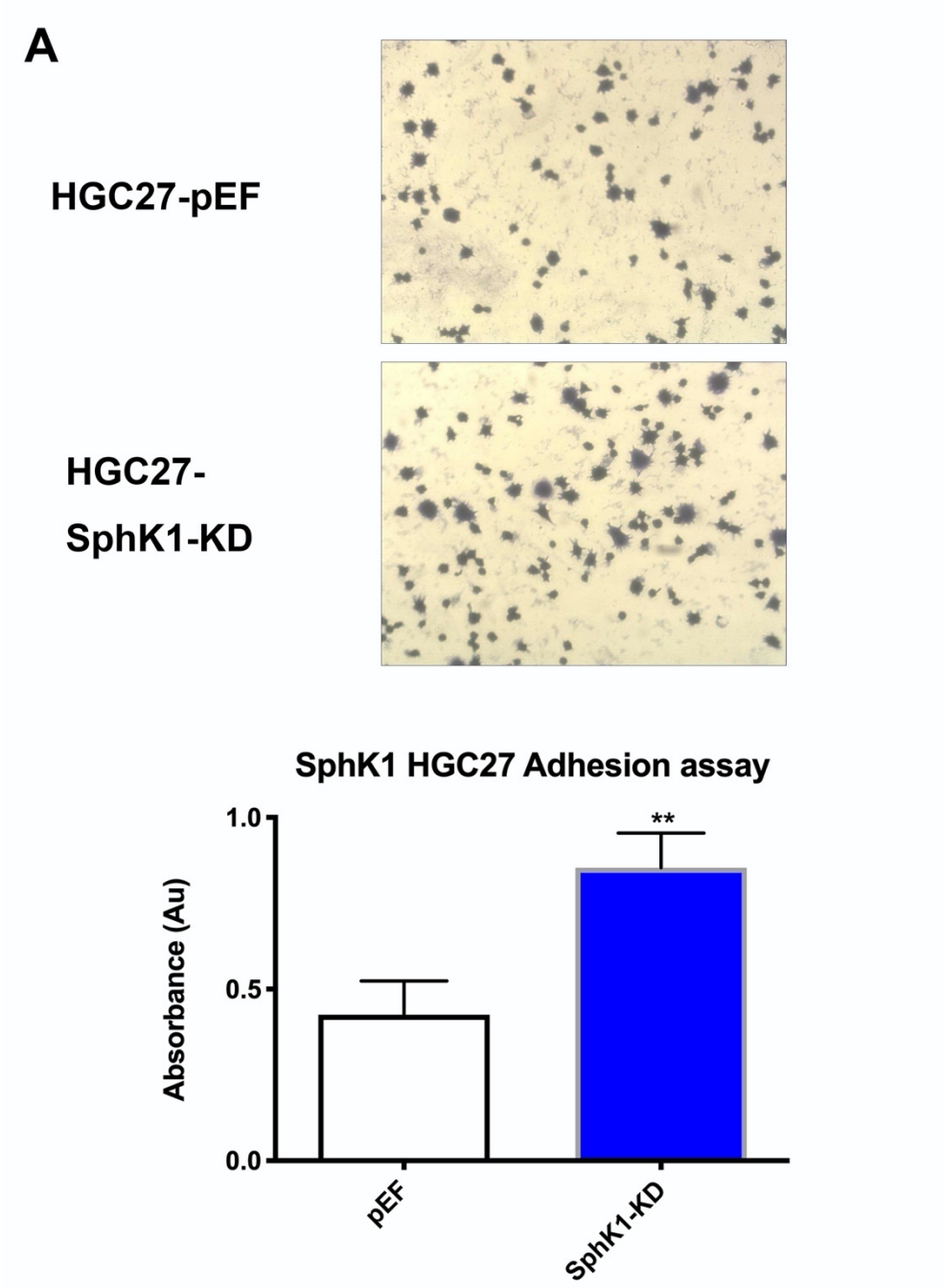

Figure 4.6 *In vitro* cell adhesion assay on SphK1 KD HGC27 cell lines
A. The absorbance, representing adherent cell numbers was quantified in both HGC27 pEF control and HGC27 SphK1 knockdown cells.
Experiments were repeated a minimum of three times. Data show represents Mean ± SEM. ** represents $p<0.01$, *** represents $p<0.001$.

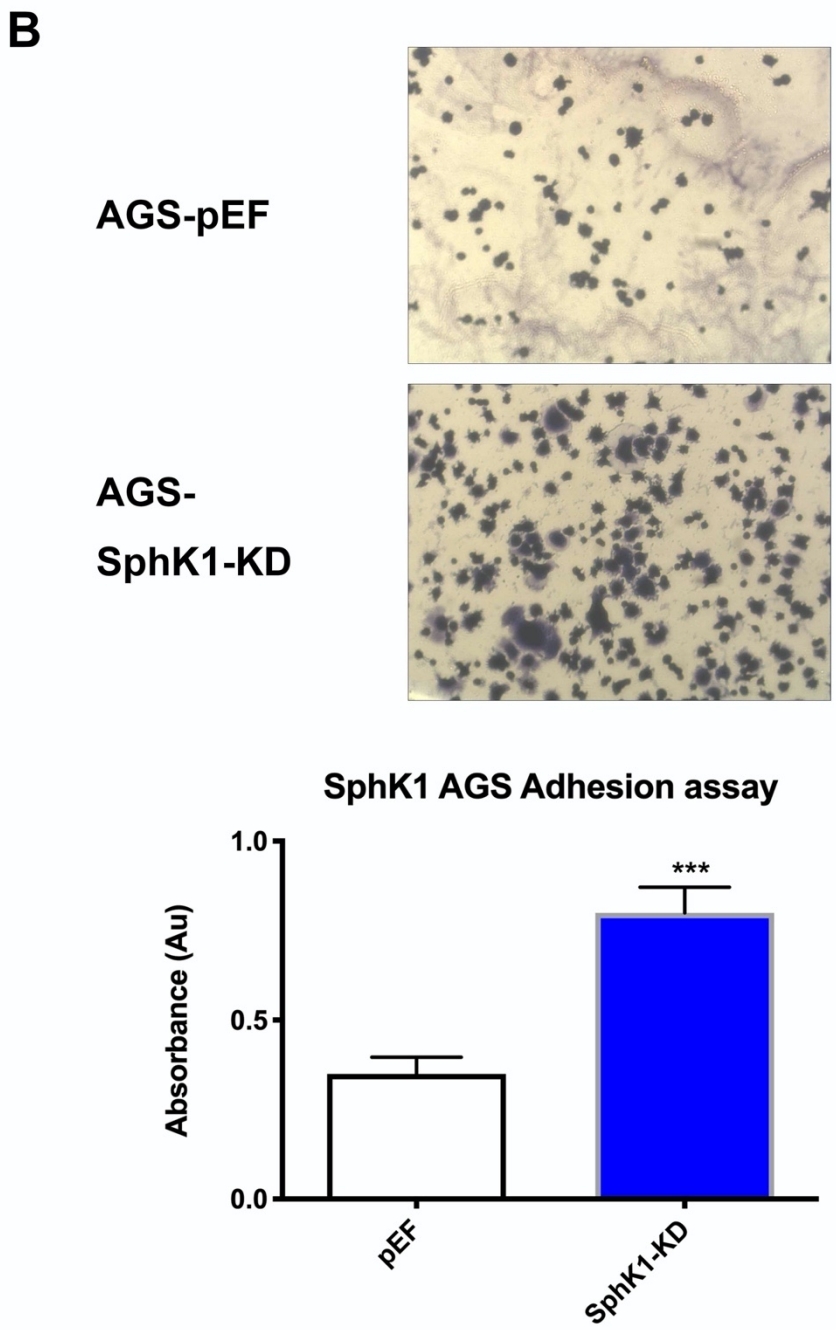

Figure 4.6 *In vitro* cell adhesion assay on SphK1 KD AGS cell lines
B. The absorbance, representing adherent cell numbers was quantified in both AGS pEF and AGS SphK1 knockdown cells. Experiments were repeated a minimum of three times. Data show represents Mean ± SEM. ** represents $p<0.01$, *** represents $p<0.001$.

4.3.6 *In vitro* cell proliferation assay

In order to examine the impact of SphK1 knockdown on the proliferative ability of HGC27 and AGS cells, an *in vitro* cell proliferation assay was conducted on the HGC27 and AGS SphK1 knockdown cell models.

Proliferation assays demonstrated that both SphK1 knockdown HGC27 (Figure 4.7A) and AGS cell lines (Figure 4.7B) exhibited significantly reduced growth rates compared to the empty vector (pEF) controls on both day 3 (both $p < 0.01$ compared to respective pEF control) and day 5 incubations (both $p < 0.001$ compared to respective pEF control).

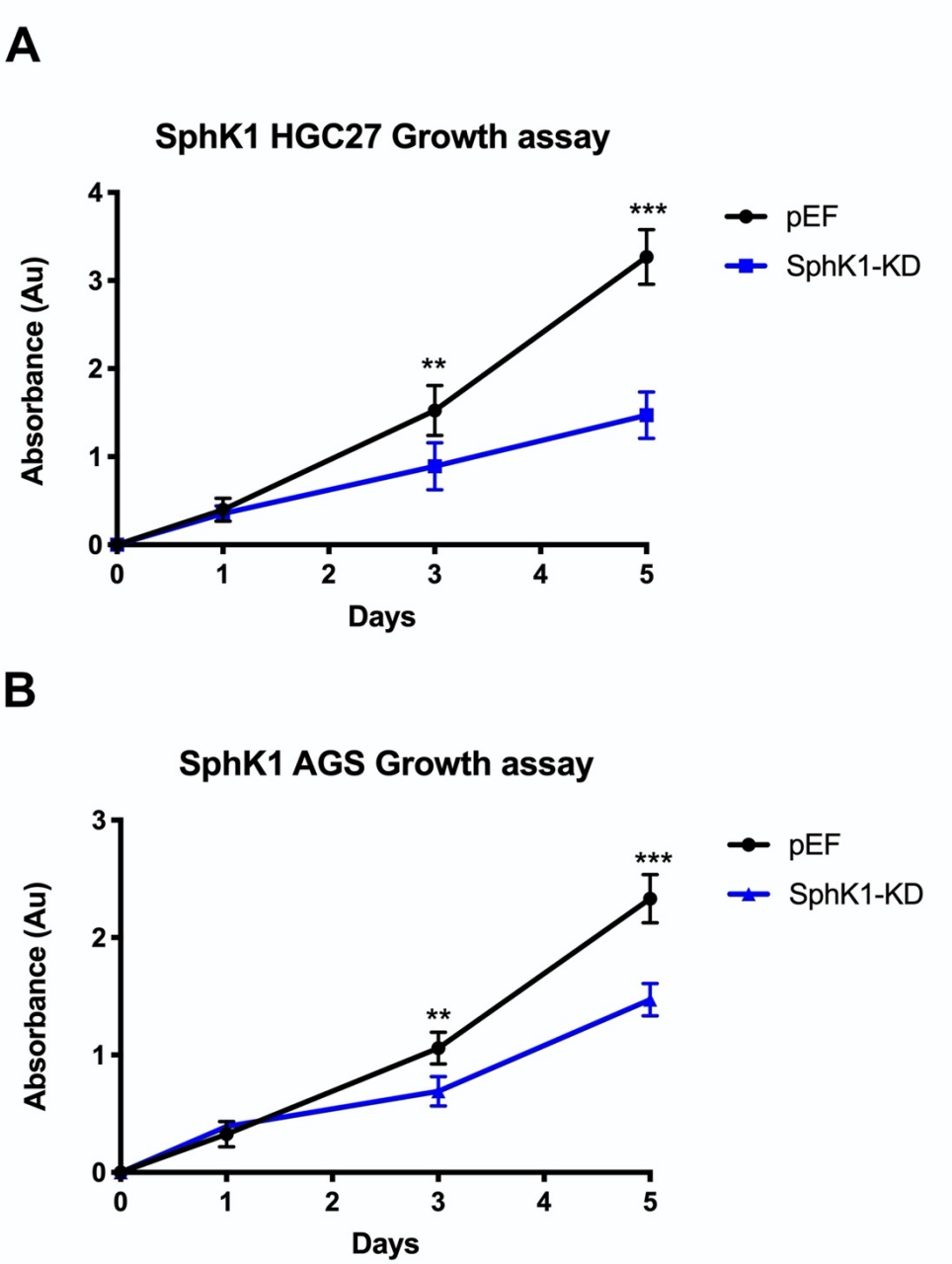

Figure 4.7*In vitro* cell proliferation assay on SphK1 knockdown HGC27 and AGS cell lines

A. The proliferative rate of HGC27 cell line on day 1, 3, 5 was analysed as cell viability against the control group in each repeat; **B.** The proliferative rate of AGS cell line on day 1, 3, 5 was analysed as cell viability against the control group in each repeat; Experiments were repeated a minimum of three times. Data shown represents Mean ± SEM. ** represents $p<0.01$, *** represents $p<0.001$.

4.3.7 *In vitro* cell migration assay

An *in vitro* wound healing assay was conducted to investigate the effect of SphK1 knockdown on HGC27 and AGS cell lines. The distance migrated between two wound edges of scratched HGC27 pEF and HGC27 SphK1-KD monolayers did not show any significant differences within the first six hours ($p > 0.05$). However, differences between the two groups were observed in the following time points, with significantly reduced rates of migration observed following SphK1-KD in comparison to the pEF control at 12, 18 and 22 hour time points ($p < 0.05$, $p < 0.05$ and $p < 0.01$ respectively) (Figure 4.8).

Similar trends were observed between AGS pEF6 and AGS SphK1-KD though significantly reduced rates of migration in the SphK1-KD, compared to the pEF control cells only appeared at 18 hours and 22 hours following wounding ($p < 0.05$ and $p < 0.01$, respectively) (Figure 4.9). In summary, downregulation of SphK1 decreased the migratory ability of HGC27 and AGS cell lines.

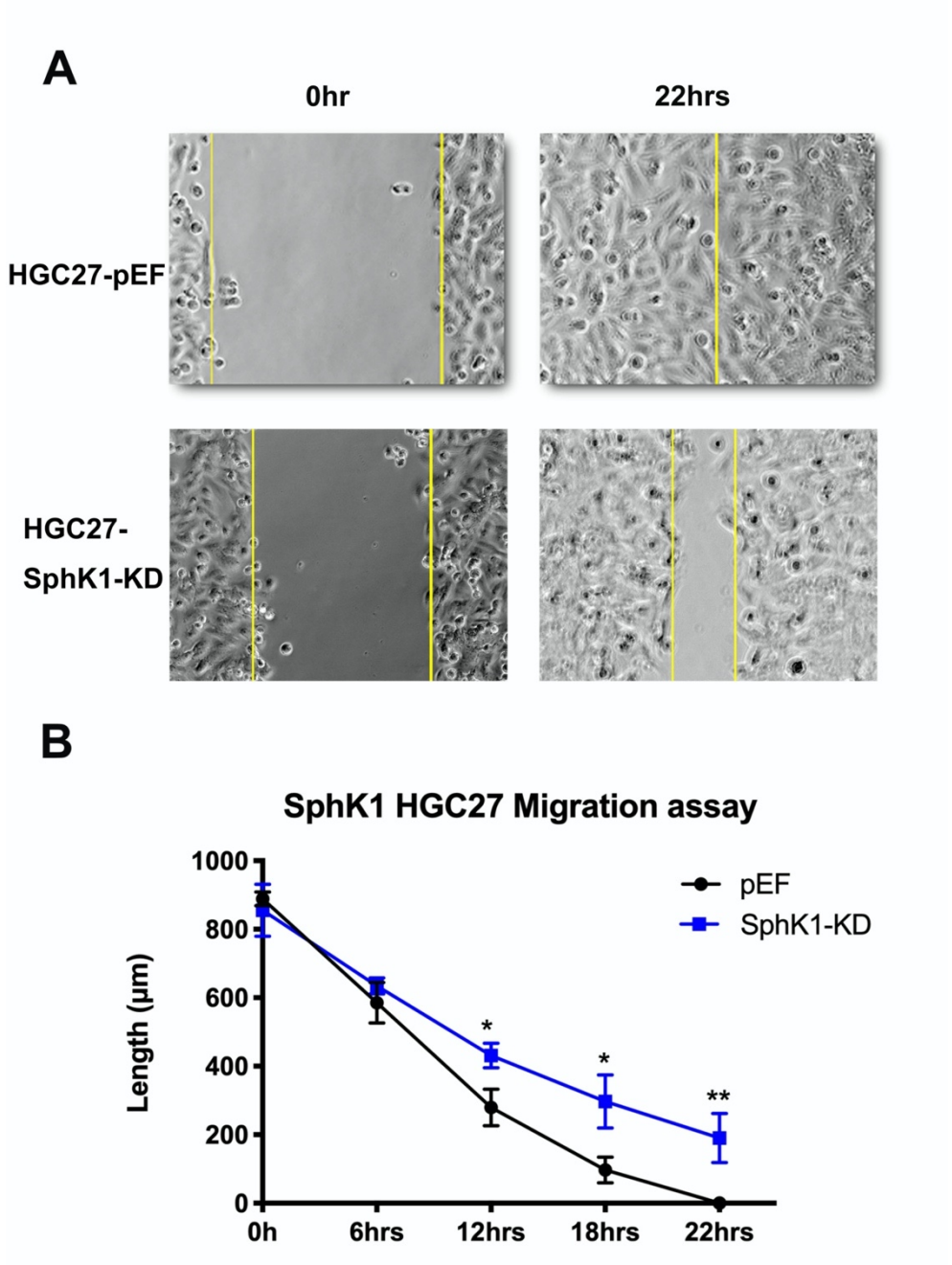

Figure 4.8*In vitro* cell migration assay on SphK1 knockdown HGC27 cell line
A. Representative images of wounds at experimental start and end points are shown. **B.** Migration assays demonstrating the effect of SphK1 knockdown on the migratory ability of HGC27 cells. The distance migrated by wound edge at each time point are plotted on a line chart. Experiments were repeated a minimum of three times. Data shown represents Mean ± SEM. * represents $p<0.05$, ** represents $p<0.01$.

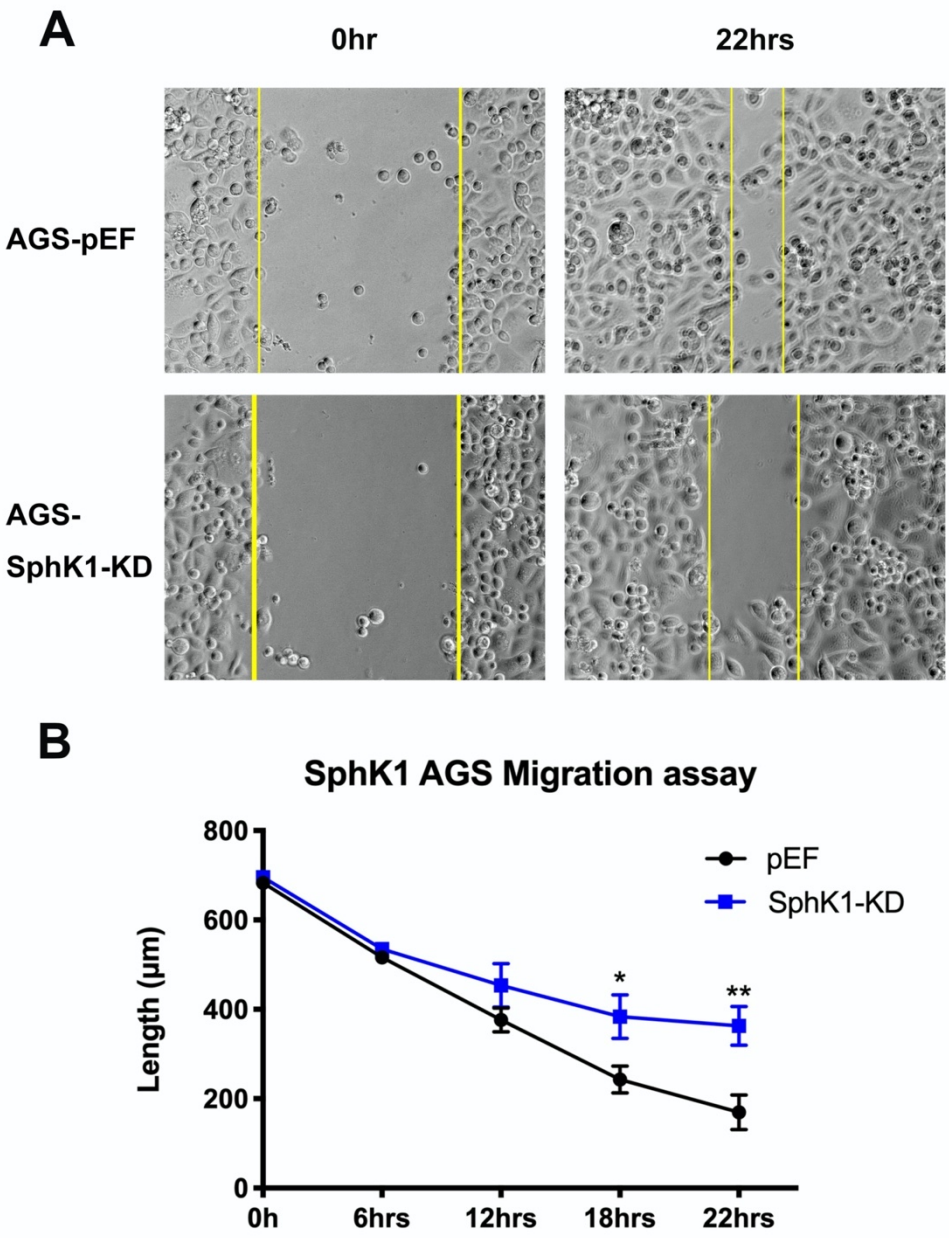

Figure 4.9 *In vitro* cell migration assay on SphK1 knockdown AGS cell line
A. Representative images of wounds at experimental start and end points are shown. **B.** Migration assays demonstrating the effect of SphK1 knockdown on the migratory ability of AGS cells. The distance migrated by wound edge at each time point are plotted on a line chart. Experiments were repeated a minimum of three times. Data shown represents Mean ± SEM. * represents $p<0.05$, ** represents $p<0.01$.

4.4 Discussion

Scientific study has demonstrated that SphK1 could regulate processes such as proliferation (Yuza et al., 2018), anti-apoptosis (Tsukamoto et al., 2015) cellular migration (Yuza et al., 2018) and invasion (Yuza et al., 2018) and angiogenesis (Dai et al., 2017).Therefore, it is of considerable importance to understand and establish the full significance of SphK1 and its expression status in human cancers. As SphK1 was directly related to the survival time of gastric cancer patients and was associated with more aggressive subtypes in the previous chapter, we further investigated the function of SphK1 and its impact on gastric cancer cells using in vitro models. We firstly screened a number of gastric cancer cell lines before choosing AGS / HCG27 as they were readily available in our lab and are commonly used cell lines to represent GC, as well as easy to grow. However, I also would like to highlight the limitations, based on the initial screen only looked at transcript, not protein level and that the study could have been further enhanced by using cell lines with weak expression to conduct over expression model (e.g. 823 and NUGC3), which would be important future work for solidifying the trends observed here.

The *in vitro* data showed that dysregulation of SphK1 contributed to cell migration, adhesion and growth which have shown similar trends to those present in the literature previously mentioned. Therefore, questions have been raised as to whether SphK1 may be useful as a therapeutic target to improve the clinical outcome of patients.

Many studies have previously indicated that SphK1 may be a potential therapeutic target. For example, an early study by Xia et al. (Xia et al., 2012), in gastric cancer cells demonstrated that SphK1 can be downregulated by miR-124, which similarly inhibited *in vivo* and *in vitro* proliferation and tumorigenicity, potentially through an observed enhancement of FOXO1 transcriptional activity and suppression of

AKT activity. A SphK1 inhibitor, SKI-II, has been used to explore SphK1's cellular role in gastric cancer cells and demonstrated the capacity to induce cell growth arrest and apoptosis via the upregulation of P27 and Bax and the downregulation of NF-κB and Bcl-2 (Li et al., 2014a). A more recent study by Wang et al. (Wang et al., 2018b), has similarly supported the importance of SphK1 in GC. In this study, they showed that SphK1 and S1PR1 appear to be a target of miR-330-3p. Overexpression of miR-330-3p caused downregulation of SphK1 and S1PR1 in a similar manner as their chemical inhibitors (FTY720 and VPC23019 respectively), having an *in vitro* and *in vivo* anti-tumour role. Furthermore, the study demonstrated that knocking down SphK1 expression in the gastric cancer cell lines MKN1 and KATO3 had a significant inhibitory effect on cellular proliferation, invasion and migration (Wang et al., 2018b). In addition, miRNA mediated downregulation of SphK1 has been reported to reduce migration of breast cancer cells, further highlighting SphK1 as a potential therapeutic target in other cancer types (Wang et al., 2019a, Cao et al., 2019, Doll et al., 2007, Sarkar et al., 2005). Overall, these findings are in keeping with the data presented in this chapter which demonstrate that targeting SphK1 reduces both gastric cancer cell proliferation and migration, though as highlighted above, we did not observe changes in invasive potential. Taken together this demonstrates and supports the potential of SphK1 as a therapeutic target. However, at the same time, another question has been raised as to which kind of target inhibitors are the most effective.

Evidence supported that matrix metalloproteinases (MMPs), extracellular proteinases, promoted variety of physiology tumour progression. The MMP family was firstly reported in 1962 (Gross and Lapiere, 1962) and the function of MMP family were seen to be degradation the extracellular matrix (ECM) (Liotta et al., 1980) and promoting epithelial-mesenchymal transition (EMT) (Xu et al., 2017b) leading to cell invasion and metastasis In the process of invasion, tumour cells pass

through the basement membrane, stroma and vascular basement membrane to enter into the blood vessels, and then transfer to distance sites. Many studies (Coussens et al., 2002, Winer et al., 2016) have indicated that the MMP degraded many important components in tissues. However, we did not observe any changes in invasion between control and SphK1 knockdown groups. One potential reason might be that different MMP members have different functions and/or are differently influenced by SphK1 expression. For example, MMP9 might play an important role in tumour invasion (Song et al., 2020) and in keeping with our results, our preliminary data suggested there was no changes in MMP9 in following SphK1 knockdown, though further investigation into such related mechanisms are needed. A previous report describing the crystal structure of SphK1 provided new direction and insight to design SphK1 inhibitors, which had aided in the development of more effective and specific inhibitors (Wang et al., 2013). Such inhibitors may be of great value as, in addition to a regulatory role of Sphk1 in basic cellular functions linked to cancer, it has also been linked to therapy resistance. For example, SphK1 has been implicated in the resistance of a number of cancers including prostate cancer (Alshaker et al., 2016), CRC (Tan et al., 2014) and HNSCC (Hazar-Rethinam et al., 2015)

Taken together, our current data and that present in the literature suggest that targeting SphK1 in gastric cancer could be an interesting therapeutic strategy. Evidence exists to suggest SphK1 may also contribute to chemo-resistance in these patients. This will be explored further in subsequent chapters.

Chapter V

SphK1 and its Implication in Gastric Cancer Chemotherapy Resistance

5.1 Introduction

Chemotherapy continues to be a key option of cancer treatment for patients and is designed to inhibit the proliferation and growth of cancer cells while limiting toxicity to host tissues (Moolgavkar et al., 2012). Frequently patients are diagnosed at a later or advanced stages of gastric cancer and will receive chemotherapy. Despite advances in chemotherapy regimens, response rates are limited by the development of resistance, resulting in poor patient prognosis. Hence, there is a strong clinical need to identify new markers or targets that could predict or combat resistance to chemotherapy.

Chemotherapy agents induce cellular stress promoting cell death mechanisms and resulting in tumour suppression and this partially occurs through inducing the generation of S1P, whereas channelling ceramide for S1P generation can give rise to chemo-resistance (Ogretmen, 2018). SphK1 is an important endogenous resource of the generation of S1P. In keeping with this an increasing number of studies have demonstrated the importance of SphK1 and SphK1 pathway in the acquisition of a resistant phenotype in numerous cancers. For example, in prostate cancer, downregulation of SphK1 expression was able to sensitise LNCaP and PC-3 prostate cancer cell lines to the chemotherapeutic agents docexaxel and camptothecin (Pchejetski et al., 2008) and enhanced SphK1 expression has been noted to result in docetaxel resistance in prostate cancer cells (Alshaker et al, 2016). Similarly in pancreatic cancer, SphK1 activity and the subsequent ratio between ceramide and S1P have been shown to correlate with gemcitabine resistance (Guillermet-Guilbert et al 2009) and more recently it has been demonstrated that miR-506 could influence chemo sensitivity through a key mechanism involving downregulation of SphK1 (Li et al., 2016c). Hence, SphK1 appears to have potential as a therapeutic target to combat drug resistance and subsequently, detection of the sphingolipid products of SphK1 potentially also having roles as predictive biomarkers of therapy-resistance.

The current chapter focuses on exploring the relationship between SphK1 and the sensitivity of gastric cancer cell lines to common chemotherapeutic agents utilised in the treatment of gastric cancer and also aims to assess the potential of SphK1 inhibitors to enhance the efficacy of chemotherapeutic agents on gastric cancer cells.

5.2 Methods and Materials

5.2.1 Cell lines and reagents

HGC27 and AGS cells, described in section 2.1 of chapter II, were used. Lines displaying SphK1 knockdown were created, using ribozyme transgenes, as described in section 2.11 of chapter II and shown in chapter IV. Culture conditions used are outlined in section 2.5.1 of chapter II.

5.2.2 Patient derived cell lines

Gastric cancer patients' primary cells were obtained from PKUCH.

Table 5-1 Gastric cancer primary cells used for drug test

Cell line name	Origin	Tissue type	Cell morphology
SphK1-H	67 year-old male patient	Adenocarcinoma	Epithelial
SphK1-L	45 year-old male	Adenocarcinoma	Epithelial

5.2.3 SphK1 inhibitor

An SphK1 inhibitor named PF543 was purchased from TOCRIS, Inc. (UK) and aliquoted into 25ml aliquots. Aliquots were stored at -20°C until required for tissue culture.

5.2.4 Cisplatin and 5-FU

Cisplatin and 5-FU were obtained from Peking University Cancer Hospital which was aliquoted into 5ml aliquots, stored at -20°C.

5.2.5 MTT cytotoxicity assays

This method is described in section 2.18.1 of the chapter II. In brief, cells were seeded and cultured in the presence or absence of cytotoxic agents or SphK1 inhibitors before the addition of MTT (final concentration 0.5mg/ml) and further culturing to allow formazan formation. Subsequently, medium was aspirated and DMSO added to solubilise crystals. Coloured solution was then read using a plate reader as an indication of cell viability.

5.3 Results

5.3.1 *In vitro* cisplatin cytotoxicity assay in AGS cell line

The role of SphK1 in chemo agent cytotoxicity of the cisplatin chemotherapeutic agent was examined using an MTT cytotoxicity assay. *In vitro* cytotoxicity assays were carried out using control and SphK1 knockdown AGS gastric cancer cell lines in combination with a concentration gradient of Cisplatin. Percentage cell survival, in comparison to untreated cells, was quantified after 48 hours of treatment with cisplatin (Figure 5.1). The IC50 of the SphK1-KD group was found to be significantly lower than that of the control group with the IC50 of the SphK1-KD group identified as 8.277μM (95% CI 7.808-8.775) and the IC50 of the control group as 13.25μM (95% CI 12.42-14.14), indicating that SphK1-KD could increase the sensitivity of the AGS cell line to cisplatin. Statistical analysis was also undertaken to compare control and SphK1-KD cell survival rates at the various cisplatin concentrations tested demonstrating significant reduction in SphK1-KD cell survival compared to control cell survival at cisplatin concentrations of 31.25μM, 15.625μM, and 7.8125μM (p=0.03, p=0.0001 and p=0.001 respectively).

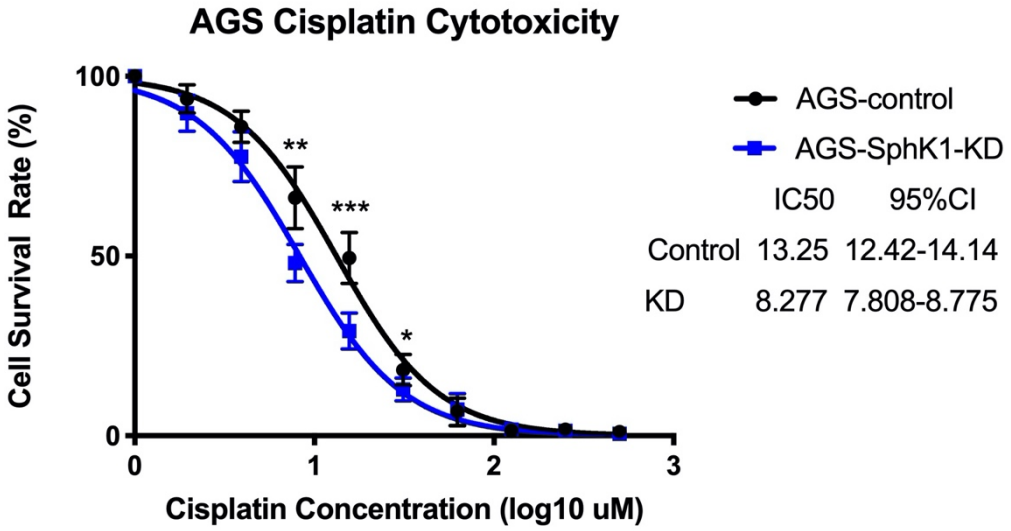

Figure 5.1 *In vitro* MTT cisplatin cytotoxicity assay in control and SphK1-KD AGS cell lines
Graphical representation of cell survival rate at different concentrations of Cisplatin. Blue line represents SphK1-KD and black line represents Control. Experiments were repeated a minimum of three times. Data shown represents Mean ± SEM. * represents $p < 0.05$, ** represents $p < 0.01$, *** represents $p < 0.001$.

5.3.2 *In vitro* cisplatin cytotoxicity assay in HGC27 cell line

In vitro cytotoxicity assay was carried out on control and SphK1 knockdown HGC27 gastric cancer cells in combination with a concentration gradient of cisplatin. Percentage cell survival, in comparison to untreated cells, was quantified after 48 hours of treatment with cisplatin (Figure 5.2). The IC50 of the SphK1-KD group was found to be significantly lower than that of the control group, with the IC50 of the SphK1-KD group identified as 8.748μM (95% CI 8.189-9.345) and the IC50 of control group as 14.44μM (95% CI 13.53-15.42), indicating SphK1 knockdown could influence the sensitivity of HGC27 cells to cisplatin. Statistical analysis were also undertaken to compare control and SphK1-KD cell survival at the various cisplatin concentrations tested, demonstrating significant reduction in SphK1-KD cell survival compared to control cell survival at cisplatin concentrations of 31.25μM, 15.625μM, 7.8125μM and 3.90625μM ($p = 0.0009$, $p = 0.001$, $p = 0.001$ and $p = 0.04$ respectively).

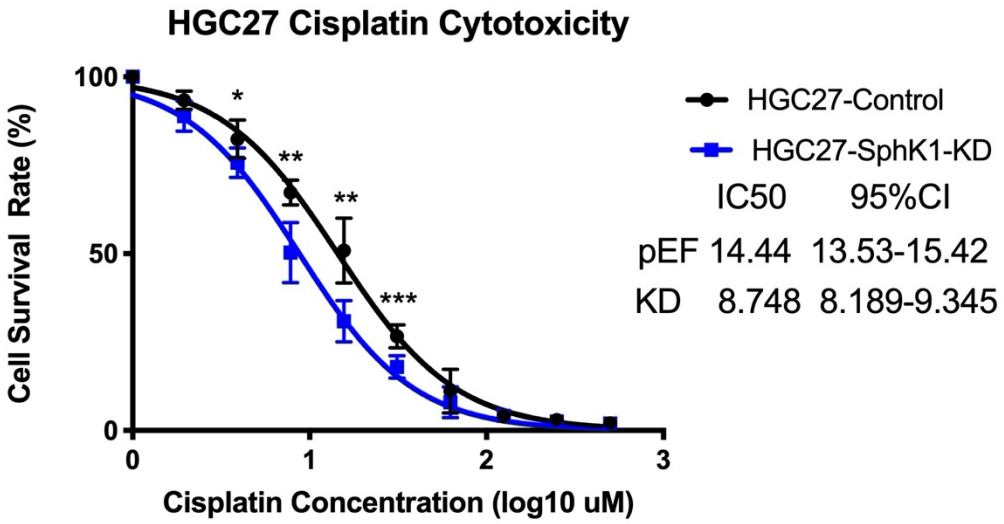

Figure 5.2 *In vitro* MTT cisplatin cytotoxicity assay in control and SphK1-KD HGC27 cell lines

Graphical representation of cell survival rate at different concentrations of Cisplatin. Blue line represents SphK1-KD and Black line represents Control. Experiments were repeated a minimum of three times. Data shown represents Mean ± SEM. * represents $p < 0.05$, ** represents $p < 0.01$, *** represents $p < 0.001$.

5.3.3 *In vitro* 5-FU cytotoxicity assay in AGS cell line

In vitro cytotoxicity assay was carried out on control and SphK1 knockdown AGS gastric cancer cell lines over a concentration gradient of 5-FU. Percentage cell survival, in comparison to untreated cells, was quantified after 48 hours of treatment with 5-FU (Figure 5.3). The IC50 of the SphK1-KD group was found to be significantly lower than that of the control group with the IC50 of the SphK1-KD group identified as 12.92μM (95% CI 11.92-14.01) and that of the control group as 35.45μM (95% CI 32.92-38.17). Statistical analysis was also undertaken to compare control and SphK1-KD cell survival rates at the various 5-FU concentrations tested, demonstrating significant reductions in SphK1-KD cell survival rates compared to control cells at 5-FU concentrations of 312.5μM, 156.25μM, 78.125μM, 39.0625μM, 19.53125μM and 9.765625μM (p = 0.004, p = 0.00005, p = 0.000003, p = 0.000004, p = 0.00002 and p = 0.0004 respectively).

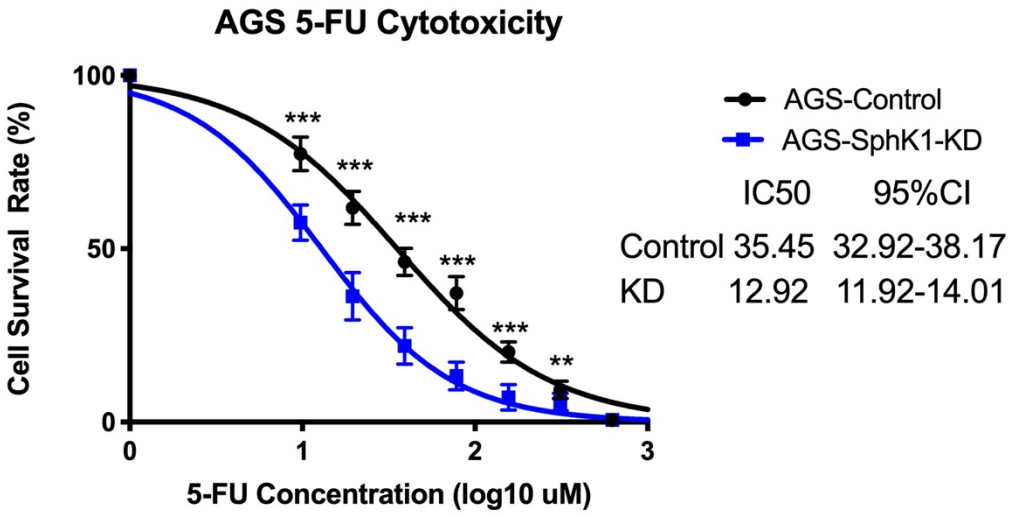

Figure 5.3 *In vitro* MTT 5-FU cytotoxicity assay in control and SphK1-KD AGS cell lines
Graphical representation of cell survival rate at different concentration of 5-FU. Blue line represents SphK1-KD and black line represents Control. Experiments were repeated a minimum of three times. Data shown represents Mean ± SEM. ** represents $p < 0.01$, *** represents $p < 0.001$.

5.3.4 *In vitro* 5-FU cytotoxicity assay in HGC27 cell line

In vitro cytotoxicity assay was carried out on control and SphK1 knockdown HGC27 gastric cancer cell lines over a concentration gradient of 5-FU. Percentage cell survival, in comparison to untreated cells, was quantified after 48 hours of treatment with 5-FU (Figure 5.4). The IC50 of SphK1-KD group was found to be significantly lower than that of the control group, with the IC50 of the SphK1-KD group identified as 12.62μM (95% CI 11.63-13.69) and the IC50 of the control group identified as 28.97μM (95% CI 27.27-30.77). Statistical analysis was also undertaken to compare control and SphK1-KD cell survival rates at the various 5-FU concentrations tested demonstrating significant reductions in SphK1-KD cell survival compared to control cell survival at 5-FU concentrations of 78.125μM, 39.0625μM, 19.53125μM and 9.765625μM ($p = 0.002$, $p = 0.000007$, $p = 0.00002$ and $p = 0.00005$ respectively).

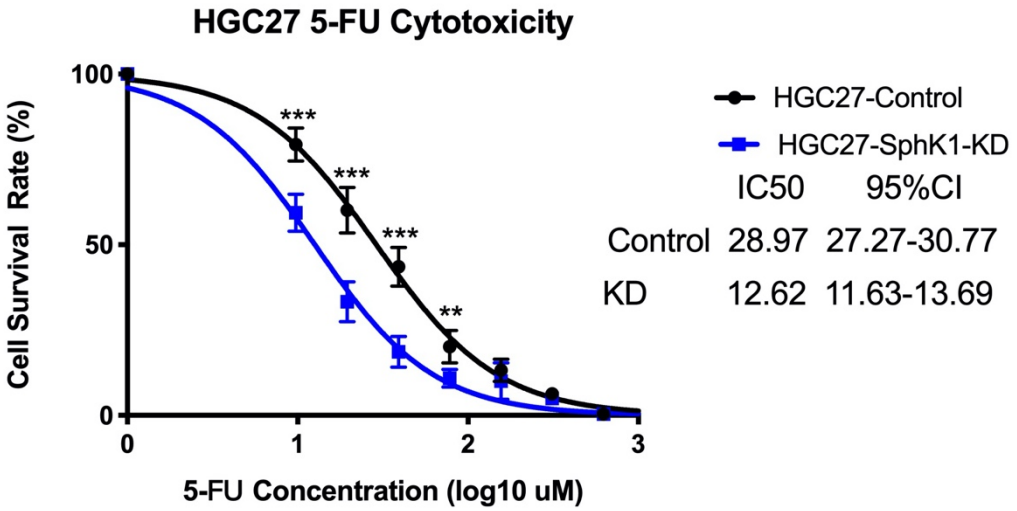

Figure 5.4 *In vitro* MTT 5-FU cytotoxicity assay in control and SphK1-KD HGC27 cell lines Graphical representation of cell survival rate at different concentrations of 5-FU. Blue line represents SphK1-KD and Black line represents Control. Experiments were repeated a minimum of three times. Data shown represents Mean ± SEM. ** represents $p < 0.01$, *** represents $p < 0.001$.

5.3.5 Impact of PF543 on *in vitro* cisplatin AGS cytotoxicity

As shown in the results above, we hypothesized that SphK1 played an important role in chemotherapy resistance and was of interest as a potential therapeutic target. Therefore, we searched for small molecule inhibitors targeting SphK1, identifying and selecting a specific small molecule inhibitor named PF543, for use in further cytotoxicity assays.

In vitro MTT cytotoxicity assays were carried out on AGS gastric cancer cell lines, over a concentration gradient of cisplatin, in the presence or absence of PF543 (12.5nM). Percentage cell survival, in comparison to untreated cells, was quantified after 48 hours of treatment with cisplatin with or without PF543 (Figure 5.5). The IC50 of the cisplatin+PF543 group was found to be significantly lower than that of the cisplatin alone group, with the IC50 of the cisplatin+PF543 group being 7.637μM (95% CI 7.230-8.143) and the IC50 of cisplatin alone group being 14.40μM (95% CI 13.67-15.18). Statistical analysis was also undertaken to compare the survival rates of AGS cells treated alone or with a combination of cisplatin+PF543, at the various cisplatin concentrations tested, identifying significantly lower survival rates in cisplatin+PF543 compared to cisplatin alone groups at cisplatin concentrations of 31.25μM, 15.625μM, and 7.8125μM and 3.90625μM (p = 0.01 p = 0.0001, p = 0.000009 and p = 0.0006 respectively).

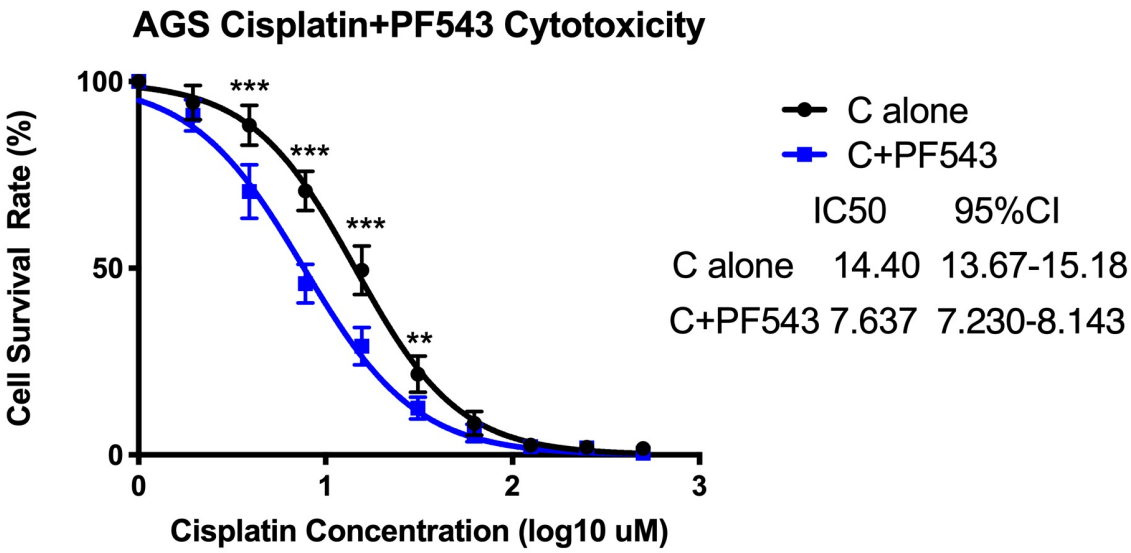

Figure 5.5 *In vitro* MTT cytotoxicity assay demonstrating the impact of PF543 on cisplatin toxicity in the AGS cell line

Graphical representation of cell survival rate at different concentrations of cisplatin alone and in combination with PF543. Blue line represents cisplatin+PF543 and black line represents cisplatin alone. Experiments were repeated a minimum of three times. Data shown represents Mean ± SEM. * represents $p < 0.01$, *** represents $p < 0.001$.

5.3.6 Impact of PF543 on *in vitro* cisplatin HGC27 cytotoxicity

In vitro cytotoxicity assays were carried out on HGC27 gastric cancer cells, over a concentration gradient of cisplatin, in the presence or absence of PF543 (12.5nM). Percentage cell survival, in comparison to untreated cells, was quantified after 48 hours of treatment with cisplatin with or without PF543 (figure 5.6). The IC50 of the cisplatin+PF543 group was found to be significantly lower than that of the cisplatin alone group, with the IC50 of the cisplatin+PF543 group being 9.195μM (95% CI 8.677-9.744) and the IC50 of cisplatin alone group being 20.43μM (95% CI 19.40-21.52). Statistical analysis was also undertaken to compare the survival rates of HGC27 cells treated with cisplatin alone or a combination of cisplatin+PF543, at the various cisplatin concentrations tested, identifying significantly lower survival rates in cisplatin+PF543 compared to cisplatin alone groups at cisplatin concentrations of 62.5μM, 31.25μM, 15.625μM, 7.8125μM and 3.90625μM (p = 0.000001, p = 0.0001, p = 0.000005, p = 0.00001 and p = 0.005 respectively).

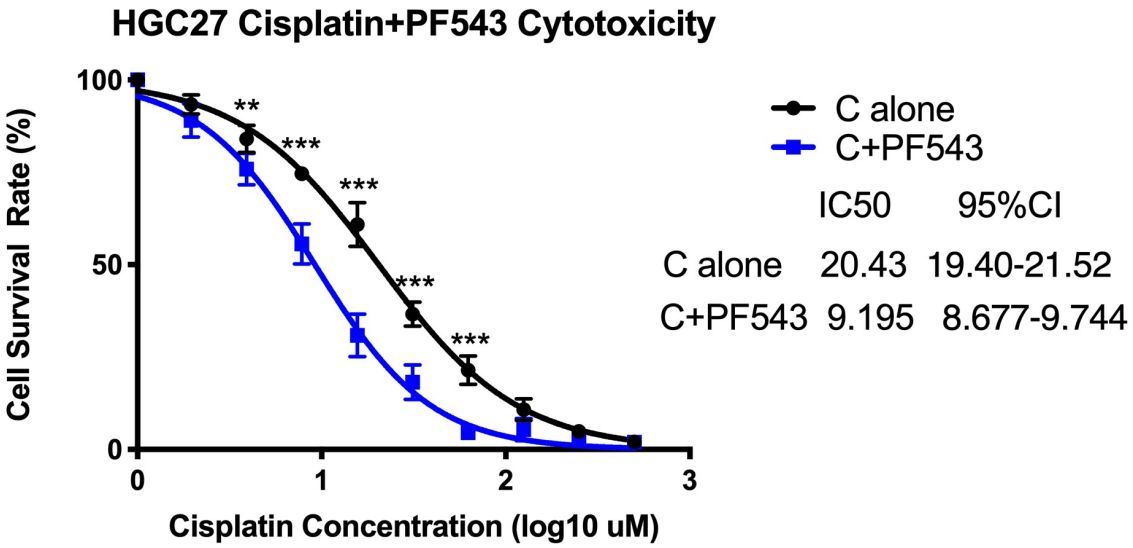

Figure 5.6 *In vitro* MTT cytotoxicity assay demonstrating the impact of PF543 on cisplatin toxicity in the HGC27 cell line

Graphical representation of cell survival rate at different concentration of cisplatin alone and cisplatin+PF543. Blue line represents cisplatin+PF543and black line represents cisplatin alone. Experiments were repeated a minimum of three times. Data shown represents Mean ± SEM. ** represents $p < 0.01$, *** represents $p < 0.001$.

5.3.7 Impact of PF543 on *in vitro* 5-FU AGS cytotoxicity

In vitro MTT cytotoxicity assays were carried out on AGS gastric cancer cells, over a concentration gradient of 5-FU, in the presence or absence of PF543 (12.5nM). Percentage cell survival, in comparison to untreated cells, was quantified after 48 hours of treatment with 5-FU with or without PF543 (Figure 5.7).The IC50 of the 5-FU+PF543 group was found to be significantly lower than that of the 5-FU alone group with the IC50 of 5-FU+PF543 group identified as 18.31μM (95% CI 16.92-19.81) and the IC50 of 5-FU alone group identified as 35.65μM (95% CI 33.20-38.28). Statistical analysis was also undertaken to compare the survival of AGS cells treated with 5-FU alone or a combination of 5-FU+PF543 at the various 5-FU concentrations tested, identifying significantly lower survival rates in 5-FU+PF543 group compared to the 5-FU alone group at 5-FU concentrations of 156.25μM, 78.125μM, 39.0625μM and 19.53125μM ($p = 0.0001$, $p = 0.000003$, $p = 0.0003$ and $p = 0.00003$ respectively).

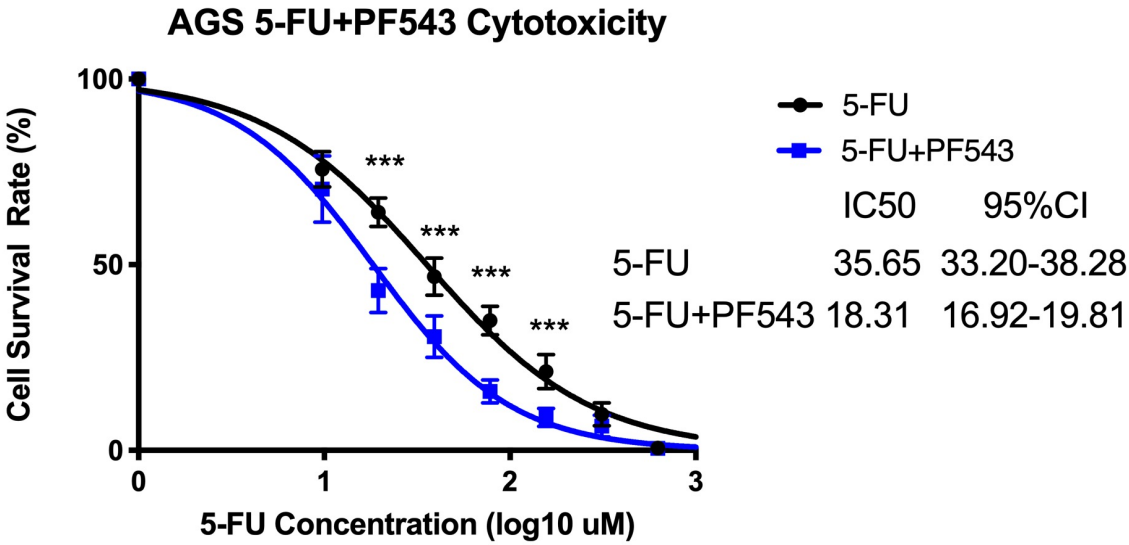

Figure 5.7 *In vitro* MTT cytotoxicity assay demonstrating the impact of PF543 on 5-FU toxicity in the AGS cell line

Graphical representation of cell survival rate at different concentrations of 5-FU alone and in combination with PF543. Blue line represents 5-FU+PF543 and Black line represents 5-FU alone. Experiments were repeated a minimum of three times. Data shown represents Mean ± SEM. *** represents $p < 0.001$.

5.3.8 Impact of PF543 on *in vitro* 5-FU HGC27 cytotoxicity

In vitro MTT cytotoxicity assays were carried out on HGC27 gastric cancer cells, over a concentration gradient of 5-FU, in the presence or absence of PF543 (12.5nM). Percentage cell survival, in comparison to untreated cells, was quantified after 48 hours of treatment with 5-FU with or without PF543 (Figure 5.8). The IC50 of the 5-FU+PF543 group was found to be significantly lower than that of the 5-FU alone group with the IC50 of the 5-FU+PF543 group identified as 12.83μM (95% CI 11.75-14.00) and the IC50 of the 5-FU alone group identified as 31.12μM (95% CI 29.12-33.26). Statistical analysis was also undertaken to compare the survival rates of HGC27 cells treated with 5-FU alone or a combination of the 5-FU+PF543 at the various 5-FU concentrations tested, identifying significantly lower survival rates in the 5-FU+PF543 group compared to 5-FU alone groups at 156.25μM, 78.125μM, 39.0625μM, 19.53125μM and 9.765625μM ($p = 0.04$, $p = 0.00001$, $p = 0.000009$, $p = 0.000003$ and $p = 0.00008$ respectively).

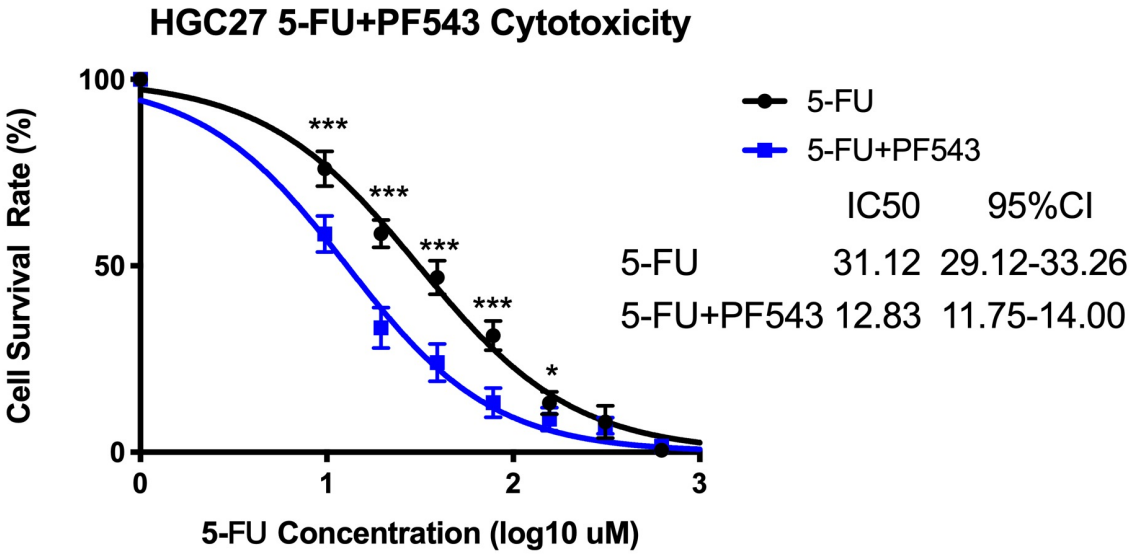

Figure 5.8 *In vitro* MTT cytotoxicity assay demonstrating the impact of PF543 on 5-FU toxicity in the HGC27 cell line

Graphical representation of cell survival rate at different concentrations of 5-FU alone and in combination with PF543. Blue line represents 5-FU+PF543 and black line represents 5-FU alone. Experiments were repeated a minimum of three times. Data shown represents Mean ± SEM. * represents $p < 0.05$, *** represents $p < 0.001$.

5.3.9 Impact of PF543 on *in vitro* cisplatin cytotoxicity in primary gastric cancer patient cell lines expressing high levels of SphK1

Previous results in human gastric cell lines have implicated a role for SphK1 in the responsiveness of these cells to chemotherapeutic agents and that targeting SphK1 can increase the sensitivity to these drugs. Following on from these results we obtained a number of primary gastric cancer lines generated in Peking University Cancer Hospital and conducted the cytotoxicity assay again.

In vitro MTT cytotoxicity assays were carried out on patient primary gastric cancer cell lines expressing high levels of SphK1 (SphK1-H) over a concentration gradient of cisplatin, in the presence or absence of PF543 (12.5nM). Percentage cell survival, in comparison to untreated cells, was quantified after 48 hours (Figure 5.9). The IC50 of the cisplatin+PF543 group was found to be significantly lower than that of the cisplatin alone group with the IC50 of the cisplatin+PF543 group identified as 14.45μM (95% CI 13.81-15.12) and the IC50 of the cisplatin alone group as 27.17μM (95% CI 25.53-28.92). Statistical analysis was also undertaken to compare the survival rates of SphK1-H primary cell lines treated with cisplatin alone or a combination of cisplatin+PF543 at the various cisplatin concentrations tested, identifying significantly lower survival rates in the cisplatin+PF543 compared to cisplatin alone groups at cisplatin concentrations at 31.25μM, 15.625μM and 7.8125μM (p = 0.03, p = 0.000006 and p = 0.0000004 respectively).

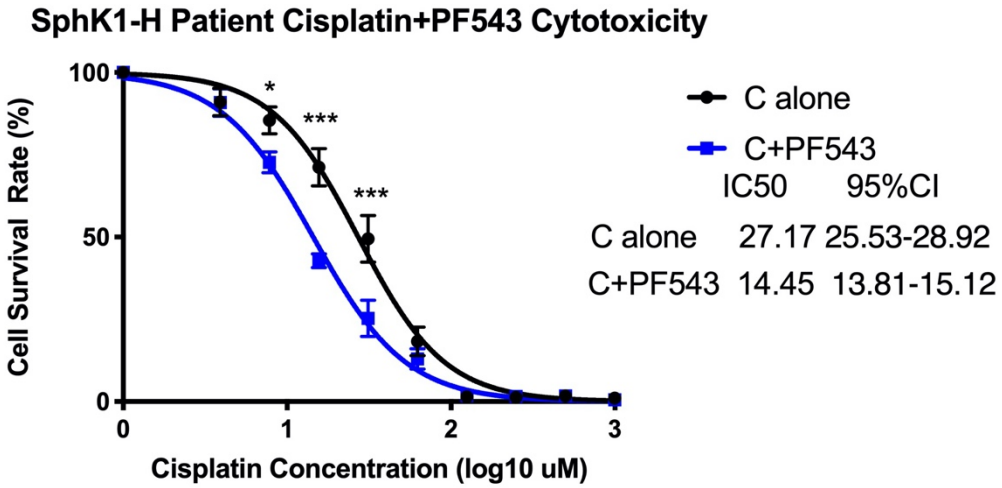

Figure 5.9 *In vitro* MTT cytotoxicity assay demonstrating the impact of PF543 on cisplatin toxicity in primary gastric cancer cell lines expressing high levels of SphK1 (SphK1-H)
Graphical representation of cell survival rate at different concentrations of cisplatin alone and in combination with PF543. Blue line represents cisplatin+PF543 and black line represents cisplatin alone. Experiments were repeated a minimum of three times. Data shown represents Mean ± SEM. * represents $p < 0.05$, *** represents $p < 0.001$.

5.3.10 Impact of PF543 on *in vitro* cisplatin cytotoxicity in primary gastric cancer patient cell lines expressing low levels of SphK1

In vitro MTT cytotoxicity assays were carried out on patient primary gastric cancer cell lines expressing low levels of SphK1 (SphK1-L), over a concentration gradient of cisplatin, in the presence or absence of PF543 (12.5nM). Percentage cell survival, in comparison to untreated cells, was quantified after 48 hours (Figure 5.10). The IC50 of the cisplatin+PF543 group was found to be similar to the cisplatin alone group, with the IC50 of the cisplatin+PF543 group identified as 33.87μM (95% CI 31.06-36.94) and the IC50 of the cisplatin alone group as 35.53μM (95% CI 32.97-38.28).

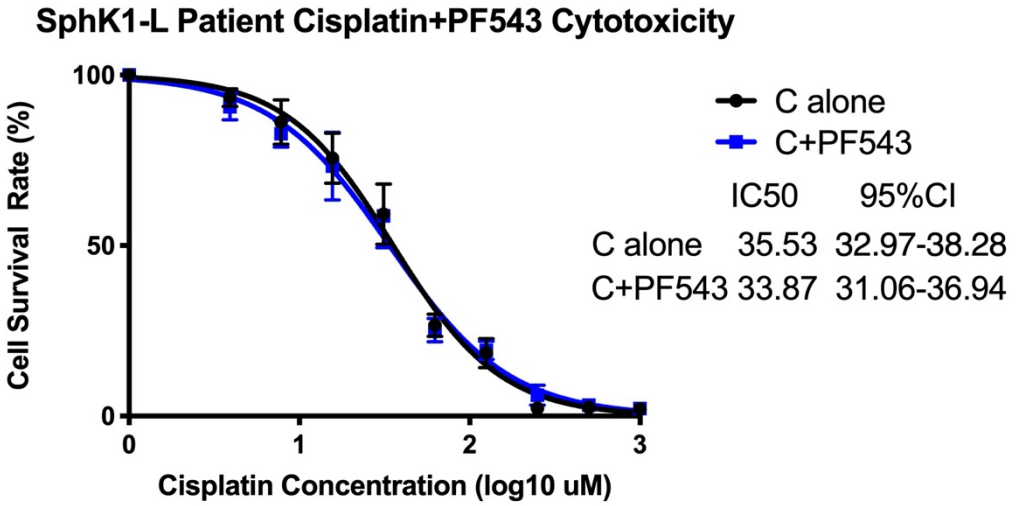

Figure 5.10 *In vitro* MTT cytotoxicity assay demonstrating the impact of PF543 on cisplatin toxicity in primary gastric cancer cell lines expressing low levels of SphK1 (SphK1-L)
Graphical representation of cell survival rate at different concentrations of cisplatin alone and in combination with PF543. Blue line represents cisplatin+PF543 and black line represents cisplatin alone. Experiments were repeated a minimum of three times. Data shown represents Mean ± SEM

5.3.11 Impact of PF543 on *in vitro* 5-FU cytotoxicity in primary gastric cancer patient cell lines expressing high levels of SphK1

In vitro MTT cytotoxicity assay were carried out on patient primary gastric cancer cell lines expressing high levels of SphK1 (SphK1-H) over a concentration gradient of 5-FU, in the presence and absence of PF543 (12.5nM). Percentage cell survival, in comparison to untreated cells, was quantified after 48 hours (Figure 5.11). The IC50 of the 5-FU+PF543 group was found to be significantly lower than that of the 5-FU alone group, with the IC50 of the 5-FU+PF543 group identified as 23.30μM (95% CI 21.56-25.18) and the IC50 of the 5-FU alone group as 53.94μM (95% CI 48.86-59.54). Statistical analysis was also undertaken to compare the survival rates of the SphK1-H primary cells treated with 5-FU alone or a combination of 5-FU+PF543, at the various concentrations tested, identifying significantly lower survival rates in the 5-FU+PF543 compared to the 5-FU alone group at 5-FU concentrations of 156.25μM, 78.125μM, 39.0625μM and 19.53125μM ($p = 0.000001$, $p = 0.00002$, $p = 0.00004$ and $p = 0.0005$ respectively).

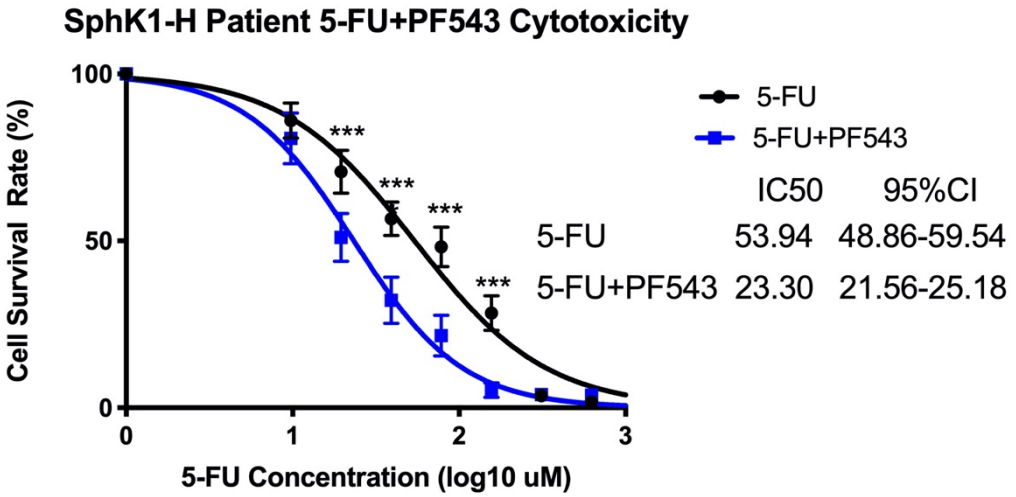

Figure 5.11 ***In vitro*** **MTT cytotoxicity assay demonstrating the impact of PF543 on 5-FU cytotoxicity in primary gastric cancer cell lines expressing high levels of SphK1 (SphK1-H)** Graphical representation of cell survival rate at different concentrations of 5-FU alone and in combination with PF543. Blue line represents 5-FU+PF543 and black line represents 5-FU alone. Experiments were repeated a minimum of three times. Data shown represents Mean ± SEM. *** represents $p < 0.001$.

5.3.12 Impact of PF543 on *in vitro* 5-FU cytotoxicity in primary gastric cancer patient cell lines expressing low levels of SphK1

In vitro MTT cytotoxicity assay was carried on patient primary gastric cancer cell lines expressing low levels of SphK1 (SphK1-L), over a concentration gradient of 5-FU, in the presence and absence of PF543 (12.5nM). Percentage cell survival, in comparison to untreated cells, was quantified after 48 hours (Figure 5.12). The IC50 of the 5-FU+PF543 group was found to be similar to the 5-FU alone group, with the IC50 of the5-FU+PF543 group identified as 40.11μM (95% CI 36.16-44.50) and the IC50 of the 5-FU alone group as 40.83μM (95% CI 36.41-45.78).

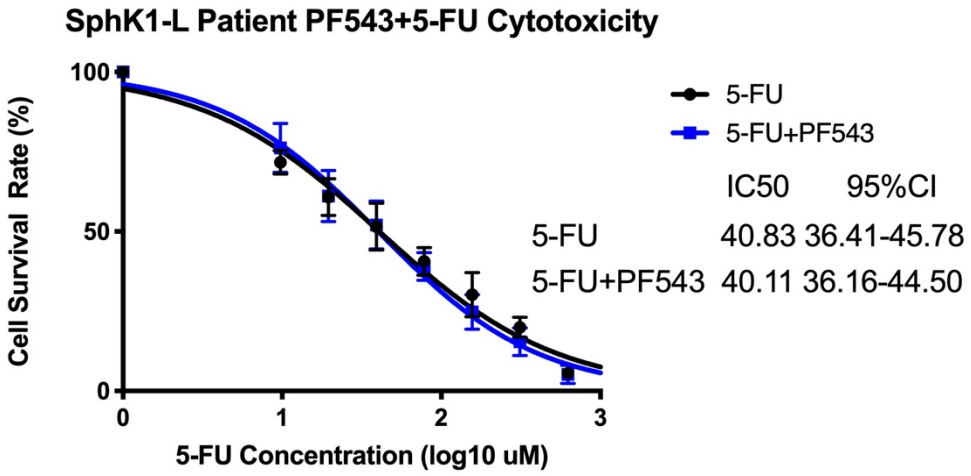

Figure 5.12 *In vitro* MTT cytotoxicity assay demonstrating the impact of PF543 on 5-FU toxicity in primary gastric cancer cell lines expressing low levels of SphK1 (SphK1-L)

Graphical representation of cell survival rate at different concentrations of 5-FU alone and in combination with PF543. Blue line represents 5-FU+PF543 and black line represents 5-FU alone. Experiments were repeated a minimum of three times. Data shown represents Mean ± SEM.

5.4 Discussion

Resistance to chemotherapeutic agents is a major issue and significant challenge in numerous human cancers and new therapy opinions combating such resistance are key interest to researchers. In recent years, new strategies, based on sensitising tumour cells to chemotherapeutic agents through the addition of relatively low toxicity small inhibitors have gained scientific interest. In such approaches, application of decreased doses of toxic agents given in combination with non-toxic or low toxicity small inhibitors with the aim of complementing treatment efficacy and sensitising cells to the toxic agent. SphK1, categorised as a bioactive lipid enzyme, is a central element in the sphingolipid rheostat (Pulkoski-Gross et al., 2015, Maceyka et al., 2012, Pyne and Pyne, 2013, Pitson, 2011, Cuvillier et al., 1996) which has been recognised as a promising therapeutic target for many types of cancer where it is frequently found to be dysregulated, contributes to progression (Wang et al., 2018b, Li et al., 2018a) and links to chemotherapeutic resistance (Li et al., 2016c, Alshaker et al., 2016). Additionally, numerous small inhibitors targeting SphK1 have been developed, raising the potential of targeting SphK1 and such processes in a clinical setting (Lima et al., 2018, Kreitzburg et al., 2018).

In our study, firstly, we performed an initial preclinical evaluation of the role of SphK1 in chemo-resistance of gastric cancer. In both AGS and HGC27 gastric cancer cell lines, displaying positive expression of SphK1, the IC50 value for both cisplatin and 5-FU was significantly decreased following SphK1 knockdown. Interestingly, cell viability and chemotherapeutic drugs are dose-dependent. At relatively high concentrations and relatively low concentrations, SphK1 appears to have a limited role in the responsiveness of the cell lines tested to these chemotherapeutic agents. However, within the appropriate drug concentration range, downregulating the expression of SphK1 expression enhanced the responsiveness of cells to the chemotherapeutic drugs. Whilst preliminary, this data suggests that

SphK1 may play a role in the chemotherapy resistance of gastric cancer. A study from Hazar-Rethinam et al., (Hazar-Rethinam et al., 2015) also indicated that knock down SphK1 could lead to the chemosensitivity of SCC cells to doxorubicin *in vitro* and *in vivo*. Similarly, SK1-I had the same function which could combat chemoresistance in SCC cells. Similarly, SphK1 has been identified as contributing to chemotherapy resistance in a number of cancers. For example in head and neck squamous cell carcinoma (HNSCC) E2F7 has been demonstrated to enhance resistance to doxorubicin through SphK1 induction and activation of AKT and subsequently that targeting or inhibition of SphK1 can enhance doxorubicin sensitivity in *in vitro* and *in vivo* models (Hazar-Rethinam et al., 2015). Similarly in pancreatic cancer, the ratio between ceramide and S1P has been suggested to predict gemcitabine resistance in pancreatic cancer cells and such resistance appeared to correlate with SphK1 activity, where targeting or inhibition of SphK1 enhanced sensitivity whereas transfection with SphK1 cDNA, and enhanced SphK1 activity, reduced sensitivity to gemcitabine (Guillermet-Guibert et al., 2009). This is further supported by a study by Li *et al*, which identified SphK1 as a target of miR-506, a miR whose reduced expression is associated with poorer prognosis in pancreatic cancer, and similarly demonstrated that targeting of SphK1 in pancreatic cancer cell lines could enhance gemcitabine sensitivity (Li et al., 2016c).

In addition to knockdown models, we also focused on identifying whether inhibition of SphK1 using small inhibitors could also alter the resistance of gastric cancer cell lines to chemotherapy drugs. We conducted a preclinical evaluation of SphK1 inhibitor, PF543, as a sensitiser for a conventional chemotherapeutic drug currently being using in clinical practice. Importantly, compared with the chemotherapy drug alone group, the IC50 of the gastric cancer cell lines with high expression of SphK1 was significantly reduced after treatment with PF543 in combination with the chemotherapy drug. Similar implications have been reported in relation to an S1P

pathway inhibitor, FTY720, which has been demonstrated to enhance the efficacy of gemcitabine when added in combination, resulting in smaller tumours compared to controls or individual therapies alone, in a clear cell renal carcinoma (CCRC) *in vivo* model (Gstalder et al., 2016).Taken together, these data indicate that SphK1 expression levels can be used as the criteria for evaluation of the resistance of gastric cancer cells and PF543 can be used as a sensitizer of chemoresistance. Subsequently, given the importance of the observed capacity of SphK1 knockdown or targeting of SphK1 with PF543 in commercial cell line models of gastric cancer we aimed to explore such relationships in a more clinically relevant model. Therefore, we used the primary cell line of gastric cancer patients in Peking University Cancer Hospital. The results showed that PF543 can effectively reduce the sensitivity to chemotherapy drugs in patients whose tumour cells displayed high expression of SphK1, but this effect was not observed in patients with low SphK1 expression. Such data is in keeping with the literature and further validates the significance of SphK1 as a potential biomarker for chemo-resistance or as a target for enhancing gastric tumour cell sensitivity to chemotherapeutics.

However, some reports have also indicated little or no impact on cellular proliferation, despite altering S1P levels, following application with some SphK1 inhibitors, including PF543 (Kharel et al., 2011, Schnute et al., 2012) and additional study is required to fully clarify their role.

In conclusion, our current data suggests that the level of SphK1 may indicate responsiveness of gastric cancer cells to chemotherapy and furthermore targeting or inhibiting SphK1 in patients with high SphK1 may be of benefit to enhance sensitivity to chemotherapy or prevent resistance. SphK1 inhibitors may therefore be of benefit to such patients but further work is required to fully establish their clinical benefit.

Chapter VI

Potential downstream mechanisms of SphK1 in gastric cancer

6.1 Introduction

SphK1 expression is dysregulated in many cancers and is associated with cancer progression and resistance to therapy (Hazar-Rethinam et al., 2015, Li et al., 2016c, Wang et al., 2018b, Li et al., 2018a, Yang et al., 2019). In keeping with this data results outlined in previous chapters have indicated that enhanced expression of SphK1 correlates with poorer survival rates of gastric cancer patients, impacts on cellular function of gastric cancer cells and also influences the ability of gastric cancer cell lines and primary cell lines derived from gastric cancer patients to respond to 5-FU and cisplatin. Taken together, this suggests a role for SphK1 in gastric cancer biology and that its expression may be useful as a potential target for reversing chemoresistance.

Mechanisms acting upstream and downstream of SphK1 are beginning to be identified. The oncogenic potential of SphK1 has previously been attributed to both gain of function, relating to enhanced S1P mediated signalling, or non-oncogenic addiction, relating to cancer cell dependence on SphK1, or this signalling system for sustained survival (Li et al., 2019a) , with little evidence suggesting SphK1 gene mutations are related to cancer (Pyne et al., 2012a). SphK1 location has been linked with its role in cancer progression with SphK1 phosphorylation state and cellular localisation being suggested to be important in cancer transformation. More recent studies have aided in establishing the mechanisms through which SphK1 acts and can be regulated. For example SphK1 has been shown to influence the process of EMT and impacts on the expression of EMT markers E-cadherin and vimentin through FAK / AKT / MMP2/9 signalling pathway (Liu et al., 2019). Other studies have also identified SphK1 as a target of a number of miRNA's, proposing regulation of SphK1 by these miRNAs contributes to their cancer related effects (Cao et al., 2019, Wang et al., 2019a).In order to further clarify the impact of SphK1 in gastric cancer biology and potential mechanisms through which SphK1 may contribute to

chemoresistance we next aimed to identify key pathways which are altered in response to enhanced levels of S1P, a product of SphK1, and may hence be mechanisms through which SphK1 exerts its role. The current chapter aims to identify potential mechanistic pathways downstream of SphK1/S1P using a protein microarray analysis.

6.2 Methods and materials

6.2.1 Cell lines and reagents

HGC27 and AGS cells, described in section 2.1 of chapter II, were used. Lines displaying SphK1 knockdown were created, using ribozyme transgenes, as described in section 2.11 of chapter II and shown in chapter IV. Culture conditions used are outlined in section 2.5.1 of chapter II.

6.2.2 Kinexus protein array and data analysis

Control AGS or AGS cells treated with S1P were cultured as outlined and described in sections 2.1 and 2.5.1 of chapter II. Protein samples from control and treated AGS cells were extracted and sent to Kinexus Bioinformatics (Canada) for microarray analysis as outlined in section 2.16 of chapter II. Results were returned following analysis and samples compared based on the percentage change from control (%CFC) or Z-ratios between control and treated AGS cells.

6.2.3 Protein extraction, quantification, SDS-PAGE and Western blot analysis

Extraction, quantification and analysis of protein expression in AGS and HGC27 SphK1 knockdown samples was undertaken as outlined in section 2.14, 2.15 and 2.17 of chapter II.

6.3 Results

6.3.1 Potential downstream signalling investigation

To explore global signalling events in AGS cells following treatment with S1P, a protein array was undertaken using the Kinexus 880 platform. The array probes with more than 850 antibodies returning information on a combination of total and phosphorylated protein expression. Figure 6.1 shows representative images from the array. Following analysis, the samples were scaled based on their percentage change from control and the top 50 upregulated total proteins shown in Table 6.1, the top 50 downregulated total proteins shown in Table 6.2, the top 50 upregulated phosphoproteins shown in Table 6.3 and the top 50 downregulated phosphoproteins shown in Table 6.4. The Kinexus array returned a vast amount of data, including the interesting observation that S1P treatment enhanced phosphorylation at Ser 473 of AKT, a key signalling molecule linked to cancer progression and therapy resistance.

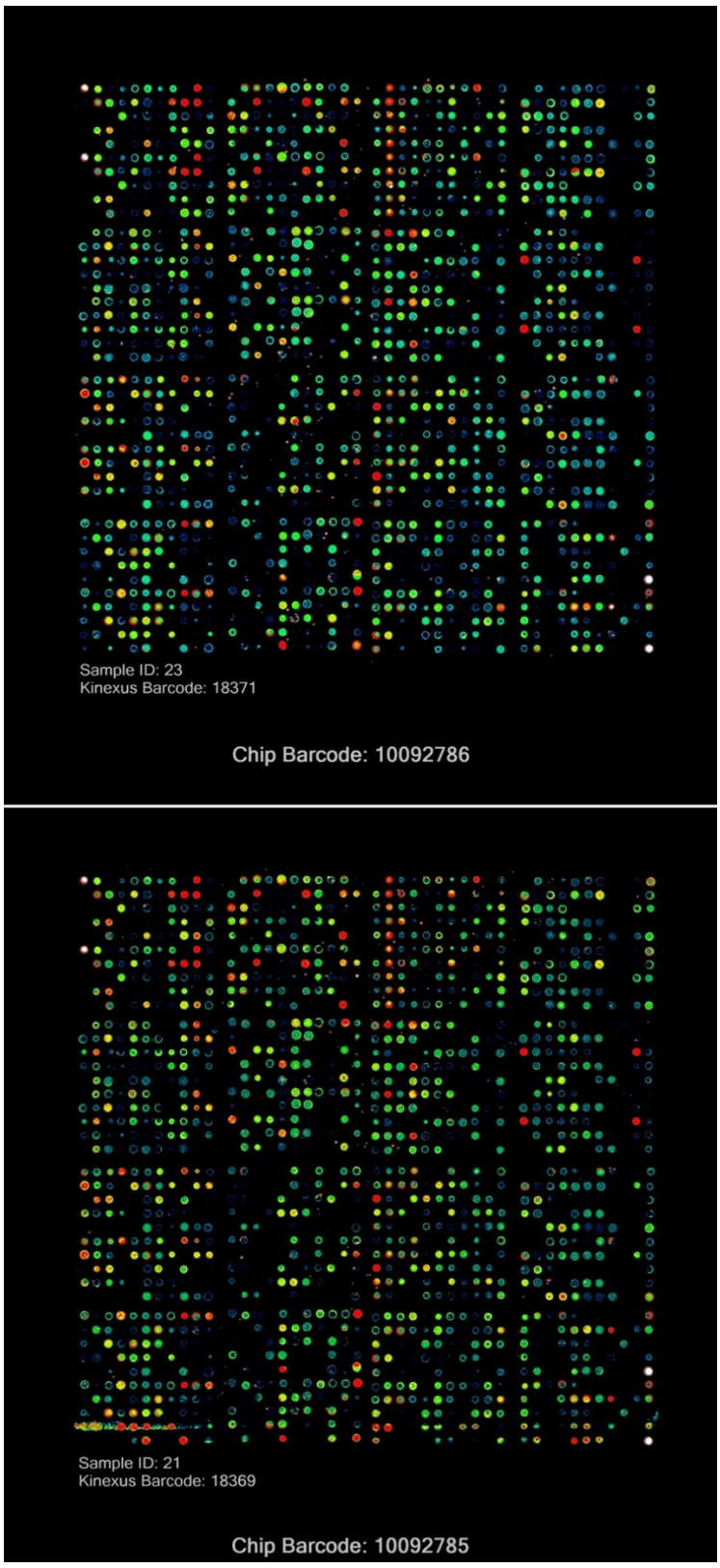

Figure 6.1 Kinexus images of array outlining comparison between AGS control (bottom, ID21) and AGS+S1P (top, ID23) protein samples.
Protein expression correlates with the signal intensity. Decreasing signal intensity corresponds with a red to orange to yellow to green to blue transition.

Table 6.1 Top 50 upregulated total proteins following S1P treatment
Data summarised from Kinexus report and is based on scaling according to percentage change from control (%CFC)

Target Protein Name	Phospho Site (Human)/Pan specific	Full Target Protein Name	Globally Normalized - AGS Control	Globally Normalized - S1P Treated AGS	%CFC (Treated from Control)
ROKa	Pan-specific	Rho-associated protein kinase 2	292	1177	308
PP2A/Ca	Pan-specific	Protein-serine phosphatase 2A - catalytic subunit - alpha isoform	110	310	186
RONa	Pan-specific	Macrophage-stimulating protein receptor alpha chain	193	513	170
Synapsin 1	Pan-specific	Synapsin 1 isoform Ia	197	515	165
Catenin b	Pan-specific	Catenin (cadherin-associated protein) beta 1	2445	5759	138
Smad2/3	Pan-specific	SMA- and mothers against decapentaplegic homolog 2/3	125	298	142
SOD (Cu/Zn)	Pan-specific	Superoxide dismutase 1	85	197	135
Smac/DIABLO	Pan-specific	Second mitochondria-derived activator of caspase	74	153	110
DUSP11	Pan-specific	Phosphatidylinositol-3,4,5-trisphosphate 5-phosphatase 2	4682	8592	86
Rac1	Pan-specific	Ras-related C3 botulinum toxin substrate 1	151	291	95
Caspase 7	Pan-specific	Caspase 7 (ICE-like apoptotic protease 3 (ICE-LAP3), Mch3)	217	399	86
IKKg/NEMO	Pan-specific	I-kappa-B kinase gamma/NF-kappa-B essential modulator	146	267	85
PKG1	Pan-specific	cGMP-dependent protein kinase 1, alpha isozyme	193	323	69
PARP1	Pan-specific	Poly [ADP-ribose] polymerase 1 (ADPRT)	7603	11788	57
BCL	Pan-specific	B-cell lymphoma protein 2 alpha	66	108	66

PTP-PEST	Pan-specific	Protein tyrosine phosphatase, non-receptor type 12	42	67	64
ZAP70	Pan-specific	Zeta-chain (TCR) associated protein-tyrosine kinase, 70 kDa	197	304	56
A-Raf	Pan-specific	A-Raf proto-oncogene serine/threonine-protein kinase	4252	6219	48
Jun	Pan-specific	Jun proto-oncogene-encoded AP1 transcription factor	176	267	54
CDK1	Pan-specific	Cyclin-dependent protein-serine kinase 1	407	611	52
STAT5A	Pan-specific	Signal transducer and activator of transcription 5A	3848	5549	46
PKC h	Pan-specific	Protein kinase C eta type	35	54	57
CDK1	Pan-specific	Cyclin-dependent protein-serine kinase 1	10352	14610	43
Cdc25B	Pan-specific	Cell division cycle 25B phosphatase	1974	2851	46
MEK5	Pan-specific	MAPK/ERK protein-serine kinase 5 (MKK5)	4413	6028	38
p38b MAPK	Pan-specific	Mitogen-activated protein-serine kinase p38 beta	5678	7722	38
HspBP1	Pan-specific	Hsp70 binding protein 1	169	242	45
VHR	Pan-specific	Dual specificity protein phosphatase 3	615	858	41
KDEL Receptor, KR10	Pan-specific	ER lumen protein retaining receptor 1	1278	1759	39
eIF2a	Pan-specific	Eukaryotic translation initiation factor 2 alpha	146	205	42
Striatin	Pan-specific	Striatin	18283	23580	31
Cdc25C	Pan-specific	Cell division cycle 25C phosphatase	4105	5414	34
MKP2	Pan-specific	MAP kinase phosphatase 2 (VH2)	237	327	39
STAT3	Pan-specific	Signal transducer and activator of transcription 3 (acute phase response factor)	1160	1555	36
ZIPK	Pan-specific	ZIP kinase (death associated protein-	3954	5194	33

		serine kinase 3 (DAPK3))			
Flt3	Pan-specific	Receptor-type tyrosine-protein kinase FLT3	6237	8103	32
Cdc25A	Pan-specific	Cell division cycle 25A phosphatase	4944	6430	32
DUSP1 (MKP1)	Pan-specific	MAP kinase phosphatase 1 (CL100, VH1)	9676	12425	30
ALK	Pan-specific	Anaplastic lymphoma kinase	16709	21155	28
SMG1	Pan-specific	Lambda/iota protein kinase C-interacting protein	43	60	41
ZIPK	Pan-specific	ZIP kinase (death associated protein-serine kinase 3 (DAPK3))	4355	5608	30
MKK7	Pan-specific	MAPK/ERK protein-serine kinase 7 (MKK7)	56	78	40
PP2A/Aa/b	Pan-specific	Protein-serine phosphatase 2A - A regulatory subunit - alpha and beta isoforms	7429	9469	29
PDK2	Pan-specific	Pyruvate dehydrogenase kinase isoform 2	10974	13879	28
LAR	Pan-specific	LCA antigen-related (LAR) receptor tyrosine phosphatase	142	192	37
Hsp47	Pan-specific	Heat shock 47 kDa protein (collagen-binding protein 1, colligin 1)	265	355	36
PP2A/Bb	Pan-specific	Protein-serine phosphatase 2A - B regulatory subunit - beta isoform	9563	12040	27
PP2Cd	Pan-specific	Protein-serine phosphatase 2C - catalytic subunit - delta isoform	187	251	36
Elk 1	Pan-specific	ETS domain-containing protein Elk-1	91	124	37
Cyclin D1	Pan-specific	Cyclin D1 (PRAD1)	18055	22432	26

Table 6.2 Top 50 downregulated total proteins following S1P treatment
Data summarised from Kinexus report and is based on scaling according to percentage change from control (%CFC)

Target Protein Name	Phospho Site (Human)/Pan specific	Full Target Protein Name	Globally Normalized - AGS Control	Globally Normalized - S1P Treated AGS	%CFC (Treated from Control)
PKCl	Pan-specific	Protein-serine kinase C lambda/iota	930	30	-97
Nek2	Pan-specific	NIMA (never-in-mitosis)-related protein-serine kinase 2	291	93	-68
p70 S6K	Pan-specific	Ribosomal protein S6 kinase beta-1	133	46	-65
MEKK1	Pan-specific	MAPK/ERK kinase kinase 1	95	36	-61
p107	Pan-specific	Retinoblastoma (Rb) protein-related p107 (PRB1)	4957	2119	-57
VGFR3	Pan-specific	Vascular endothelial growth factor receptor-protein-tyrosine kinase 3 (VEGFR3)	12503	5557	-55
Akt2 (PkBb)	Pan-specific	RAC-beta serine/threonine-protein kinase	60	27	-54
Yes	Pan-specific	Yamaguchi sarcoma proto-oncogene-encoded tyrosine kinase	62	28	-54
Wee1	Pan-specific	Wee1 protein-tyrosine kinase	9047	4870	-45
SMG1	Pan-specific	Lambda/iota protein kinase C-interacting protein	76	41	-45
p35	Pan-specific	CDK5 regulatory subunit p25 and p35	7045	3866	-44
Raf1	Pan-specific	Raf1 proto-oncogene-encoded protein-serine kinase	3184	1761	-44
TYK2	Pan-specific	Protein-tyrosine kinase 2 (Jak-related)	11456	6566	-42
MKK6	Pan-specific	MAPK/ERK protein-serine kinase 6 (MKK6)	18788	11100	-40

TBK1	Pan-specific	Serine/threonine-protein kinase TBK1	6040	3584	-40
4E-BP1	Pan-specific	Eukaryotic translation initiation factor 4E binding protein 1 (PHAS1)	237	142	-39
PKG1b-NT	Pan-specific	cGMP-dependent protein kinase 1, beta isozyme	4487	2758	-38
STAT6	Pan-specific	Signal transducer and activator of transcription 6	4719	2930	-37
MEK3	Pan-specific	MAPK/ERK protein-serine kinase 3 beta isoform (MKK3 beta)	2029	1292	-36
NFkappa B p65	Pan-specific	NF-kappa-B p65 nuclear transcription factor	4102	2614	-35
Bak	Pan-specific	Bcl2 homologous antagonist/killer (BCK2L7)	2839	1856	-34
PAK3	Pan-specific	p21-activated kinase 3 (beta) (serine/threonine-protein kinase PAK 3)	3567	2333	-34
PP4C (X/C)	Pan-specific	Protein-serine phosphatase X - catalytic subunit (PPX/C)	86	57	-33
MSH2	Pan-specific	DNA mismatch repair protein mutS homolog2, colon cancer, nonpolyposis type 1	455	302	-33
Hsc70	Pan-specific	Heat shock 70 kDa protein 8	2545	1713	-32
MEK5	Pan-specific	MAPK/ERK protein-serine kinase 5 (MKK5)	1943	1313	-32
JNK2	Pan-specific	Jun N-terminus protein-serine kinase (stress-activated protein kinase (SAPK)) 2	67	46	-31
FasL	Pan-specific	Tumor necrosis factor ligand, member 6	321	223	-30
SNF1lK	Pan-specific	Serine/threonine-protein kinase SIK1	130	91	-29

Caveolin 1	Pan-specific	Caveolin 1	67	47	-29
Cdc2 p34	Pan-specific	Cyclin-dependent protein-serine kinase 1	4204	2974	-28
PAK a	Pan-specific	p21-activated kinase 1 (alpha) (serine/threonine-protein kinase PAK 1)	3965	2812	-28
Lck	Pan-specific	Lymphocyte-specific protein-tyrosine kinase	2435	1738	-28
Src	Pan-specific	Src proto-oncogene-encoded protein-tyrosine kinase	1347	964	-28
Cdc25C	Pan-specific	Cell division cycle 25C phosphatase	4263	3094	-27
IRAK1	Pan-specific	Interleukin 1 receptor-associated kinase 1 (Pelle-like protein kinase)	41	30	-26
PKCz	Pan-specific	Protein-serine kinase C zeta	2564	1889	-25
SG2NA	Pan-specific	Striatin-3	9530	7030	-25
MELK	Pan-specific	Maternal embryonic leucine zipper kinase	6425	4755	-25
FAS	Pan-specific	Tumor necrosis factor superfamily member 6 (Apo1, CD95)	4279	3171	-25
CDK9	Pan-specific	Cyclin-dependent protein-serine kinase 9	3153	2349	-25
Wip1	Pan-specific	Protein phosphatase 1D	3144	2373	-24
CDK6	Pan-specific	Cyclin-dependent protein-serine kinase 6	4196	3178	-23
Hsp90	Pan-specific	Heat shock 90 kDa protein alpha/beta	2917	2209	-23
PDK3	Pan-specific	Pyruvate dehydrogenase kinase isoform 3	485	367	-23
Bcl2	Pan-specific	B-cell lymphoma protein 2 alpha	182	139	-23
PKD (PKCm)	Pan-specific	Protein-serine kinase C mu (Protein kinase D)	2506	1920	-22
PSD-95	Pan-specific	Disks large homolog 4	455	349	-22

MEK3b	Pan-specific	MAPK/ERK protein-serine kinase 3 beta isoform (MKK3 beta)	217	169	-21
IAP1	Pan-specific	Cellular inhibitor of apoptosis protein 1 (baculoviral IAP repeat-containing protein 3, apoptosis inhibitor 2 (API2))	34	27	-20

Table 6.3 Top 50 upregulated phospho- proteins following S1P treatment
Data summarised from Kinexus report and is based on scaling according to percentage change from control (%CFC)

Target Protein Name	Phospho Site (Human)	Full Target Protein Name	Globally Normalized - AGS Control	Globally Normalized - S1P Treated AGS	%CFC (Treated from Control)
STAT1	Y701	Signal transducer and activator of transcription 1 alpha	283	976	249
Tau	S199/202	Microtubule-associated protein tau	317	903	189
RSK1/2	S221/S227	Ribosomal S6 protein-serine kinase 1	771	2046	169
Mnk1	T197+T202	MAP kinase-interacting protein-serine kinase 1 (calmodulin-activated)	54	148	179
STAT5A	S780	Signal transducer and activator of transcription 5A	168	417	151
Raf1	S259	Raf1 proto-oncogene-encoded protein-serine kinase	33	81	147
Vimentin	S33	Vimentin	134	309	134
Rb	T821	Retinoblastoma-associated protein 1	328	712	120
Tau	S422	Microtubule-associated protein tau	331	699	114
S6	S235	40S ribosomal protein S6	264	555	112
4E-BP1	T45	Eukaryotic translation initiation factor 4E binding protein 1 (PHAS1)	133	281	114
PTEN	S380/S382/S385	Phosphatidylinositol-3,4,5-trisphosphate 3-phosphatase and protein phosphatase and tensin homolog deleted on chromosome 10	579	1191	108
Rad17	S645	Rad17 homolog	92	176	93
JAK2	Y1007+Y1008	Janus protein-tyrosine kinase 2	34	63	89

APP	T743	Amyloid beta A4 protein	1006	1732	74
Rac1/cdc42	S71	Ras-related C3 botulinum toxin substrate 1	164	290	79
Rb	S795	Retinoblastoma-associated protein 1	60	102	72
Met	Y1230/Y1234/Y1235	Hepatocyte growth factor (HGF) receptor-tyrosine kinase	223	366	66
BMX (Etk)	Y40	Bone marrow X protein-tyrosine kinase	46	76	69
IR/IGF1R	Y1162/Y1163	Insulin receptor / Insulin-like growth factor 1 receptor	175	284	64
Kit	Y721	Mast/stem cell growth factor receptor Kit	204	327	62
Akt1 (PKBa)	S473	RAC-alpha serine/threonine-protein kinase	1756	2717	57
SHP2	S576	Protein-tyrosine phosphatase 1D (SHP2, SHPTP2, Syp, PTP2C)	204	326	62
p53	S392	Tumor suppressor protein p53 (antigenNY-CO-13)	510	802	59
PTEN	S380/T382/T383	Phosphatidylinositol-3,4,5-trisphosphate 3-phosphatase and protein phosphatase and tensin homolog deleted on chromosome 10	154	243	60
FRS2	Y349	Fibroblast growth factor receptor substrate 2	1785	2704	53
Cyclin E	T395	Cyclin E1	927	1417	55
Huntingtin	S421	Huntington's disease protein	47	76	62
Chk1	S280	Checkpoint protein-serine kinase 1	275	424	56
p70 S6K	S424	Ribosomal protein S6 kinase beta-1	106	165	58
Estrongen Receptor	S104	Estrogen receptor alpha	334	507	54
PKA Cb	S338	cAMP-dependent protein-serine kinase catalytic subunit beta	1107	1648	51

VEGFR2	Y1214	Vascular endothelial growth factor receptor-tyrosine kinase 2 (Flk1)	86	134	57
eIF4G	S1232	Eukaryotic translation initiation factor 4 gamma 1	568	851	52
PYK2	Y579	Protein-tyrosine kinase 2	112	171	54
Tau	S404	Microtubule-associated protein tau	349	522	51
IkBa	Y42	Inhibitor of NF-kappa-B alpha (MAD3)	158	239	53
B23 (NPM)	T199	B23 (nucleophosmin, numatrin, nucleolar protein NO38)	216	324	51
IRS1	Y1179	Insulin receptor substrate 1	4316	6144	44
Rb	S612	Retinoblastoma-associated protein 1	6413	8997	42
IRS1	S639	Insulin receptor substrate 1	109	163	51
MST3	T184	Mammalian STE20-like protein-serine kinase 3	2332	3314	44
Tau	S199	Microtubule-associated protein tau	533	772	47
CDK1/CDC2	T161	Cyclin-dependent protein-serine kinase 1/2	157	231	49
Tau	T231	Microtubule-associated protein tau	212	306	46
JNK 1/2/3	T183/Y185	Jun N-terminus protein-serine kinase (stress-activated protein kinase (SAPK)) 1/2/3	362	519	45
FKHR	S319	Forkhead box protein O1	154	223	47
FAK	S722	Focal adhesion protein-tyrosine kinase	425	603	44
Jun	T91	Jun proto-oncogene-encoded AP1 transcription factor	796	1112	41
IkBe	S22	NF-kappa-B inhibitor epsilon	137	197	45

Table 6.4: Top 50 downregulated phospho-proteins following S1P treatment
Data summarised from Kinexus report and is based on scaling according to percentage change from control (%CFC)

Target Protein Name	Phospho Site (Human)	Full Target Protein Name	Globally Normalized - AGS Control	Globally Normalized - S1P Treated AGS	%CFC (Treated from Control)
p38a MAPK	T180/Y182	Mitogen-activated protein-serine kinase p38 alpha	1447	29	-98
PKCe	S729	Protein-serine kinase C epsilon	2125	446	-79
RSK1/2/3	T573	Ribosomal S6 protein-serine kinase 1	123	51	-58
Rb	S608	Retinoblastoma-associated protein 1	50	23	-54
MEK1	S298	MAPK/ERK protein-serine kinase 1 (MKK1)	61	29	-52
Msk1	S376	Mitogen & stress-activated protein-serine kinase 1	88	42	-51
Myc	S373	Myc proto-oncogene protein	630	305	-51
PKCt	S695	Protein-serine kinase C theta	307	184	-39
Ron	Y1238	Macrophage-stimulating protein receptor alpha chain	48	29	-39
RelB	S552	Transcription factor RelB	820	516	-36
Tyrosine Hydroxylase	S40	Tyrosine hydroxylase isoform a	72	47	-34
Src	Y418	Src proto-oncogene-encoded protein-tyrosine kinase	487	331	-31
FAK	Y576+Y577	Focal adhesion protein-tyrosine kinase	744	512	-30
Ezrin	T567	Cytovillin 2	87	60	-30
IRAK4	T345+S346	Interleukin 1 receptor-associated kinase 4	57	39	-30
TBK1	S172	Serine/threonine -protein kinase TBK1	30149	20945	-30

PPP1R11	Y64	Protein phosphatase 1 regulatory subunit 11	4351	3031	-29
p70 S6K	T421/S424	Ribosomal protein S6 kinase beta-1	31	22	-28
Tau	T205	Microtubule-associated protein tau	474	337	-28
MEK1	T386	MAPK/ERK protein-serine kinase 1 (MKK1)	75	55	-26
eIF2a	S52	Eukaryotic translation initiation factor 2 alpha	947	693	-26
EGFR	Y1197	Epidermal growth factor receptor-tyrosine kinase	168	124	-25
Ephrin-B2	Y316	EPH-related receptor tyrosine kinase ligand 5	241	179	-25
p38d MAPK	Y182	Mitogen-activated protein-serine kinase p38 delta (MAPK13)	5911	4408	-24
CDK6	Y13	Cyclin-dependent protein-serine kinase 6	272	208	-23
Bcr	Y177	Breakpoint cluster region protein	4658	3583	-22
PKCm (PKD)	S916	Protein-serine kinase C mu (Protein kinase D)	1501	1157	-22
EGFR	Y998	Epidermal growth factor receptor-tyrosine kinase	4428	3425	-22
SMC1	S957	Structural maintenance of chromosomes protein 1A	3751	2934	-21
MEK2 mouse	T394	MAPK/ERK protein-serine kinase 2 (MKK2) (mouse)	6514	5101	-21
PKCd	Y311	Protein-serine kinase C delta	9051	7144	-20
c-Cbl	Y700	Signal transduction protein CBL	241	191	-20

PDGFRa	S847+pY849	Platelet-derived growth factor receptor kinase alpha	4655	3794	-17
Rb	T356	Retinoblastoma-associated protein 1	62	50	-17
MST3	T190	Mammalian STE20-like protein-serine kinase 3	7021	5725	-17
eIF4B	S422	Eukaryotic translation initiation factor 4B	325	268	-17
Lck	Y394	Lymphocyte-specific protein-tyrosine kinase	1706	1410	-16
Kit	Y703	Mast/stem cell growth factor receptor Kit	6356	5263	-16
MKK3	S218	MAPK/ERK protein-serine kinase 3 beta isoform (MKK3 beta)	5446	4512	-16
4E-BP1	S65	Eukaryotic translation initiation factor 4E binding protein 1 (PHAS1)	129	108	-16
PKCg	T514	Protein-serine kinase C gamma	7394	6191	-15
ERK1	Y204	Extracellular regulated protein-serine kinase 1 (p44 MAP kinase)	2180	1827	-15
AurKB	S227	Aurora Kinase B (serine/threonine protein kinase 12)	6818	5751	-15
A-Raf	Y302	A-Raf proto-oncogene serine/threonine-protein kinase	10667	9010	-14
GSK3a	T19+pS21	Glycogen synthase-serine kinase 3 alpha	45	38	-14
PKCt	S676	Protein-serine kinase C theta	340	290	-14
Jun	S73	Jun proto-oncogene-encoded AP1 transcription factor	2205	1911	-12

TrkB	Y705	BNDF/NT3/4/5 receptor-tyrosine kinase	194	170	-11
ASK1	S966	Apoptosis signal regulating protein-serine kinase 1	146	130	-10
Gab1	Y627	GRB2-associated binder 1	134	121	-8

6.3.2 Potential downstream signalling investigation

Following on from the initial summary of the most up and down-regulated proteins, the results of the Kinexus micro array were further analysed by a bioinformatician, Dr You Zhou, Systems Immunity Research Institute, Division of Infection and Immunity, Cardiff University. At the same time, we gave Dr. You the following inclusion and exclusion criteria

- Related to tumour progression in human.
- Related to chemotherapy resistance
- Related to clinical significance

The data indicated that there were a number of protein candidates demonstrating significantly changed levels of phosphorylation after the addition of S1P in AGS cells. One of the most significant changes was seen in Protein Kinase B (Akt/PKB).

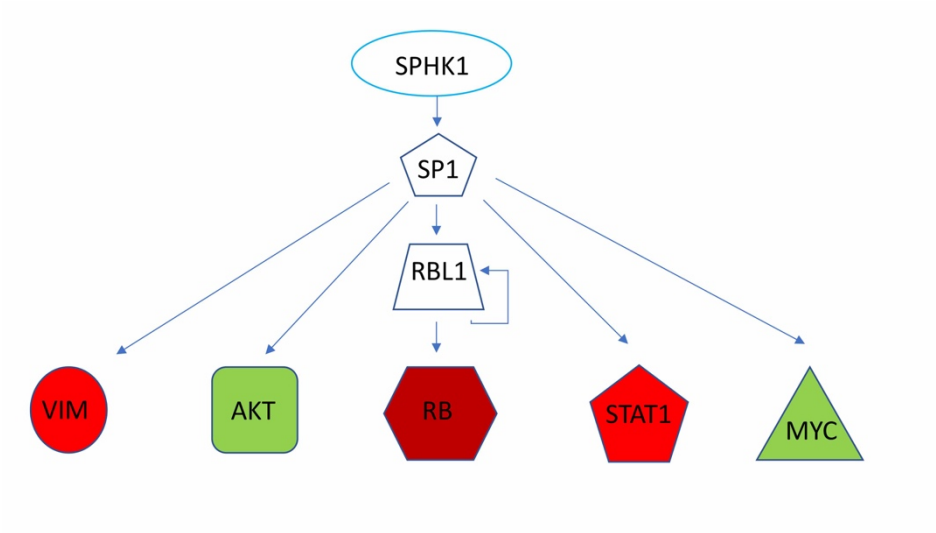

Figure 6.2 Bioinformatics analysis of the KinexusTM protein-array data.
Red represents upregulated and Green represents downregulated.

6.3.3 Potential downstream signalling investigation

Previous analysis highlighted AKT as a potential pathway downstream of SphK1/S1P. Given the significance of AKT/mammalian target of rapamycin (mTOR) in cell signalling and cancer cell survival, we further aimed to verify the protein expression level of total AKT and its phosphorylation at Ser473 between HGC27/AGS pEF and HGC27/AGS-SphK1-KD cell lines as this may be a key molecule governing the effects brought about by SphK1 suppression. It was found that downregulation of SphK1 correlated with the decrease of AKT Ser473, but appeared to have no influence on total AKT protein levels. Furthermore, we explored the downstream protein mTOR which is often activated by AKT. Interestingly, a decrease in p-mTOR (Ser2448), and potentially total m-TOR expression was discovered following SphK1 knockdown (Figure 6.3).

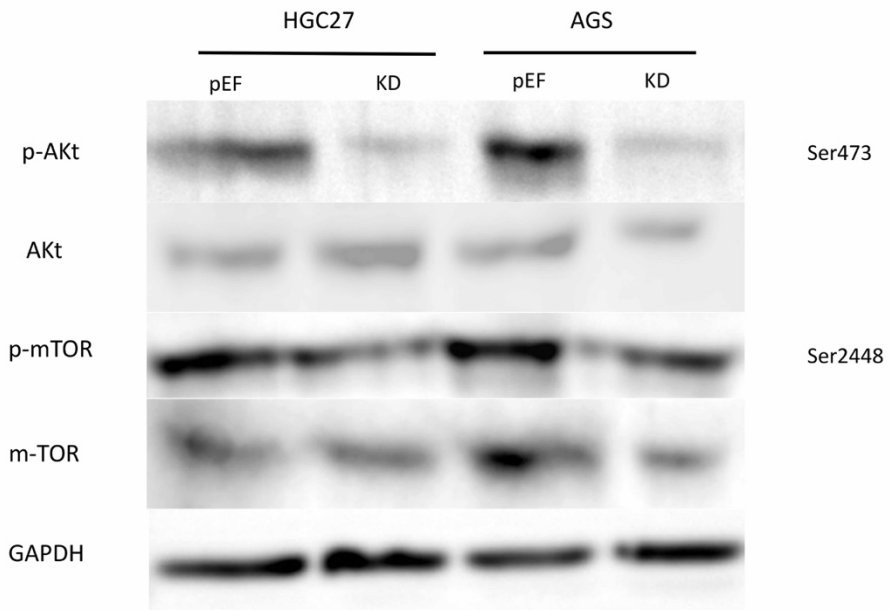

Figure 6.3 Western blotting verification of potential mechanistic actions, examining the relationship between SphK1 and AKT/m-TOR
Western blot verification on the protein expression level of AKT, AKT ser473, mTOR and mTOR Ser2448 in protein extracts from AGS/HGC27 SphK1-KD and AGS/HGC27 pEF.

6.4 Discussion

Both the literature and data presented throughout this thesis have demonstrated a role for SphK1 in promoting cancer progression and enhancing resistance to chemotherapy. Whilst the mechanisms downstream of SphK1 are beginning to be elucidated.

Currently, a number of pathways have been identified as acting downstream of SphK1 to regulate its pro-cancerous effects. For example, in CRC cell lines the inhibition of SphK1 resulted in a decreased migratory capacity and also reduced expression of FAK / pFAK as well as the EMT markers Slug, vimentin and N-cadherin, whilst enhancing E-cadherin levels. Consistent with this, chemical inhibition of FAK has similar effects to SphK1 inhibition on migration and EMT marker expression suggesting a link between SphK1, FAK and EMT in CRC (Xu et al., 2017a). Additional work subsequently explored this relationship in clinical samples and its impact on metastasis, demonstrating an up regulation of SphK1, vimentin, FAK and pFAK, and downregulation of E-cadherin, in metastatic compared to non-metastatic tumour and also, using knockdown and over-expression models, demonstrated SphK1 was involved in migration, EMT traits and regulated the expression of pFAK, MMP2/9 and AKT, which could subsequently be removed through FAK inhibition (Liu et al., 2019). Further studies focusing on lung cancer have similarly suggested links with the AKT pathway. Overexpression or knockdown A549 models have demonstrated SphK1 to be linked with invasion and migration, EMT marker (E-cadherin and Snail) expression and activation of AKT, where enhanced SphK1 brought about activation of AKT and subsequently traits associated with SphK1 overexpression could be negated through AKT inhibition (Zhu et al., 2015). This observation is similarly supported in an additional study exploring the impact of the long non coding (Lnc)RNA HULC in non-small cell lung cancer (NSCLC) (Liu et al., 2018). In this study the authors demonstrate HULC can

enhance SphK1 expression and levels of phospho-AKT, but not total levels of AKT and that inhibition of SphK1 or AKT is able to reduce the cellular effects of HULC, whilst SphK1 inhibition can also reduce AKT phosphorylation but was not itself inhibited by AKT inhibition (Liu et al., 2018).

In our study, we aimed to identify potential signalling pathways in which SphK1 could be linked and which may account for its observed role in cancer progression and chemoresistance. We conducted a Kinexus protein microarray following treatment with S1P in AGS cells to screen a large number of protein and phosphoproteins which highlighted AKT as a potential partner. This observation was interesting given the potential links observed in other cancers between SphK1 and AKT (Liu et al., 2018, Zhu et al., 2015, Liu et al., 2019). This was further validated using conventional western blot techniques in both AGS and HGC27 gastric cell models, where ribozyme transgene suppression of SphK1 reduced phosphorylation of AKT, but not total protein levels, and mTOR and appeared to further confirm the relationship. In addition to the AKT link, bioinformatics analysis also suggested a potential relationship with vimentin and a number of FAK phospho-residues were also seen to be altered following S1P treatment.

Similarly, potential links between FAK and vimentin were also observed following S1P treatment and scaling of phosphoproteins, though in our study S1P treatment brought about a decrease in the phosphorylation in the catalytic loop Y576/Y577 residues and an increase in S722 phosphorylation, which may potentially contrast with proposed SphK1 FAK links (Liu et al., 2019, Xu et al., 2017a). However, this may be due to the use of S1P treatment for the Kinexus microarray work, which in itself presents some limitations. For example, whilst SphK1 is a key kinase involved in the generation of S1P, the levels of S1P receptors within the cell line were not characterised/quantified making it difficult to understand the full significance and similarly it may not highlight any non-S1P related impacts of SphK1 within the cell

line. Hence direct observations following SphK1 manipulation should be clarified in the future. The reason why we used AGS for the Kinexus microarray is that AGS was readily available in our lab and was purchased from a commercial company with stable characters. Due to the cost of sending sample and the time limitation, we utilised AGS due to its readiness at the time of the Kinexus study and as it was a representative line used in our earlier work. of cell line at the time of study. This model provides preliminary insight, additional work characterizing effects of S1P treatment or SphK1 manipulation on a range of gastric cell lines are key in establishing downstream effectors. Netherthless, due to the indication that SphK1 or S1P signalling can influence phosphorylation and activation of AKT is of relevance and suggests that this relationship is common across many cancer types. AKT is a key pathway (Porta et al., 2014) across cancer types and is involved in the regulation of numerous cellular traits involved in cancer progression, including survival, proliferation and migration and represents a pathway of interest for therapeutic intervention. Enhanced activation of AKT is observed in many malignancies including gastric cancer where some reports have indicated links with poorer outlooks and resistance to chemotherapy (Oki et al., 2005, Almhanna et al., 2011, Cinti et al., 2008, Nam et al., 2003).

Taken together with the data from previous chapters the relationship between SphK1 and AKT in gastric cancer represents an interesting avenue to explore.

Chapter VII

General Discussion

7.1 Introduction

In the past decades, gastric cancer has become the fifth largest malignant tumour in the world (Bray et al., 2018), which seriously threatens the survival and health of the population. In China, gastric cancer is also an important fatal factor threatening the population. Although the incidence of gastric cancer has decreased in recent years, our 5-year survival rate still has a significant difference with our neighbours Japan and South Korea (Chen et al., 2018b), and also, the poor response to chemotherapy drugs for patients in advanced stages is one of the important reasons for poor survival. Therefore, the discovery of new molecular targets for treatment of gastric cancer has been the focus and direction of doctors and scientists working on gastric cancer research.

SphKs is a sphingosine metabolizing enzyme found in different organisms. SphKs have been identified in mammals. SphK1 is an oncogenic enzyme and the activity of SphK1 is closely associated to cell transformation, proliferation and tumour cell survival (Li et al., 2009). Our research hopes to define the function of SphK1 in gastric cancer and discover whether SphK1 serves as a new molecular markers for predicting the development and progression of gastric cancer.

7.2 Biological characteristics of SphK1

In 1998, Olivera et al. (Olivera et al., 1998) for the first time extracted SphK1 from rat kidney cells with a relative molecular mass of 49kDa. Subsequently, Kohham et al., (Kohama et al., 1998) successfully purified two SphK1 variants rats, named SphK1 a and SphK1b, respectively, and found that the amino acid sequences of the two differ only in the 382-388 polypeptides. In 2006, Venkataraman (Venkataraman et al., 2006) found that there are three SphK1 subtypes in the human body, named SphK1a, SphK1b, SphK1c. SphKs are members of the evolutionarily conserved

lipidase family, and the putative amino acid sequences of SphKs provided by NCBI are derived from thirty species spanning 4 epigenetic phyla.

7.3 SphK1 biological function

7.3.1 SphK1 and sphingosine 1 phosphate

S1P, Sphingosine (SP) and Ceramide (Cer) are key molecules involved in the process of sphingolipid metabolism. The effects of signalling molecules are manifested in important cellular processes including cancer progression. S1P is widely present in cells of various tissue systems in eukaryotes such as sputum (eg gastrointestinal tract, endocrine, reproductive), respiratory system and blood, lymphoid tissue, etc.) (Limaye, 2008). As a special ligand for the GPCR, the biological effects of S1P are mainly mediated by the GPCR family, including five specific subtypes, also known as S1PRs(1-5) (Zhang et al., 2007). S1P regulates different pathologies and physiological processes, including tumour formation, lymphocyte response, immune and allergic reactions, and angiogenesis and maturation. S1P not only act as a second messenger in the cell, but also act as an intercellular signalling molecule to interact with the S1P receptor on the cell surface to produce a wide range of biological effects, such as inhibition of apoptosis, stimulation of cell proliferation and regulation of adhesion molecule expression (Kim et al., 2009).

It has been reported that S1P plays an important role in regulating the survival and development of tumours. The rate-limiting enzyme that catalyses the production of S1P is SphK1. Hormones play a very important role in the development of tumours. SphK1 affects cell proliferation by regulating S1P production. It has multiple functions in areas such as death, migration and adhesion molecule expression (Hannun and Obeid, 2008). In addition to many bioactive agents that activate SphK1, receptor-type tyrosine kinases and intracellular proto-oncoproteins also activate

SphK1. The expression of SphK1 not only stimulates cell growth, but also leads to malignant transformation of cells. Therefore, the SphK1 / S1P pathway has been investigated as a signalling pathway for apoptosis and proliferation in recent years.

7.4 The role of SphK1 in tumorigenesis

7.4.1 SphK1 and tumour cell proliferation, apoptosis

SphK1 can be activated by many growth factors, cytokines and mitogens, and PDGF, PMA, TNF-a, FCS can activate SphK1. Although the molecular mechanisms by which these growth factors activate SphK1 are not fully understood, they demonstrate the importance of SphK1 in the development of tumorigenesis. At the same time, since its activation involves translocation to the cell membrane, it is speculated that its location is also important for its signalling function. Pitson et al., (Pitson et al., 2005) suggested that phosphorylation of SphK1 and its translocation from cytoplasm to membrane may be the key to the malignant phenotype of cells, which not only promotes the proliferation of malignant cells, but also protects the apoptotic pathway. Chamberlain et al., (Safadi-Chamberlain et al., 2005) used Myr-SphK1 to inhibit SphK1 activity; they hypothesized that the inhibition mechanism of SphK1 after anti-tumour therapy depends on p53, however, studies have found that in the p53 (-) human promyelocytic leukemia cell line HL-60, SphK1 was also down-regulated after addition of doxorubicin and etoposide, suggesting that SphK1 inhibition in these cells does not depend on the expression of p53. The experimental data on human pro-adenocarcinoma cell lines PC-3 and LNCaP showed that SphK1 was down-regulated after anti-tumour treatment regardless of the status of p53 in these cell lines, suggesting that multiple pathways may be involved (Neubauer et al., 2016). In terms of the significance of SphK1 inhibition in tumour apoptosis, it is speculated that by inhibiting SphK1, Cer produced by stimulating factors will not be

converted into S1P, and S1P is responsible for shifting tumour cells away form an apoptotic stat to a proflierative growth state. Contrary to the function of SphK1, SphK2 functions to induce apoptosis, but it has not yet been studied in detail in the pathogenesis or treatment of tumours.

The strong evidence that SphK1 initially became a potential target for cancer research comes from data from Vada et al. which found that SphK1 may be a product of an oncogene, in nude mice by using a classical cell transformation model. Fibroblasts overexpressing SphK1 phenotypes in tissue culture acquire the ability to form tumours. In many tumour tissues (such as stomach, rectum, small intestine, brain, breast, colon, lung, ovary, uterus, kidney), the expression of SphK1 mRNA is significantly higher than that of healthy controls (Summary in Table 1.3). Wang et al. (Wang et al., 2018b) reported SphK1 was expressed level in GC tissues and peripheral blood. The expression of SphK1 in tumour tissue was higher than that in normal tissue. In addition, S1P produced by SphK1 was more expressed in tumour patients' serum than in normal patients' serum in another dataset (Wang et al., 2018b).Similarly, downregulation of SphK1 expression will result in slower tumour cell growth, promote apoptosis and enhance chemotherapy sensitivity. Malavaud et al. (Malavaud et al., 2010) used the different effects of the topoisomerase inhibitor camptothecin and the anti-microtubule drug paclitaxel on human prostate cancer cell lines PC-3 and LNCaP to study their association with SphK1 and subsequent Cer/S1P. The relationship between the results showed that only in the cell lines sensitive to these chemotherapeutic drugs, SphK1 was significantly inhibited and the Cer/S1P ratio was increased, and tumour cells showed significant apoptosis, confirming that SphK1 is an important factor in tumour cell sensitivity. Visentin et al., (Visentin et al., 2006) found that neutralization of S1P with a specific monoclonal antibody significantly slowed the growth of multidrug-resistant tumours in murine

xenografts and allogeneic models, such as lung cancer, colon cancer, breast cancer, and melanin tumour and ovarian cancer.

7.4.2 S1P, SphK1 and tumour angiogenesis

Angiogenesis is a key link in tumour growth and metabolism. The method of anti-tumour angiogenesis has developed rapidly. Nowadays, bevacizumab (Avastin; Genentech CA), an anti-vascular endothelial growth factor (VEGF) antibody combined with traditional chemotherapy drugs for the treatment of colorectal cancer has been widely used. Recently, more and more evidence has shown that S1P is one of the most effective angiogenic factors. S1P is more effective than VEGF or hepatocyte growth factor (HGF) in promoting endothelial cell migration, thus promoting angiogenesis (Milstien and Spiegel, 2006). OH-Lee et al (Lee et al., 1999) showed that S1P combined with EDG-1 can stimulate DNA synthesis and induce vascular endothelial cell migration in vascular endothelial cells and is stronger than basic fibroblast growth factor (bFGF) and VEGF. S1P induces endothelial cell migration and adhesion and promotes the formation of tubular structures in endothelial cells. S1P stimulates umbilical vein endothelial cells to form a tubular structure in the extracellular matrix. The most direct evidence for S1P-promoting tumour angiogenesis comes from the use of anti-S1P murine monoclonal antibody (mAb) as a molecular sponge to selectively absorb and neutralize S1P, ie, human malignant tumours treated with mAbs in mice, this treatment blocks endothelial cell migration and capillary formation, inhibits angiogenesis induced by VEGF and bFGF, and prevents tumour-associated angiogenesis, while also preventing the release of pro-angiogenic cytokines from tumours (VEGF, IL-2 and IL-6).

SphK1 mainly affects tumour angiogenesis by generating S1P. Many tumour-associated growth factors and angiogenic factors can be phosphorylated by SphK1 promoting their downstream signal transduction. At the same time, there is some

evidence that SphK1 is involved in angiogenesis. Endothelial cells removed from serum and extracellular media display improved survival rates following overexpression of SphK1, suggesting that SphK1 plays an important role in angiogenesis under stress conditions (Whetton et al., 2003). After knocking out the SphK1 gene, mice died of haemorrhage due to dysplasia of the endothelial cells in the embryonic stage, so SphK1 may play a decisive role in the formation and maturation of new blood vessels.

7.5 Relationship between SphK1 and gastric cancer

7.5.1 Expression of SphK1 in gastric cancer tissues

In the early stage, we conducted a large-scale tissue microarray screening of freshly matched gastric cancer tissue samples from gastric cancer patients admitted to our hospital (PKUCH) from 2006 to 2007. We aimed to get identify differences at the transcription level and lay the foundation for further research. In 322 freshly matched gastric cancer tissues, we found that the expression of SphK1 in tumour tissues was significantly upregulated by tissue microarray screening, which was statistically significant. After further refinement analysis, we found that SphK1 was positively correlated with the advanced TNM stage of the patient's tumour and the degree of lymph node metastasis, which is consistent with the experimental results in other tumours (Wang et al., 2018b).

Comparing to Li et al. (Li et al., 2009) who detected SphK1 in normal gastric mucosa epithelium, gastric cancer cell line, gastric cancer tissues and matched normal tissues by RT-PCR, western blot and immunohistochemistry in 10 normal human gastric mucosa tissues and 175 gastric cancer tissues. The expression of SphK1 in gastric cancer at mRNA and protein levels was significantly higher than that in normal gastric tissues. 115 of the 175 gastric cancer tissues expressed SphK1 protein

(65.7%). The expression of SphK1 protein in gastric cancer was associated with multiple clinical and pathological factors such as clinical stage, T stage and M stage and vascular invasion in gastric cancer patients, which was consistent with the results of our study (Table 3.5). Patients with expression of SphK1 protein had shorter survival time, and the survival rate of patients was negatively correlated with the expression level of SphK1 protein which we clarify in Figure 3.4. Next, in order to test the expression of SphK1 at the protein level, we collected paraffin-embedded sections of gastric cancer patients in our hospital for immunohistochemistry. We found that the expression of SphK1 in gastric cancer patients was significantly higher than that in normal tissues adjacent to the cancer, and it was statistically significant. This is consistent with our findings on the level of transcription on tissue microarrays. Our study found that patients with positive SphK1 expression had significantly shorter survival than patients with negative SphK1 expression, both in terms of overall survival and disease-free survival, and we concluded that this might be related to intracellular function of SphK1. In the Cox regression model, we found that SphK1 can be used as an independent prognostic factor for patients with gastric cancer. Based on the above studies, we can speculate that SphK1 can be used as a good molecular target for predicting the prognosis of patients with gastric cancer.

At the same time, we did have limitations in our study. Firstly, we used fresh frozen samples from 2006 to 2007, and we extracted RNA in 2014. Therefore, it is possible that such long storage may have resulted in increased RNA degradation and thus affected the results of our study. However, it is suggested from the literature that Kelly et al. (Kelly et al., 2019) reported that 11 years storage didn't affect the integrity and histomorphology of tissues preserved under qualified preservation conditions. The biobank of PKUCH is a qualified one with worldwide standards. In addition, the expression rate of SphK1 at the protein level was about 34% in our study and the expression rate of SphK1 in Li et.al., (Li et al., 2009) article is as high

as 66%. The reason for this difference might be due to the antibody factor and the lower indoor temperature in the laboratory

Our research not only draws conclusions at the RNA level, but also from protein level which make our results reliable. And also, our results indicate SphK1 might be a promising targeting in gastric cancer treatment (Chapter III).

7.5.2 SphK1 and proliferation of gastric cancer cells

Yin et al. (Yin et al., 2019) reported that GC cells promoting autophagy in HPMCs, was inhibited by blocking TGF-β1 secreted by GC cells, while inhibiting expression of SphK1 in HPMC can inhibit TGF-β1-induced autophagy. SphK1 regulates HPMC autophagy and promotes the growth of GC cells *in vitro* and *in vivo*. Overexpression of SphK1 can induce fibrosis in HPMCs. Mechanically, elevated SphK1 levels promoted tumour bioactive sphingolipid dysregulation, of which ceramide decreased and S1P increased (Yin et al., 2019).

Similarly, we established an SphK1 knockdown cell line and carried out cell function studies to observe the impact of knockdown of SphK1 on cancer cell function. My *in vitro* data showed that dysregulation of SphK1 contributed to the cell migration, adhesion and growth which are similar trends to those present in the literature previously mentioned. Therefore, questions have been arisen as to whether SphK1 may be useful as a therapeutic target to improve the clinical outcome of patients (Chapter IV).

Here, I also want to clarify the limitations of our research. In functional assays, due to time and budget issues, we only knocked down gastric cancer cell lines with high SphK1 expression, rather than overexpressed SphK1 in gastric cancer cell lines with low SphK1 expression. Therefore, our evidence was not sufficiently strong. At the

same time, the establishment of knock down gene expression cell lines has off-target effects. Therefore, it is more convincing to establish overexpression cell lines and compare them with existing research.

At the same time, we should have more experiments such as cell cycle and apoptosis to observe whether SphK1 affects tumour biological behaviour through these processes. In confirming the effect of SphK1 on tumour cells, limited conclusions can be drawn with only one experiment method, such as migration. It should be verified at the level of molecular markers, such as whether migration affects EMT and detect molecular markers such as E-cadherin, N-cadherin, Snail, Slug and Vimentin.

.

7.5.3 SphK1 and chemoresistance of gastric cancer cells

A major challenge in developing effective cancer therapies involves implementation of effective treatment regimen, using biomarkers to identify patients who might benefit from the treatment and making the conventional chemotherapeutic approaches more effective and resilient to resistance mechanisms in the patients by using molecule antagonist and agonist.

Research has indicated that chemotherapy resistance occurs when inhibited the expression of SphK1 (Li et al., 2016c). For example, inhibited expression of SphK1 enhances docetaxel and camptothecin sensitivity in LNCaP and PC-3 cells (prostate cancer cells), respectively (Pchejetski et al., 2008). Similar result suggests that elevated SphK1 promoted daunorubicin resistance in leukaemia cells (Sobue et al., 2008), cisplatin resistance in lung cancer cells (Min et al., 2005) docetaxel resistance in prostate cancer cell (Alshaker et al., 2016) and oxaliplatin resistance in colon cancer cells (Nemoto et al., 2009). Furthermore, an additional study has demonstrated the ability of SphK1 to bring about the overexpression of transcript

levels of the downstream transcription factor, E2F7, mediating the chemoresistance of anthracycline in HNSCC (Hazar-Rethinam et al., 2015). Another study has demonstrated the capacity of a SphK inhibitor to repair the resistance to etoposide and doxorubicin through inducing apoptosis, a finding that is identical to the observation that reduced ceramide accumulation and sustained SphK1 activity may result in chemotherapeutic resistance (Heffernan-Stroud and Obeid, 2013).

In our study, we performed an initial preclinical evaluation of the role of SphK1 in chemoresistance of gastric cancer. In all two SphK1 high expression gastric cancer cell lines (AGS and HGC27), the IC50 was significantly decreased in SphK1-KD group comparing with SphK1 control group both following treatment with cisplatin or 5-FU according to different drug concentrations. Interestingly, cell viability and chemotherapeutic drugs are dose dependent. At relatively high concentrations and relatively low concentrations, SphK1 has a limited role in chemotherapy resistance, but within the appropriate drug concentration range, downregulating the expression of SphK1 expression was significantly decreasing the IC50 concentration of chemotherapeutic drugs. Furthermore, we also studied the small molecule inhibitor of SphK1, named PF543. After using PF543 to inhibit SphK1, we found that compared with no small molecule inhibitors group, the small molecule inhibitor group could significantly reduce the IC50 of chemotherapy drugs in both the AGS or HGC27 cell line and in the cisplatin or fluorouracil chemotherapy group. Wang et al. (Wang et al., 2018a) reported that the use of PF543 in TNBC cells increased the sensitivity of the cells to chemotherapy drugs which showed similar findings to ours. At the same time, we used the patient derived primary cell lines established in PKUCH and selected one which showed high expression of SphK1 and one with low expression of SphK1 for subsequent research. The experimental group treated with PF543 showed that PF543 in the SphK1 high expression group significantly increased the sensitivity of chemotherapy, but not in the low expression group. This

preliminarily indicated that SphK1 play a role in the chemotherapy resistance of gastric cancer (Chapter V).

In my future research, I would like to build up a mouse model to further verify that knockdown of SphK1 can contribute to chemosensitivity in gastric cancer cell. This would further investigate whether SphK1 can be a potential target to covert chemoresistance of gastric cancer patients.

Our research has well demonstrated at the cellular level that reducing SphK1 expression enhanced the chemosensitivity of fluorouracil and cisplatin. At the same time, in the primary cells derived from patients and gastric cancer cell lines, it has also been proved that the use of small molecule inhibitors PF543 in high expression of SphK1 cell lines lead to increase in the sensitivity of cells to chemotherapy. On the other hand, there is no such effect in a patient derived primary cell line with low expression of SphK1. However, these studies are all at the 2-Dimensional level, and they couldn't simulate the real environment in the human body. With the continuous advancement of research technology, emerging Patient Derived Organoids (PDO) (Vlachogiannis et al., 2018) and Patient Derived Tumour Xenograft (PDTX) (Ben-David et al., 2017) have further simulated the microenvironment in human tumour. Therefore, our research should further validate our hypotheses on these models.

7.6 The mechanisms of SphK1 in gastric cancer cells

Previous research has focused on the study of the function and the effect on chemoresistance of SphK1 in cells. SphK1 localized to the endoplasmic reticulum within the cytoplasm, and many molecules activate SphK1 and promoted its expression. These factors include seven transmembrane receptor activators, tyrosine kinase receptors, pro-inflammatory factors, immunoglobulins, calcium ions and protein kinase receptors. Activation of SphK1 is achieved by translocation to the

vicinity of the cell membrane, and this translocation requires phosphorylation of ERK at the Ser225 site, which also increases the expression of SphK1. Other experiments have demonstrated this from another perspective. SphK1 cannot be translocated near the cell membrane in cells with SphK1 Ser225 mutations, and thus does not promote cell proliferation and survival (Ren et al., 2002).

Another study demonstrated that the deletion of SphK1 inhibited the growth of thymic lymphomas in p53 null mice and extended the survival time. SphK1 enhances the expression of sphingosine and ceramide, in order to mediate P53 tumour suppressive role in cancer, and also influences the cell cycle process and chemosensitivity (Heffernan-Stroud et al., 2012). The study of Liu et al. (Liu et al., 2019) indicated that SphK1 was overexpressed in colon cancer, which affected the prognosis, metastasis and survival of patients. SphK1 affected the metastasis through affecting cancer cell EMT. At the same time, elevated expression of SphK1 promoted the expression of p-FAK, AKT and MMP2/9. FAK small inhibitors inhibited the expression of the above proteins and the inactivation of FAK signalling pathways (Liu et al., 2019).

In recent years, research discovered that SphK1 is a target of micro RNA (miRNA), and that this will subsequently impact many downstream signalling pathways. Wang et al. study (Wang et al., 2019a) demonstrated that miR-506-3p directly targeted and inhibited SphK1 expression on osteosarcoma. In this study, transfection with miR-506-3p mimics reduced the ability of invasion of osteosarcoma cell lines, which could be subsequently reversed through SphK1 overexpression. Furthermore, miR-506-3p played an important role in MET and autophagy. Similarly, a study by Cao et al. (Cao et al., 2019), also highlighted a link between SphK1 and miR-128 in PTC and FTC. In this study SphK1 was identified as a target of miR-128 and the expression of SphK1 was reduced in PTC and FTC tissues where it notably showed a negative correlation with miR-128 expression. Additionally, the inhibitory effect

of miR-128 on growth rate and tumour weight identified using *in vivo* models also appeared to suppress SphK1 expression. SphK1 plays an important role in the occurrence and development of cancer and affects different signalling pathways.

NF-κB is well established as a key signalling pathway in apoptosis and as being involved in cancer development and progression (Zhang et al., 2017). In keeping with SphK1's role, links between SphK1 and NF-κB have been previously observed. One such study by Alvarez et al. (Alvarez et al., 2010) have demonstrated a role for SphK1/S1P in apoptosis through regulation of NF-κB signalling by ubiquitination of TRAF2, RIP1, IκB kinase, IκBa and the degradation of IκBa (Alvarez et al., 2010). Further links have also been demonstrated in a subsequent study by Liang et al. (Liang et al., 2013) indicating that overexpression of SphK1 and subsequent upregulation of S1P drives a persistent amplification loop from SphK1/S1P/S1PR1 to NF-κB/IL-6/STAT3 (Liang et al., 2013).

In our study, we aimed to identify potential signalling pathways in which SphK1 could be linked and which may account for its observed role in cancer progression and chemoresistance. Our observation was interesting given the potential links observed in other cancers between SphK1 and AKT (Liu et al., 2018, Zhu et al., 2015, Liu et al., 2019). This was further validated using conventional western blot techniques in both AGS and HGC27 gastric cell models, where ribozyme transgene suppression of SphK1 reduced phosphorylation of AKT, but not total protein levels, and mTOR and appeared to further confirm the relationship. In addition to the AKT link, bioinformatics analysis also suggested a potential relationship with vimentin and a number of FAK phospho-residues were also seen to be altered following S1P treatment (Chapter VI). Furthermore, Peng et al. (Peng et al., 2010) reported that in cisplatin-resistant cell lines, there was a higher phosphorylation of Akt. At the same time, inhibition of Akt phosphorylation made drug-resistant cells sensitive to cisplatin. In addition, if the phosphorylation of Akt / mTOR was inhibited in

common ovarian cell lines, cancer cells could be made more sensitive to cisplatin. This study also strongly confirmed that resistance to cisplatin works through the Akt / mTOR pathway which explained the high expression SphK1 activation Akt / mTOR signalling pathway which affects drug gastric cancer patient chemoresistance.

In our research, due to the fact that the knock down cell line was not yet established and commercial SphK1 inhibitors were not available at that time, we chose to use exogenous S1P instead. This is another limitation in our research. Therefore, we will use the established knockdown cell line and SphK1 inhibitor to explore the downstream signalling pathway in the future. Furthermore, in establishing an over-expression cell line, we can compare the same change of signalling pathway in the knockdown and over-expression cell lines.

7.7 Conclusion

In summary, SphK1 is overexpressed in many types of tumours and plays a role in promoting growth, cell apoptosis, and angiogenesis. SphK1expression is closely related to cell biological behaviour such as proliferation, migration and apoptosis of human gastric cancer cells and the occurrence and metastasis of GC. However, the up-regulated expression of SphK1 in tumour cells and its role in tumorigenesis and development and chemoresistance and related molecular mechanisms are still unclear, and further in-depth studies are needed. However, based on my current research, I believe that SphK1 is expected to become a potential new target for gastric cancer therapy and play a significant role in GC chemoresistance.

Chapter VIII

References

ACHARYA, S., YAO, J., LI, P., ZHANG, C., LOWERY, F. J., ZHANG, Q., GUO, H., QU, J., YANG, F., WISTUBA, II, PIWNICA-WORMS, H., SAHIN, A. A. & YU, D. 2019. Sphingosine Kinase 1 Signaling Promotes Metastasis of Triple-Negative Breast Cancer. *Cancer Res,* 79**,** 4211-4226.

AKAO, Y., BANNO, Y., NAKAGAWA, Y., HASEGAWA, N., KIM, T. J., MURATE, T., IGARASHI, Y. & NOZAWA, Y. 2006. High expression of sphingosine kinase 1 and S1P receptors in chemotherapy-resistant prostate cancer PC3 cells and their camptothecin-induced up-regulation. *Biochem Biophys Res Commun,* 342**,** 1284-90.

AL-BATRAN, S. E., HOFHEINZ, R. D., PAULIGK, C., KOPP, H. G., HAAG, G. M., LULEY, K. B., MEILER, J., HOMANN, N., LORENZEN, S., SCHMALENBERG, H., PROBST, S., KOENIGSMANN, M., EGGER, M., PRASNIKAR, N., CACA, K., TROJAN, J., MARTENS, U. M., BLOCK, A., FISCHBACH, W., MAHLBERG, R., CLEMENS, M., ILLERHAUS, G., ZIRLIK, K., BEHRINGER, D. M., SCHMIEGEL, W., POHL, M., HEIKE, M., RONELLENFITSCH, U., SCHULER, M., BECHSTEIN, W. O., KONIGSRAINER, A., GAISER, T., SCHIRMACHER, P., HOZAEEL, W., REICHART, A., GOETZE, T. O., SIEVERT, M., JAGER, E., MONIG, S. & TANNAPFEL, A. 2016. Histopathological regression after neoadjuvant docetaxel, oxaliplatin, fluorouracil, and leucovorin versus epirubicin, cisplatin, and fluorouracil or capecitabine in patients with resectable gastric or gastro-oesophageal junction adenocarcinoma (FLOT4-AIO): results from the phase 2 part of a multicentre, open-label, randomised phase 2/3 trial. *Lancet Oncol,* 17**,** 1697-1708.

ALEMANY, R., VAN KOPPEN, C. J., DANNEBERG, K., TER BRAAK, M. & MEYER ZU HERINGDORF, D. 2007. Regulation and functional roles of sphingosine kinases. *Naunyn Schmiedebergs Arch Pharmacol,* 374**,** 413-28.

ALLEMANI, C., MATSUDA, T., DI CARLO, V., HAREWOOD, R., MATZ, M., NIKSIC, M., BONAVENTURE, A., VALKOV, M., JOHNSON, C. J., ESTEVE, J., OGUNBIYI, O. J., AZEVEDO, E. S. G., CHEN, W. Q., ESER, S., ENGHOLM, G., STILLER, C. A., MONNEREAU, A., WOODS, R. R., VISSER, O., LIM, G. H., AITKEN, J., WEIR, H. K., COLEMAN, M. P. & GROUP, C. W. 2018. Global surveillance of trends in cancer survival 2000-14 (CONCORD-3): analysis of individual records for 37 513 025 patients diagnosed with one of 18 cancers from 322 population-based registries in 71 countries. *Lancet,* 391**,** 1023-1075.

ALMHANNA, K., STROSBERG, J. & MALAFA, M. 2011. Targeting AKT protein kinase in gastric cancer. *Anticancer Res,* 31**,** 4387-92.

ALSHAKER, H., WANG, Q., KAWANO, Y., ARAFAT, T., BOHLER, T., WINKLER, M., COOPER, C. & PCHEJETSKI, D. 2016. Everolimus (RAD001) sensitizes prostate cancer cells to docetaxel by down-regulation of HIF-1alpha and sphingosine kinase 1. *Oncotarget,* 7**,** 80943-80956.

ALVAREZ, S. E., HARIKUMAR, K. B., HAIT, N. C., ALLEGOOD, J., STRUB, G. M., KIM, E. Y., MACEYKA, M., JIANG, H., LUO, C., KORDULA, T., MILSTIEN, S. & SPIEGEL, S. 2010. Sphingosine-1-phosphate is a missing cofactor for the E3 ubiquitin ligase TRAF2. *Nature,* 465**,** 1084-8.

ARA, T., SONG, L., SHIMADA, H., KESHELAVA, N., RUSSELL, H. V., METELITSA, L. S., GROSHEN, S. G., SEEGER, R. C. & DECLERCK, Y. A. 2009. Interleukin-6 in the bone marrow microenvironment promotes the growth and survival of neuroblastoma cells. *Cancer Res,* 69**,** 329-37.

ARNOLD, M., RUTHERFORD, M. J., BARDOT, A., FERLAY, J., ANDERSSON, T. M., MYKLEBUST, T. A., TERVONEN, H., THURSFIELD, V., RANSOM, D., SHACK, L., WOODS, R. R., TURNER, D., LEONFELLNER, S., RYAN, S., SAINT-JACQUES, N., DE, P., MCCLURE, C., RAMANAKUMAR, A. V., STUART-PANKO, H., ENGHOLM, G., WALSH, P. M., JACKSON, C., VERNON, S., MORGAN, E., GAVIN, A., MORRISON, D. S., HUWS, D. W., PORTER, G., BUTLER, J., BRYANT, H., CURROW, D. C., HIOM, S., PARKIN, D. M., SASIENI, P., LAMBERT, P. C., MOLLER, B., SOERJOMATARAM, I. & BRAY, F. 2019. Progress in cancer survival, mortality, and incidence in seven high-income countries 1995-2014 (ICBP SURVMARK-2): a population-based study. *Lancet Oncol,* 20**,** 1493-1505.

AUERNHAMMER, C. J., BOUSQUET, C. & MELMED, S. 1999. Autoregulation of pituitary corticotroph SOCS-3 expression: characterization of the murine SOCS-3 promoter. *Proc Natl Acad Sci U S A,* 96**,** 6964-9.

BANG, Y. J., IM, S. A., LEE, K. W., CHO, J. Y., SONG, E. K., LEE, K. H., KIM, Y. H., PARK, J. O., CHUN, H. G., ZANG, D. Y., FIELDING, A., ROWBOTTOM, J., HODGSON, D., O'CONNOR, M. J., YIN, X. & KIM, W. H. 2015. Randomized, Double-Blind Phase II Trial With Prospective Classification by ATM Protein Level to Evaluate the Efficacy and Tolerability of Olaparib Plus Paclitaxel in Patients With Recurrent or Metastatic Gastric Cancer. *J Clin Oncol,* 33**,** 3858-65.

BANG, Y. J., KIM, Y. W., YANG, H. K., CHUNG, H. C., PARK, Y. K., LEE, K. H., LEE, K. W., KIM, Y. H., NOH, S. I., CHO, J. Y., MOK, Y. J., KIM, Y. H., JI, J., YEH, T. S., BUTTON, P., SIRZEN, F., NOH, S. H. & INVESTIGATORS, C. T. 2012. Adjuvant capecitabine and oxaliplatin for gastric cancer after D2 gastrectomy (CLASSIC): a phase 3 open-label, randomised controlled trial. *Lancet,* 379**,** 315-21.

BANG, Y. J., VAN CUTSEM, E., FEYEREISLOVA, A., CHUNG, H. C., SHEN, L., SAWAKI, A., LORDICK, F., OHTSU, A., OMURO, Y., SATOH, T., APRILE, G., KULIKOV, E., HILL, J., LEHLE, M., RUSCHOFF, J., KANG, Y. K. & TO, G. A. T. I. 2010. Trastuzumab in combination with chemotherapy versus chemotherapy alone for treatment of HER2-positive advanced gastric or gastro-oesophageal junction cancer (ToGA): a phase 3, open-label, randomised controlled trial. *Lancet,* 376**,** 687-97.

BANG, Y. J., XU, R. H., CHIN, K., LEE, K. W., PARK, S. H., RHA, S. Y., SHEN, L., QIN, S., XU, N., IM, S. A., LOCKER, G., ROWE, P., SHI, X., HODGSON, D., LIU, Y. Z. & BOKU, N. 2017. Olaparib in combination with paclitaxel in patients with advanced gastric cancer who have progressed following first-line therapy (GOLD): a double-blind, randomised, placebo-controlled, phase 3 trial. *Lancet Oncol,* 18**,** 1637-1651.

BARAN, Y., SALAS, A., SENKAL, C. E., GUNDUZ, U., BIELAWSKI, J., OBEID, L. M. & OGRETMEN, B. 2007. Alterations of ceramide/sphingosine 1-phosphate rheostat involved in the regulation of resistance to

imatinib-induced apoptosis in K562 human chronic myeloid leukemia cells. *J Biol Chem,* 282**,** 10922-34.

BAYERL, M. G., BRUGGEMAN, R. D., CONROY, E. J., HENGST, J. A., KING, T. S., JIMENEZ, M., CLAXTON, D. F. & YUN, J. K. 2008. Sphingosine kinase 1 protein and mRNA are overexpressed in non-Hodgkin lymphomas and are attractive targets for novel pharmacological interventions. *Leuk Lymphoma,* 49**,** 948-54.

BEIDER, K., ROSENBERG, E., BITNER, H., SHIMONI, A., LEIBA, M., KOREN-MICHOWITZ, M., RIBAKOVSKY, E., KLEIN, S., OLAM, D., WEISS, L., WALD, H., ABRAHAM, M., GALUN, E., PELED, A. & NAGLER, A. 2017. The Sphingosine-1-Phosphate Modulator FTY720 Targets Multiple Myeloma via the CXCR4/CXCL12 Pathway. *Clin Cancer Res,* 23**,** 1733-1747.

BEKTAS, M., JOLLY, P. S., MULLER, C., EBERLE, J., SPIEGEL, S. & GEILEN, C. C. 2005. Sphingosine kinase activity counteracts ceramide-mediated cell death in human melanoma cells: role of Bcl-2 expression. *Oncogene,* 24**,** 178-87.

BEN-DAVID, U., HA, G., TSENG, Y. Y., GREENWALD, N. F., OH, C., SHIH, J., MCFARLAND, J. M., WONG, B., BOEHM, J. S., BEROUKHIM, R. & GOLUB, T. R. 2017. Patient-derived xenografts undergo mouse-specific tumor evolution. *Nat Genet,* 49**,** 1567-1575.

BLAIR, V., MARTIN, I., SHAW, D., WINSHIP, I., KERR, D., ARNOLD, J., HARAWIRA, P., MCLEOD, M., PARRY, S., CHARLTON, A., FINDLAY, M., COX, B., HUMAR, B., MORE, H. & GUILFORD, P. 2006. Hereditary diffuse gastric cancer: diagnosis and management. *Clin Gastroenterol Hepatol,* 4**,** 262-75.

BOLLRATH, J. & GRETEN, F. R. 2009. IKK/NF-kappaB and STAT3 pathways: central signalling hubs in inflammation-mediated tumour promotion and metastasis. *EMBO Rep,* 10**,** 1314-9.

BOLLRATH, J., PHESSE, T. J., VON BURSTIN, V. A., PUTOCZKI, T., BENNECKE, M., BATEMAN, T., NEBELSIEK, T., LUNDGREN-MAY, T., CANLI, O., SCHWITALLA, S., MATTHEWS, V., SCHMID, R. M., KIRCHNER, T., ARKAN, M. C., ERNST, M. & GRETEN, F. R. 2009. gp130-mediated Stat3 activation in enterocytes regulates cell survival and cell-cycle progression during colitis-associated tumorigenesis. *Cancer Cell,* 15**,** 91-102.

BONHOURE, E., LAURET, A., BARNES, D. J., MARTIN, C., MALAVAUD, B., KOHAMA, T., MELO, J. V. & CUVILLIER, O. 2008. Sphingosine kinase-1 is a downstream regulator of imatinib-induced apoptosis in chronic myeloid leukemia cells. *Leukemia,* 22**,** 971-9.

BORNSCHEIN, J., SELGRAD, M., WARNECKE, M., KUESTER, D., WEX, T. & MALFERTHEINER, P. 2010. H. pylori infection is a key risk factor for proximal gastric cancer. *Dig Dis Sci,* 55**,** 3124-31.

BRAY, F., FERLAY, J., SOERJOMATARAM, I., SIEGEL, R. L., TORRE, L. A. & JEMAL, A. 2018. Global cancer statistics 2018: GLOBOCAN estimates of incidence and mortality worldwide for 36 cancers in 185 countries. *CA Cancer J Clin,* 68**,** 394-424.

BRENNAN, C. W., VERHAAK, R. G., MCKENNA, A., CAMPOS, B., NOUSHMEHR, H., SALAMA, S. R., ZHENG, S., CHAKRAVARTY, D., SANBORN, J. Z., BERMAN, S. H., BEROUKHIM, R., BERNARD, B., WU, C. J., GENOVESE, G., SHMULEVICH, I., BARNHOLTZ-SLOAN, J., ZOU, L., VEGESNA, R., SHUKLA, S. A., CIRIELLO, G., YUNG, W. K., ZHANG, W., SOUGNEZ, C., MIKKELSEN, T., ALDAPE, K., BIGNER, D. D., VAN MEIR, E. G., PRADOS, M., SLOAN, A., BLACK, K. L., ESCHBACHER, J., FINOCCHIARO, G., FRIEDMAN, W., ANDREWS, D. W., GUHA, A., IACOCCA, M., O'NEILL, B. P., FOLTZ, G., MYERS, J., WEISENBERGER, D. J., PENNY, R., KUCHERLAPATI, R., PEROU, C. M., HAYES, D. N., GIBBS, R., MARRA, M., MILLS, G. B., LANDER, E., SPELLMAN, P., WILSON, R., SANDER, C., WEINSTEIN, J., MEYERSON, M., GABRIEL, S., LAIRD, P. W., HAUSSLER, D., GETZ, G., CHIN, L. & NETWORK, T. R. 2013. The somatic genomic landscape of glioblastoma. *Cell,* 155**,** 462-77.

BRINKMANN, V., DAVIS, M. D., HEISE, C. E., ALBERT, R., COTTENS, S., HOF, R., BRUNS, C., PRIESCHL, E., BAUMRUKER, T., HIESTAND, P., FOSTER, C. A., ZOLLINGER, M. & LYNCH, K. R. 2002. The immune modulator FTY720 targets sphingosine 1-phosphate receptors. *J Biol Chem,* 277**,** 21453-7.

BRITTEN, C. D., GARRETT-MAYER, E., CHIN, S. H., SHIRAI, K., OGRETMEN, B., BENTZ, T. A., BRISENDINE, A., ANDERTON, K., CUSACK, S. L., MAINES, L. W., ZHUANG, Y., SMITH, C. D. & THOMAS, M. B. 2017. A Phase I Study of ABC294640, a First-in-Class Sphingosine Kinase-2 Inhibitor, in Patients with Advanced Solid Tumors. *Clin Cancer Res,* 23**,** 4642-4650.

BROCKLYN, J. R. 2010. Regulation of cancer cell migration and invasion by sphingosine-1-phosphate. *World J Biol Chem,* 1**,** 307-12.

CANCER GENOME ATLAS, N. 2012. Comprehensive molecular characterization of human colon and rectal cancer. *Nature,* 487**,** 330-7.

CANCER GENOME ATLAS RESEARCH, N. 2014. Comprehensive molecular characterization of gastric adenocarcinoma. *Nature,* 513**,** 202-9.

CANCER GENOME ATLAS RESEARCH, N., KANDOTH, C., SCHULTZ, N., CHERNIACK, A. D., AKBANI, R., LIU, Y., SHEN, H., ROBERTSON, A. G., PASHTAN, I., SHEN, R., BENZ, C. C., YAU, C., LAIRD, P. W., DING, L., ZHANG, W., MILLS, G. B., KUCHERLAPATI, R., MARDIS, E. R. & LEVINE, D. A. 2013. Integrated genomic characterization of endometrial carcinoma. *Nature,* 497**,** 67-73.

CAO, X. Z., BIN, H. & ZANG, Z. N. 2019. MiR-128 suppresses the growth of thyroid carcinoma by negatively regulating SPHK1. *Biomed Pharmacother,* 109**,** 1960-1966.

CATLETT-FALCONE, R., LANDOWSKI, T. H., OSHIRO, M. M., TURKSON, J., LEVITZKI, A., SAVINO, R., CILIBERTO, G., MOSCINSKI, L., FERNANDEZ-LUNA, J. L., NUNEZ, G., DALTON, W. S. & JOVE, R. 1999. Constitutive activation of Stat3 signaling confers resistance to apoptosis in human U266 myeloma cells. *Immunity,* 10**,** 105-15.

CHEN, H. S., LU, A. Q., YANG, P. Y., LIANG, J., WEI, Y., SHANG, Y. W. & LI, Q.

2019. MicroRNA-28-5p regulates glioma cell proliferation, invasion and migration by targeting SphK1. *Eur Rev Med Pharmacol Sci,* 23**,** 6621-6628.

CHEN, J., QI, Y., ZHAO, Y., KACZOROWSKI, D., COUTTAS, T. A., COLEMAN, P. R., DON, A. S., BERTOLINO, P., GAMBLE, J. R., VADAS, M. A., XIA, P. & MCCAUGHAN, G. W. 2018a. Deletion of sphingosine kinase 1 inhibits liver tumorigenesis in diethylnitrosamine-treated mice. *Oncotarget,* 9**,** 15635-15649.

CHEN, W., SUN, K., ZHENG, R., ZENG, H., ZHANG, S., XIA, C., YANG, Z., LI, H., ZOU, X. & HE, J. 2018b. Cancer incidence and mortality in China, 2014. *Chin J Cancer Res,* 30**,** 1-12.

CHEN, Y. C., FANG, W. L., WANG, R. F., LIU, C. A., YANG, M. H., LO, S. S., WU, C. W., LI, A. F., SHYR, Y. M. & HUANG, K. H. 2016. Clinicopathological Variation of Lauren Classification in Gastric Cancer. *Pathol Oncol Res,* 22**,** 197-202.

CHEONG, J. H., YANG, H. K., KIM, H., KIM, W. H., KIM, Y. W., KOOK, M. C., PARK, Y. K., KIM, H. H., LEE, H. S., LEE, K. H., GU, M. J., KIM, H. Y., LEE, J., CHOI, S. H., HONG, S., KIM, J. W., CHOI, Y. Y., HYUNG, W. J., JANG, E., KIM, H., HUH, Y. M. & NOH, S. H. 2018. Predictive test for chemotherapy response in resectable gastric cancer: a multi-cohort, retrospective analysis. *Lancet Oncol,* 19**,** 629-638.

CHOI, I. J., KIM, C. G., LEE, J. Y., KIM, Y. I., KOOK, M. C., PARK, B. & JOO, J. 2020. Family History of Gastric Cancer and Helicobacter pylori Treatment. *N Engl J Med,* 382**,** 427-436.

CHOI, I. J., KOOK, M. C., KIM, Y. I., CHO, S. J., LEE, J. Y., KIM, C. G., PARK, B. & NAM, B. H. 2018. Helicobacter pylori Therapy for the Prevention of Metachronous Gastric Cancer. *N Engl J Med,* 378**,** 1085-1095.

CINTI, C., VINDIGNI, C., ZAMPARELLI, A., LA SALA, D., EPISTOLATO, M. C., MARRELLI, D., CEVENINI, G. & TOSI, P. 2008. Activated Akt as an indicator of prognosis in gastric cancer. *Virchows Arch,* 453**,** 449-55.

COHEN, J. A., BARKHOF, F., COMI, G., HARTUNG, H. P., KHATRI, B. O., MONTALBAN, X., PELLETIER, J., CAPRA, R., GALLO, P., IZQUIERDO, G., TIEL-WILCK, K., DE VERA, A., JIN, J., STITES, T., WU, S., ARADHYE, S., KAPPOS, L. & GROUP, T. S. 2010. Oral fingolimod or intramuscular interferon for relapsing multiple sclerosis. *N Engl J Med,* 362**,** 402-15.

COLLABORATORS, G. B. D. S. C. 2020. The global, regional, and national burden of stomach cancer in 195 countries, 1990-2017: a systematic analysis for the Global Burden of Disease study 2017. *Lancet Gastroenterol Hepatol,* 5**,** 42-54.

CORDI, A. A., LACOSTE, J. M., DESCOMBES, J. J., COURCHAY, C., VANHOUTTE, P. M., LAUBIE, M. & VERBEUREN, T. J. 1995. Design, synthesis, and structure-activity relationships of a new series of alpha-adrenergic agonists: spiro[(1,3-diazacyclopent-1-ene)-5,2'-(1',2',3',4'-tetrahydronaphthalene)]. *J Med Chem,* 38**,** 4056-69.

COUSSENS, L. M., FINGLETON, B. & MATRISIAN, L. M. 2002. Matrix metalloproteinase inhibitors and cancer: trials and tribulations. *Science,* 295**,** 2387-92.

CUNNINGHAM, D., ALLUM, W. H., STENNING, S. P., THOMPSON, J. N., VAN DE VELDE, C. J., NICOLSON, M., SCARFFE, J. H., LOFTS, F. J., FALK, S. J., IVESON, T. J., SMITH, D. B., LANGLEY, R. E., VERMA, M., WEEDEN, S., CHUA, Y. J. & PARTICIPANTS, M. T. 2006. Perioperative chemotherapy versus surgery alone for resectable gastroesophageal cancer. *N Engl J Med,* 355**,** 11-20.

CUNNINGHAM, D. & CHUA, Y. J. 2007. East meets west in the treatment of gastric cancer. *N Engl J Med,* 357**,** 1863-5.

CUVILLIER, O., PIRIANOV, G., KLEUSER, B., VANEK, P. G., COSO, O. A., GUTKIND, S. & SPIEGEL, S. 1996. Suppression of ceramide-mediated programmed cell death by sphingosine-1-phosphate. *Nature,* 381**,** 800-3.

DAI, L., LIU, Y., XIE, L., WU, X., QIU, L. & DI, W. 2017. Sphingosine kinase 1/sphingosine-1-phosphate (S1P)/S1P receptor axis is involved in ovarian cancer angiogenesis. *Oncotarget,* 8**,** 74947-74961.

DATTA, A., LOO, S. Y., HUANG, B., WONG, L., TAN, S. S., TAN, T. Z., LEE, S. C., THIERY, J. P., LIM, Y. C., YONG, W. P., LAM, Y., KUMAR, A. P. & YAP, C. T. 2014. SPHK1 regulates proliferation and survival responses in triple-negative breast cancer. *Oncotarget,* 5**,** 5920-33.

DEMICCO, E. G., FARRIS, A. B., 3RD, BABA, Y., AGBOR-ETANG, B., BERGETHON, K., MANDAL, R., DAIVES, D., FUKUOKA, J., SHIMIZU, M., DIAS-SANTAGATA, D., OGINO, S., IAFRATE, A. J., GAISSERT, H. A. & MINO-KENUDSON, M. 2011. The dichotomy in carcinogenesis of the distal esophagus and esophagogastric junction: intestinal-type vs cardiac-type mucosa-associated adenocarcinoma. *Mod Pathol,* 24**,** 1177-90.

DENG, J., LIU, Y., LEE, H., HERRMANN, A., ZHANG, W., ZHANG, C., SHEN, S., PRICEMAN, S. J., KUJAWSKI, M., PAL, S. K., RAUBITSCHEK, A., HOON, D. S., FORMAN, S., FIGLIN, R. A., LIU, J., JOVE, R. & YU, H. 2012. S1PR1-STAT3 signaling is crucial for myeloid cell colonization at future metastatic sites. *Cancer Cell,* 21**,** 642-54.

DING, B. B., YU, J. J., YU, R. Y., MENDEZ, L. M., SHAKNOVICH, R., ZHANG, Y., CATTORETTI, G. & YE, B. H. 2008. Constitutively activated STAT3 promotes cell proliferation and survival in the activated B-cell subtype of diffuse large B-cell lymphomas. *Blood,* 111**,** 1515-23.

DOLL, F., PFEILSCHIFTER, J. & HUWILER, A. 2007. Prolactin upregulates sphingosine kinase-1 expression and activity in the human breast cancer cell line MCF7 and triggers enhanced proliferation and migration. *Endocr Relat Cancer,* 14**,** 325-35.

EATOCK, M. M., TEBBUTT, N. C., BAMPTON, C. L., STRICKLAND, A. H., VALLADARES-AYERBES, M., SWIEBODA-SADLEJ, A., VAN CUTSEM, E., NANAYAKKARA, N., SUN, Y. N., ZHONG, Z. D., BASS, M. B., ADEWOYE, A. H. & BODOKY, G. 2013. Phase II randomized, double-blind, placebo-controlled study of AMG 386 (trebananib) in combination with cisplatin and capecitabine in patients with metastatic gastro-oesophageal cancer. *Ann Oncol,* 24**,** 710-8.

EREZ-ROMAN, R., PIENIK, R. & FUTERMAN, A. H. 2010. Increased ceramide synthase 2 and 6 mRNA levels in breast cancer tissues and correlation

with sphingosine kinase expression. *Biochem Biophys Res Commun,* 391**,** 219-23.

FALCONE, A. 2003. Future strategies and adjuvant treatment of gastric cancer. *Ann Oncol,* 14 Suppl 2**,** ii45-7.

FERLAY, J., SOERJOMATARAM, I., DIKSHIT, R., ESER, S., MATHERS, C., REBELO, M., PARKIN, D. M., FORMAN, D. & BRAY, F. 2015. Cancer incidence and mortality worldwide: sources, methods and major patterns in GLOBOCAN 2012. *Int J Cancer,* 136**,** E359-86.

FERLAY, J., STELIAROVA-FOUCHER, E., LORTET-TIEULENT, J., ROSSO, S., COEBERGH, J. W., COMBER, H., FORMAN, D. & BRAY, F. 2013. Cancer incidence and mortality patterns in Europe: estimates for 40 countries in 2012. *Eur J Cancer,* 49**,** 1374-403.

FERRO, A., PELETEIRO, B., MALVEZZI, M., BOSETTI, C., BERTUCCIO, P., LEVI, F., NEGRI, E., LA VECCHIA, C. & LUNET, N. 2014. Worldwide trends in gastric cancer mortality (1980-2011), with predictions to 2015, and incidence by subtype. *Eur J Cancer,* 50**,** 1330-44.

FOSS, F. W., JR., MATHEWS, T. P., KHAREL, Y., KENNEDY, P. C., SNYDER, A. H., DAVIS, M. D., LYNCH, K. R. & MACDONALD, T. L. 2009. Synthesis and biological evaluation of sphingosine kinase substrates as sphingosine-1-phosphate receptor prodrugs. *Bioorg Med Chem,* 17**,** 6123-36.

FRENCH, K. J., SCHRECENGOST, R. S., LEE, B. D., ZHUANG, Y., SMITH, S. N., EBERLY, J. L., YUN, J. K. & SMITH, C. D. 2003. Discovery and evaluation of inhibitors of human sphingosine kinase. *Cancer Res,* 63**,** 5962-9.

FRENCH, K. J., UPSON, J. J., KELLER, S. N., ZHUANG, Y., YUN, J. K. & SMITH, C. D. 2006. Antitumor activity of sphingosine kinase inhibitors. *J Pharmacol Exp Ther,* 318**,** 596-603.

FUCHS, C. S., DOI, T., JANG, R. W., MURO, K., SATOH, T., MACHADO, M., SUN, W., JALAL, S. I., SHAH, M. A., METGES, J. P., GARRIDO, M., GOLAN, T., MANDALA, M., WAINBERG, Z. A., CATENACCI, D. V., OHTSU, A., SHITARA, K., GEVA, R., BLEEKER, J., KO, A. H., KU, G., PHILIP, P., ENZINGER, P. C., BANG, Y. J., LEVITAN, D., WANG, J., ROSALES, M., DALAL, R. P. & YOON, H. H. 2018. Safety and Efficacy of Pembrolizumab Monotherapy in Patients With Previously Treated Advanced Gastric and Gastroesophageal Junction Cancer: Phase 2 Clinical KEYNOTE-059 Trial. *JAMA Oncol,* 4**,** e180013.

FUCHS, C. S., TOMASEK, J., YONG, C. J., DUMITRU, F., PASSALACQUA, R., GOSWAMI, C., SAFRAN, H., DOS SANTOS, L. V., APRILE, G., FERRY, D. R., MELICHAR, B., TEHFE, M., TOPUZOV, E., ZALCBERG, J. R., CHAU, I., CAMPBELL, W., SIVANANDAN, C., PIKIEL, J., KOSHIJI, M., HSU, Y., LIEPA, A. M., GAO, L., SCHWARTZ, J. D., TABERNERO, J. & INVESTIGATORS, R. T. 2014. Ramucirumab monotherapy for previously treated advanced gastric or gastro-oesophageal junction adenocarcinoma (REGARD): an international, randomised, multicentre, placebo-controlled, phase 3 trial. *Lancet,* 383**,** 31-39.

FUKASE, K., KATO, M., KIKUCHI, S., INOUE, K., UEMURA, N., OKAMOTO, S., TERAO, S., AMAGAI, K., HAYASHI, S., ASAKA, M. & JAPAN GAST STUDY,

G. 2008. Effect of eradication of Helicobacter pylori on incidence of metachronous gastric carcinoma after endoscopic resection of early gastric cancer: an open-label, randomised controlled trial. *Lancet,* 372**,** 392-7.

FURUYA, H., SHIMIZU, Y., TAMASHIRO, P. M., IINO, K., BIELAWSKI, J., CHAN, O. T. M., PAGANO, I. & KAWAMORI, T. 2017. Sphingosine kinase 1 expression enhances colon tumor growth. *J Transl Med,* 15**,** 120.

FYRST, H. & SABA, J. D. 2010. An update on sphingosine-1-phosphate and other sphingolipid mediators. *Nat Chem Biol,* 6**,** 489-97.

GACHECHILADZE, M., TICHY, T., KOLEK, V., GRYGARKOVA, I., KLEIN, J., MGEBRISHVILI, G., KHARAISHVILI, G., JANIKOVA, M., SMICKOVA, P., CIERNA, L., PITSON, S., MADDELEIN, M. L., CUVILLIER, O. & SKARDA, J. 2019. Sphingosine kinase-1 predicts overall survival outcomes in non-small cell lung cancer patients treated with carboplatin and navelbine. *Oncol Lett,* 18**,** 1259-1266.

GAO, M. Q., GAO, H., HAN, M., LIU, K. L., PENG, J. J. & HAN, Y. T. 2017. Hispidulin suppresses tumor growth and metastasis in renal cell carcinoma by modulating ceramide-sphingosine 1-phosphate rheostat. *Am J Cancer Res,* 7**,** 1501-1514.

GAO, S. P., MARK, K. G., LESLIE, K., PAO, W., MOTOI, N., GERALD, W. L., TRAVIS, W. D., BORNMANN, W., VEACH, D., CLARKSON, B. & BROMBERG, J. F. 2007. Mutations in the EGFR kinase domain mediate STAT3 activation via IL-6 production in human lung adenocarcinomas. *J Clin Invest,* 117**,** 3846-56.

GAO, X. Y., LI, L., WANG, X. H., WEN, X. Z., JI, K., YE, L., CAI, J., JIANG, W. G. & JI, J. F. 2015. Inhibition of sphingosine-1-phosphate phosphatase 1 promotes cancer cells migration in gastric cancer: Clinical implications. *Oncol Rep,* 34**,** 1977-87.

GOTTESMAN, M. M., FOJO, T. & BATES, S. E. 2002. Multidrug resistance in cancer: role of ATP-dependent transporters. *Nat Rev Cancer,* 2**,** 48-58.

GRIVENNIKOV, S., KARIN, E., TERZIC, J., MUCIDA, D., YU, G. Y., VALLABHAPURAPU, S., SCHELLER, J., ROSE-JOHN, S., CHEROUTRE, H., ECKMANN, L. & KARIN, M. 2009. IL-6 and Stat3 are required for survival of intestinal epithelial cells and development of colitis-associated cancer. *Cancer Cell,* 15**,** 103-13.

GROSS, J. & LAPIERE, C. M. 1962. Collagenolytic activity in amphibian tissues: a tissue culture assay. *Proc Natl Acad Sci U S A,* 48**,** 1014-22.

GROUP, G., PAOLETTI, X., OBA, K., BURZYKOWSKI, T., MICHIELS, S., OHASHI, Y., PIGNON, J. P., ROUGIER, P., SAKAMOTO, J., SARGENT, D., SASAKO, M., VAN CUTSEM, E. & BUYSE, M. 2010. Benefit of adjuvant chemotherapy for resectable gastric cancer: a meta-analysis. *JAMA,* 303**,** 1729-37.

GSTALDER, C., ADER, I. & CUVILLIER, O. 2016. FTY720 (Fingolimod) Inhibits HIF1 and HIF2 Signaling, Promotes Vascular Remodeling, and Chemosensitizes in Renal Cell Carcinoma Animal Model. *Mol Cancer Ther,* 15**,** 2465-2474.

GUILLERMET-GUIBERT, J., DAVENNE, L., PCHEJETSKI, D., SAINT-LAURENT, N.,

BRIZUELA, L., GUILBEAU-FRUGIER, C., DELISLE, M. B., CUVILLIER, O., SUSINI, C. & BOUSQUET, C. 2009. Targeting the sphingolipid metabolism to defeat pancreatic cancer cell resistance to the chemotherapeutic gemcitabine drug. *Mol Cancer Ther,* 8**,** 809-20.

HANNUN, Y. A. & OBEID, L. M. 2008. Principles of bioactive lipid signalling: lessons from sphingolipids. *Nat Rev Mol Cell Biol,* 9**,** 139-50.

HANSON, M. A., ROTH, C. B., JO, E., GRIFFITH, M. T., SCOTT, F. L., REINHART, G., DESALE, H., CLEMONS, B., CAHALAN, S. M., SCHUERER, S. C., SANNA, M. G., HAN, G. W., KUHN, P., ROSEN, H. & STEVENS, R. C. 2012. Crystal structure of a lipid G protein-coupled receptor. *Science,* 335**,** 851-5.

HANYU, T., NAGAHASHI, M., ICHIKAWA, H., ISHIKAWA, T., KOBAYASHI, T. & WAKAI, T. 2018. Expression of phosphorylated sphingosine kinase 1 is associated with diffuse type and lymphatic invasion in human gastric cancer. *Surgery,* 163**,** 1301-1306.

HASUIKE, N., ONO, H., BOKU, N., MIZUSAWA, J., TAKIZAWA, K., FUKUDA, H., ODA, I., DOYAMA, H., KANEKO, K., HORI, S., IISHI, H., KUROKAWA, Y., MUTO, M. & GASTROINTESTINAL ENDOSCOPY GROUP OF JAPAN CLINICAL ONCOLOGY, G. 2018. A non-randomized confirmatory trial of an expanded indication for endoscopic submucosal dissection for intestinal-type gastric cancer (cT1a): the Japan Clinical Oncology Group study (JCOG0607). *Gastric Cancer,* 21**,** 114-123.

HAZAR-RETHINAM, M., DE LONG, L. M., GANNON, O. M., TOPKAS, E., BOROS, S., VARGAS, A. C., DZIENIS, M., MUKHOPADHYAY, P., SIMPSON, F., ENDO-MUNOZ, L. & SAUNDERS, N. A. 2015. A novel E2F/sphingosine kinase 1 axis regulates anthracycline response in squamous cell carcinoma. *Clin Cancer Res,* 21**,** 417-27.

HEDVAT, M., HUSZAR, D., HERRMANN, A., GOZGIT, J. M., SCHROEDER, A., SHEEHY, A., BUETTNER, R., PROIA, D., KOWOLIK, C. M., XIN, H., ARMSTRONG, B., BEBERNITZ, G., WENG, S., WANG, L., YE, M., MCEACHERN, K., CHEN, H., MOROSINI, D., BELL, K., ALIMZHANOV, M., IOANNIDIS, S., MCCOON, P., CAO, Z. A., YU, H., JOVE, R. & ZINDA, M. 2009. The JAK2 inhibitor AZD1480 potently blocks Stat3 signaling and oncogenesis in solid tumors. *Cancer Cell,* 16**,** 487-97.

HEFFERNAN-STROUD, L. A., HELKE, K. L., JENKINS, R. W., DE COSTA, A. M., HANNUN, Y. A. & OBEID, L. M. 2012. Defining a role for sphingosine kinase 1 in p53-dependent tumors. *Oncogene,* 31**,** 1166-75.

HEFFERNAN-STROUD, L. A. & OBEID, L. M. 2013. Sphingosine kinase 1 in cancer. *Adv Cancer Res,* 117**,** 201-35.

HIRASAWA, T., GOTODA, T., MIYATA, S., KATO, Y., SHIMODA, T., TANIGUCHI, H., FUJISAKI, J., SANO, T. & YAMAGUCHI, T. 2009. Incidence of lymph node metastasis and the feasibility of endoscopic resection for undifferentiated-type early gastric cancer. *Gastric Cancer,* 12**,** 148-52.

HLA, T. & MACIAG, T. 1990. An abundant transcript induced in differentiating human endothelial cells encodes a polypeptide with structural similarities to G-protein-coupled receptors. *J Biol Chem,* 265**,** 9308-13.

HONG, D., KURZROCK, R., KIM, Y., WOESSNER, R., YOUNES, A., NEMUNAITIS, J., FOWLER, N., ZHOU, T., SCHMIDT, J., JO, M., LEE, S. J., YAMASHITA, M., HUGHES, S. G., FAYAD, L., PIHA-PAUL, S., NADELLA, M. V., MOHSENI, M., LAWSON, D., REIMER, C., BLAKEY, D. C., XIAO, X., HSU, J., REVENKO, A., MONIA, B. P. & MACLEOD, A. R. 2015. AZD9150, a next-generation antisense oligonucleotide inhibitor of STAT3 with early evidence of clinical activity in lymphoma and lung cancer. *Sci Transl Med,* 7**,** 314ra185.

HU, Y., HUANG, C., SUN, Y., SU, X., CAO, H., HU, J., XUE, Y., SUO, J., TAO, K., HE, X., WEI, H., YING, M., HU, W., DU, X., CHEN, P., LIU, H., ZHENG, C., LIU, F., YU, J., LI, Z., ZHAO, G., CHEN, X., WANG, K., LI, P., XING, J. & LI, G. 2016. Morbidity and Mortality of Laparoscopic Versus Open D2 Distal Gastrectomy for Advanced Gastric Cancer: A Randomized Controlled Trial. *J Clin Oncol,* 34**,** 1350-7.

ILLUZZI, G., BERNACCHIONI, C., AURELI, M., PRIONI, S., FRERA, G., DONATI, C., VALSECCHI, M., CHIGORNO, V., BRUNI, P., SONNINO, S. & PRINETTI, A. 2010. Sphingosine kinase mediates resistance to the synthetic retinoid N-(4-hydroxyphenyl)retinamide in human ovarian cancer cells. *J Biol Chem,* 285**,** 18594-602.

ISOMOTO, H., SHIKUWA, S., YAMAGUCHI, N., FUKUDA, E., IKEDA, K., NISHIYAMA, H., OHNITA, K., MIZUTA, Y., SHIOZAWA, J. & KOHNO, S. 2009. Endoscopic submucosal dissection for early gastric cancer: a large-scale feasibility study. *Gut,* 58**,** 331-6.

ITO, M., TAKATA, S., TATSUGAMI, M., WADA, Y., IMAGAWA, S., MATSUMOTO, Y., TAKAMURA, A., KITAMURA, S., MATSUO, T., TANAKA, S., HARUMA, K. & CHAYAMA, K. 2009. Clinical prevention of gastric cancer by Helicobacter pylori eradication therapy: a systematic review. *J Gastroenterol,* 44**,** 365-71.

JANJIGIAN, Y. Y., BENDELL, J., CALVO, E., KIM, J. W., ASCIERTO, P. A., SHARMA, P., OTT, P. A., PELTOLA, K., JAEGER, D., EVANS, J., DE BRAUD, F., CHAU, I., HARBISON, C. T., DORANGE, C., TSCHAIKA, M. & LE, D. T. 2018. CheckMate-032 Study: Efficacy and Safety of Nivolumab and Nivolumab Plus Ipilimumab in Patients With Metastatic Esophagogastric Cancer. *J Clin Oncol,* 36**,** 2836-2844.

JAPANESE GASTRIC CANCER, A. 2017. Japanese gastric cancer treatment guidelines 2014 (ver. 4). *Gastric Cancer,* 20**,** 1-19.

JAPANESE GASTRIC CANCER, A. 2020. Japanese gastric cancer treatment guidelines 2018 (5th edition). *Gastric Cancer*.

JEFFERY, D. R., MARKOWITZ, C. E., REDER, A. T., WEINSTOCK-GUTTMAN, B. & TOBIAS, K. 2011. Fingolimod for the treatment of relapsing multiple sclerosis. *Expert Rev Neurother,* 11**,** 165-83.

JOHNSON, K. R., JOHNSON, K. Y., CRELLIN, H. G., OGRETMEN, B., BOYLAN, A. M., HARLEY, R. A. & OBEID, L. M. 2005. Immunohistochemical distribution of sphingosine kinase 1 in normal and tumor lung tissue. *J Histochem Cytochem,* 53**,** 1159-66.

JU, T., GAO, D. & FANG, Z. Y. 2016. Targeting colorectal cancer cells by a novel sphingosine kinase 1 inhibitor PF-543. *Biochem Biophys Res Commun,*

470**,** 728-734.

KAPITONOV, D., ALLEGOOD, J. C., MITCHELL, C., HAIT, N. C., ALMENARA, J. A., ADAMS, J. K., ZIPKIN, R. E., DENT, P., KORDULA, T., MILSTIEN, S. & SPIEGEL, S. 2009. Targeting sphingosine kinase 1 inhibits Akt signaling, induces apoptosis, and suppresses growth of human glioblastoma cells and xenografts. *Cancer Res,* 69**,** 6915-23.

KATAI, H., MIZUSAWA, J., KATAYAMA, H., KUNISAKI, C., SAKURAMOTO, S., INAKI, N., KINOSHITA, T., IWASAKI, Y., MISAWA, K., TAKIGUCHI, N., KAJI, M., OKITSU, H., YOSHIKAWA, T., TERASHIMA, M. & STOMACH CANCER STUDY GROUP OF JAPAN CLINICAL ONCOLOGY, G. 2019. Single-arm confirmatory trial of laparoscopy-assisted total or proximal gastrectomy with nodal dissection for clinical stage I gastric cancer: Japan Clinical Oncology Group study JCOG1401. *Gastric Cancer,* 22**,** 999-1008.

KAURAH, P., MACMILLAN, A., BOYD, N., SENZ, J., DE LUCA, A., CHUN, N., SURIANO, G., ZAOR, S., VAN MANEN, L., GILPIN, C., NIKKEL, S., CONNOLLY-WILSON, M., WEISSMAN, S., RUBINSTEIN, W. S., SEBOLD, C., GREENSTEIN, R., STROOP, J., YIM, D., PANZINI, B., MCKINNON, W., GREENBLATT, M., WIRTZFELD, D., FONTAINE, D., COIT, D., YOON, S., CHUNG, D., LAUWERS, G., PIZZUTI, A., VACCARO, C., REDAL, M. A., OLIVEIRA, C., TISCHKOWITZ, M., OLSCHWANG, S., GALLINGER, S., LYNCH, H., GREEN, J., FORD, J., PHAROAH, P., FERNANDEZ, B. & HUNTSMAN, D. 2007. Founder and recurrent CDH1 mutations in families with hereditary diffuse gastric cancer. *JAMA,* 297**,** 2360-72.

KAWAMORI, T., KANESHIRO, T., OKUMURA, M., MAALOUF, S., UFLACKER, A., BIELAWSKI, J., HANNUN, Y. A. & OBEID, L. M. 2009. Role for sphingosine kinase 1 in colon carcinogenesis. *FASEB J,* 23**,** 405-14.

KAWAMORI, T., OSTA, W., JOHNSON, K. R., PETTUS, B. J., BIELAWSKI, J., TANAKA, T., WARGOVICH, M. J., REDDY, B. S., HANNUN, Y. A., OBEID, L. M. & ZHOU, D. 2006. Sphingosine kinase 1 is up-regulated in colon carcinogenesis. *FASEB J,* 20**,** 386-8.

KELLY, R., ALBERT, M., DE LADURANTAYE, M., MOORE, M., DOKUN, O. & BARTLETT, J. M. S. 2019. RNA and DNA Integrity Remain Stable in Frozen Tissue After Long-Term Storage at Cryogenic Temperatures: A Report from the Ontario Tumour Bank. *Biopreserv Biobank,* 17**,** 282-287.

KHAREL, Y., MATHEWS, T. P., GELLETT, A. M., TOMSIG, J. L., KENNEDY, P. C., MOYER, M. L., MACDONALD, T. L. & LYNCH, K. R. 2011. Sphingosine kinase type 1 inhibition reveals rapid turnover of circulating sphingosine 1-phosphate. *Biochem J,* 440**,** 345-53.

KIM, H. S., YOON, G., RYU, J. Y., CHO, Y. J., CHOI, J. J., LEE, Y. Y., KIM, T. J., CHOI, C. H., SONG, S. Y., KIM, B. G., BAE, D. S. & LEE, J. W. 2015. Sphingosine kinase 1 is a reliable prognostic factor and a novel therapeutic target for uterine cervical cancer. *Oncotarget,* 6**,** 26746-56.

KIM, R. H., TAKABE, K., MILSTIEN, S. & SPIEGEL, S. 2009. Export and functions of sphingosine-1-phosphate. *Biochim Biophys Acta,* 1791**,** 692-6.

KIM, S. T., CRISTESCU, R., BASS, A. J., KIM, K. M., ODEGAARD, J. I., KIM, K., LIU,

X. Q., SHER, X., JUNG, H., LEE, M., LEE, S., PARK, S. H., PARK, J. O., PARK, Y. S., LIM, H. Y., LEE, H., CHOI, M., TALASAZ, A., KANG, P. S., CHENG, J., LOBODA, A., LEE, J. & KANG, W. K. 2018. Comprehensive molecular characterization of clinical responses to PD-1 inhibition in metastatic gastric cancer. *Nat Med,* 24**,** 1449-1458.

KOHAMA, T., OLIVERA, A., EDSALL, L., NAGIEC, M. M., DICKSON, R. & SPIEGEL, S. 1998. Molecular cloning and functional characterization of murine sphingosine kinase. *J Biol Chem,* 273**,** 23722-8.

KOHNO, M., MOMOI, M., OO, M. L., PAIK, J. H., LEE, Y. M., VENKATARAMAN, K., AI, Y., RISTIMAKI, A. P., FYRST, H., SANO, H., ROSENBERG, D., SABA, J. D., PROIA, R. L. & HLA, T. 2006. Intracellular role for sphingosine kinase 1 in intestinal adenoma cell proliferation. *Mol Cell Biol,* 26**,** 7211-23.

KREITZBURG, K. M., FEHLING, S. C., LANDEN, C. N., GAMBLIN, T. L., VANCE, R. B., AREND, R. C., KATRE, A. A., OLIVER, P. G., VAN WAARDENBURG, R., ALVAREZ, R. D. & YOON, K. J. 2018. FTY720 enhances the anti-tumor activity of carboplatin and tamoxifen in a patient-derived xenograft model of ovarian cancer. *Cancer Lett,* 436**,** 75-86.

KUNKEL, G. T., MACEYKA, M., MILSTIEN, S. & SPIEGEL, S. 2013. Targeting the sphingosine-1-phosphate axis in cancer, inflammation and beyond. *Nat Rev Drug Discov,* 12**,** 688-702.

LADEIRAS-LOPES, R., PEREIRA, A. K., NOGUEIRA, A., PINHEIRO-TORRES, T., PINTO, I., SANTOS-PEREIRA, R. & LUNET, N. 2008. Smoking and gastric cancer: systematic review and meta-analysis of cohort studies. *Cancer Causes Control,* 19**,** 689-701.

LAUREN, P. 1965. The Two Histological Main Types of Gastric Carcinoma: Diffuse and So-Called Intestinal-Type Carcinoma. An Attempt at a Histo-Clinical Classification. *Acta Pathol Microbiol Scand,* 64**,** 31-49.

LE SCOLAN, E., PCHEJETSKI, D., BANNO, Y., DENIS, N., MAYEUX, P., VAINCHENKER, W., LEVADE, T. & MOREAU-GACHELIN, F. 2005. Overexpression of sphingosine kinase 1 is an oncogenic event in erythroleukemic progression. *Blood,* 106**,** 1808-16.

LECLERCQ, T. M. & PITSON, S. M. 2006. Cellular signalling by sphingosine kinase and sphingosine 1-phosphate. *IUBMB Life,* 58**,** 467-72.

LEE, H., DENG, J., KUJAWSKI, M., YANG, C., LIU, Y., HERRMANN, A., KORTYLEWSKI, M., HORNE, D., SOMLO, G., FORMAN, S., JOVE, R. & YU, H. 2010. STAT3-induced S1PR1 expression is crucial for persistent STAT3 activation in tumors. *Nat Med,* 16**,** 1421-8.

LEE, H., HERRMANN, A., DENG, J. H., KUJAWSKI, M., NIU, G., LI, Z., FORMAN, S., JOVE, R., PARDOLL, D. M. & YU, H. 2009. Persistently activated Stat3 maintains constitutive NF-kappaB activity in tumors. *Cancer Cell,* 15**,** 283-93.

LEE, J., LIM, D. H., KIM, S., PARK, S. H., PARK, J. O., PARK, Y. S., LIM, H. Y., CHOI, M. G., SOHN, T. S., NOH, J. H., BAE, J. M., AHN, Y. C., SOHN, I., JUNG, S. H., PARK, C. K., KIM, K. M. & KANG, W. K. 2012a. Phase III trial comparing capecitabine plus cisplatin versus capecitabine plus cisplatin with concurrent capecitabine radiotherapy in completely

resected gastric cancer with D2 lymph node dissection: the ARTIST trial. *J Clin Oncol,* 30**,** 268-73.

LEE, J., LIM DO, H., KIM, S., PARK, S. H., PARK, J. O., PARK, Y. S., LIM, H. Y., CHOI, M. G., SOHN, T. S., NOH, J. H., BAE, J. M., AHN, Y. C., SOHN, I., JUNG, S. H., PARK, C. K., KIM, K. M. & KANG, W. K. 2012b. Phase III trial comparing capecitabine plus cisplatin versus capecitabine plus cisplatin with concurrent capecitabine radiotherapy in completely resected gastric cancer with D2 lymph node dissection: the ARTIST trial. *J Clin Oncol,* 30**,** 268-73.

LEE, J., SOHN, I., DO, I. G., KIM, K. M., PARK, S. H., PARK, J. O., PARK, Y. S., LIM, H. Y., SOHN, T. S., BAE, J. M., CHOI, M. G., LIM, D. H., MIN, B. H., LEE, J. H., RHEE, P. L., KIM, J. J., CHOI, D. I., TAN, I. B., DAS, K., TAN, P., JUNG, S. H., KANG, W. K. & KIM, S. 2014. Nanostring-based multigene assay to predict recurrence for gastric cancer patients after surgery. *PLoS One,* 9**,** e90133.

LEE, J., VAN HUMMELEN, P., GO, C., PALESCANDOLO, E., JANG, J., PARK, H. Y., KANG, S. Y., PARK, J. O., KANG, W. K., MACCONAILL, L. & KIM, K. M. 2012c. High-throughput mutation profiling identifies frequent somatic mutations in advanced gastric adenocarcinoma. *PLoS One,* 7**,** e38892.

LEE, M. J., VAN BROCKLYN, J. R., THANGADA, S., LIU, C. H., HAND, A. R., MENZELEEV, R., SPIEGEL, S. & HLA, T. 1998. Sphingosine-1-phosphate as a ligand for the G protein-coupled receptor EDG-1. *Science,* 279**,** 1552-5.

LEE, O. H., KIM, Y. M., LEE, Y. M., MOON, E. J., LEE, D. J., KIM, J. H., KIM, K. W. & KWON, Y. G. 1999. Sphingosine 1-phosphate induces angiogenesis: its angiogenic action and signaling mechanism in human umbilical vein endothelial cells. *Biochem Biophys Res Commun,* 264**,** 743-50.

LEUNG, W. K., LIN, S. R., CHING, J. Y., TO, K. F., NG, E. K., CHAN, F. K., LAU, J. Y. & SUNG, J. J. 2004. Factors predicting progression of gastric intestinal metaplasia: results of a randomised trial on Helicobacter pylori eradication. *Gut,* 53**,** 1244-9.

LEWIS, C. S., VOELKEL-JOHNSON, C. & SMITH, C. D. 2016. Suppression of c-Myc and RRM2 expression in pancreatic cancer cells by the sphingosine kinase-2 inhibitor ABC294640. *Oncotarget,* 7**,** 60181-60192.

LI, F., WANG, J., ZHU, Y., LIU, L., FENG, W., SHI, W., WANG, Q., ZHANG, Q., CHAI, L. & LI, M. 2018a. SphK1/S1P Mediates PDGF-Induced Pulmonary Arterial Smooth Muscle Cell Proliferation via miR-21/BMPRII/Id1 Signaling Pathway. *Cell Physiol Biochem,* 51**,** 487-500.

LI, J., GUAN, H. Y., GONG, L. Y., SONG, L. B., ZHANG, N., WU, J., YUAN, J., ZHENG, Y. J., HUANG, Z. S. & LI, M. 2008. Clinical significance of sphingosine kinase-1 expression in human astrocytomas progression and overall patient survival. *Clin Cancer Res,* 14**,** 6996-7003.

LI, J., QIN, S., XU, J., XIONG, J., WU, C., BAI, Y., LIU, W., TONG, J., LIU, Y., XU, R., WANG, Z., WANG, Q., OUYANG, X., YANG, Y., BA, Y., LIANG, J., LIN, X., LUO, D., ZHENG, R., WANG, X., SUN, G., WANG, L., ZHENG, L., GUO,

H., WU, J., XU, N., YANG, J., ZHANG, H., CHENG, Y., WANG, N., CHEN, L., FAN, Z., SUN, P. & YU, H. 2016a. Randomized, Double-Blind, Placebo-Controlled Phase III Trial of Apatinib in Patients With Chemotherapy-Refractory Advanced or Metastatic Adenocarcinoma of the Stomach or Gastroesophageal Junction. *J Clin Oncol,* 34**,** 1448-54.

LI, J., SONG, Z., WANG, Y., YIN, Y., LIU, Y., YUAN, R. & NAN, X. 2016b. Overexpression of SphK1 enhances cell proliferation and invasion in triple-negative breast cancer via the PI3K/AKT signaling pathway. *Tumour Biol,* 37**,** 10587-93.

LI, J., WU, H., LI, W., YIN, L., GUO, S., XU, X., OUYANG, Y., ZHAO, Z., LIU, S., TIAN, Y., TIAN, Z., JU, J., NI, B. & WANG, H. 2016c. Downregulated miR-506 expression facilitates pancreatic cancer progression and chemoresistance via SPHK1/Akt/NF-kappaB signaling. *Oncogene,* 35**,** 5501-5514.

LI, J., ZHANG, B., BAI, Y., LIU, Y., ZHANG, B. & JIN, J. 2019a. Upregulation of sphingosine kinase 1 is associated with recurrence and poor prognosis in papillary thyroid carcinoma. *Oncol Lett,* 18**,** 5374-5382.

LI, M. H., SWENSON, R., HAREL, M., JANA, S., STOLARZEWICZ, E., HLA, T., SHAPIRO, L. H. & FERRER, F. 2015. Antitumor Activity of a Novel Sphingosine-1-Phosphate 2 Antagonist, AB1, in Neuroblastoma. *J Pharmacol Exp Ther,* 354**,** 261-8.

LI, P. H., WU, J. X., ZHENG, J. N. & PEI, D. S. 2014a. A sphingosine kinase-1 inhibitor, SKI-II, induces growth inhibition and apoptosis in human gastric cancer cells. *Asian Pac J Cancer Prev,* 15**,** 10381-5.

LI, W., YU, C. P., XIA, J. T., ZHANG, L., WENG, G. X., ZHENG, H. Q., KONG, Q. L., HU, L. J., ZENG, M. S., ZENG, Y. X., LI, M., LI, J. & SONG, L. B. 2009. Sphingosine kinase 1 is associated with gastric cancer progression and poor survival of patients. *Clin Cancer Res,* 15**,** 1393-9.

LI, W. Q., MA, J. L., ZHANG, L., BROWN, L. M., LI, J. Y., SHEN, L., PAN, K. F., LIU, W. D., HU, Y., HAN, Z. X., CRYSTAL-MANSOUR, S., PEE, D., BLOT, W. J., FRAUMENI, J. F., JR., YOU, W. C. & GAIL, M. H. 2014b. Effects of Helicobacter pylori treatment on gastric cancer incidence and mortality in subgroups. *J Natl Cancer Inst,* 106.

LI, Z., SHAN, F., YING, X., ZHANG, Y., E, J. Y., WANG, Y., REN, H., SU, X. & JI, J. 2019b. Assessment of Laparoscopic Distal Gastrectomy After Neoadjuvant Chemotherapy for Locally Advanced Gastric Cancer: A Randomized Clinical Trial. *JAMA Surg*.

LI, Z., WANG, Y., SHAN, F., YING, X., WU, Z., XUE, K., MIAO, R., ZHANG, Y. & JI, J. 2018b. ypTNM staging after neoadjuvant chemotherapy in the Chinese gastric cancer population: an evaluation on the prognostic value of the AJCC eighth edition cancer staging system. *Gastric Cancer,* 21**,** 977-987.

LIANG, J., NAGAHASHI, M., KIM, E. Y., HARIKUMAR, K. B., YAMADA, A., HUANG, W. C., HAIT, N. C., ALLEGOOD, J. C., PRICE, M. M., AVNI, D., TAKABE, K., KORDULA, T., MILSTIEN, S. & SPIEGEL, S. 2013. Sphingosine-1-phosphate links persistent STAT3 activation, chronic

intestinal inflammation, and development of colitis-associated cancer. *Cancer Cell,* 23**,** 107-20.

LIAO, C. Y., SONG, M. J., GAO, Y., MAUER, A. S., REVZIN, A. & MALHI, H. 2018. Hepatocyte-Derived Lipotoxic Extracellular Vesicle Sphingosine 1-Phosphate Induces Macrophage Chemotaxis. *Front Immunol,* 9**,** 2980.

LIMA, S., TAKABE, K., NEWTON, J., SAURABH, K., YOUNG, M. M., LEOPOLDINO, A. M., HAIT, N. C., ROBERTS, J. L., WANG, H. G., DENT, P., MILSTIEN, S., BOOTH, L. & SPIEGEL, S. 2018. TP53 is required for BECN1- and ATG5-dependent cell death induced by sphingosine kinase 1 inhibition. *Autophagy,* 14**,** 942-957.

LIMAYE, V. 2008. The role of sphingosine kinase and sphingosine-1-phosphate in the regulation of endothelial cell biology. *Endothelium,* 15**,** 101-12.

LIMAYE, V., LI, X., HAHN, C., XIA, P., BERNDT, M. C., VADAS, M. A. & GAMBLE, J. R. 2005. Sphingosine kinase-1 enhances endothelial cell survival through a PECAM-1-dependent activation of PI-3K/Akt and regulation of Bcl-2 family members. *Blood,* 105**,** 3169-77.

LIOTTA, L. A., TRYGGVASON, K., GARBISA, S., HART, I., FOLTZ, C. M. & SHAFIE, S. 1980. Metastatic potential correlates with enzymatic degradation of basement membrane collagen. *Nature,* 284**,** 67-8.

LIU, H., SUGIURA, M., NAVA, V. E., EDSALL, L. C., KONO, K., POULTON, S., MILSTIEN, S., KOHAMA, T. & SPIEGEL, S. 2000. Molecular cloning and functional characterization of a novel mammalian sphingosine kinase type 2 isoform. *J Biol Chem,* 275**,** 19513-20.

LIU, L., ZHOU, X. Y., ZHANG, J. Q., WANG, G. G., HE, J., CHEN, Y. Y., HUANG, C., LI, L. & LI, S. Q. 2018. LncRNA HULC promotes non-small cell lung cancer cell proliferation and inhibits the apoptosis by up-regulating sphingosine kinase 1 (SPHK1) and its downstream PI3K/Akt pathway. *Eur Rev Med Pharmacol Sci,* 22**,** 8722-8730.

LIU, S. Q., XU, C. Y., WU, W. H., FU, Z. H., HE, S. W., QIN, M. B. & HUANG, J. A. 2019. Sphingosine kinase 1 promotes the metastasis of colorectal cancer by inducing the epithelialmesenchymal transition mediated by the FAK/AKT/MMPs axis. *Int J Oncol,* 54**,** 41-52.

LIU, Y., DENG, J., WANG, L., LEE, H., ARMSTRONG, B., SCUTO, A., KOWOLIK, C., WEISS, L. M., FORMAN, S. & YU, H. 2012. S1PR1 is an effective target to block STAT3 signaling in activated B cell-like diffuse large B-cell lymphoma. *Blood,* 120**,** 1458-65.

LIU, Y., ZHU, Z., CAI, H., LIU, Q., ZHOU, H. & ZHU, Z. 2014. SKI-II reverses the chemoresistance of SGC7901/DDP gastric cancer cells. *Oncol Lett,* 8**,** 367-373.

LONG, J. S., EDWARDS, J., WATSON, C., TOVEY, S., MAIR, K. M., SCHIFF, R., NATARAJAN, V., PYNE, N. J. & PYNE, S. 2010. Sphingosine kinase 1 induces tolerance to human epidermal growth factor receptor 2 and prevents formation of a migratory phenotype in response to sphingosine 1-phosphate in estrogen receptor-positive breast cancer cells. *Mol Cell Biol,* 30**,** 3827-41.

LUNET, N., VALBUENA, C., VIEIRA, A. L., LOPES, C., LOPES, C., DAVID, L.,

CARNEIRO, F. & BARROS, H. 2007. Fruit and vegetable consumption and gastric cancer by location and histological type: case-control and meta-analysis. *Eur J Cancer Prev,* 16**,** 312-27.

LUTZ, M. P., ZALCBERG, J. R., DUCREUX, M., AJANI, J. A., ALLUM, W., AUST, D., BANG, Y. J., CASCINU, S., HOLSCHER, A., JANKOWSKI, J., JANSEN, E. P., KISSLICH, R., LORDICK, F., MARIETTE, C., MOEHLER, M., OYAMA, T., ROTH, A., RUESCHOFF, J., RUHSTALLER, T., SERUCA, R., STAHL, M., STERZING, F., VAN CUTSEM, E., VAN DER GAAST, A., VAN LANSCHOT, J., YCHOU, M., OTTO, F. & FIRST ST GALLEN, E. G. C. C. E. P. 2012. Highlights of the EORTC St. Gallen International Expert Consensus on the primary therapy of gastric, gastroesophageal and oesophageal cancer - differential treatment strategies for subtypes of early gastroesophageal cancer. *Eur J Cancer,* 48**,** 2941-53.

MA, J. L., ZHANG, L., BROWN, L. M., LI, J. Y., SHEN, L., PAN, K. F., LIU, W. D., HU, Y., HAN, Z. X., CRYSTAL-MANSOUR, S., PEE, D., BLOT, W. J., FRAUMENI, J. F., JR., YOU, W. C. & GAIL, M. H. 2012. Fifteen-year effects of Helicobacter pylori, garlic, and vitamin treatments on gastric cancer incidence and mortality. *J Natl Cancer Inst,* 104**,** 488-92.

MACDONALD, J. S., SMALLEY, S. R., BENEDETTI, J., HUNDAHL, S. A., ESTES, N. C., STEMMERMANN, G. N., HALLER, D. G., AJANI, J. A., GUNDERSON, L. L., JESSUP, J. M. & MARTENSON, J. A. 2001. Chemoradiotherapy after surgery compared with surgery alone for adenocarcinoma of the stomach or gastroesophageal junction. *N Engl J Med,* 345**,** 725-30.

MACEYKA, M., HARIKUMAR, K. B., MILSTIEN, S. & SPIEGEL, S. 2012. Sphingosine-1-phosphate signaling and its role in disease. *Trends Cell Biol,* 22**,** 50-60.

MAINES, L. W., FITZPATRICK, L. R., FRENCH, K. J., ZHUANG, Y., XIA, Z., KELLER, S. N., UPSON, J. J. & SMITH, C. D. 2008. Suppression of ulcerative colitis in mice by orally available inhibitors of sphingosine kinase. *Dig Dis Sci,* 53**,** 997-1012.

MALAVAUD, B., PCHEJETSKI, D., MAZEROLLES, C., DE PAIVA, G. R., CALVET, C., DOUMERC, N., PITSON, S., RISCHMANN, P. & CUVILLIER, O. 2010. Sphingosine kinase-1 activity and expression in human prostate cancer resection specimens. *Eur J Cancer,* 46**,** 3417-24.

MATULA, K., COLLIE-DUGUID, E., MURRAY, G., PARIKH, K., GRABSCH, H., TAN, P., LALWANI, S., GARAU, R., ONG, Y., BAIN, G., SMITH, A. D., URQUHART, G., BIELAWSKI, J., FINNEGAN, M. & PETTY, R. 2015. Regulation of cellular sphingosine-1-phosphate by sphingosine kinase 1 and sphingosine-1-phopshate lyase determines chemotherapy resistance in gastroesophageal cancer. *BMC Cancer,* 15**,** 762.

MERA, R., FONTHAM, E. T., BRAVO, L. E., BRAVO, J. C., PIAZUELO, M. B., CAMARGO, M. C. & CORREA, P. 2005. Long term follow up of patients treated for Helicobacter pylori infection. *Gut,* 54**,** 1536-40.

MILSTIEN, S. & SPIEGEL, S. 2006. Targeting sphingosine-1-phosphate: a novel

avenue for cancer therapeutics. *Cancer Cell,* 9**,** 148-50.

MIN, J., VAN VELDHOVEN, P. P., ZHANG, L., HANIGAN, M. H., ALEXANDER, H. & ALEXANDER, S. 2005. Sphingosine-1-phosphate lyase regulates sensitivity of human cells to select chemotherapy drugs in a p38-dependent manner. *Mol Cancer Res,* 3**,** 287-96.

MITRA, P., OSKERITZIAN, C. A., PAYNE, S. G., BEAVEN, M. A., MILSTIEN, S. & SPIEGEL, S. 2006. Role of ABCC1 in export of sphingosine-1-phosphate from mast cells. *Proc Natl Acad Sci U S A,* 103**,** 16394-9.

MOEHLER, M., BALTIN, C. T., EBERT, M., FISCHBACH, W., GOCKEL, I., GRENACHER, L., HOLSCHER, A. H., LORDICK, F., MALFERTHEINER, P., MESSMANN, H., MEYER, H. J., PALMQVIST, A., ROCKEN, C., SCHUHMACHER, C., STAHL, M., STUSCHKE, M., VIETH, M., WITTEKIND, C., WAGNER, D. & MONIG, S. P. 2015. International comparison of the German evidence-based S3-guidelines on the diagnosis and multimodal treatment of early and locally advanced gastric cancer, including adenocarcinoma of the lower esophagus. *Gastric Cancer,* 18**,** 550-63.

MOOLGAVKAR, S. H., HOLFORD, T. R., LEVY, D. T., KONG, C. Y., FOY, M., CLARKE, L., JEON, J., HAZELTON, W. D., MEZA, R., SCHULTZ, F., MCCARTHY, W., BOER, R., GORLOVA, O., GAZELLE, G. S., KIMMEL, M., MCMAHON, P. M., DE KONING, H. J. & FEUER, E. J. 2012. Impact of reduced tobacco smoking on lung cancer mortality in the United States during 1975-2000. *J Natl Cancer Inst,* 104**,** 541-8.

MORUNO MANCHON, J. F., UZOR, N. E., FINKBEINER, S. & TSVETKOV, A. S. 2016. SPHK1/sphingosine kinase 1-mediated autophagy differs between neurons and SH-SY5Y neuroblastoma cells. *Autophagy,* 12**,** 1418-24.

NAGAHASHI, M., ABE, M., SAKIMURA, K., TAKABE, K. & WAKAI, T. 2018a. The role of sphingosine-1-phosphate in inflammation and cancer progression. *Cancer Sci,* 109**,** 3671-3678.

NAGAHASHI, M., RAMACHANDRAN, S., KIM, E. Y., ALLEGOOD, J. C., RASHID, O. M., YAMADA, A., ZHAO, R., MILSTIEN, S., ZHOU, H., SPIEGEL, S. & TAKABE, K. 2012. Sphingosine-1-phosphate produced by sphingosine kinase 1 promotes breast cancer progression by stimulating angiogenesis and lymphangiogenesis. *Cancer Res,* 72**,** 726-35.

NAGAHASHI, M., YAMADA, A., KATSUTA, E., AOYAGI, T., HUANG, W. C., TERRACINA, K. P., HAIT, N. C., ALLEGOOD, J. C., TSUCHIDA, J., YUZA, K., NAKAJIMA, M., ABE, M., SAKIMURA, K., MILSTIEN, S., WAKAI, T., SPIEGEL, S. & TAKABE, K. 2018b. Targeting the SphK1/S1P/S1PR1 Axis That Links Obesity, Chronic Inflammation, and Breast Cancer Metastasis. *Cancer Res,* 78**,** 1713-1725.

NAM, S. Y., LEE, H. S., JUNG, G. A., CHOI, J., CHO, S. J., KIM, M. K., KIM, W. H. & LEE, B. L. 2003. Akt/PKB activation in gastric carcinomas correlates with clinicopathologic variables and prognosis. *APMIS,* 111**,** 1105-13.

NEMOTO, S., NAKAMURA, M., OSAWA, Y., KONO, S., ITOH, Y., OKANO, Y., MURATE, T., HARA, A., UEDA, H., NOZAWA, Y. & BANNO, Y. 2009. Sphingosine kinase isoforms regulate oxaliplatin sensitivity of human

colon cancer cells through ceramide accumulation and Akt activation. *J Biol Chem,* 284**,** 10422-32.

NEUBAUER, H. A., PHAM, D. H., ZEBOL, J. R., MORETTI, P. A., PETERSON, A. L., LECLERCQ, T. M., CHAN, H., POWELL, J. A., PITMAN, M. R., SAMUEL, M. S., BONDER, C. S., CREEK, D. J., GLIDDON, B. L. & PITSON, S. M. 2016. An oncogenic role for sphingosine kinase 2. *Oncotarget,* 7**,** 64886-64899.

O'SULLIVAN, C. & DEV, K. K. 2013. The structure and function of the S1P1 receptor. *Trends Pharmacol Sci,* 34**,** 401-12.

OGRETMEN, B. 2018. Sphingolipid metabolism in cancer signalling and therapy. *Nat Rev Cancer,* 18**,** 33-50.

OH, C. M., WON, Y. J., JUNG, K. W., KONG, H. J., CHO, H., LEE, J. K., LEE, D. H., LEE, K. H. & COMMUNITY OF POPULATION-BASED REGIONAL CANCER, R. 2016. Cancer Statistics in Korea: Incidence, Mortality, Survival, and Prevalence in 2013. *Cancer Res Treat,* 48**,** 436-50.

OHTA, H., YATOMI, Y., SWEENEY, E. A., HAKOMORI, S. & IGARASHI, Y. 1994. A possible role of sphingosine in induction of apoptosis by tumor necrosis factor-alpha in human neutrophils. *FEBS Lett,* 355**,** 267-70.

OKI, E., BABA, H., TOKUNAGA, E., NAKAMURA, T., UEDA, N., FUTATSUGI, M., MASHINO, K., YAMAMOTO, M., IKEBE, M., KAKEJI, Y. & MAEHARA, Y. 2005. Akt phosphorylation associates with LOH of PTEN and leads to chemoresistance for gastric cancer. *Int J Cancer,* 117**,** 376-80.

OLIVEIRA, C., PINHEIRO, H., FIGUEIREDO, J., SERUCA, R. & CARNEIRO, F. 2015. Familial gastric cancer: genetic susceptibility, pathology, and implications for management. *Lancet Oncol,* 16**,** e60-70.

OLIVERA, A., KOHAMA, T., TU, Z., MILSTIEN, S. & SPIEGEL, S. 1998. Purification and characterization of rat kidney sphingosine kinase. *J Biol Chem,* 273**,** 12576-83.

ORR GANDY, K. A. & OBEID, L. M. 2013. Targeting the sphingosine kinase/sphingosine 1-phosphate pathway in disease: review of sphingosine kinase inhibitors. *Biochim Biophys Acta,* 1831**,** 157-66.

PAL, S. K., DRABKIN, H. A., REEVES, J. A., HAINSWORTH, J. D., HAZEL, S. E., PAGGIARINO, D. A., WOJCIAK, J., WOODNUTT, G. & BHATT, R. S. 2017. A phase 2 study of the sphingosine-1-phosphate antibody sonepcizumab in patients with metastatic renal cell carcinoma. *Cancer,* 123**,** 576-582.

PANNEER SELVAM, S., DE PALMA, R. M., OAKS, J. J., OLEINIK, N., PETERSON, Y. K., STAHELIN, R. V., SKORDALAKES, E., PONNUSAMY, S., GARRETT-MAYER, E., SMITH, C. D. & OGRETMEN, B. 2015. Binding of the sphingolipid S1P to hTERT stabilizes telomerase at the nuclear periphery by allosterically mimicking protein phosphorylation. *Sci Signal,* 8**,** ra58.

PARK, Y. K., YOON, H. M., KIM, Y. W., PARK, J. Y., RYU, K. W., LEE, Y. J., JEONG, O., YOON, K. Y., LEE, J. H., LEE, S. E., YU, W., JEONG, S. H., KIM, T., KIM, S., NAM, B. H. & GROUP, C. 2018. Laparoscopy-assisted versus Open D2 Distal Gastrectomy for Advanced Gastric Cancer: Results From a Randomized Phase II Multicenter Clinical Trial (COACT 1001). *Ann*

Surg, 267**,** 638-645.

PARRILL, A. L., WANG, D., BAUTISTA, D. L., VAN BROCKLYN, J. R., LORINCZ, Z., FISCHER, D. J., BAKER, D. L., LILIOM, K., SPIEGEL, S. & TIGYI, G. 2000. Identification of Edg1 receptor residues that recognize sphingosine 1-phosphate. *J Biol Chem,* 275**,** 39379-84.

PAUGH, S. W., PAUGH, B. S., RAHMANI, M., KAPITONOV, D., ALMENARA, J. A., KORDULA, T., MILSTIEN, S., ADAMS, J. K., ZIPKIN, R. E., GRANT, S. & SPIEGEL, S. 2008. A selective sphingosine kinase 1 inhibitor integrates multiple molecular therapeutic targets in human leukemia. *Blood,* 112**,** 1382-91.

PCHEJETSKI, D., DOUMERC, N., GOLZIO, M., NAYMARK, M., TEISSIE, J., KOHAMA, T., WAXMAN, J., MALAVAUD, B. & CUVILLIER, O. 2008. Chemosensitizing effects of sphingosine kinase-1 inhibition in prostate cancer cell and animal models. *Mol Cancer Ther,* 7**,** 1836-45.

PCHEJETSKI, D., GOLZIO, M., BONHOURE, E., CALVET, C., DOUMERC, N., GARCIA, V., MAZEROLLES, C., RISCHMANN, P., TEISSIE, J., MALAVAUD, B. & CUVILLIER, O. 2005. Sphingosine kinase-1 as a chemotherapy sensor in prostate adenocarcinoma cell and mouse models. *Cancer Res,* 65**,** 11667-75.

PEEST, U., SENSKEN, S. C., ANDREANI, P., HANEL, P., VAN VELDHOVEN, P. P. & GRALER, M. H. 2008. S1P-lyase independent clearance of extracellular sphingosine 1-phosphate after dephosphorylation and cellular uptake. *J Cell Biochem,* 104**,** 756-72.

PENG, D. J., WANG, J., ZHOU, J. Y. & WU, G. S. 2010. Role of the Akt/mTOR survival pathway in cisplatin resistance in ovarian cancer cells. *Biochem Biophys Res Commun,* 394**,** 600-5.

PETRELLI, N. J. 2004. The debate is over; it's time to move on. *J Clin Oncol,* 22**,** 2041-2.

PHAROAH, P. D., GUILFORD, P., CALDAS, C. & INTERNATIONAL GASTRIC CANCER LINKAGE, C. 2001. Incidence of gastric cancer and breast cancer in CDH1 (E-cadherin) mutation carriers from hereditary diffuse gastric cancer families. *Gastroenterology,* 121**,** 1348-53.

PI, J., TAO, T., ZHUANG, T., SUN, H., CHEN, X., LIU, J., CHENG, Y., YU, Z., ZHU, H. H., GAO, W. Q., SUO, Y., WEI, X., CHAN, P., ZHENG, X., TIAN, Y., MORRISEY, E., ZHANG, L. & ZHANG, Y. 2017. A MicroRNA302-367-Erk1/2-Klf2-S1pr1 Pathway Prevents Tumor Growth via Restricting Angiogenesis and Improving Vascular Stability. *Circ Res,* 120**,** 85-98.

PITMAN, M. R., POWELL, J. A., COOLEN, C., MORETTI, P. A., ZEBOL, J. R., PHAM, D. H., FINNIE, J. W., DON, A. S., EBERT, L. M., BONDER, C. S., GLIDDON, B. L. & PITSON, S. M. 2015. A selective ATP-competitive sphingosine kinase inhibitor demonstrates anti-cancer properties. *Oncotarget,* 6**,** 7065-83.

PITSON, S. M. 2011. Regulation of sphingosine kinase and sphingolipid signaling. *Trends Biochem Sci,* 36**,** 97-107.

PITSON, S. M., MORETTI, P. A., ZEBOL, J. R., LYNN, H. E., XIA, P., VADAS, M. A. & WATTENBERG, B. W. 2003. Activation of sphingosine kinase 1 by ERK1/2-mediated phosphorylation. *EMBO J,* 22**,** 5491-500.

PITSON, S. M., XIA, P., LECLERCQ, T. M., MORETTI, P. A., ZEBOL, J. R., LYNN, H. E., WATTENBERG, B. W. & VADAS, M. A. 2005. Phosphorylation-dependent translocation of sphingosine kinase to the plasma membrane drives its oncogenic signalling. *J Exp Med,* 201**,** 49-54.

PODBIELSKA, M., KROTKIEWSKI, H. & HOGAN, E. L. 2012. Signaling and regulatory functions of bioactive sphingolipids as therapeutic targets in multiple sclerosis. *Neurochem Res,* 37**,** 1154-69.

POHL, H., SIROVICH, B. & WELCH, H. G. 2010. Esophageal adenocarcinoma incidence: are we reaching the peak? *Cancer Epidemiol Biomarkers Prev,* 19**,** 1468-70.

PORTA, C., PAGLINO, C. & MOSCA, A. 2014. Targeting PI3K/Akt/mTOR Signaling in Cancer. *Front Oncol,* 4**,** 64.

POSTMA, F. R., JALINK, K., HENGEVELD, T. & MOOLENAAR, W. H. 1996. Sphingosine-1-phosphate rapidly induces Rho-dependent neurite retraction: action through a specific cell surface receptor. *EMBO J,* 15**,** 2388-92.

PRICEMAN, S. J., SHEN, S., WANG, L., DENG, J., YUE, C., KUJAWSKI, M. & YU, H. 2014. S1PR1 is crucial for accumulation of regulatory T cells in tumors via STAT3. *Cell Rep,* 6**,** 992-999.

PULKOSKI-GROSS, M. J., DONALDSON, J. C. & OBEID, L. M. 2015. Sphingosine-1-phosphate metabolism: A structural perspective. *Crit Rev Biochem Mol Biol,* 50**,** 298-313.

PYNE, N. J. & PYNE, S. 2010. Sphingosine 1-phosphate and cancer. *Nat Rev Cancer,* 10**,** 489-503.

PYNE, N. J. & PYNE, S. 2017. Sphingosine 1-Phosphate Receptor 1 Signaling in Mammalian Cells. *Molecules,* 22.

PYNE, N. J., TONELLI, F., LIM, K. G., LONG, J., EDWARDS, J. & PYNE, S. 2012a. Targeting sphingosine kinase 1 in cancer. *Adv Biol Regul,* 52**,** 31-8.

PYNE, S., EDWARDS, J., OHOTSKI, J. & PYNE, N. J. 2012b. Sphingosine 1-phosphate receptors and sphingosine kinase 1: novel biomarkers for clinical prognosis in breast, prostate, and hematological cancers. *Front Oncol,* 2**,** 168.

PYNE, S., LEE, S. C., LONG, J. & PYNE, N. J. 2009. Role of sphingosine kinases and lipid phosphate phosphatases in regulating spatial sphingosine 1-phosphate signalling in health and disease. *Cell Signal,* 21**,** 14-21.

PYNE, S. & PYNE, N. J. 2011. Translational aspects of sphingosine 1-phosphate biology. *Trends Mol Med,* 17**,** 463-72.

PYNE, S. & PYNE, N. J. 2013. New perspectives on the role of sphingosine 1-phosphate in cancer. *Handb Exp Pharmacol***,** 55-71.

QIN, Z., DAI, L., TRILLO-TINOCO, J., SENKAL, C., WANG, W., RESKE, T., BONSTAFF, K., DEL VALLE, L., RODRIGUEZ, P., FLEMINGTON, E., VOELKEL-JOHNSON, C., SMITH, C. D., OGRETMEN, B. & PARSONS, C. 2014. Targeting sphingosine kinase induces apoptosis and tumor regression for KSHV-associated primary effusion lymphoma. *Mol Cancer Ther,* 13**,** 154-64.

QIU, M. Z., CAI, M. Y., ZHANG, D. S., WANG, Z. Q., WANG, D. S., LI, Y. H. & XU, R. H. 2013. Clinicopathological characteristics and prognostic analysis

of Lauren classification in gastric adenocarcinoma in China. *J Transl Med,* 11**,** 58.

REBOUISSOU, S., AMESSOU, M., COUCHY, G., POUSSIN, K., IMBEAUD, S., PILATI, C., IZARD, T., BALABAUD, C., BIOULAC-SAGE, P. & ZUCMAN-ROSSI, J. 2009. Frequent in-frame somatic deletions activate gp130 in inflammatory hepatocellular tumours. *Nature,* 457**,** 200-4.

REN, J., DONG, L., XU, C. B. & PAN, B. R. 2002. Expression of sphingosine kinase gene in the interactions between human gastric carcinoma cell and vascular endothelial cell. *World J Gastroenterol,* 8**,** 602-7.

RISS, T. L., MORAVEC, R. A., NILES, A. L., DUELLMAN, S., BENINK, H. A., WORZELLA, T. J. & MINOR, L. 2004. Cell Viability Assays. *In:* SITTAMPALAM, G. S., COUSSENS, N. P., BRIMACOMBE, K., GROSSMAN, A., ARKIN, M., AULD, D., AUSTIN, C., BEJCEK, B., GLICKSMAN, M., INGLESE, J., IVERSEN, P. W., LI, Z., MCGEE, J., MCMANUS, O., MINOR, L., NAPPER, A., PELTIER, J. M., RISS, T., TRASK, O. J., JR. & WEIDNER, J. (eds.) *Assay Guidance Manual.* Bethesda (MD).

ROMANI, R., MANNI, G., DONATI, C., PIRISINU, I., BERNACCHIONI, C., GARGARO, M., PIRRO, M., CALVITTI, M., BAGAGLIA, F., SAHEBKAR, A., CLERICI, G., MATINO, D., POMILI, G., DI RENZO, G. C., TALESA, V. N., PUCCETTI, P. & FALLARINO, F. 2018. S1P promotes migration, differentiation and immune regulatory activity in amniotic-fluid-derived stem cells. *Eur J Pharmacol,* 833**,** 173-182.

ROSA, R., MARCIANO, R., MALAPELLE, U., FORMISANO, L., NAPPI, L., D'AMATO, C., D'AMATO, V., DAMIANO, V., MARFE, G., DEL VECCHIO, S., ZANNETTI, A., GRECO, A., DE STEFANO, A., CARLOMAGNO, C., VENEZIANI, B. M., TRONCONE, G., DE PLACIDO, S. & BIANCO, R. 2013. Sphingosine kinase 1 overexpression contributes to cetuximab resistance in human colorectal cancer models. *Clin Cancer Res,* 19**,** 138-47.

ROSEN, H., STEVENS, R. C., HANSON, M., ROBERTS, E. & OLDSTONE, M. B. 2013. Sphingosine-1-phosphate and its receptors: structure, signaling, and influence. *Annu Rev Biochem,* 82**,** 637-62.

RUAN, H., DONG, J., ZHOU, X., XIONG, J., WANG, H., ZHONG, X. & CAO, X. 2017. Multicenter phase II study of apatinib treatment for metastatic gastric cancer after failure of second-line chemotherapy. *Oncotarget,* 8**,** 104552-104559.

RUCKHABERLE, E., RODY, A., ENGELS, K., GAETJE, R., VON MINCKWITZ, G., SCHIFFMANN, S., GROSCH, S., GEISSLINGER, G., HOLTRICH, U., KARN, T. & KAUFMANN, M. 2008. Microarray analysis of altered sphingolipid metabolism reveals prognostic significance of sphingosine kinase 1 in breast cancer. *Breast Cancer Res Treat,* 112**,** 41-52.

SADDOUGHI, S. A., GENCER, S., PETERSON, Y. K., WARD, K. E., MUKHOPADHYAY, A., OAKS, J., BIELAWSKI, J., SZULC, Z. M., THOMAS, R. J., SELVAM, S. P., SENKAL, C. E., GARRETT-MAYER, E., DE PALMA, R. M., FEDAROVICH, D., LIU, A., HABIB, A. A., STAHELIN, R. V., PERROTTI, D. & OGRETMEN, B. 2013. Sphingosine analogue drug FTY720 targets I2PP2A/SET and mediates lung tumour suppression via activation of

PP2A-RIPK1-dependent necroptosis. *EMBO Mol Med,* 5**,** 105-21.

SAFADI-CHAMBERLAIN, F., WANG, L. P., PAYNE, S. G., LIM, C. U., STRATFORD, S., CHAVEZ, J. A., FOX, M. H., SPIEGEL, S. & SUMMERS, S. A. 2005. Effect of a membrane-targeted sphingosine kinase 1 on cell proliferation and survival. *Biochem J,* 388**,** 827-34.

SAKURAMOTO, S., SASAKO, M., YAMAGUCHI, T., KINOSHITA, T., FUJII, M., NASHIMOTO, A., FURUKAWA, H., NAKAJIMA, T., OHASHI, Y., IMAMURA, H., HIGASHINO, M., YAMAMURA, Y., KURITA, A., ARAI, K. & GROUP, A.-G. 2007. Adjuvant chemotherapy for gastric cancer with S-1, an oral fluoropyrimidine. *N Engl J Med,* 357**,** 1810-20.

SALAS, A., PONNUSAMY, S., SENKAL, C. E., MEYERS-NEEDHAM, M., SELVAM, S. P., SADDOUGHI, S. A., APOHAN, E., SENTELLE, R. D., SMITH, C., GAULT, C. R., OBEID, L. M., EL-SHEWY, H. M., OAKS, J., SANTHANAM, R., MARCUCCI, G., BARAN, Y., MAHAJAN, S., FERNANDES, D., STUART, R., PERROTTI, D. & OGRETMEN, B. 2011. Sphingosine kinase-1 and sphingosine 1-phosphate receptor 2 mediate Bcr-Abl1 stability and drug resistance by modulation of protein phosphatase 2A. *Blood,* 117**,** 5941-52.

SANO, T., SASAKO, M., MIZUSAWA, J., YAMAMOTO, S., KATAI, H., YOSHIKAWA, T., NASHIMOTO, A., ITO, S., KAJI, M., IMAMURA, H., FUKUSHIMA, N., FUJITANI, K. & STOMACH CANCER STUDY GROUP OF THE JAPAN CLINICAL ONCOLOGY, G. 2017. Randomized Controlled Trial to Evaluate Splenectomy in Total Gastrectomy for Proximal Gastric Carcinoma. *Ann Surg,* 265**,** 277-283.

SARKAR, S., MACEYKA, M., HAIT, N. C., PAUGH, S. W., SANKALA, H., MILSTIEN, S. & SPIEGEL, S. 2005. Sphingosine kinase 1 is required for migration, proliferation and survival of MCF-7 human breast cancer cells. *FEBS Lett,* 579**,** 5313-7.

SASAKO, M., SAKURAMOTO, S., KATAI, H., KINOSHITA, T., FURUKAWA, H., YAMAGUCHI, T., NASHIMOTO, A., FUJII, M., NAKAJIMA, T. & OHASHI, Y. 2011. Five-year outcomes of a randomized phase III trial comparing adjuvant chemotherapy with S-1 versus surgery alone in stage II or III gastric cancer. *J Clin Oncol,* 29**,** 4387-93.

SATO, K., MALCHINKHUU, E., HORIUCHI, Y., MOGI, C., TOMURA, H., TOSAKA, M., YOSHIMOTO, Y., KUWABARA, A. & OKAJIMA, F. 2007. Critical role of ABCA1 transporter in sphingosine 1-phosphate release from astrocytes. *J Neurochem,* 103**,** 2610-9.

SCHNUTE, M. E., MCREYNOLDS, M. D., KASTEN, T., YATES, M., JEROME, G., RAINS, J. W., HALL, T., CHRENCIK, J., KRAUS, M., CRONIN, C. N., SAABYE, M., HIGHKIN, M. K., BROADUS, R., OGAWA, S., CUKYNE, K., ZAWADZKE, L. E., PETERKIN, V., IYANAR, K., SCHOLTEN, J. A., WENDLING, J., FUJIWARA, H., NEMIROVSKIY, O., WITTWER, A. J. & NAGIEC, M. M. 2012. Modulation of cellular S1P levels with a novel, potent and specific inhibitor of sphingosine kinase-1. *Biochem J,* 444**,** 79-88.

SENDLER, A., DITTLER, H. J., FEUSSNER, H., NEKARDA, H., BOLLSCHWEILER, E., FINK, U., HELMBERGER, H., HOFLER, H. & SIEWERT, J. R. 1995.

Preoperative staging of gastric cancer as precondition for multimodal treatment. *World J Surg,* 19**,** 501-8.

SHAW, D., BLAIR, V., FRAMP, A., HARAWIRA, P., MCLEOD, M., GUILFORD, P., PARRY, S., CHARLTON, A. & MARTIN, I. 2005. Chromoendoscopic surveillance in hereditary diffuse gastric cancer: an alternative to prophylactic gastrectomy? *Gut,* 54**,** 461-8.

SHI, J. H. & SUN, S. C. 2018. Tumor Necrosis Factor Receptor-Associated Factor Regulation of Nuclear Factor kappaB and Mitogen-Activated Protein Kinase Pathways. *Front Immunol,* 9**,** 1849.

SHIMIZU, Y., FURUYA, H., TAMASHIRO, P. M., IINO, K., CHAN, O. T. M., GOODISON, S., PAGANO, I., HOKUTAN, K., PERES, R., LOO, L. W. M., HERNANDEZ, B., NAING, A., CHONG, C. D. K., ROSSER, C. J. & KAWAMORI, T. 2018. Genetic deletion of sphingosine kinase 1 suppresses mouse breast tumor development in an HER2 transgenic model. *Carcinogenesis,* 39**,** 47-55.

SHITARA, K., OZGUROGLU, M., BANG, Y. J., DI BARTOLOMEO, M., MANDALA, M., RYU, M. H., FORNARO, L., OLESINSKI, T., CAGLEVIC, C., CHUNG, H. C., MURO, K., GOEKKURT, E., MANSOOR, W., MCDERMOTT, R. S., SHACHAM-SHMUELI, E., CHEN, X., MAYO, C., KANG, S. P., OHTSU, A., FUCHS, C. S. & INVESTIGATORS, K.-. 2018. Pembrolizumab versus paclitaxel for previously treated, advanced gastric or gastro-oesophageal junction cancer (KEYNOTE-061): a randomised, open-label, controlled, phase 3 trial. *Lancet,* 392**,** 123-133.

SIEWERT, J. R. & STEIN, H. J. 1998. Classification of adenocarcinoma of the oesophagogastric junction. *Br J Surg,* 85**,** 1457-9.

SMALLEY, S. R., BENEDETTI, J. K., HALLER, D. G., HUNDAHL, S. A., ESTES, N. C., AJANI, J. A., GUNDERSON, L. L., GOLDMAN, B., MARTENSON, J. A., JESSUP, J. M., STEMMERMANN, G. N., BLANKE, C. D. & MACDONALD, J. S. 2012. Updated analysis of SWOG-directed intergroup study 0116: a phase III trial of adjuvant radiochemotherapy versus observation after curative gastric cancer resection. *J Clin Oncol,* 30**,** 2327-33.

SOBUE, S., NEMOTO, S., MURAKAMI, M., ITO, H., KIMURA, A., GAO, S., FURUHATA, A., TAKAGI, A., KOJIMA, T., NAKAMURA, M., ITO, Y., SUZUKI, M., BANNO, Y., NOZAWA, Y. & MURATE, T. 2008. Implications of sphingosine kinase 1 expression level for the cellular sphingolipid rheostat: relevance as a marker for daunorubicin sensitivity of leukemia cells. *Int J Hematol,* 87**,** 266-75.

SOLIMINI, N. L., LUO, J. & ELLEDGE, S. J. 2007. Non-oncogene addiction and the stress phenotype of cancer cells. *Cell,* 130**,** 986-8.

SONG, L., LI, X. X., LIU, X. Y., WANG, Z., YU, Y., SHI, M., JIANG, B. & HE, X. P. 2020. EFEMP2 Suppresses the Invasion of Lung Cancer Cells by Inhibiting Epithelial-Mesenchymal Transition (EMT) and Down-Regulating MMPs. *Onco Targets Ther,* 13**,** 1375-1396.

SONG, L., XIONG, H., LI, J., LIAO, W., WANG, L., WU, J. & LI, M. 2011. Sphingosine kinase-1 enhances resistance to apoptosis through activation of PI3K/Akt/NF-kappaB pathway in human non-small cell lung cancer. *Clin Cancer Res,* 17**,** 1839-49.

SONGUN, I., PUTTER, H., KRANENBARG, E. M., SASAKO, M. & VAN DE VELDE, C. J. 2010. Surgical treatment of gastric cancer: 15-year follow-up results of the randomised nationwide Dutch D1D2 trial. *Lancet Oncol,* 11**,** 439-49.

SPIEGEL, S. & MILSTIEN, S. 2011. The outs and the ins of sphingosine-1-phosphate in immunity. *Nat Rev Immunol,* 11**,** 403-15.

SUKOCHEVA, O., WADHAM, C., HOLMES, A., ALBANESE, N., VERRIER, E., FENG, F., BERNAL, A., DERIAN, C. K., ULLRICH, A., VADAS, M. A. & XIA, P. 2006. Estrogen transactivates EGFR via the sphingosine 1-phosphate receptor Edg-3: the role of sphingosine kinase-1. *J Cell Biol,* 173**,** 301-10.

SUKOCHEVA, O., WANG, L., VERRIER, E., VADAS, M. A. & XIA, P. 2009. Restoring endocrine response in breast cancer cells by inhibition of the sphingosine kinase-1 signaling pathway. *Endocrinology,* 150**,** 4484-92.

SUKOCHEVA, O. A. 2018. Expansion of Sphingosine Kinase and Sphingosine-1-Phosphate Receptor Function in Normal and Cancer Cells: From Membrane Restructuring to Mediation of Estrogen Signaling and Stem Cell Programming. *Int J Mol Sci,* 19.

SZAKACS, G., PATERSON, J. K., LUDWIG, J. A., BOOTH-GENTHE, C. & GOTTESMAN, M. M. 2006. Targeting multidrug resistance in cancer. *Nat Rev Drug Discov,* 5**,** 219-34.

TABERNERO, J., HOFF, P. M., SHEN, L., OHTSU, A., SHAH, M. A., CHENG, K., SONG, C., WU, H., ENG-WONG, J., KIM, K. & KANG, Y. K. 2018. Pertuzumab plus trastuzumab and chemotherapy for HER2-positive metastatic gastric or gastro-oesophageal junction cancer (JACOB): final analysis of a double-blind, randomised, placebo-controlled phase 3 study. *Lancet Oncol,* 19**,** 1372-1384.

TAHA, T. A., HANNUN, Y. A. & OBEID, L. M. 2006. Sphingosine kinase: biochemical and cellular regulation and role in disease. *J Biochem Mol Biol,* 39**,** 113-31.

TAKABE, K., KIM, R. H., ALLEGOOD, J. C., MITRA, P., RAMACHANDRAN, S., NAGAHASHI, M., HARIKUMAR, K. B., HAIT, N. C., MILSTIEN, S. & SPIEGEL, S. 2010. Estradiol induces export of sphingosine 1-phosphate from breast cancer cells via ABCC1 and ABCG2. *J Biol Chem,* 285**,** 10477-86.

TAKABE, K., PAUGH, S. W., MILSTIEN, S. & SPIEGEL, S. 2008. "Inside-out" signaling of sphingosine-1-phosphate: therapeutic targets. *Pharmacol Rev,* 60**,** 181-95.

TAN, S. S., KHIN, L. W., WONG, L., YAN, B., ONG, C. W., DATTA, A., SALTO-TELLEZ, M., LAM, Y. & YAP, C. T. 2014. Sphingosine kinase 1 promotes malignant progression in colon cancer and independently predicts survival of patients with colon cancer by competing risk approach in South asian population. *Clin Transl Gastroenterol,* 5**,** e51.

THE CANCER GENOME ATLAS RESEARCH, N., ANALYSIS WORKING GROUP: DANA-FARBER CANCER, I., INSTITUTE FOR SYSTEMS, B., UNIVERSITY OF SOUTHERN, C., MEMORIAL SLOAN KETTERING CANCER, C.,

AGENCY, B. C. C., THE, E., EDYTHE, L. B. I., CENTER, M. D. A. C., HARVARD MEDICAL, S., UNIVERSITY OF NORTH, C., VANDERBILT, U., ASAN MEDICAL, C., UNIVERSITY OF, M., NATIONAL CANCER, I., CASE WESTERN RESERVE, U., UNIVERSITY OF CALIFORNIA AT SANTA, C., DUKE, U., UNIVERSITY OF, M., UNIVERSITY OF, P., BROWN, U., BRIGHAM, WOMEN'S, H., NATIONAL CANCER, C., NATIONWIDE CHILDREN'S, H., WASHINGTON, U., GREATER POLAND CANCER, C., LEUVEN, K. U., GENOME SEQUENCING CENTER: THE, E., EDYTHE, L. B. I., WASHINGTON UNIVERSITY IN ST, L., GENOME CHARACTERIZATION CENTERS, B. C. C. A., THE, E., EDYTHE, L. B. I., HARVARD MEDICAL, S. B., WOMEN'S HOSPITAL, M. D. A. C. C., CENTER, M. D. A. C., UNIVERSITY OF SOUTHERN CALIFORNIA EPIGENOME, C., THE SIDNEY KIMMEL COMPREHENSIVE CANCER CENTER AT JOHNS HOPKINS, U., GENOME DATA ANALYSIS CENTERS: THE, E., EDYTHE, L. B. I., MEMORIAL SLOAN-KETTERING CANCER, C., INSTITUTE FOR SYSTEMS, B., UNIVERSITY OF CALIFORNIA, S. C., CENTER, M. D. A. C., BROWN, U., UNIVERSITY OF CALIFORNIA SAN, F., BIOSPECIMEN CORE RESOURCE: THE RESEARCH INSTITUTE AT NATIONWIDE CHILDREN'S, H., INTERNATIONAL GENOMICS, C., TISSUE SOURCE SITES: BUCK INSTITUTE FOR RESEARCH ON, A., CHONNAM NATIONAL UNIVERSITY MEDICAL, S., CITY CLINICAL ONCOLOGY, D., CURELINE, CENTER, U. N. C. L. C. C., GREATER POLAND CANCER, C., HELEN, F. G. C. C., RESEARCH, I., KEIMYUNG UNIVERSITY SCHOOL OF, M., INTERNATIONAL GENOMICS, C., ONTARIO TUMOUR, B., PUSAN NATIONAL UNIVERSITY, H., UNIVERSITY OF PITTSBURGH SCHOOL OF, M., DISEASE WORKING GROUP: MEMORIAL SLOAN-KETTERING CANCER, C., DUKE, U., ASAN MEDICAL, C., YONSEI UNIVERSITY COLLEGE OF, M., CENTER, M. D. A. C., NATIONAL CANCER, I., DATA COORDINATION CENTER, S. R. A. I., PROJECT TEAM: NATIONAL CANCER, I., FREDERICK, S., ANALYSIS WORKING GROUP DANA-FARBER CANCER, I., INSTITUTE FOR SYSTEMS, B., UNIVERSITY OF SOUTHERN, C., MEMORIAL SLOAN KETTERING CANCER, C., AGENCY, B. C. C., THE ELI EDYTHE, L. B. I., CENTER, M. D. A. C., HARVARD MEDICAL, S., UNIVERSITY OF NORTH, C., VANDERBILT, U., ASAN MEDICAL, C., UNIVERSITY OF, M., NATIONAL CANCER, I., CASE WESTERN RESERVE, U., UNIVERSITY OF CALIFORNIA AT SANTA, C., DUKE, U., UNIVERSITY OF, M., UNIVERSITY OF, P., BROWN, U., BRIGHAM, WOMEN'S, H., NATIONAL CANCER, C., NATIONWIDE CHILDREN'S, H., WASHINGTON, U., GREATER POLAND CANCER, C., LEUVEN, K. U., GENOME SEQUENCING CENTER THE ELI EDYTHE, L. B. I., WASHINGTON UNIVERSITY IN ST, L., GENOME CHARACTERIZATION CENTERS, B. C. C. A., et al. 2014. Comprehensive molecular characterization of gastric adenocarcinoma. *Nature*.

THUMKEO, D., WATANABE, S. & NARUMIYA, S. 2013. Physiological roles of Rho and Rho effectors in mammals. *Eur J Cell Biol,* 92**,** 303-15.

TONELLI, F., LIM, K. G., LOVERIDGE, C., LONG, J., PITSON, S. M., TIGYI, G., BITTMAN, R., PYNE, S. & PYNE, N. J. 2010. FTY720 and (S)-FTY720 vinylphosphonate inhibit sphingosine kinase 1 and promote its

proteasomal degradation in human pulmonary artery smooth muscle, breast cancer and androgen-independent prostate cancer cells. *Cell Signal,* 22**,** 1536-42.

TORRE, L. A., BRAY, F., SIEGEL, R. L., FERLAY, J., LORTET-TIEULENT, J. & JEMAL, A. 2015. Global cancer statistics, 2012. *CA Cancer J Clin,* 65**,** 87-108.

TSUKAMOTO, S., HUANG, Y., KUMAZOE, M., LESNICK, C., YAMADA, S., UEDA, N., SUZUKI, T., YAMASHITA, S., KIM, Y. H., FUJIMURA, Y., MIURA, D., KAY, N. E., SHANAFELT, T. D. & TACHIBANA, H. 2015. Sphingosine Kinase-1 Protects Multiple Myeloma from Apoptosis Driven by Cancer-Specific Inhibition of RTKs. *Mol Cancer Ther,* 14**,** 2303-12.

VADAS, M., XIA, P., MCCAUGHAN, G. & GAMBLE, J. 2008. The role of sphingosine kinase 1 in cancer: oncogene or non-oncogene addiction? *Biochim Biophys Acta,* 1781**,** 442-7.

VAN BROCKLYN, J. R., JACKSON, C. A., PEARL, D. K., KOTUR, M. S., SNYDER, P. J. & PRIOR, T. W. 2005. Sphingosine kinase-1 expression correlates with poor survival of patients with glioblastoma multiforme: roles of sphingosine kinase isoforms in growth of glioblastoma cell lines. *J Neuropathol Exp Neurol,* 64**,** 695-705.

VAN CUTSEM, E., DE HAAS, S., KANG, Y. K., OHTSU, A., TEBBUTT, N. C., MING XU, J., PENG YONG, W., LANGER, B., DELMAR, P., SCHERER, S. J. & SHAH, M. A. 2012. Bevacizumab in combination with chemotherapy as first-line therapy in advanced gastric cancer: a biomarker evaluation from the AVAGAST randomized phase III trial. *J Clin Oncol,* 30**,** 2119-27.

VAN CUTSEM, E., DICATO, M., GEVA, R., ARBER, N., BANG, Y., BENSON, A., CERVANTES, A., DIAZ-RUBIO, E., DUCREUX, M., GLYNNE-JONES, R., GROTHEY, A., HALLER, D., HAUSTERMANS, K., KERR, D., NORDLINGER, B., MARSHALL, J., MINSKY, B. D., KANG, Y. K., LABIANCA, R., LORDICK, F., OHTSU, A., PAVLIDIS, N., ROTH, A., ROUGIER, P., SCHMOLL, H. J., SOBRERO, A., TABERNERO, J., VAN DE VELDE, C. & ZALCBERG, J. 2011. The diagnosis and management of gastric cancer: expert discussion and recommendations from the 12th ESMO/World Congress on Gastrointestinal Cancer, Barcelona, 2010. *Ann Oncol,* 22 Suppl 5**,** v1-9.

VENANT, H., RAHMANIYAN, M., JONES, E. E., LU, P., LILLY, M. B., GARRETT-MAYER, E., DRAKE, R. R., KRAVEKA, J. M., SMITH, C. D. & VOELKEL-JOHNSON, C. 2015. The Sphingosine Kinase 2 Inhibitor ABC294640 Reduces the Growth of Prostate Cancer Cells and Results in Accumulation of Dihydroceramides In Vitro and In Vivo. *Mol Cancer Ther,* 14**,** 2744-52.

VENKATA, J. K., AN, N., STUART, R., COSTA, L. J., CAI, H., COKER, W., SONG, J. H., GIBBS, K., MATSON, T., GARRETT-MAYER, E., WAN, Z., OGRETMEN, B., SMITH, C. & KANG, Y. 2014. Inhibition of sphingosine kinase 2 downregulates the expression of c-Myc and Mcl-1 and induces apoptosis in multiple myeloma. *Blood,* 124**,** 1915-25.

VENKATARAMAN, K., THANGADA, S., MICHAUD, J., OO, M. L., AI, Y., LEE, Y. M., WU, M., PARIKH, N. S., KHAN, F., PROIA, R. L. & HLA, T. 2006.

Extracellular export of sphingosine kinase-1a contributes to the vascular S1P gradient. *Biochem J,* 397**,** 461-71.

VISENTIN, B., VEKICH, J. A., SIBBALD, B. J., CAVALLI, A. L., MORENO, K. M., MATTEO, R. G., GARLAND, W. A., LU, Y., YU, S., HALL, H. S., KUNDRA, V., MILLS, G. B. & SABBADINI, R. A. 2006. Validation of an anti-sphingosine-1-phosphate antibody as a potential therapeutic in reducing growth, invasion, and angiogenesis in multiple tumor lineages. *Cancer Cell,* 9**,** 225-38.

VLACHOGIANNIS, G., HEDAYAT, S., VATSIOU, A., JAMIN, Y., FERNANDEZ-MATEOS, J., KHAN, K., LAMPIS, A., EASON, K., HUNTINGFORD, I., BURKE, R., RATA, M., KOH, D. M., TUNARIU, N., COLLINS, D., HULKKI-WILSON, S., RAGULAN, C., SPITERI, I., MOORCRAFT, S. Y., CHAU, I., RAO, S., WATKINS, D., FOTIADIS, N., BALI, M., DARVISH-DAMAVANDI, M., LOTE, H., ELTAHIR, Z., SMYTH, E. C., BEGUM, R., CLARKE, P. A., HAHNE, J. C., DOWSETT, M., DE BONO, J., WORKMAN, P., SADANANDAM, A., FASSAN, M., SANSOM, O. J., ECCLES, S., STARLING, N., BRACONI, C., SOTTORIVA, A., ROBINSON, S. P., CUNNINGHAM, D. & VALERI, N. 2018. Patient-derived organoids model treatment response of metastatic gastrointestinal cancers. *Science,* 359**,** 920-926.

WADDELL, T., CHAU, I., CUNNINGHAM, D., GONZALEZ, D., OKINES, A. F., OKINES, C., WOTHERSPOON, A., SAFFERY, C., MIDDLETON, G., WADSLEY, J., FERRY, D., MANSOOR, W., CROSBY, T., COXON, F., SMITH, D., WATERS, J., IVESON, T., FALK, S., SLATER, S., PECKITT, C. & BARBACHANO, Y. 2013. Epirubicin, oxaliplatin, and capecitabine with or without panitumumab for patients with previously untreated advanced oesophagogastric cancer (REAL3): a randomised, open-label phase 3 trial. *Lancet Oncol,* 14**,** 481-9.

WALDUM, H. L. & BRENNA, C. 1993. Classification of gastric carcinomas. *Hum Pathol,* 24**,** 114-5.

WANG, C., MAO, J., REDFIELD, S., MO, Y., LAGE, J. M. & ZHOU, X. 2014a. Systemic distribution, subcellular localization and differential expression of sphingosine-1-phosphate receptors in benign and malignant human tissues. *Exp Mol Pathol,* 97**,** 259-65.

WANG, D., BAO, F., TENG, Y., LI, Q. & LI, J. 2019a. MicroRNA-506-3p initiates mesenchymal-to-epithelial transition and suppresses autophagy in osteosarcoma cells by directly targeting SPHK1. *Biosci Biotechnol Biochem,* 83**,** 836-844.

WANG, F., MENG, W., WANG, B. & QIAO, L. 2014b. Helicobacter pylori-induced gastric inflammation and gastric cancer. *Cancer Lett,* 345**,** 196-202.

WANG, J., KNAPP, S., PYNE, N. J., PYNE, S. & ELKINS, J. M. 2014c. Crystal Structure of Sphingosine Kinase 1 with PF-543. *ACS Med Chem Lett,* 5**,** 1329-33.

WANG, L., YI, T., KORTYLEWSKI, M., PARDOLL, D. M., ZENG, D. & YU, H. 2009. IL-17 can promote tumor growth through an IL-6-Stat3 signaling pathway. *J Exp Med,* 206**,** 1457-64.

WANG, S., LIANG, Y., CHANG, W., HU, B. & ZHANG, Y. 2018a. Triple Negative Breast Cancer Depends on Sphingosine Kinase 1 (SphK1)/Sphingosine-1-Phosphate (S1P)/Sphingosine 1-Phosphate Receptor 3 (S1PR3)/Notch Signaling for Metastasis. *Med Sci Monit,* 24**,** 1912-1923.

WANG, W., HUANG, M. C. & GOETZL, E. J. 2007. Type 1 sphingosine 1-phosphate G protein-coupled receptor (S1P1) mediation of enhanced IL-4 generation by CD4 T cells from S1P1 transgenic mice. *J Immunol,* 178**,** 4885-90.

WANG, Y., SHEN, Y., SUN, X., HONG, T. L., HUANG, L. S. & ZHONG, M. 2019b. Prognostic roles of the expression of sphingosine-1-phosphate metabolism enzymes in non-small cell lung cancer. *Transl Lung Cancer Res,* 8**,** 674-681.

WANG, Z. & CHEN, W. 2013. Emerging Roles of SIRT1 in Cancer Drug Resistance. *Genes Cancer,* 4**,** 82-90.

WANG, Z., MIN, X., XIAO, S. H., JOHNSTONE, S., ROMANOW, W., MEININGER, D., XU, H., LIU, J., DAI, J., AN, S., THIBAULT, S. & WALKER, N. 2013. Molecular basis of sphingosine kinase 1 substrate recognition and catalysis. *Structure,* 21**,** 798-809.

WANG, Z., QU, H., GONG, W. & LIU, A. 2018b. Up-regulation and tumor-promoting role of SPHK1 were attenuated by miR-330-3p in gastric cancer. *IUBMB Life,* 70**,** 1164-1176.

WANG, Z., XING, J., CAI, J., ZHANG, Z., LI, F., ZHANG, N., WU, J., CUI, M., LIU, Y., CHEN, L., YANG, H., ZHENG, Z., WANG, X., GAO, C., WANG, Z., FAN, Q., ZHU, Y., REN, S., ZHANG, C., LIU, M., JI, J. & SU, X. 2019c. Short-term surgical outcomes of laparoscopy-assisted versus open D2 distal gastrectomy for locally advanced gastric cancer in North China: a multicenter randomized controlled trial. *Surg Endosc,* 33**,** 33-45.

WEN, J., ZHENG, T., HU, K., ZHU, C., GUO, L. & YE, G. 2017. Promoter methylation of tumor-related genes as a potential biomarker using blood samples for gastric cancer detection. *Oncotarget,* 8**,** 77783-77793.

WHETTON, A. D., LU, Y., PIERCE, A., CARNEY, L. & SPOONCER, E. 2003. Lysophospholipids synergistically promote primitive hematopoietic cell chemotaxis via a mechanism involving Vav 1. *Blood,* 102**,** 2798-802.

WILKE, H., MURO, K., VAN CUTSEM, E., OH, S. C., BODOKY, G., SHIMADA, Y., HIRONAKA, S., SUGIMOTO, N., LIPATOV, O., KIM, T. Y., CUNNINGHAM, D., ROUGIER, P., KOMATSU, Y., AJANI, J., EMIG, M., CARLESI, R., FERRY, D., CHANDRAWANSA, K., SCHWARTZ, J. D., OHTSU, A. & GROUP, R. S. 2014. Ramucirumab plus paclitaxel versus placebo plus paclitaxel in patients with previously treated advanced gastric or gastro-oesophageal junction adenocarcinoma (RAINBOW): a double-blind, randomised phase 3 trial. *Lancet Oncol,* 15**,** 1224-35.

WINER, A., JANOSKY, M., HARRISON, B., ZHONG, J., MOUSSAI, D., SIYAH, P., SCHATZ-SIEMERS, N., ZENG, J., ADAMS, S. & MIGNATTI, P. 2016. Inhibition of Breast Cancer Metastasis by Presurgical Treatment with

an Oral Matrix Metalloproteinase Inhibitor: A Preclinical Proof-of-Principle Study. *Mol Cancer Ther,* 15**,** 2370-2377.

WORTHLEY, D. L., PHILLIPS, K. D., WAYTE, N., SCHRADER, K. A., HEALEY, S., KAURAH, P., SHULKES, A., GRIMPEN, F., CLOUSTON, A., MOORE, D., CULLEN, D., ORMONDE, D., MOUNKLEY, D., WEN, X., LINDOR, N., CARNEIRO, F., HUNTSMAN, D. G., CHENEVIX-TRENCH, G. & SUTHERS, G. K. 2012. Gastric adenocarcinoma and proximal polyposis of the stomach (GAPPS): a new autosomal dominant syndrome. *Gut,* 61**,** 774-9.

WU, M. S., SHUN, C. T., WU, C. C., HSU, T. Y., LIN, M. T., CHANG, M. C., WANG, H. P. & LIN, J. T. 2000. Epstein-Barr virus-associated gastric carcinomas: relation to H. pylori infection and genetic alterations. *Gastroenterology,* 118**,** 1031-8.

XIA, J., WU, Z., YU, C., HE, W., ZHENG, H., HE, Y., JIAN, W., CHEN, L., ZHANG, L. & LI, W. 2012. miR-124 inhibits cell proliferation in gastric cancer through down-regulation of SPHK1. *J Pathol,* 227**,** 470-80.

XIA, P., GAMBLE, J. R., WANG, L., PITSON, S. M., MORETTI, P. A., WATTENBERG, B. W., D'ANDREA, R. J. & VADAS, M. A. 2000. An oncogenic role of sphingosine kinase. *Curr Biol,* 10**,** 1527-30.

XIONG, H., WANG, J., GUAN, H., WU, J., XU, R., WANG, M., RONG, X., HUANG, K., HUANG, J., LIAO, Q., FU, Y. & YUAN, J. 2014. SphK1 confers resistance to apoptosis in gastric cancer cells by downregulating Bim via stimulating Akt/FoxO3a signaling. *Oncol Rep,* 32**,** 1369-73.

XU, C. Y., LIU, S. Q., QIN, M. B., ZHUGE, C. F., QIN, L., QIN, N., LAI, M. Y. & HUANG, J. A. 2017a. SphK1 modulates cell migration and EMT-related marker expression by regulating the expression of p-FAK in colorectal cancer cells. *Int J Mol Med,* 39**,** 1277-1284.

XU, Y., DONG, B., HUANG, J., KONG, W., XUE, W., ZHU, Y., ZHANG, J. & HUANG, Y. 2016. Sphingosine kinase 1 is overexpressed and promotes adrenocortical carcinoma progression. *Oncotarget,* 7**,** 3233-44.

XU, Y., QIN, L., SUN, T., WU, H., HE, T., YANG, Z., MO, Q., LIAO, L. & XU, J. 2017b. Twist1 promotes breast cancer invasion and metastasis by silencing Foxa1 expression. *Oncogene,* 36**,** 1157-1166.

YANG, L., HU, H., DENG, Y. & BAI, Y. 2014. [Role of SPHK1 regulates multi-drug resistance of small cell lung cancer and its clinical significance]. *Zhongguo Fei Ai Za Zhi,* 17**,** 769-77.

YANG, L., ZHENG, R., WANG, N., YUAN, Y., LIU, S., LI, H., ZHANG, S., ZENG, H. & CHEN, W. 2018. Incidence and mortality of stomach cancer in China, 2014. *Chin J Cancer Res,* 30**,** 291-298.

YANG, P., ZHOU, Y., CHEN, B., WAN, H. W., JIA, G. Q., BAI, H. L. & WU, X. T. 2009. Overweight, obesity and gastric cancer risk: results from a meta-analysis of cohort studies. *Eur J Cancer,* 45**,** 2867-73.

YANG, Y., ZHAO, J., HAO, D., WANG, X., WANG, T., LI, H. & LV, B. 2019. Increased SPK1 expression promotes cell growth by activating the ERK1/2 signaling in non-small-cell lung cancer. *Anticancer Drugs,* 30**,** 458-465.

YCHOU, M., BOIGE, V., PIGNON, J. P., CONROY, T., BOUCHE, O., LEBRETON, G.,

DUCOURTIEUX, M., BEDENNE, L., FABRE, J. M., SAINT-AUBERT, B., GENEVE, J., LASSER, P. & ROUGIER, P. 2011. Perioperative chemotherapy compared with surgery alone for resectable gastroesophageal adenocarcinoma: an FNCLCC and FFCD multicenter phase III trial. *J Clin Oncol,* 29**,** 1715-21.

YE, L., SUN, P. H., MALIK, M. F., MASON, M. D. & JIANG, W. G. 2014. Capillary morphogenesis gene 2 inhibits growth of breast cancer cells and is inversely correlated with the disease progression and prognosis. *J Cancer Res Clin Oncol,* 140**,** 957-67.

YIN, S., MIAO, Z., TAN, Y., WANG, P., XU, X., ZHANG, C., HOU, W., HUANG, J. & XU, H. 2019. SPHK1-induced autophagy in peritoneal mesothelial cell enhances gastric cancer peritoneal dissemination. *Cancer Med,* 8**,** 1731-1743.

YOHE, S. 2015. Molecular Genetic Markers in Acute Myeloid Leukemia. *J Clin Med,* 4**,** 460-78.

YOSHIDA, K., KODERA, Y., KOCHI, M., ICHIKAWA, W., KAKEJI, Y., SANO, T., NAGAO, N., TAKAHASHI, M., TAKAGANE, A., WATANABE, T., KAJI, M., OKITSU, H., NOMURA, T., MATSUI, T., YOSHIKAWA, T., MATSUYAMA, J., YAMADA, M., ITO, S., TAKEUCHI, M. & FUJII, M. 2019. Addition of Docetaxel to Oral Fluoropyrimidine Improves Efficacy in Patients With Stage III Gastric Cancer: Interim Analysis of JACCRO GC-07, a Randomized Controlled Trial. *J Clin Oncol,* 37**,** 1296-1304.

YOSHIKAWA, T., TERASHIMA, M., MIZUSAWA, J., NUNOBE, S., NISHIDA, Y., YAMADA, T., KAJI, M., FUKUSHIMA, N., HATO, S., CHODA, Y., YABUSAKI, H., YOSHIDA, K., ITO, S., TAKENO, A., YASUDA, T., KAWACHI, Y., KATAYAMA, H., FUKUDA, H., BOKU, N., SANO, T. & SASAKO, M. 2019. Four courses versus eight courses of adjuvant S-1 for patients with stage II gastric cancer (JCOG1104 [OPAS-1]): an open-label, phase 3, non-inferiority, randomised trial. *Lancet Gastroenterol Hepatol,* 4**,** 208-216.

YOSHIMURA, A., NAKA, T. & KUBO, M. 2007. SOCS proteins, cytokine signalling and immune regulation. *Nat Rev Immunol,* 7**,** 454-65.

YU, H. & JOVE, R. 2004. The STATs of cancer--new molecular targets come of age. *Nat Rev Cancer,* 4**,** 97-105.

YU, H., KORTYLEWSKI, M. & PARDOLL, D. 2007. Crosstalk between cancer and immune cells: role of STAT3 in the tumour microenvironment. *Nat Rev Immunol,* 7**,** 41-51.

YU, H., PARDOLL, D. & JOVE, R. 2009. STATs in cancer inflammation and immunity: a leading role for STAT3. *Nat Rev Cancer,* 9**,** 798-809.

YU, J., HUANG, C., SUN, Y., SU, X., CAO, H., HU, J., WANG, K., SUO, J., TAO, K., HE, X., WEI, H., YING, M., HU, W., DU, X., HU, Y., LIU, H., ZHENG, C., LI, P., XIE, J., LIU, F., LI, Z., ZHAO, G., YANG, K., LIU, C., LI, H., CHEN, P., JI, J., LI, G. & CHINESE LAPAROSCOPIC GASTROINTESTINAL SURGERY STUDY, G. 2019. Effect of Laparoscopic vs Open Distal Gastrectomy on 3-Year Disease-Free Survival in Patients With Locally Advanced Gastric Cancer: The CLASS-01 Randomized Clinical Trial. *JAMA,* 321**,** 1983-1992.

YUZA, K., NAKAJIMA, M., NAGAHASHI, M., TSUCHIDA, J., HIROSE, Y., MIURA, K., TAJIMA, Y., ABE, M., SAKIMURA, K., TAKABE, K. & WAKAI, T. 2018. Different Roles of Sphingosine Kinase 1 and 2 in Pancreatic Cancer Progression. *J Surg Res,* 232**,** 186-194.

ZHANG, H., DESAI, N. N., OLIVERA, A., SEKI, T., BROOKER, G. & SPIEGEL, S. 1991. Sphingosine-1-phosphate, a novel lipid, involved in cellular proliferation. *J Cell Biol,* 114**,** 155-67.

ZHANG, J., HONBO, N., GOETZL, E. J., CHATTERJEE, K., KARLINER, J. S. & GRAY, M. O. 2007. Signals from type 1 sphingosine 1-phosphate receptors enhance adult mouse cardiac myocyte survival during hypoxia. *Am J Physiol Heart Circ Physiol,* 293**,** H3150-8.

ZHANG, K., CHEN, H., WU, G., CHEN, K. & YANG, H. 2014a. High expression of SPHK1 in sacral chordoma and association with patients' poor prognosis. *Med Oncol,* 31**,** 247.

ZHANG, Q., LENARDO, M. J. & BALTIMORE, D. 2017. 30 Years of NF-kappaB: A Blossoming of Relevance to Human Pathobiology. *Cell,* 168**,** 37-57.

ZHANG, Y., WANG, Y., WAN, Z., LIU, S., CAO, Y. & ZENG, Z. 2014b. Sphingosine kinase 1 and cancer: a systematic review and meta-analysis. *PLoS One,* 9**,** e90362.

ZHANG, Z., YAN, Z., YUAN, Z., SUN, Y., HE, H. & MAI, C. 2015. SPHK1 inhibitor suppresses cell proliferation and invasion associated with the inhibition of NF-kappaB pathway in hepatocellular carcinoma. *Tumour Biol,* 36**,** 1503-9.

ZHAO, X., HE, W., LI, J., HUANG, S., WAN, X., LUO, H. & WU, D. 2015. MiRNA-125b inhibits proliferation and migration by targeting SphK1 in bladder cancer. *Am J Transl Res,* 7**,** 2346-54.

ZHENG, H., TAKAHASHI, H., MURAI, Y., CUI, Z., NOMOTO, K., MIWA, S., TSUNEYAMA, K. & TAKANO, Y. 2007. Pathobiological characteristics of intestinal and diffuse-type gastric carcinoma in Japan: an immunostaining study on the tissue microarray. *J Clin Pathol,* 60**,** 273-7.

ZHOU, P., HUANG, G., ZHAO, Y., ZHONG, D., XU, Z., ZENG, Y., ZHANG, Y., LI, S. & HE, F. 2014. MicroRNA-363-mediated downregulation of S1PR1 suppresses the proliferation of hepatocellular carcinoma cells. *Cell Signal,* 26**,** 1347-54.

ZHU, L., WANG, Z., LIN, Y., CHEN, Z., LIU, H., CHEN, Y., WANG, N. & SONG, X. 2015. Sphingosine kinase 1 enhances the invasion and migration of non-small cell lung cancer cells via the AKT pathway. *Oncol Rep,* 33**,** 1257-63.

ZHU, Y. J., YOU, H., TAN, J. X., LI, F., QIU, Z., LI, H. Z., HUANG, H. Y., ZHENG, K. & REN, G. S. 2017. Overexpression of sphingosine kinase 1 is predictive of poor prognosis in human breast cancer. *Oncol Lett,* 14**,** 63-72.

ZONDAG, G. C., POSTMA, F. R., ETTEN, I. V., VERLAAN, I. & MOOLENAAR, W. H. 1998. Sphingosine 1-phosphate signalling through the G-protein-coupled receptor Edg-1. *Biochem J,* 330 (Pt 2)**,** 605-9.

ZUKER, M. 2003. Mfold web server for nucleic acid folding and hybridization

prediction. *Nucleic Acids Res,* 31**,** 3406-15.